An Investigation into the Role of Complement Factor H in the Retina

A Thesis Submitted to University College London

for the Degree of

Doctor of Philosophy in Ocular Cell Biology

By

Jennifer A.E. Williams

April 2012

Supervisor – Prof. Stephen E. Moss

UCL Institute of Ophthalmology

11-43 Bath Street, London, EC1V 9EL

Declaration

I, Jennifer Williams, confirm that the work presented in this thesis is my own. Where information has been derived from other sources, I confirm that this has been indicated in the thesis.

Jennifer A. E. Williams

25th April 2012

Abstract

Age-related macular degeneration (AMD) is the leading cause of visual impairment in the UK. In 2005, the first publication of a genome-wide associated study identified a single nucleotide polymorphism in complement factor H (CFH) as a genetic risk factor for AMD. CFH is a secreted regulator of the alternative complement pathway and therefore key to controlling the inflammatory response. Prior to 2005, little was known about the role of CFH in the retina. This study addresses this question in order to understand how this protein could contribute towards AMD pathology.

Initial experiments confirmed that retinal pigment epithelial (RPE) cells are capable of secreting detectable levels of CFH, and that RPE cells were able to enhance the secretion of CFH in response to inflammatory stimuli. The main focus of this study was to characterise the effect of loss of CFH on young and aged retina in *Cfh*$^{-/-}$ mice. Immunohistochemical studies revealed that signs of stress and re-distribution of complement proteins appear at one year of age. Genome-wide microarray analysis of the RPE and choroid or neuroretina, showed that loss of CFH has little effect on gene expression in young mice but that the impact of CFH loss increases with age. The largest group of genes to change were involved in antigen presentation and immunity suggesting that CFH has an important role in immune regulation in the eye.

Analysis of visual function using electoretinograms revealed that dysfunction seen at two years was not present at one year, indicating that age-related gene expression changes are likely to be involved in the pathogenic process in these mice. This study reveals the importance of CFH in maintaining retinal health and good visual function with age.

Acknowledgements

First and foremost, I would like to thank Prof. Steve Moss for accepting me into his lab as a PhD student back in 2007. He has been a wonderful supervisor who has always had time for me and spent many hours poring over data, talks, reports and thesis drafts! More than this he has given me confidence in my ability and the encouragement to continue in my scientific career. I would also like to thank the MRC-Laboratory for Molecular Cell Biology for awarding me a place on their PhD programme and all the support that goes with it. Many thanks also to Prof. John Greenwood who has been like a deputy supervisor to me. Many other Principal Investigators have also given up their time to discuss my data and progress including my thesis committee, Prof. Mary Collins, Dr. Franck Pichaud and Prof. Karl Matter, my second supervisor Dr. Virginia Calder and my graduate tutor Prof. Alison Hardcastle, to whom I am very grateful. Thanks to Prof. Mogens Holst Nissen and Dr. Carsten Faber for collaborative work on the microarray and to Prof. Paul Morgan for his generous gifts of antibodies. I would also like to thank my previous scientific mentors who taught me all the 'basics' and encouraged me to undertake this PhD including, Dr. Sandy Buchan, Dr. Steve Young, Prof. Steve Watson and Dr. Andrew Pearce of the University of Birmingham and Dr. Dilniya Fattah from my time at GlaxoSmithKline.

The Institute of Ophthalmology has been a fantastic place to learn. Many core facility staff members have made this possible, including Claire Cox, Aida Jokubaityte, Charmie Kodituwakku, Nicky Gent and the BRU staff. I would also like to take this opportunity to thank individually, all those who have helped in my training over the past 4 years including, Becca Longbottom, my amazing mentor who has taught me more things than I can list here!; Matt Hayes who has been very helpful in troubleshooting and suggesting new experiments; Jenny McKenzie for her help with qPCR and DART-PCR; Anna Tsapara for her help with primary porcine RPE isolation; Xiaomeng Wang for her help with the animals; Hari Jayaram for assistance with perfusing mice; Katy Coxon for help with the FPLC; Clare Futter and Emily Eden for help with EM; Robin Howes and Peter Munro for assistance with electron and confocal microscopy; Jean Lawrence and lovely Mike Powner for help with immunohistochemistry; Shalini Jadeja for teaching me how to flatmount; Nipurna Jina and Daniel Paull for microarray analysis assistance;

Ah-Lai Law for teaching me how to use dissection tools (and couscous offerings) and Vineeta Tripathi for the generous loan of a laptop!

Many people both at the LMCB and IoO have been a pleasure to be around in the last 4/5 years. Sweet Adam and 'Dream-Team' co-founder Lux were excellent 'Team-Western' buddies and I hope their blots are still coming out clean. Jay, Emily and Natalie have really made the IoO a great place to work, have tea, eat biscuits and have lunch with, hopefully this will continue! Rachel, Ingrid, Katharina and James have generated a friendly and fun office environment. New arrivals have made losing old friends to foreign shores a lot easier including, Apostolos, Hui, Sterenn, Tom, Simon and Mafalda. My 'lovely year group' at the LMCB, Andrew, Clare, Fran, Mark and Maz have honestly made moving to London worthwhile. Living at the Clenesca residence and making the skits could not have been more fun! 'Library Club' members Clare, JK and Natalie have made writing this thesis more fun than I thought possible. JK, cruise ship labs will open one day!

I would also like to thank my non-work friends (there aren't very many!) for putting up with me and staying in touch, including Betsey, Marianne, Sarah, Tracey, Eirin, Anthony, Claire, Lisa, Emma, Feng, Mei and Abi.

Above all I would like to thank my loving family for just being there. Thanks and love goes to my Grandma Searle, Auntie Kate, Ellen, Owen and to my Mum & Dad.

List of contents

List of figures

List of tables

List of abbreviations

A2E	N-retinylidene-N-retinyl-ethanolamine
aa	amino acid
ABCA4	adenosine triphosphate-binding cassette, subfamily A, member 4
AFG3L2	AFG3 (ATPase family gene 3)-like 2
AGE	advanced glycation end-product
aHUS	atypical haemolytic uraemic syndrome
AMD	age-related macular degeneration
AP	apical process
ANOVA	analysis of variance
ARMS2	age-related maculopathy susceptibility protein 2
AU	arbitrary unit
BI	basal infolding
BlamD	basal laminar deposit
BlinD	basal linear deposit
BM	Bruch's membrane
BRB	blood-retinal barrier
BSA	bovine serum albumin
C4BP	C4b binding protein
CACNA1S	calcium channel, voltage-dependent, L type, alpha 1S subunit
CC	choriocapillaris
CDH2	cadherin 2
cDNA	complementary DNA
CEP	carboxyethyl pyrrole
CFH	complement factor H
CFHR1	complement factor H-related protein 1
CHX	cycloheximide
CNV	choroidal neovascularisation
CR	complement receptor
CRIg	complement receptor of the immunoglobulin superfamily
CRIT	C2 receptor inhibitor trispanning
CRP	c-reactive protein

CRRY	complement receptor type-1 related gene Y
CTSE	cathepsin E
Cy3	cyanine 3
DAF	decay-accelerating factor
DAPI	4’,6-diamidino-2-phenylindole
DART-PCR	data analysis for real-time PCR
DBI	diazepam binding inhibitor
DDD	dense deposit disease
DMEM	Dulbecco’s modified Eagle’s medium
DMSO	dimethyl sulphoxide
DNA	deoxyribonucleic acid
DYNLT1	dynein light chain Tctex-type 1
EAAU	experimental autoimmune anterior uveitis
ECM	extracellular matrix
EDTA	ethylenediaminetetraacetic acid
ERG	electroretinogram
FC	fold change
FCS	foetal calf serum
FE	fenestrated endothelium
FHL1	factor H-like 1
FITC	fluoroscein-5-isothiocyanate
FU	fluorescence unit
G	gauge
GCL	ganglion cell layer
GFAP	glial fibrillary acidic protein
H	histidine
HAMP	host associated molecular pattern
HTRA1	high-temperature requirement A 1
IFN	interferon
Ig	immunoglobulin
IL	interleukin
ILM	inner limiting membrane

INL	inner nuclear layer
IPA®	Ingenuity Pathway Analysis®
IPL	inner plexiform layer
IS	inner segment
ITGAV	integrin alpha V
Kb	kilobase
kDa	kiloDalton
L	lipofuscin
Ly	lysosome
mAb	monoclonal antibody
MAC	membrane attack complex
MAP-1	MBL/ficolin associated protein-1
MASP	MBL-associated serine protease
MBL	mannose-binding lectin
MCM6	minichromosome maintenance deficient 6
MCP	membrane co-factor protein
MCP-1	monocyte chemotactic protein-1
MIRL	membrane inhibitor of reactive lysis
ML	Melano-lipofuscin
MPI	mean pixel intensity
mRNA	messenger ribonucleic acid
OLM	outer limiting membrane
ONL	outer nuclear layer
OPL	outer plexiform layer
OS	outer segment
P	phagosome
pAb	polyclonal antibody
PAGE	polyacrylamide gel electrophoresis
PAMP	pathogen-associated molecular pattern
PBS	phosphate buffered saline
PCA	principal component analysis
PDT	photo dynamic therapy

PEDF	pigment epithelium-derived factor
PECAM1	platelet endothelial cell adhesion molecule 1
PFA	paraformaldehyde
PR	photoreceptor
Poly	polyanionic
PTTG1	pituitary tumour-transforming gene 1
RBC	red blood cell
RBP7	retinol binding protein 7
RIN	RNA integrity number
RMA	robust multiarray average
RNA	ribonucleic acid
RPE	retinal pigment epithelium/epithelial
rpm	revolutions per minute
rRNA	ribosomal RNA
RT	room temperature
RT qPCR	real-time quantitative polymerase chain reaction
SNCA	synuclein alpha
SCR	short complement repeat
S.D.	standard deviation
SDS	sodium dodecyl sulphate
SERPING1	serpin peptidase inhibitor clade G member 1
sMAP	small MBL associated protein
SNP	single nucleotide polymorphism
STAT1	signal transducer and activator of transcription 1
TCA	trichloroacetic acid
TIMP3	tissue inhibitor of matrix metalloproteinase 3
TLR	toll-like receptor
TNF	tumour necrosis factor
VEP	visual evoked potential
WT	wild-type
Y	tyrosine
ZRANB3	zinc finger RAN binding domain containing 3

Chapter 1: Introduction

1.1. The complement system

The sophisticated complement system, present in mammals today, acts as the frontline defence against invading pathogens. Additionally, it facilitates the removal of modified and dead host cells. This system has evolved within multicellular organisms over millions of years with the earliest homologs dating back to 550 million years ago in the horseshoe crab, *Carcinoscorpius rotundicauda* (Zhu *et al.,* 2005). Family members share conserved structural motifs and domains indicative of evolutionary multiple exon shuffling and gene duplication.

The complement system in mammals consists of over 30 soluble and membrane bound proteins which either act as activators, regulators or receptors of innate immunity. The proteins work together to discriminate pathogens and modified self from normal host cells and initiate their removal whilst protecting neighbouring host cells. This is done through the recognition of pathogen or host-associated molecular patterns (P- and HAMPs). Identification of a pathogen or modified self causes activation of a cascade whereby the activating components sequentially cleave each other leading to several effector functions that initiate the pathogen's removal. The cascade style response is biologically beneficial as it allows rapid amplification when a fast response is necessary. Moreover, the cascade can be regulated at each level so to have increased control over the immune response and to make it appropriate to the level required for the initiating stimulus.

Paul Ehrlich coined the term, 'complement system' in the late 1890s to describe the complementary action of the heat labile proteins in serum to that of specific heat stable proteins (now known to be antibodies). Originally complement was thought only to assist the function of antibodies, however in the 1930s complement's independent role in the innate recognition of microbes was described. Over recent years it has emerged that complement also plays a key role in adaptive immunity and immune homeostasis. It is also important in the removal of cellular debris such as apoptosed cells and immune complexes.

1.1.1. The complement system

The activators of the complement system are a collection of inactive proteases (zymogens) which require cleavage to become active. There are three activation pathways of these zymogens which make up the complement system: the classical, lectin and alternative (Figure 1.1). Each pathway has its own mechanism that enables it to distinguish between foreign and host cells. Between these three activation pathways a huge range of PAMPs can initiate activation of the system.

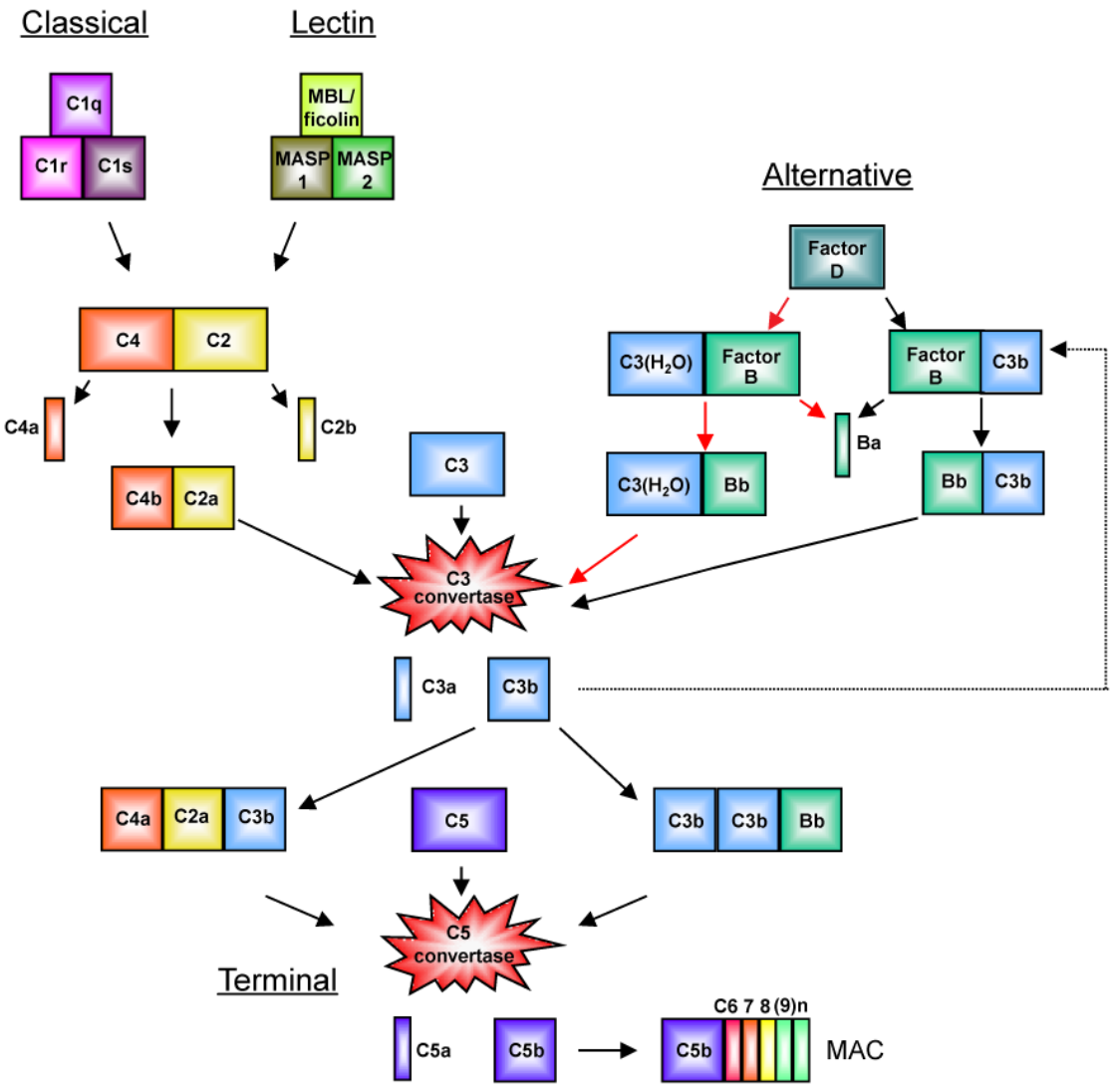

Figure 1.1. Activation pathways of the complement cascade
The classical, lectin and alternative pathways of complement once activated lead to the central formation of a C3 convertase (C4b2a or C3bBb). Red arrows indicate the tick-over component of the alternative pathway, where C3 convertase $C3(H_2O)Bb$ is constantly produced at low levels. Terminal activation of the pathway includes generation of C5 convertase (C4b2a3b or $C3b_2Bb$) and membrane attack complex (MAC, C5b678(9)n). Activation of the pathway leads to generation of anaphylatoxins (C3a, C4a and C5a) and opsonins (C3b and C4b).

The classical pathway is unique in that it bridges the innate and adaptive immune systems. The initiator of the pathway is C1 which is made up of three subunits, C1q, C1r and C1s. These subunits come together upon activation, which relies heavily upon antigen-antibody (Immunoglobulin (Ig) M or IgG_1 and IgG_3) complexes. In addition C1q can bind PAMPs present on microbes (Mintz *et al.,* 1995), pentraxins (Nauta *et al.,* 2003), deoxyribonucleic acid (DNA) (Garlatti *et al.,* 2010), polyanionic molecules and apoptotic bodies (Korb and Ahearn, 1997). Activation causes cleavage of C1r and C1s exposing protease activity which goes on to cleave C4 and C2, generating the smaller fragments C4a and C2b. The larger C4 fragment, C4b, binds covalently to target surfaces. The larger C2 fragment, C2a, binds C4b on target surfaces to form the enzymatic complex C3 convertase, C4b2a.

In the lectin pathway, collectins (mannose-binding lectin (MBL), L-, H- or M-ficolin) associate with MBL-associated serine proteases (MASPs). The collectins have many binding sites and together have a broad specificity for terminal carbohydrates on microbial glycoproteins. Once collectins bind to a PAMP, associated MASPs become activated and cleave C4 and C2 in the same manner as the classical pathway.

The alternative pathway of complement activation is different in that it is constantly active at a low level by the tick-over pathway. In this pathway C3 is continually hydrolysed by water into $C3(H_2O)$ in the serum (Lachmann and Halbwachs, 1975). An exposed thioester group in $C3(H_2O)$ can bind to the inactive serine protease, Factor B. Factor B is subsequently cleaved by Factor D releasing a small fragment Ba and revealing the active serine protease site in the larger Bb fragment. $C3(H_2O)Bb$ acts as a fluid phase C3 convertase, converting C3 to C3a and C3b.

The generation of C3b is the key step to amplifying the tick-over pathway for full-blown activation. At this step, regulators of the pathway mop up free C3b preventing full-blown activation. Unlike the other two pathways, the discrimination between host and pathogen comes from the regulators rather than the activators. Complement factor H (CFH) recognises HAMPs such as glycosaminoglycans present on the surface of host cells. C3b can only activate the cascade if bound to a surface which is unprotected

by regulators such as CFH or its membrane bound homologues (see Section 1.1.3). C3b like C3(H_2O) binds Factor B and is cleaved by Factor D to form C3bBb. C3bBb is an active C3 convertase with twice the convertase activity of C3(H_2O)Bb and can therefore amplify the tick-over pathway (Bexborn *et al.,* 2008).

C3 convertase is stabilised by association with the soluble protein properdin which increases its half-life tenfold (Fearon and Austen, 1975). More recently it has emerged that properdin can initiate activation of the alternative pathway by recruiting serum C3b as a platform for C3 convertase formation. Properdin has been shown to direct C3b towards apoptotic and necrotic cells, and also pathogens through its PAMP recognition ability (Spitzer *et al.,* 2007). The alternative pathway can also become activated in response to lectin or classical pathway activation, since both drive the formation of C3b. Once C3b concentrations outweigh the balance kept by regulators, alternative pathway activation can proceed. To add to the complexity of this cascade new evidence suggests there may be several bypass pathways which are capable of activating the cascade in the absence of key components (Huber-Lang *et al.,* 2006).

1.1.2. Complement effector functions

All pathways, although activated by different molecules, converge in the formation of the central complement enzyme, C3 convertase, and from this point all pathways lead to the same downstream effects. C3 convertase causes the breakdown of C3 whose products in turn allow the formation of C5 convertase (C4b2a3b or C3b_2Bb) which releases further pro-inflammatory proteins. The result of complement activation is the initiation of pathogen, apoptotic cell and immune complex clearance. This is achieved in three ways. Firstly, the small break down products, C3a, C4a and C5a act as pro-inflammatory anaphylatoxins which attract leucocytes expressing chemokine receptors. Anaphylatoxins enhance this process by acting on endothelial cells to increase vascular permeability (Schraufstatter *et al.,* 2002). Once recruited, mast cells, granulocytes and macrophages are activated by C3a and C5a (Klos *et al.,* 2009).

Secondly, opsonins C3b, iC3b, C3d, C3dg and C4b which are released by enzymatic cleavages, covalently bind to amino and hydroxyl groups on the surface of cells and

basement membranes via an active thioester. Although opsonins cannot discriminate between host and pathogen surfaces, C3b has been shown to preferentially bind microbial carbohydrates (Sahu *et al.,* 1994). Opsonins target the attracted leucocytes to pathogens to enhance their clearance. Complement receptors (CR) 1, 3 and 4 mediate phagocytosis through C3 fragment recognition. C3b and C3d also stimulate antigen uptake for processing by professional antigen presenting cells by binding to the B-cell receptor and CR2 (Dempsey *et al.,* 1996). C3b coated pathogens can also be cleared by binding to CR1 receptors on red blood cells which transport pathogens to phagocytes in the liver and spleen in a process called immune adherence (Nelson, Jr., 1953).

Finally, complement can directly clear pathogens by the formation of membrane attack complex (MAC). MAC formation is the terminal part of the cascade where C5b released upon C5 cleavage by C5 convertase binds to C6 and C7 in their fluid phase, this complex attaches to the surface of cells and forms a pore with C8 and multiple molecules of C9. C9 is able to penetrate the lipid bilayer of the cell envelope where it polymerises to create pores. Multiple pores disrupt membrane integrity and can cause cell lysis. Sublytic levels of MAC are also able to promote inflammation by inducing functional changes in host cells (work published from our group, Lueck *et al.,* 2011).

In summary the main effector functions of the complement cascade are the generation of inflammatory mediators, anaphylactic peptides, cytolytic and antimicrobial compounds and the recruitment of leucocytes. Unlike the adaptive immune system, the complement system can act very fast, and within five minutes of activation, C3b opsonisation is maximal with 20 million molecules deposited per target cell (Ollert *et al.,* 1994).

1.1.3. Complement regulation

The complement cascade is tightly regulated in order to determine the level and length of the amplification which is appropriate for clearance of the target. A proportionate and targeted defence prevents unnecessary amplification and bystander

damage of host cells. Proteins which regulate the pathway target one of the four main stages of the cascade:

1. Activation of the pathway
2. C3 convertase formation, decay and by-product degradation
3. C5 convertase formation , decay and by-product degradation
4. MAC assembly and function

As is the nature of a cascade, regulators which target components earlier in the cascade indirectly inhibit the formation of components further down the cascade. The first level of regulation is preventing activation of the cascade by regulating either the classical or lectin pathways (the alternative pathway is constantly active). The soluble serpin peptidase inhibitor clade G member 1 (SERPING1) regulates activation of both the classical and lectin pathways by blocking serine protease function in C1r, C1s and MASP2 (Cicardi *et al.,* 2005). Both MBL/ficolin associated protein-1 (MAP-1) and small MBL associated protein (sMAP) regulate activation of the lectin pathway by competing with MASPs for binding to MBL or ficolins (Degn *et al.,* 2010). Complement regulators which sequester C3b, inhibit the amplification of the tick-over pathway into full blown alternative pathway activation, these include CFH, factor H-like 1 (FHL-1) (Zipfel *et al.,* 1999), CR1, membrane co-factor protein (MCP) and complement receptor of the immunoglobulin superfamily (CRIg) (Wiesmann *et al.,* 2006).

The major class of inhibitors act at the level of the C3 convertase which indirectly prevents the formation of C5 convertase. By sequestering the proteins the complexes are composed of, formation of the complex is inhibited (as mentioned above in the alternative pathway). The formation of the classical/lectin pathway C3 convertase, (C4b2a), is inhibited by C2 receptor inhibitor trispanning (CRIT) which sequesters C2 (Inal *et al.,* 2005) and blocks its cleavage by C1 complex or MASPs. If C3 convertases are able to form, several regulators are able to promote its dissociation. Factor I, in association with a co-factor, (CFH, FHL-1, MCP, C4b binding protein (C4BP) or CR1) accelerates the decay of all C3 convertases, through cleavage of the alpha chain of C3b or C4b (Bokisch *et al.,* 1975). Several regulators accelerate the decay of C3 convertases

independent of Factor I. CFH, FHL-1, decay-accelerating factor (DAF), MCP and CR1 accelerate the decay of C3bBb through the interaction with C3b whereas C4BP and CR1 accelerate the decay of C4b2a through interaction with C4b. Generation of C3 convertase leads to the production of anaphylatoxin C3a which is degraded by carboxypeptidase N therefore inhibiting inflammation (Bokisch and Muller-Eberhard, 1970).

Finally terminal complement regulators regulate C5 convertase formation, its decay, degradation of it by-products and MAC assembly. Complement factor H-related protein 1 (CFHR1) inhibits the formation of C5 convertase and MAC assembly (Heinen *et al.,* 2009) whereas clusterin, vitronectin and membrane inhibitor of reactive lysis (CD59, MIRL) inhibit MAC assembly and function only. Carboxypeptidase N in addition to degrading C3a can also degrade C5a (Bokisch and Muller-Eberhard, 1970).

Rodents possess another complement regulator which is not expressed in humans, complement receptor type-1 related gene Y (CRRY) which has the co-factor and decay accelerating properties of MCP and DAF (Molina, 2002). Additionally in mice, the CD59 gene is duplicated leading to protein expression of both CD59a and CD59b (Harris *et al.,* 2003), however, CD59a is the main regulator of MAC formation (Baalasubramanian *et al.,* 2004).

Complement regulatory proteins fall into two main categories, those which are membrane bound and those which are soluble and are secreted (Table 1.1). Cells are protected by expressing the membrane bound regulators and the molecules which attract the soluble ones. Biomembranes such as Bruch's membrane in the eye and the glomerular basement membrane in the kidney are dependent on the soluble regulators since they do not have the capacity to express the membrane bound regulators.

The expression and distribution of complement regulatory proteins differs between cell types and from tissue to tissue. Importantly these proteins can become up or down-regulated in order to fine tune local needs, for instance during an infection.

Complement regulator	Abbreviation (& CD antigen)	Level of Regulation	Primary Ligands	Pathways Regulated	Function
C4 binding protein	C4BP	2	C4	CP, LP, AP	Sequesters C4, acts as a co-factor for Factor I and accelerates the decay of C3 convertases
Carboxypeptidase N	CBPN	2, 3	C3a, C4a, C5a	CP, LP, AP	Cleaves and partially inacivates anaphylatoxins
Complement factor H	CFH	1, 2	C3b	AP	Sequesters C3b, acts as a cofactor for Factor I and accelerates the decay of C3 convertases
Complement factor H related protein 1	CFHR1	3, 4	C5 convertase, MAC	Terminal	Inhibits C5 convertase formation and MAC assembly
Complement factor I	CFI	2	C3b, C4b	CP, LP, AP	Cleaves C4b, C3b and iC3b when bound to a co-factor
Clusterin	CLU	4	C7, C8, C9, MAC	Terminal	Inhibits MAC assembly and function
Factor H-like 1	FHL1	1, 2	C3b	AP	Sequesters C3b, acts as a cofactor for Factor I and accelerates the decay of C3 convertases
MBL/ficolin associated protein-1	MAP-1	1	MBL, ficolins	LP	Sequesters MBL and ficolins
Small MBL associated protein	sMAP	1	MBL	LP	Sequesters MBL
Serpin peptidase inhibitor clade G member 1	SERPING1	1	C1r, C1s, MASP2	CP, LP	Blocks serine protease activity
Vitronectin	VTN	4	C5b-7, MAC	Terminal	Blocks C5b-7 membrane binding and C9 polymerisation
C2 receptor inhibitor trispaning	CRIT	1	C2	CP, LP	Sequesters C2
Complement receptor 1	CR1 (CD35)	1, 2	C3b, C4b	CP, LP, AP	Acts as a cofactor for Factor I and accelerates the decay of C3
Complement receptor type-1 related gene Y	CRRY	1, 2	C3b, C4b	CP, LP, AP	Murine homolog of MCP and DAF
Complement regulator of the immunoglobulin super-family	CRIg	1, 2	C3b	AP	Sequesters C3b
Decay accelerating factor	DAF (CD55)	2	C3b, C4b	CP, LP, AP	Accelerates the decay of C3 convertases
Membrane co-factor protein	MCP (CD46)	1, 2	C3b, C4b	CP, LP, AP	Sequesters C3b, acts as a cofactor for Factor I and accelerates the decay of C3 convertases
Membrane inhibitor of reactive lysis	MIRL (CD59)	4	C8, MAC	Terminal	Inhibits MAC assembly and function

Table 1.1. Regulators of the complement system

Soluble (red) and membrane-bound (blue) regulators of the complement system act at different levels of the cascade,1; activation of the pathway 2; C3 convertase formation, decay or by-products, 3; C5 convertase formation, decay or by-products 4; membrane attack complex (MAC) assembly or function. By targeting different primary ligands, complement regulators can target one or more of the activation pathways (classical (CP), lectin (LP) or alternative (AP)) or the terminal pathway. Table adapted from Zipfel and Skerka, 2009.

1.1.4. Complement synthesis

The majority of complement proteins in the body circulate in the blood. They are synthesised in the liver and their secretion is rapidly enhanced in response to tissue injury and inflammation and are therefore termed acute phase proteins. Interleukin-1 (IL-1), IL-6 and interferon γ (IFNγ) are the main cytokines shown to stimulate transcription of complement genes (Volanakis, 1995). Unlike other acute phase proteins, complement proteins are also synthesised in extra-hepatic sites, which are more responsive to inflammatory changes than the liver (Volanakis, 1995). A vast array of tissues and cell types have been shown to express complement proteins, discussion of which is beyond the scope of this introduction, see review by Morgan and Gasque (1997).

1.1.5. Complement and disease

There are several ways in which the complement system can bring about disease:

1. Inappropriate activation of the complement system caused by ischemia reperfusion injury, burns, apoptosis and necrosis.
2. Extreme activation of the complement system which saturates host defence mechanisms such as antibody mediated autoimmunity, immune complex disease and sepsis.
3. Deficiency or mutation in one of the activatory complement proteins causing susceptibility to infection. For example, individuals with properdin deficiency have a higher susceptibility to *Nisseria* infections.
4. Deficiency or mutation in one of the complement proteins leading to a lack of host defence for example, atypical haemolytic uraemic syndrome (aHUS), paroxysmal nocturnal haemoglobinuria and age-related macular degeneration (AMD).

Dysregulated or misdirected complement activation can result in severe pathology in several organ systems. The absence of just one complement protein has the ability to disrupt the whole cascade resulting in a variety of diseases (Holers, 2008; Carroll and Sim, 2011; Degn *et al.,* 2011). More commonly individuals contain polymorphisms which affect the function or expression of a complement protein.

1.1.6. Ocular complement expression and eye diseases

Complement is continuously active at a low level in the eye in order to function as a front line defence ready to react quickly to an appropriate challenge (Sohn *et al.,* 2000). However complement is also involved in protecting host tissue from innocent bystander destruction. Complement expression is important in both the front and back of the eye. The balance between offence and defence is a crucial function of complement within the eye and factors which disrupt this balance can cause disease.

Ocular tolerance is an important feature of immune privilege in the eye. To achieve this, the anterior chamber uses immune deviation to react to antigens to promote the generation of regulatory T-cells and suppress delayed type hypersensitivity. In the anterior chamber iC3b has been shown to be important in inducing tolerance to new antigens (Sohn *et al.,* 2003).

The cornea expresses many complement factors which mediate the generation of anaphylatoxins and MAC (Mondino and Sumner, 1990; Mondino *et al.,* 1996) to defend this exposed tissue from pathogens in the environment. To minimise damage to host tissue, the cornea also expresses complement regulators. A loss in expression of these complement regulators is believed to contribute towards corneal disease. Complement activation is believed to be a contributing factor in ulceration of the cornea (Mondino *et al.,* 1978; Cleveland *et al.,* 1983).

Anterior uveitis, the most common form of uveitis, features inflammation of the iris and anterior chamber. The inflammation is brought about by an autoimmune response to ocular antigens. In a mouse model of the disease, experimental autoimmune anterior uveitis (EAAU), Jha *et al.,* (2006a; 2006b) show that complement activation is required for disease development and they observe a concomitant upregulation of complement regulators. Complement regulation is important to disease development since *Daf*$^{-/-}$ mice develop a more severe phenotype of EAAU (An *et al.,* 2009) whereas administration of recombinant CRRY suppresses disease development (Manickam *et al.,* 2010). Administration of Factor B antibodies but not C4 antibodies also suppressed

EAAU development, suggesting it is the alternative pathway of complement activation which is most important for EAAU development (Manickam *et al.,* 2011).

Complement is also an important feature in the health of the retina. Complement dysregulation is implicated in AMD. This was first indicated when complement activation products were identified in drusen (Mullins *et al.,* 2000; Johnson *et al.,* 2000). The development of choroidal neovascularisation (CNV), a feature of AMD, has been shown in an animal model to be partly dependent on complement activation (Bora *et al.,* 2005). Furthermore, administration of recombinant CD59 suppresses CNV in these mice (Bora *et al.,* 2010). The involvement of complement in AMD was strengthened when in 2005, four separate studies identified the same single nucleotide polymorphism (SNP) in a complement regulator, CFH, as a major risk factor for AMD (Edwards *et al.,* 2005; Hageman *et al.,* 2005; Haines *et al.,* 2005; Klein *et al.,* 2005). Prior to describing AMD, I will first introduce CFH in more detail.

1.2. Complement factor H

CFH is a secreted glycoprotein whose main function is to regulate the activation of the alternative complement pathway. CFH was first described by Nilsson and Mueller-Eberhand in 1965 as the fifth factor of complement which brings thermostability to the heat labile complex of complement (Nilsson and Mueller-Eberhard, 1965). The role of this protein in the complement system has now been well characterised. Thus, CFH's regulatory function is mediated via its interaction with glycosaminoglycans present on host surfaces and the cleavage product of C3, C3b. CFH regulates the alternative pathway both in fluid phase and on host surfaces by three separate actions:

1. Competing with Factor B for binding to C3b thereby impeding the formation of C3 convertase.
2. Accelerating the decay of C3 convertase (C3bBb) through interaction with C3b.
3. Acting as a co-factor for Factor I-mediated degradation of C3b to iC3b.

1.2.1. CFH structure

CFH is composed of 1213 amino acids (aa) which after glycosylation forms a 155 kDa glycoprotein (Ripoche *et al.,* 1988). The protein consists of 20 short complement repeats (SCR) each of which are between 51-62 aa and are connected by a linker sequence of 3-8 aa. Each repeat contains four invariant cysteine residues which form two disulphide bonds stabilising the folding of the protein into complement control modules also known as sushi domains (Interpro database reference: IPR000436). CFH has an elongated structure of β-pleated sheets which are folded back to bring the N- and C-terminal regions into close proximity (Aslam and Perkins, 2001). The crystal structure of the full length protein has yet to be elucidated because of its size, glycosylation and inter-SCR flexibility. Instead, structures of CFH protein fragments have been studied. CFH is a member of a structurally related family of proteins called regulators of complement activation which all contain SCR motifs and whose genes are located in a cluster on human chromosome 1q31.3-32.2. Members of this family include, CFH, CR2, C4BP, DAF, CR1, MCP, CFHR1-3 and CRRY in rodents.

1.2.2. Binding partners of CFH

CFH is able to regulate the complement pathway by binding C3b. Using surface plasmon resonance and deletion mutants in functional assays, several regions of the protein have been identified as having C3b binding capacity (Schmidt *et al.,* 2008) (Figure 1.2). N-terminal SCR 1-4 was the first C3b binding region to be identified and is now well characterised (Gordon *et al.,* 1995). This region confers the co-factor and decay accelerating properties of the protein (Wu *et al.,* 2009). Full length CFH has a 100 fold greater affinity for C3b than SCR 1-4 alone therefore the possibility for additional C3b binding sites were hypothesised. Indeed, a second C3b binding region was identified in the C-terminal SCRs 19-20 using deletion mutants (Jokiranta *et al.,* 2000), and exhibits strong binding to C3b. Two other regions, SCR 6-8 (Sharma and Pangburn, 1996) and 8-15 (Schmidt *et al.,* 2008) have both been identified as having weak C3b binding capability, however the exact locations within these regions are disputed.

The ability of the alternative complement pathway to distinguish self from pathogen or modified self lies in the capacity of CFH to bind polyanionic molecules such as sialic acid, heparan sulphate and other glycosaminoglycans expressed on host cells. In fact the affinity of CFH for C3b is enhanced by the presence of polyanionic structures which helps to direct the protection of CFH towards host cell surfaces (Meri and Pangburn, 1990; Kelly *et al.,* 2010). Two regions of the protein have been identified to bind polyanions, SCR 7 in the middle of the protein (Blackmore *et al.,* 1996) and SCR 19-20 in the C-terminus (Blackmore *et al.,* 1998b). In the retina, recombinant SCR 6-8 fragments specifically bind heparan sulphate and dermatan sulphate present on choroidal vessels, Bruch's membrane and retinal pigment epithelium (RPE) (Clark *et al.,* 2010).

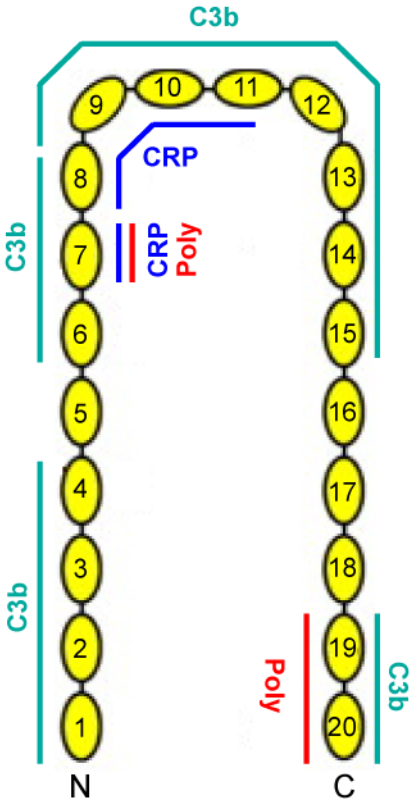

Figure 1.2. Structure and binding partners of complement factor H
CFH is composed of 20 short complement repeats (SCR, yellow) connected by small linkers. The protein has a folded back structure bringing the N- and C- terminal regions into close proximity. Several regions of the protein have been identified as binding regions for C3b (green), c-reactive protein (CRP, blue) and polyanionic molecules (Poly, red). The Y402H SNP associated with increased AMD susceptibilty is located in SCR 7. This figure is modified from Kieslich *et al.*, 2011.

Integral to CFH's function is its ability to bind simultaneously to both C3b and polyanions, and although the structure of this relationship has not been fully elucidated, computer modelling suggests that CFH binds one C3b molecule via its two terminal C3b binding sites whilst binding polyanionic structures (Morgan *et al.,* 2011).

CFH also has the capacity to self-associate and form oligomers with dimerisation sites located in SCR 6-8 and 16-20 (Perkins *et al.,* 1991; Nan *et al.,* 2008b). The functional significance of this oligomerisation is not known but this property may play a role in aggregation of the protein found in disease-related protein deposits such as drusen. Oligomerisation of the protein is influenced by local zinc and copper concentrations (Nan *et al.,* 2008a). It is proposed that C3b may be sterically blocked when CFH aggregates, however oligomerisation may alternatively maximise the ability of CFH to bind both C3b and polyanions simultaneously.

CFH also has binding capacity for c-reactive protein (CRP) (Okemefuna *et al.,* 2010; Perkins *et al.,* 2010). CRP is an acute phase protein which circulates in the blood and is up-regulated by inflammation. CRP binds to pathogenic surfaces and necrotic cells and can activate the classical complement pathway (Mihlan *et al.,* 2011). CFH has been shown to have two regions which bind CRP, SCR 7 and 8-11 (Jarva *et al.,* 1999). Binding to CRP has been disputed because of reports showing that CRP binding to CFH requires prior denaturation (Hakobyan *et al.,* 2008). However it is also argued that denatured CRP is present on necrotic cells and the presence of CFH on necrotic and apoptotic cells helps to remove them safely (Mihlan *et al.,* 2009). It has recently been shown that CFH binds non-denatured CRP when CRP is at high concentrations such as in times of inflammation (Okemefuna *et al.,* 2010). CFH has also been shown to bind annexin 2, DNA and histones on apoptotic cells which may limit inflammation during their phagocytosis (Leffler *et al.,* 2010). CFH also binds fibromodullin (Sjoberg *et al.,* 2005), a constituent of extracellular matrix, and adrenomedullin (Pio *et al.,* 2001; Martinez *et al.,* 2003) which is a multifunctional peptide secreted by the RPE with a role in inflammation. This enables the protection of acellular host structures such as Bruch's membrane in the eye (Udono *et al.,* 2000).

Finally, microorganisms have evolved to protect themselves from complement attack by expressing complement regulator-acquiring surface proteins which bind to proteins such as CFH. These include M-protein of *Streptococcus pyogenes* (Horstmann *et al.,* 1988; Blackmore *et al.,* 1998a; Kraiczy *et al.,* 2004), OspE (Hellwage *et al.,* 2001), BpCRASP-2 (Hartmann *et al.,* 2006), BpCRASP-3 (Kraiczy *et al.,* 2003) of *Borrelia*

burgdoferi, Gpm1p of *Candida albicans* (Poltermann *et al.,* 2007), Tuf of *Pseudomonas aeruginosa* (Kunert *et al.,* 2007) LfhA of *Leptospira interrogans* (Verma *et al.,* 2006) and factor-H binding protein of Nisseria meningitides (Madico *et al.,* 2006).

1.2.3. CFH synthesis and expression

The *CFH* gene is located on chromosome 1 in both humans (1q31.3) and mice (1F). The gene contains 22 exons and yields a transcript of 4.1 kb in humans and 4.4 kb in mice. The *CFH* messenger ribonucleic acid (mRNA) is 71% homologous between humans and mice in the coding region and the 5' flanking region has 60% identity. The *CFH* gene is located within the CFH related gene cluster which also contains five CFH-related genes, *CFHR1-5*.

In the human gene, three glucocorticoid response elements, two acute phase signals, two 3'-5'-cyclic adenosine monophosphate responsive elements, a retinoic acid response element and an IFNγ activation site have been identified in the promoter region (Munoz-Canoves *et al.,* 1990; Ward *et al.,* 1997). Both mouse and human genes share a histone H4 transcription factor binding site which is speculated to be involved in the IFNγ mediated up-regulation of CFH (Vik, 1996).

The majority of plasma CFH is made by the liver in both humans and rodents (Morris *et al.,* 1982; Schwaeble *et al.,* 1987; Mandal and Ayyagari, 2006). In humans, CFH plasma concentrations range from 120-790 μg/ml (Weiler *et al.,* 1976; Charlesworth *et al.,* 1979; Adinolfi *et al.,* 1981; Sim and DiScipio, 1982). Like other complement factors, CFH is also secreted locally by many cell types in distinct tissues including monocytes, fibroblasts, endothelial cells, epithelial cells, glomerular mesangial cells, B-cells, oligodendrocytes and astrocytes, (Friese *et al.,* 1999).

1.2.4. Factor H-like protein 1

FHL1 is a splice variant consisting of the first 9 exons of *CFH* (Estaller *et al.,* 1991). FHL-1 is therefore a truncated version of CFH that contains SCR 1-7 and four additional hydrophobic C-terminal aa. The concentration of FHL-1 in plasma is tenfold lower than that of CFH (Kotarsky *et al.,* 1998). Nevertheless, FHL-1 is capable of regulating the

alternative complement pathway through binding of C3b in its N-terminus and the polyanion binding site in SCR 7 (Misasi *et al.,* 1989). FHL-1, like CFH is also secreted by extra-hepatic sources however studies have revealed that the two proteins have tissue-specific differences in their expression and regulation (Friese *et al.,* 1999).

1.2.5. CFH-related proteins

The CFH related proteins, CFHR1-5, are by implication structurally similar to CFH, in that they were first identified using polyclonal antibodies to CFH, but unlike FHL-1 are transcribed from different genes (Zipfel and Skerka, 1994). With their structural similarities it is unsurprising that their functions suggest roles in complement regulation. Indeed, CFHR1 has been shown to regulate C5 convertase activity and MAC formation (Heinen *et al.,* 2009) and CFHR5 is capable of regulating C3 convertase activity (McRae *et al.,* 2005). CFHR3 and 4 have been shown to have C3b binding capacity (Hellwage *et al.,* 1999).

1.2.6. Diseases associated with CFH

Several CFH mutations have been linked to pathology of the kidney. The kidney is particularly vulnerable because of its high exposure to blood and complement components within it. Since the glomerular basement membrane does not express membrane bound complement regulators, it is dependent on soluble ones for its protection. Therefore mutations which affect the function of soluble complement regulators often manifest within this organ.

One of the major causes of the childhood kidney disease, aHUS, are mutations in the C-terminus of CFH which affect the binding of this protein to polyanions, C3b or both (Perez-Caballero *et al.,* 2001). This leads to less control over the activation of the alternative pathway, the consequences of which manifest first in the kidney where most damage occurs. Consistent with this, a mouse which lacks the C-terminal domain of CFH develops spontaneous aHUS (Pickering *et al.,* 2007). aHUS can also be caused and or exacerbated by mutations in other complement proteins including Factor I, Factor B, C3b and MCP (Fremeaux-Bacchi *et al.,* 2008).

An aa deletion in the N-terminal C3b binding domain of CFH causes dense deposit disease (DDD), (Licht *et al.,* 2006). DDD, is a disease which manifests at the glomerular basement membrane of the kidney. This also occurs in *Cfh*$^{-/-}$ pigs, humans and mice (Pickering *et al.,* 2002). Humans with DDD often also develop soft drusen in their eyes, an acknowledged risk indicator for AMD, and their composition is similar, suggesting a common or similar molecular pathogenesis (D'souza *et al.,* 2009). However, unlike in AMD, DDD patients do not exhibit retinal damage.

There have also been reports that Alzheimer's disease (Zetterberg *et al.,* 2008) and myocardial infarction (Kardys *et al.,* 2006) are associated with mutations in CFH, however both of these associations have been disputed (Stark *et al.,* 2007; Hamilton *et al.,* 2007).

As previously mentioned, a common SNP in CFH is a significant risk factor for AMD. This SNP involves a histidine substitution for tyrosine at position 402 of the protein (Y402H), within a cluster of positively charged aa in SCR 7. Initially the broad binding capacity of this domain, known to bind C3b, CRP and polyanionic molecules, was thought to be the disease causing mechanism of this SNP. Although many groups have now studied this, a clear answer has yet to be found. It is has been shown that this SNP does not affect the secretion of the protein (Yu *et al.,* 2007) nor its affinity to C3b (Skerka *et al.,* 2007; Yu *et al.,* 2007; Schmidt *et al.,* 2008; Kelly *et al.,* 2010). Several studies show that the SNP causes a diminished binding to CRP (Laine *et al.,* 2007; Skerka *et al.,* 2007; Yu *et al.,* 2007; Okemefuna *et al.,* 2010), a stronger affinity for DNA and necrotic cells (Sjoberg *et al.,* 2007) and a higher propensity to dimerise (Fernando *et al.,* 2007). But there are conflicting reports as to whether glycosaminoglycan binding is affected (Clark *et al.,* 2006; Herbert *et al.,* 2007; Yu *et al.,* 2007). Before discussing the link between CFH and AMD, I will first introduce the affected cells and tissues of the retina.

1.3. Retina

The eye can be functionally split into two halves (Figure 1.3A). The anterior half includes the cornea, iris, lens and ciliary body which together focus light onto the posterior half of the eye. Here the sensory retina processes light into electrical signals that are transmitted to the visual cortex via the optic nerve. The retina is a multi-layered structure of predominantly neurons (neuroretina) and RPE. Bruch's membrane separates the retina from the outer choroidal capillary network, the choriocapillaris.

1.3.1. Neuroretina

The neuroretina is a neural tissue containing neurons, glial cells and blood vessels. The neurons form three main cellular layers, the innermost photoreceptors, the bipolar, horizontal and amacrine cell layer, and the outermost ganglion cell layer. Toluidine blue staining of the neuroretina reveals 6 visually distinct layers (Figure 1.3B). The innermost layer contains the photoreceptor inner and outer segments (IS and OS) which synthesise and store the photosensitive pigments. Inward of the photoreceptors lies the outer nuclear layer (ONL) which contains the nuclei of the photoreceptors. The outer plexiform layer (OPL) contains synapses between the photoreceptors, bipolar and horizontal neurons. The inner nuclear layer (INL) lies in the middle of the retina and contains the nuclei of the bipolar, horizontal and amacrine neurons. Inward of the INL is the inner plexiform layer (IPL) which contains synapses between the bipolar, amacrine and ganglion cell layers. The innermost layer bordering the vitreous humour is the ganglion cell layer (GCL) which contains the cell bodies of the ganglion cells.

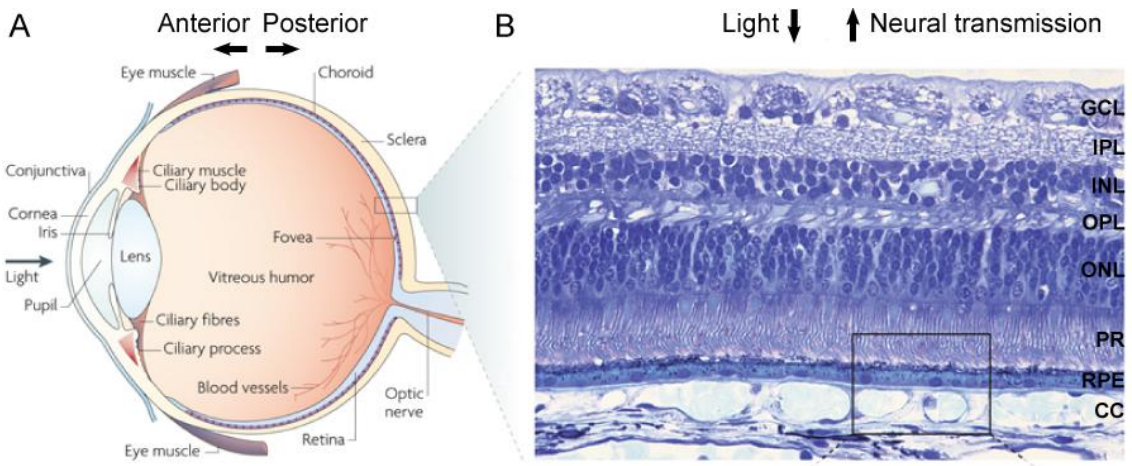

Figure 1.3. Structure of the human eye and retina
(A) Schematic of the eye which can be anatomically split into two halves; the anterior and posterior segments. Light enters through the pupil and is focused by the lens onto the light sensitive retina. (B) The retina is a multi-layered structure where light travels outward and neural transmission inward. The layers consist of the outermost choriocappilaris (CC) which perfuses the overlying retinal pigment epithelium (RPE) which in turn support the light sensitive photoreceptors (PR). The PR nuclei lie within the outer nuclear layer (ONL) and form synapses with second-order neurons in the outer plexifrom layer (OPL), whose nuclei lie within the inner nuclear layer (INL). Second-order neurons form synapses with ganglion cells in the inner plexiform layer (IPL) whose cell bodies lie within the innermost ganglion cell layer (GCL). (C) The RPE is a polarised monolayer whose apical surface contain apical processes (AP) which interdigitate between the outer segments (OS) of rod and cone PRs. Their basal surface form basal infoldings (BI) to aid diffusion with the CC. The Bruch's membrane (BM) separates the RPE from the CC and is composed of five layers; the basement membranes of the RPE and CC (red), two collagen layers and a central elastic fibre layer (striped). Figure modified from Wright *et al.*, (2010).

1.3.1.1. Photoreceptors

There are two types of photoreceptors; rods and cones. In humans, the peripheral retina contains predominantly rods which are sensitive to low levels of light whereas cones are the dominating photoreceptor of central vision. Three types of cones, which are sensitive to either long (red), medium (green) or short (blue) wavelengths of light, allow colour vision. In nocturnal rodents the majority of photoreceptors are rods (Carter-Dawson and LaVail, 1979). Photoreceptors are made up of IS and OS connected by a cilium, with the nucleus located between the cilium and the synaptic terminal. The photosensitive pigment, opsin, is composed of a G-protein coupled receptor bound by a chromophore, 11-cis-retinal. The photosensitive opsins are synthesised in the IS and are transported to the OS, whereas the chromophore is regenerated

through delivery to the RPE as part of the visual cycle. Rod OS contain rhodopsin which is packed into membranous discs distinct from the ciliary plasma membrane, whereas cone-opsins are stacked on invaginations of the ciliary plasma membrane.

1.3.1.2. Glial cells

The retina, as with other parts of the central nervous system, contains non-neuronal glial cells which support the function of both the neurons and blood vessels to maintain homeostasis. The retina contains three types of glial cells; Müller cells, astrocytes and microglia. Müller cells span the length of the retina between the two limiting membranes. Their apical villi form adherens junctions and desmosomes with each other and the IS of the photoreceptors to form the outer limiting membrane (OLM). Their wide endfeet along with the basement membrane form the inner limiting membrane (ILM), separating the vitreous from the retina. Müller cell processes form a close relationship with axons and blood vessels. They have a multitude of functions such as structural support, maintenance of ionic homeostasis, metabolic support and regulation of blood flow (Bringmann *et al.,* 2006). Astrocytes also support the functions of neurons and blood vessels, but are restricted to the GCL. Microglia are tissue resident macrophages which aid phagocytosis of dying cells and debris.

1.3.2. Retinal pigment epithelium

The RPE is a cobblestone monolayer of polarised pigmented epithelium which under normal conditions is mitotically inactive. Located between the choroid and the neuroretina, the RPE is integral to homeostasis of the retina (Figure 1.3C). The apical surface of the RPE forms sheet-like microvilli which extend up into the interphotoreceptor matrix and engulf the OS of the photoreceptors upon daily circadian shedding. The basal surface of the RPE forms convoluted infoldings which maximise the surface area for metabolic exchange with the choroidal vasculature. The RPE is polarised whereby the apical and basal halves differ in their structure, secretion of factors, expression of membrane bound proteins, organisation of organelles and junctional proteins. The six major functions of RPE have been comprehensively reviewed by Strauss (2005) and are summarised below.

1.3.2.1. Phagocytosis of shed outer segments

Photoreceptor OS are continually turned over to prevent build-up of photo-oxidation by-products. Each day roughly 10% of the most distal OS is shed and phagocytosed by the RPE (Young and Bok, 1969). The shedding of OS is regulated by circadian rhythms where lights off initiates a wave of cone OS shedding and lights on initiates a burst of rod OS shedding. The three main steps of OS phagocytosis are binding, signalling events and subsequent internalisation. The $\alpha_v\beta_5$ integrin, expressed on the apical surface of the RPE, must become activated for binding (Finnemann *et al.,* 1997). Activation of $\alpha_v\beta_5$ initiates a signalling cascade whereby activated focal adhesion kinase phosphorylates and activates the tyrosine kinase *c-mer,* which leads to downstream second messenger signalling. Tyrosine kinase signalling triggers an increase of intracellular inositol 1,4,5-triphosphate, Ca^{2+} mobilisation and stimulates actin dynamics via modulators such as annexin 2 (Law *et al.,* 2009) to drive OS internalisation.

1.3.2.2. Preventing light induced oxidation

The retina is exposed to almost constant light during conscious hours. A combination of light and a high oxygen and lipid content together favour oxidative reactions, leading to the potential generation of toxic free radicals. The RPE limits this process by the expression of antioxidants, pigment granules and repair mechanisms. Most importantly, the specialised organelles containing the pigment melanin, melanosomes, are polarised towards the apical surface of the cell for maximal absorption of scattered light. In rodents there is movement of melanosomes into the apical processes upon lights on. Although the reason for this movement is not known, it is speculated that it is related to the physical constraints of phagocytosis (Futter *et al.,* 2004). This process has not been studied in humans or primates.

1.3.2.3. Selective transport

Tight junctions which seal neighbouring RPE cells together are important in maintaining the outer blood-retinal barrier (BRB). These tight junctions control the paracellular transport of water, ions, metabolites, proteins and cells between the choroid and the retina. Therefore the RPE must regulate the bi-directional transport of

these substances to meet the needs of the retina. The retina requires delivery of glucose, nutrients, retinal and lipids, and the removal of metabolites and metabolic water, and RPE cells are equipped with transporters for these substances on both apical and basal surfaces.

1.3.2.4. Visual cycle

11-*cis*-retinal is transformed by light energy to all-*trans*-retinal in the OS. Conversion of all-*trans*-retinal back to 11-*cis*-retinal takes place in the visual cycle which occurs in two steps. The first step is carried out in the photoreceptors where all-*trans*-retinal is transported to the cytosolic space where it reacts with phosphatidylethanolamine and retinol dehydrogenase to become all-*trans*-retinol. Since photoreceptors lack the enzymes required for re-isomerisation, all-*trans*-retinol is transported to the RPE via interstitial retinol binding proteins. In the RPE, cellular retinol binding proteins guide the all-*trans*-retinol to an enzyme complex which esterifies, re-isomerises and oxidises it into 11-*cis*-retinal. The delivery of 11-*cis*-retinal back to the photoreceptors completes the visual cycle (Thompson and Gal, 2003).

1.3.2.5. Secretion by the RPE

The RPE secretes a variety of proteins to maintain the structure and function of the retina, Bruch's membrane and choroid. Some proteins are secreted in a polarised fashion in order to carry out specialised functions such as the neuroprotective and anti-angiogenic pigment epithelium-derived factor (PEDF) which is secreted apically (Becerra *et al.,* 2004). The RPE secrete a variety of proteins and enzymes to maintain turnover of the extracellular matrix, growth factors and several immunological proteins including complement components, chemokines and interleukins. Secretion by RPE cells is regulated, in part, by intracellular free Ca^{2+} which is tightly regulated by the expression of transporters and ion channels (Rosenthal and Strauss, 2002).

1.3.2.6. Buffering of ions in the subretinal space

Effective electrical conductance in neurons is dependent on the buffering of ions by neighbouring non-neuronal cells. In the retina this is achieved by Müller glia cells and the RPE cells. The excitability of the photoreceptors is dependent on the

concentrations of ions in the subretinal space. RPE cells maintain ion homeostasis in this part of the retina by controlling the K^+ conductance across their apical and basal membranes. In the dark, photoreceptors maintain a dark current which involves influx of Na^+ and Ca^{2+} and efflux of K^+. RPE cells buffer the subretinal K^+ concentration by transporting K^+ ions from the subretinal space towards the choroid. However, upon light stimulus K^+ efflux from the photoreceptors declines and the K^+ concentration in the subretinal space diminishes. The RPE counteracts this by switching from basolateral to apical efflux of K^+. This process must be fast to keep up with neuronal transmission and RPE cells are therefore equipped with voltage-gated K^+ channels (Wimmers *et al.,* 2007).

1.3.3. Bruch's membrane

Bruch's membrane is an acellular pentalaminar structure which separates the choroid from the RPE. It provides structural support, acts as a scaffold for bio-active molecules, and forms part of the BRB to regulate movement of waste and nutrients between the RPE and the choroid. The five layers consist of a central lamina of elastic fibres sandwiched between two collagen layers, with two external basement membrane layers of the RPE and the choroid. Its composition and turnover is maintained by both the choroid and RPE (Booij *et al.,* 2010).

1.3.4. Blood supply

The retina has two blood supplies (Figure 1.4). The outer retina is dependent on the blood supply of the choroid which has the highest perfusion rate in the body. The second blood supply, the retinal vessels, supports the retina between the ILM and OLM. Due to the multi-layered nature of the retina, the retinal vessels form three separate plexuses. The inner plexus contains the larger vessels and a capillary network. During development, vessels from the inner plexus dive down towards the outer edge of the INL and anastomose to form a deep capillary plexus. Finally, a third plexus called the intermediate capillary plexus forms between the inner and deep plexuses along the inner edge of the INL.

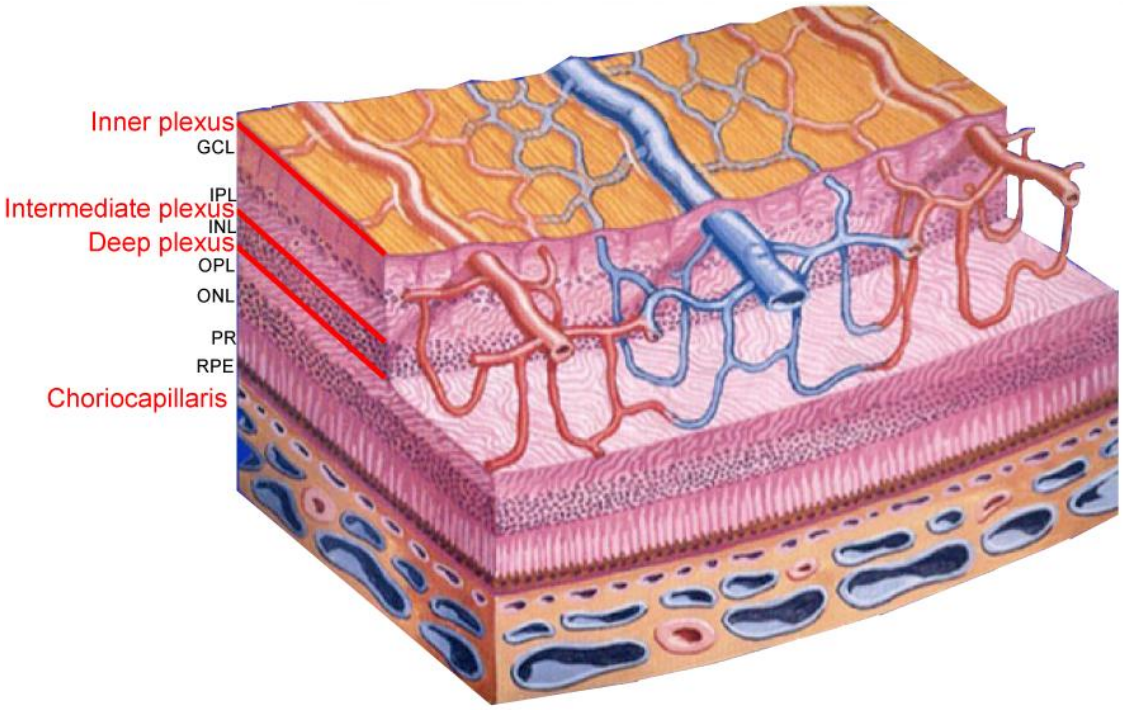

Figure 1.4. Vascular beds in the retina
The retina is perfused by two separate blood supplies (labelled in red). The choriocapillaris is composed of highly fenestrated endothelium and perfuses the outer retina. The inner retina is perfused by the retinal vessels which are composed of three plexuses. The inner plexus develops first and contains arteries, veins and smaller vessels conatined within the ganglion cell layer (GCL). Blood vessels from the inner plexus dive outwards to form two capillary beds, the intermediate and deep plexuses, which form on either side of the inner nuclear layer (INL). IPL; inner plexiform layer; OPL; outer plexiform layer, ONL; outer nuclear layer, PR; photoreceptors, RPE; retinal pigment epithelium. Figure adapted from www.retinadoctor.com.au.

1.3.5. Blood-retinal barrier

The BRB is essential for maintaining homeostasis within the retina. It is comparable to the blood-brain barrier which regulates transport of ions, proteins, fluid and cells to and from the brain. The two blood supplies of the retina means that there is both an inner and outer BRB. The inner BRB refers to the retinal vessels where the vascular endothelial cells are connected by tight junctions restricting diffusion paracellularly. Müller cells, astrocytes and pericytes are also thought to contribute toward the barrier properties of the inner BRB. The outer BRB is maintained by Bruch's membrane and tight junctions between RPE cells, because the endothelial cells of the choriocapillaris are heavily fenestrated and hence permeable.

1.3.6. Immune regulation in the retina

The eye is considered an immune privileged site where several immunoregulatory mechanisms exist to protect vulnerable neural tissue by minimising bystander damage involved with inflammation. Such mechanisms include the BRB, immune deviation to self-antigens and secretion of immunosuppressive cytokines (Streilein, 2003). Breakdown of immune privilege can lead to autoimmune responses, infection and immune-mediated diseases such as uveitis and AMD.

The RPE plays an important role in maintaining immune privilege of the subretinal space but also compensating for it by taking on several immune-related functions (Zamiri *et al.,* 2007). The RPE expresses membrane bound receptors for immune recognition (toll-like receptors (TLR), Fcγ receptors, complement receptors) and antigen presentation (major histocompatibility complexes I & II) (Detrick and Hooks, 2010). RPE cells are able to respond to and secrete a variety of cytokines and chemokines. In a normal state the RPE secretes immunosuppressive cytokines such as transforming growth factor-β, IL-10 and IFNβ. However, RPE cells also secrete several pro-inflammatory cytokines and chemokines for example in response to C5a (Fukuoka *et al.,* 2003), CRP (Wang *et al.,* 2010) or fibronectin (Austin *et al.,* 2009) stimulation. Expression of membrane-bound and soluble cytokine receptors also allows the RPE to adapt its functions to the surrounding cytokine environment. For example, IL-1β (Holtkamp *et al.,* 1998), tumour necrosis factor-α (TNFα) (An *et al.,* 2008), IFNγ (Nagineni *et al.,* 2007) or a combination of IFNγ, TNFα and IL-1β (Li *et al.,* 2007; Kutty *et al.,* 2010; Nagineni *et al.,* 2011) all induce changes in RPE secretion.

1.3.7. Specialisations of the macula

The macula is a specialised central region of the retina in humans and primates. In the centre of the macula there is a roughly 1 mm region called the fovea which has the highest visual acuity and is exclusively populated by cone photoreceptors. Although several structural and morphological differences have been found between the macula and the peripheral retina, the region still remains largely uncharacterised. Unique anatomical features of the macula include the foveal avascular zone (Gariano *et al.,* 2000) and a high density of photoreceptors which is responsible for this region having

the highest metabolic rate in the retina. The RPE cells underlying the macula have been shown to be more pigmented and smaller (Streeten, 1969), and the elastin layer of the Bruch's membrane at this region is six fold thinner in order to aid fast diffusion (Chong *et al.,* 2005). The macula has a yellow appearance which is due to the presence of macula pigments, lutein and zeaxanthin (Bone *et al.,* 1985). The macula is a vulnerable area of the retina since several retinal diseases manifest in this region including macular telangiectasia, progressive cone dystrophy, rod-cone dystrophy, benign concentric macular dystrophy, Stargardt's disease, Batten's disease and AMD.

1.4. Age-related macular degeneration

AMD, as the name suggests, is a disease in which the macula of elderly people progressively degenerates. Originally described as guttate senile choroiditis by Nettleship in 1884, AMD is the leading cause of legal blindness in western countries, and causes 8.7% of blindness worldwide (Resnikoff *et al.,* 2004). Although the macula is a comparatively small area of the whole retina, it accounts for the majority of central vision and therefore any degeneration in this area causes a significant impact on sight.

There are two main subcategories of AMD, atrophic (formerly known as dry) and neovascular (formerly known as wet). Early stages of the disease are characterised by a change in retinal pigmentation and the presence of extracellular lipoproteinaceous deposits, termed drusen, basal to the RPE. Progression of the disease in the majority of patients is atrophic, characterised by detachment and death of the RPE and subsequent atrophy of overlaying photoreceptors. On average, 15% of patients will progress to neovascular AMD where the growth of choroidal vessels into the retina causes haemorrhage and scarring (Ferris, III *et al.,* 1984). However, rare cases of AMD have also exhibited the neovascular form switching to the atrophic form or in other cases, both types progressing at once.

1.4.1. Early clinical symptoms

The earliest clinical signs of AMD are the formation of basal laminar and linear deposits (BlamD, BlinD). BlamD form between the RPE basal plasma membrane and the RPE basal lamina, and consist of membranous debris and collagen. BlinD form within the

inner collagenous layer of the Bruch's membrane, and consist of vesicular material (Curcio and Millican, 1999).

In addition to these deposits, drusen form between the basal lamina of the RPE and the inner collagenous layer of the Bruch's membrane. Drusen are yellowish extracellular deposits visible by fundoscopic eye examination. The presence of drusen is a normal feature of ageing, however a change in number, size, colour, shape, distribution or solid appearance can be an indicator for early signs of AMD. Clinicians categorise these features of drusen to diagnose patients and predict progression of the disease (Pauleikhoff *et al.,* 1990). Drusen are extracellular aggregates whose contents include lipids, carbohydrates, cellular materials and over 140 proteins. A proteomic comparison of drusen from AMD sufferers and age-matched controls showed they shared 65% of the same proteins (Crabb *et al.,* 2002). The composition of drusen is similar to that of extracellular deposits seen in other diseases such as atherosclerosis and amyloidosis, suggesting common processes in their pathogenesis (Mullins *et al.,* 2000).

The origins of drusen are not fully characterised, although they are thought to be a combination of RPE debris, including phagocytosed material from the photoreceptors, extruded basally (Anderson *et al.,* 2001; Malek *et al.,* 2003), and plasma proteins from the choroid diffusing across Bruch's membrane. The driving force for their formation is also not fully understood, although a commonly held view is that complement activation and inflammation are key processes in drusen biogenesis. This is supported by the significant presence of complement and inflammatory proteins found in drusen (Mullins *et al.,* 2000; Hageman *et al.,* 2001; Johnson *et al.,* 2001).

Enhanced lipofuscin in the RPE is another early sign of AMD (Marmorstein *et al.,* 2002). Lipofuscin is an autofluorescent mix of coloured lipid-soluble pigments. Like drusen, the presence of lipofuscin is also a normal feature of ageing (Wing *et al.,* 1978) and its biogenesis is not fully understood. Disruption to the visual cycle can lead to a build-up of toxic bis-retinoids such as N-retinylidene-N-retinyl-ethanolamine (A2E) and photo-oxidation of these molecules contributes to lipofuscin generation. Lipofuscin is not

easily digested or catabolised by RPE cells, and as it accumulates it becomes vulnerable to peroxidation generating damaging reactive oxygen species. Like drusen, it is not clear whether lipofuscin formation is a primary cause of AMD, a risk factor or an early secondary effect.

1.4.2. Late stage disease

Progression of atrophic AMD is characterised by the loss of RPE cells which leads to degeneration of the overlying photoreceptors. Cell death can extend into the outer retinal layers resulting in dramatic thinning of the retina in the macula. As compensation for the loss of RPE, surrounding RPE proliferate and become hyperpigmented.

Neovascular AMD is the main cause of sudden irreversible vision loss. Blood vessels from the choroid penetrate Bruch's membrane and can advance into the photoreceptor layers where they may anastomose with retinal blood vessels. These blood vessels are often leaky causing haemorrhage and detachment of the RPE. Formation of disciform scars in the RPE and neural layers of the macula causes permanent irreversible damage and is the main cause of vision loss in AMD. Several constituents of drusen, C3a, C5a (Rohrer *et al.,* 2009), carboxyethyl pyrrole (CEP) adducts (Ebrahem *et al.,* 2006) and bis-retinoids (Iriyama *et al.,* 2009), have been shown to stimulate neovascularisation of the choroid.

1.4.3. Pathogenesis

AMD is a multifactorial disease whose pathogenesis is determined by many genetic and environmental factors, which makes this disease interesting to study but difficult to resolve. The use of large population based studies have helped to characterise prevalence of the disease in different populations and investigate candidate risk factors. The major studies have been undertaken in America (The Beaver Dam eye study) (Klein *et al.,* 1992), The Netherlands (The Rotterdam study) (Vingerling *et al.,* 1995)) and Australia (The Blue Mountain eye study) (Mitchell *et al.,* 1995). All studies show an age-specific frequency for AMD amongst the population.

1.4.3.1. Environmental risks to AMD

Several environmental factors have been shown to be associated with AMD. These include sunlight exposure (Taylor *et al.,* 1990), alcohol consumption (Chong *et al.,* 2008), hyerptension and cardiovascular disease (Hogg *et al.,* 2008), smoking (Klein *et al.,* 2008), and body mass index (Seddon *et al.,* 2003). Of these, smoking has had the most consistent results, and is now well established as a risk factor for AMD. Smoking can link into two main theories of AMD, inflammation and oxidative stress. Smoking impairs the generation of antioxidants, possibly by stimulating inflammation. Smoking has also been shown to decrease plasma levels of CFH (Esparza-Gordillo *et al.,* 2004), luteal pigment in the retina (Hammond, Jr. *et al.,* 1996), reduce choroidal blood flow (Bettman *et al.,* 1958), reduce drug detoxification by the RPE, activate the immune system, and potentiate nicotine angiogenic activities (Pryor *et al.,* 1983; Beatty *et al.,* 2000; Suner *et al.,* 2004). In contrast, eating fish and omega-3 fatty acids were found to be protective against AMD (Seddon *et al.,* 2006).

1.4.3.2. Genetic predisposition to AMD

Since the 1960s, clinicians have reported the high frequency of family members of an AMD patient who also develop the disease (Braley, 1966) pointing to the role of genetics in the aetiology of AMD. Familial aggregation studies such as the Rotterdam study showed that a quarter of late stage AMD cases were genetically determined (Klaver *et al.,* 1998). A large scale study on monozygotic and dizygotic twins showed that genetics determined 46% of overall disease susceptibility, which increased to 67% for intermediate and 71% for late-stage disease. Therefore the likelihood of progressing to late stage disease is more dependent on genetic rather than environmental influence (Seddon *et al.,* 2005a).

The first gene found to be associated with AMD was adenosine triphosphate-binding cassette, subfamily A, member 4 (*ABCA4*). This gene was chosen as a candidate gene for a gene association study because of its association with a juvenile form of AMD, Stargardt disease. Here they observed that mutations in the *ABCA4* gene associated with 4% of AMD patients tested. Although the same group went on to replicate their results in a larger cohort, indeed showing a larger effect of the gene (Allikmets, 2000),

no other groups have been able to replicate their findings. Many studies since 1997 have identified the association of other candidate genes with AMD (Haddad *et al.,* 2006; Katta *et al.,* 2009), and genome wide linkage studies have identified regions of the genome which segregate with known AMD susceptibility markers at a higher frequency in cases than in controls (Deangelis *et al.,* 2011). Two chromosomal regions with the most consistent logarithm of odds score are 1q23.3-31.1 and 10q26.

A new era of studying complex genetic diseases began when the first (as regarded by the National Human Genome Research Institute) genome wide association study, was published in 2005. This study examined over 100,000 SNPs throughout the human genome with the aim of identifying common risk alleles for AMD (Klein *et al.,* 2005). Using 96 cases and 50 controls, this study identified a SNP in *CFH* to have a large effect size, where being heterozygous increased risk 4.6 fold and homozygous 7.4 fold. *CFH* is located on chromosome 1q within a region highly associated with AMD susceptibility. This SNP, rs1061170, replaces a thymine with a cytosine at position 1277 in exon 9 which leads to a histidine (H) to tyrosine (Y) mutation at position 402 (Y402H), in SCR 7 of the protein. The association of the Y402H mutation with AMD was a landmark discovery with three other separate studies reported in the same year corroborating the finding (Edwards *et al.,* 2005; Hageman *et al.,* 2005; Haines *et al.,* 2005).

Other SNPs in *CFH* have also been shown to associate with AMD, several of which have been suggested to have a larger effect than Y402H. A further study showed four common haplotypes surrounding *CFH*, two of which offer protection and two which confer risk to AMD (Li *et al.,* 2006).

After *CFH*, age-related maculopathy susceptibility protein 2 (*ARMS2*) is the gene with the second largest odds ratio (Rivera *et al.,* 2005), and like *CFH* it lies within a region highly associated to AMD susceptibility, 10q26. The cellular function of ARMS2 is still unknown, and the localisation of the protein is disputed between the mitochondria (Kanda *et al.,* 2007) and cytosol (Wang *et al.,* 2009b), and other studies have reported ARMS2 to be secreted component of the extracellular matrix (Kortvely *et al.,* 2010). Results from genome-wide scans also implicated a gene next to ARMS2 on 10q26,

high-temperature requirement A 1, (*HTRA1*). HTRA1 is a serine protease which in the retina has been shown to act on fibromodulin, clusterin, disintegrin, metalloproteinase domain-containing protein 9 and vitronectin (An *et al.,* 2010) and its overexpression in mice showed altered elastogenesis of Bruch's membrane (Vierkotten *et al.,* 2011). Several SNPs in this gene have now been shown to associate with AMD risk but a SNP in the promoter region has been the most consistent. This SNP has been shown to enhance mRNA expression in RPE (An *et al.,* 2010).

To date, over 50 genes have been implicated in the pathogenesis of AMD, confirming its complex-genetic disease definition. The majority of these have only been identified in one or two studies, with a similar number of studies unable to confirm the original findings (Lotery and Trump, 2007; Katta *et al.,* 2009), and the majority conveying only small effects. Since clinical symptoms and progression vary vastly between AMD patients, therefore it may be that different haplotypes are responsible for different categories of the disease. However, allelic variations in four of the genes, *CFH*, *ARMS2*, *C2* and *CFB* account for more than half of the genetic risk (Maller *et al.,* 2006), highlighting the significance of the complement system to AMD.

1.4.4. Disease mechanisms in AMD

By definition, age has the largest influence on AMD susceptibility. In the United States of America, prevalence in the 5th decade of life is 2.1% however this increases to over 35% in the 9th decade (Friedman *et al.,* 2004). Ageing of the retina is associated with several well-characterised structural and functional changes which are thought to predispose the retina to AMD. The additive effect of environmental and genetic risk factors to ageing tips the balance from homeostasis to pathology. There are four main mechanisms which become dysregulated with normal ageing, and the following sections describe how normal ageing affects these cellular functions and how they predispose the retina to AMD.

1.4.4.1. Oxidative stress

The retina is one of the most vulnerable tissues to oxidative damage in the body. It has the highest consumption of oxygen, an almost constant exposure to light and contains an unusually high lipid content rich in unsaturated fatty-acids. Oxidation of lipids generates highly reactive molecules that can cause free-radical chain reactions, and lipid peroxidation products which modify proteins. These lipid peroxidation products have been shown to affect lysosomal degradation, and influence exocytosis of un-degraded proteins from the basal side of the RPE (Krohne *et al.,* 2010). This material extruded basally from the RPE contributes towards the formation of drusen. Although the retina is well equipped with antioxidant enzymes (Cai *et al.,* 2000) normal ageing in the RPE is associated with a decrease in these enzymes and also melanin (Bonilha, 2008). Melanin content reduces with age because there is an increased tendency for melanosomes to fuse with both lysosomes (melanolysosomes) and lipofuscin (melanolipofuscin), diminishing the anti-oxidative capacity of melanin (Sarna *et al.,* 2003). Additionally, lipofuscin which is known to increase with age, is particularly toxic when oxidised (Wassell *et al.,* 1999).

The study of ageing has largely focused on the accumulative effects of oxidative stress on macromolecules and the accumulation of nuclear and mitochondrial mutations (Van *et al.,* 2003; Kregel and Zhang, 2007; Romano *et al.,* 2010). The consequences of oxidative stress cause dysregulation of numerous RPE functions (Cai *et al.,* 2000; Jarrett *et al.,* 2008), including the ability of RPE cells to regulate complement deposition on the cell surface (Thurman *et al.,* 2009).

There are several reports which directly or indirectly highlight the role of oxidative stress in AMD. For example, AMD patients who supplement their diet with anti-oxidants slow the progression of disease (Age-related Eye Disease Study, 2001), and proteomic analysis showed that drusen from AMD patients contain more oxidised lipids and protein adducts resulting from oxidative damage than those from age-matched controls (Crabb *et al.,* 2002). The most common adduction of proteins found in AMD eyes is CEP, which is an oxidative fragment of docosahexaenoic acid (the most abundant long chain polyunsaturated fatty acid in the retina) (Gu *et al.,* 2003). Indeed,

mice injected with albumin conjugated with CEP develop AMD-like symptoms (Hollyfield *et al.,* 2008; Hollyfield *et al.,* 2010). Furthermore, mice lacking anti-oxidants develop a geographic atrophy-like phenotype (Imamura *et al.,* 2006).

Both environmental and genetic risk factors, which either increase oxidative stress or decrease the capacity of the retina to cope with oxidative stress, increase AMD susceptibility. Smoking, the most consistent environmental risk factor for AMD is known to reduce antioxidant levels, and cause mitochondrial DNA damage (Wang *et al.,* 2009a), and several SNPs in anti-oxidant enzymes increase the risk of AMD.

1.4.4.2. Lipid metabolism

Photoreceptors contain an unusually high lipid content, making up 15% of the total wet weight compared to 1% in other cells (Wright *et al.,* 2010). The phagocytosis of shed photoreceptor OS therefore involves coping with a significant level of lipid metabolism. Internalised OS are contained within phagosomes which fuse with lysosomes for degradation and recycling (Kevany and Palczewski, 2010). Normal ageing has been shown to decrease lysosomal efficiency which leads to an accumulation of un-degradable lipid that in turn enhances the risk of lipid peroxidation (discussed above) and the formation of lipofuscin within the RPE (Wing *et al.,* 1978; Rajawat *et al.,* 2009). Lipofuscin causes dysfunction of several RPE cell activities including interference with melanin (Wang *et al.,* 2006), clogging of the cytoplasm (Yasukawa *et al.,* 2007), inhibition of mitochondrial function (Vives-Bauza *et al.,* 2008) and is vulnerable to photo-oxidation (Schutt *et al.,* 2000).

Several genetic risk factors have linked dysregulation of lipid metabolism with AMD susceptibility. Mutations in genes involved in lipid metabolism associated with AMD susceptibility are summarised in Table 1.2.

Gene Name	Gene Symbol	Gene Location	Function	Variation	Role
Adenosine triphosphate-binding cassette transporter, subfamily A, member 4	ABCA4	1p22.1	Involved in the visual cycle	G1961E, D2177N	Harmful
Apolipoprotein E	APOE	19q13.32	Mediates binding, internalisation and metabolism of lipoproteins	E4 allele	Protective
Elongation of very long chain fatty acids	ELOV4	6q14.1	Biosynthesis of fatty acids	M229V	Harmful
Paraoxonase 1	PON1	7q21.3	Hydrolyses lipid peroxides	M55L, Q192R	Harmful
Hepatic lipase	LIPC	15q21.3	Metabolisn of triglycerides and high-density lipoprotein cholesterol	rs10468017 in promoter region	Harmful

Table 1.2. Mutations in proteins involved in lipid transport or metabolism which are associated with age-related macular degeneration susceptibility

1.4.4.3. Immune regulation

Dysregulation of the immune system is accepted to be a key feature in AMD progression. Normal ageing of the retina is associated with immunological activation which can induce a low-grade inflammation named para-inflammation (Chen *et al.,* 2008; Xu *et al.,* 2009; Chen *et al.,* 2010). Features of para-inflammation include the activation of complement, activation of microglia in the neuroretina and accumulation of microglia in the outer retina. In AMD, immunological activation of the retina is uncontrolled and several features of the disease suggest that immune dysregulation may be a primary cause for disease onset. Initially the composition of drusen was the main point of evidence. However systemic characterisation of AMD patients has shown that CRP, IL-6, factor D and complement activation products are all elevated (Seddon *et al.,* 2005b; Scholl *et al.,* 2008), and patients with choroidal neovascularisation showed higher proportions of activated circulating monocytes (Cousins *et al.,* 2004). Both CRP and amyloid P, known activators of the classical complement pathway, are also elevated in the choroid of AMD patients (Seddon *et al.,* 2004; Johnson *et al.,* 2006). A mouse model for AMD corroborated the role of the immune system in the pathogenesis of AMD where monocyte chemotactic protein-1 (MCP1) and MCP1 receptor null mice develop an AMD-like phenotype (Ambati *et al.,* 2003).

SNPs in proteins involved in the immune system (Table 1.3), and in particular the complement system (Table 1.4), confirm the role of the immune system in AMD susceptibility.

Gene Name	Gene Symbol	Gene Location	Function	Variation	Role
Chemokine (C-X3-C motif) receptor 1	CX3CR1	3p22.2	Chemokine receptor	V249I, T280M	Harmful
Toll-like receptor 3	TLR3	4q35.1	Binds dsRNA & associated with viral infection	L412F	Protective
Toll-like receptor 4	TLR4	9q33.1	Involved in recognition of lipopolysaccharide	D299G	Harmful

Table 1.3. Mutations in immunological proteins associated with age-related macular degeneration susceptibility

Gene Name	Gene Symbol	Gene Location	Function	Variation	Role
Complement component 2	C2	6p21.33	Component of the classical and lectin complement pathways	E318D	Protective
Complement component 3	C3	19p13.3	Central component of the complement pathway	S80F/G, R102G	Harmful
Complement factor B	CFB	6p21.33	Component of the alternative complement pathway	L9H, R32Q, R32W	Protective
Complement factor H	CFH	1q31.3	Regulates the alternative complement pathway	Y402H, I62V	Harmful
Complement factor H-related 1 & 3	CFHR1&3	1q31.3	CFHR1 regulates the terminal complement pathway, CFHR3 function unknown	Deletion	Protective
Complement factor H-related 5	CFHR5	1q31.3	Possible alternative complement pathway regulation	D169D	Protective
Complement Factor I	CFI	4q25	Regulates the alternative complement pathway	non coding region	Harmful

Table 1.4. Mutations in complement proteins associated with age-related macular degeneration susceptibility

1.4.4.4. Bruch's membrane structure and turnover

Normal ageing of Bruch's membrane causes it to become thicker, stiffer, have an altered chemical composition and accumulate cell debris (Okubo *et al.,* 1999; Ugarte *et al.,* 2006). With normal ageing, Bruch's membrane alterations compromise diffusion of nutrients from the choroid to the retina. Patients with AMD are less able to cope with the normal effects of ageing in the retina since the combination of inflammation,

oxidative stress and altered lipid metabolism further compromises Bruch's membrane. Bruch's membrane in AMD eyes contains modifications such as an increase in lipid content and proteins modified by advanced glycation end-products (AGE). These AGE modifications have been shown to enhance protein cross-linking, be detrimental to cellular function, and are hypothesised to contribute towards the formation of drusen (Baynes, 2001; Glenn *et al.,* 2009).

Bruch's membrane composition in AMD patients has also been shown to lose its ability to bind CFH (Kelly *et al.,* 2010). Bruch's membrane heavily relies upon CFH since it does not express surface bound complement regulators. Loss of the ability to bind CFH makes this site more vulnerable to uncontrolled complement activation. Decreased binding may be due to a SNP in CFH or composition of Bruch's membrane. Expression of tissue inhibitor of matrix metalloproteinase 3 (TIMP3) expression is enhanced in the Bruch's membrane of AMD patients (Kamei and Hollyfield, 1999). *TIMP3*, known to be associated with a juvenile form of macular degeneration, also contains a SNP associated with AMD, highlighting its role in the disease. SNPs in proteins of the extracellular matrix or enzymes involved in their turnover that are found to be associated with AMD susceptibility are summarised in Table 1.5.

Gene Name	Gene Symbol	Gene Location	Function	Variation	Role
Tissue inhibitor of metalloproteinase 3	TIMP3	22q12.3	Inactivates metalloproteinases	SNP rs9621532, two intronic	Harmful
Hemicentin 1	HMCN1	1q25.34	Maintenance of ECM integrity	Q5345R	Harmful
Fibulin 5	FBLN5	14q32.12	Involved in polymerisation of elastin	V60L, R71Q, P87S, I169T,	Harmful
Matrix metalloproteinase 9	MMP9	20q13.2	Degradation of ECM	Microsatellite repeat in promoter region	Harmful
HtrA serine peptidase 1	HTRA1	10q26.13	Degradation of ECM	SNP in promoter region	Harmful

Table 1.5. Mutations in extracellular matrix (ECM) proteins or enzymes involved in their turnover associated with age-related macular degeneration susceptibility

1.4.4.5. RPE dysfunction

One of the main effects of ageing is the dysfunction of the RPE. Without a fully functioning RPE, the neuroretina cannot be supported, causing it to thin with age. Drusen are an early sign of RPE dysfunction. Environmental and genetic factors predispose people to AMD because they hinder the ability of the retina to cope with the normal ageing process. Because the RPE serves many homeostatic functions, death or dysfunction of these cells has a dramatic effect on phenotype, and could at least partly explain why AMD is so variable amongst sufferers.

1.4.5. AMD therapies

Only in the past two decades have therapies for AMD become available for patients, however these are limited to the neovascular form of AMD. Although neovascular AMD represents only 15% of AMD patients, it accounts for the majority of visual loss associated with this disease.

Thermal laser therapy, one of the first treatments for neovascular AMD, uses lasers to photocoagulate the CNV membranes disrupting new vessel growth. The disadvantage of this therapy was that it also caused destruction of overlying healthy tissue (Kallitsis *et al.,* 2007). This treatment was improved when Novartis developed Visudyne®, a photosensitiser which can be injected intravenously and is subsequently activated by a laser in the region of the neovascularisation. This photodynamic therapy (PDT) generates the release of damaging free radicals in a localised area and destroys the CNV membranes without damaging the overlying retina.

Currently, new biological reagents have been developed for the treatment of neovascular AMD which achieve better outcomes than PDT (Ciulla and Rosenfeld, 2009). These therapies target vascular endothelial growth factor (VEGF) which is a potent inducer of CNV. The first anti-VEGF treatment was pegaptanib sodium (Macugen®, Pfizer) which is a pegylated aptamer that targets only the $VEGF_{A165}$ isoform. This has been superseded by the generation of a monoclonal antibody fragment, ranibizumab (Lucentis®, Novartis) which recognises all $VEGF_A$ isoforms. Although patient outcomes have been very effective in a proportion of patients

treated (Horster *et al.,* 2011), it does not work for everyone and the treatment is expensive. In some instances to save costs, AMD patients are treated with a cheaper alternative, bevacizumab (Avastin®, Roche) which is a full-length humanised monoclonal antibody to $VEGF_A$. In fact, bevacizumab was the predecessor to ranibizumab and both were developed by Genentech. Bevacizumab is licensed for treatment of colorectal carcinoma, although it has been prescribed 'off-label' to AMD patients. Another anti-VEGF treatment currently under clinical trials, is VEGF Trap-Eye which has a higher affinity for VEGF than monoclonal antibodies (Heier *et al.,* 2011). VEGF Trap-Eye consists of the extracellular portions of VEGF receptors 1 and 2 fused to the fragment crystallisable region of human IgG.

The expense of new biological treatments may be mitigated by the development of pharmacogenetics which could, in the future, impact how AMD patients are treated. With increasing knowledge of genetic risk alleles, more studies are being carried out to assess the success of AMD treatments in relation to individual genotype (Nischler *et al.,* 2011; Wickremasinghe *et al.,* 2011). In the future it may be possible to genotype patients prior to choosing personalised treatment options.

Patients with atrophic AMD have considerably fewer treatment options available to them. At present, treatment strategies involve dietary supplementation with anti-oxidants and zinc (Olson *et al.,* 2011), a recommendation to stop smoking and regular check-ups to monitor progression to the neovascular form. Since 85% of patients have atrophic AMD, there is a substantial unmet clinical need for licensed treatments. With fast progress in unravelling AMD pathogenesis, many targets for potential atrophic AMD treatments have been identified and are under current clinical trial (reviewed by Yehoshua *et al.,* 2011) such as anti-inflammatories, anti-oxidants, complement inhibitors, immunosuppressant agents, TLR inhibitors, stem cell therapies (Du *et al.,* 2011) and PEDF gene therapy (Rasmussen *et al.,* 2001).

1.5. Thesis aims

The molecular mechanisms by which SNPs in CFH are associated with AMD susceptibility have not been clearly defined. In part, this is due to a lack of understanding of the role of CFH within the retina. A report which characterised aged *Cfh*$^{-/-}$ mice demonstrated an important requirement for CFH in maintaining a healthy retina (Coffey *et al.,* 2007). Through studying the secretion of CFH from RPE cells and further characterisation of the *Cfh*$^{-/-}$ mouse, this thesis aims to investigate the role of CFH in the retina, in order to clarify its significance in AMD pathogenesis.

Chapter 2: Materials and Methods

All reagents were purchased from Sigma Aldrich unless specified otherwise. Catalogue numbers are indicated in brackets after company name.

2.1. *In vitro* techniques

2.1.1. Cell culture

ARPE19, a spontaneously arising immortalised human RPE cell line, was used between passages 20-30. ARPE19 and primary porcine RPE were maintained in either high glucose Dulbecco's modified Eagle's medium (DMEM, Invitrogen, 41965-039) containing 292 μg/ml L-glutamine or X-VIVO™ 15 (Lonza, BE04-418F). Media were supplemented with 100 IU/ml penicillin and 100 μg/ml streptomycin (PAA Laboratories Ltd, P11-010). DMEM was additionally supplemented with 10% or 1% heat-inactivated foetal calf serum (FCS-Invitrogen, 10108-165). ARPE19 cells were passaged with 0.05% trypsin - 0.53 mM ethylenediaminetetraacetic acid (EDTA) (Invitrogen, 15400-054) in Dulbecco's phosphate buffered saline (PBS-Invitrogen, 14200067). Cells were grown in a 37°C humidified incubator with 5% CO_2.

2.1.2. Primary porcine RPE isolation

Sow's eyes were obtained from Cheale Meats Ltd and delivered on ice on the morning of slaughter. Once external tissue was removed, eyes were soaked in a 2.5% povidone-iodine solution (Videne-Williams Medical Supplies, D748980) for 10 min and washed in an antibiotic solution containing 1000 IU/ml penicillin and 1 mg/ml streptomycin for 5 min. In a sterile hood, the anterior halves were dissected with a scalpel and discarded along with the lens and vitreous humour. The posterior eyecups were filled with PBS. The neuroretinas were carefully peeled away from the underlying RPE, disconnected at the optic nerve head and discarded along with the PBS. 2 ml of 10X trypsin in PBS (0.5% Trypsin - 5.3 mM EDTA, Invitrogen, 15400-054) was added to eyecups and incubated for 30 min at 37°C. Trypsinised RPE were harvested by gentle agitation and washed in DMEM containing 10% FCS for 5 min at 800 revolutions per minute (rpm) at room temperature (RT) using an Eppendorf 5810 R centrifuge. RPE cells were pooled and plated at approximately one eye/9.6cm^2.

2.1.3. Secretion assay

RPE cells were grown to confluency in a 6-well plate (Nunc) prior to use in secretion assays. Cells were washed twice in PBS to remove traces of FCS from the culture medium. 1.2 ml of serum-free DMEM or X-VIVO™ 15 containing 100 IU/ml penicillin and 100 μg/ml streptomycin was added per well. For the zero time point, media was added and immediately removed from one well. Plates were then placed into an incubator wrapped in wet tissue paper to prevent evaporation. In each 6-well plate four of the remaining wells were treated in an 'accumulative' fashion whereby spent media were collected from one well at 2 h, the second at 4 h, the third at 6 h and the last at 8 h (or in an extended time course 8, 24, 48 and 72 h). One well was treated in a 'serial' fashion whereby spent media was collected and replaced with fresh serum-free media each time the accumulative samples were collected. After collection of spent media at various time points, cells were washed with PBS and lysed in boiling 2X sodium dodecyl sulphate-polyacrylamide gel electrophoresis (SDS-PAGE) sample buffer (0.125 M Tris-HCl-pH 6.8, 25% glycerol, 5.4% dithiothreitol, 2% SDS, 0.02% bromophenol blue). Prior to precipitation, cell debris in spent media was pelleted for 3 min at 13,000 rpm in a table top centrifuge at RT. The supernatant was transferred into a fresh Eppendorf tube and where described, 100 μl of 10 μg/ml goat IgG (dissolved in DMEM) was added per sample.

2.1.3.1. Cytokine stimulation

For cytokine stimulation, IL-1β, IFNγ and TNFα (R&D Systems, 201-LB, 285-IF, 210-TA) were diluted in 1.2 ml DMEM containing 100 IU/ml penicillin and 100 μg/ml streptomycin. A range of concentrations (0-200 ng/ml) was tested and spent media collected after 8 h. Further experiments applied 100 ng/ml IFNγ, with spent media collected in both an accumulative and serial fashion over 8 h.

2.1.3.2. Cycloheximide treatment

Cycloheximide was dissolved in dimethyl sulphoxide (DMSO) and diluted to 10 μM in DMEM containing 100 IU/ml penicillin and 100 μg/ml streptomycin. 1.2 ml of DMEM containing or DMSO (vehicle control) was applied to ARPE19 cells in an 8 h secretion assay as described in Section 2.1.3.

2.2. Protein isolation and analysis techniques

2.2.1. Trichloroacetic acid precipitation

One volume of trichloroacetic acid (TCA) was added to four volumes of spent media, mixed, and incubated for a minimum of 30 min at 4°C. Precipitated proteins were pelleted in a table top centrifuge at 13,000 rpm for 10 min at 4°C. The supernatant was discarded and the pellet washed twice in 200 µl ice-cold acetone. The pellet was dried at 95°C for 10 min and re-solubilised in 20 µl 2X SDS-PAGE sample buffer (described in Section 2.1.3).

2.2.2. Acetone precipitation

One volume of ice cold acetone was added to 1.4 volumes of spent media, mixed, and incubated for 5 min at RT. Precipitated proteins were pelleted in a table top centrifuge at 13,000 rpm for 3 min at RT. The pellet was dried at 95°C for 10 min and re-solubilised in 20 µl 2X SDS-PAGE sample buffer (described in Section 2.1.3).

2.2.3. Ammonium sulphate cut

Saturated ammonium sulphate was added to spent media to give a final concentration of either 5% or 29%. Samples were mixed and rotated for 45 min at RT. Precipitated proteins were pelleted in a table top centrifuge at 13,000 rpm for 15 min at RT. Supernatants were transferred to a fresh tube and the pellet re-solubilised in 20 µl 2X SDS-PAGE sample buffer (described in Section 2.1.3). Further volumes of saturated ammonium sulphate were added to recovered supernatant to increase the final concentration of ammonium sulphate, and the following steps repeated (from 5% to 14, 25, 32, 41 and 50% ammonium sulphate, or from 29% to 55, 62, 67 and 71% ammonium sulphate).

2.2.4. Heparin-agarose pull-down

Heparin-agarose type I was washed twice in PBS, and pelleted in a table top centrifuge at 13,000 rpm for 1 min at RT. One volume of heparin-agarose was added to two volumes of spent media and rotated for 3.5 h at RT. The heparin-agarose was again pelleted and the supernatant precipitated with TCA (as described in Section 2.2.1). Heparin-agarose was washed six times in PBS. Finally, 150 µl of 2X SDS-PAGE sample

buffer (described in Section 2.1.3) was added to the pellets and incubated for 5 min at 95°C to solubilise proteins. Tubes were centrifuged and samples were analysed by SDS-PAGE and western blotting.

2.2.5. Polyacrylamide gel electrophoresis

Resolving gels for SDS-PAGE were 0.375 M Tris-HCl (pH 8.8) and 8% acrylamide/Bis-acrylamide for CFH analysis, and 10% in all other analyses. Stacking gels were 0.125 M Tris-HCl (pH 6.8) and 4% acrylamide/Bis-acrylamide. Gels contained 0.1% SDS and were polymerised with 0.05% ammonium persulphate and 0.1% tetramethylethylenediamine. Samples from Sections 2.2.1-4 were denatured for 5 min at 95°C prior to loading alongside a suitable molecular weight ladder (Bio-Rad, 161-0374). Gels were run in electrophoresis grade SDS-running buffer (0.025 M Tris, 0.192 M glycine, 0.1% SDS, National Diagnostics, EC-870) at 80 mV until proteins were stacked along the resolving/stacking interface upon which the voltage was increased to 150 mV.

Proteins were transferred from gels onto PVDF membrane (GE Healthcare, RPN303F) via wet transfer. For this, the membrane was activated in methanol for 5 min at RT and rinsed in transfer buffer (10% methanol, 0.025 M Tris, 0.192 M glycine, National Diagnostics, EC-880). The gel and membrane were sandwiched between filter papers and sponges soaked in transfer buffer. Transfer sandwiches were immersed in a tank of transfer buffer and run at 400 mA for 30 min per gel on ice.

2.2.6. Western blotting

All incubation steps were carried out on an orbital shaker. Membranes were blocked in blocking buffer (PBS-7% skimmed milk) for 1 h at RT. Primary antibodies were diluted (according to Table 2.1) in blocking buffer and applied to membranes overnight at 4°C. Membranes were washed six times for 5 min in washing buffer (PBS - 0.05% Tween). Horseradish peroxidise conjugated secondary antibodies were diluted in PBS - 3.5% milk, 0.025% Tween (according to Table 2.1) and applied to membranes for 1 h at RT. Membranes were again washed six times for 5 min in washing buffer. Membranes were developed using an enhanced chemiluminescence detection system (GE

Healthcare, RPN2109), for 3 min at RT and immediately developed using a Konica Minolta SRX-101A X-ray developer and X-ray film (Fuji photofilm, MRX 1824).

Antibody target	Antibody Clone/Type	Antibody Species	Immunogen Species	Conjugated	Antibody Concentration	Dilution	Source	Catalogue Number
α-Tubulin	Z022, IgG_1, mAb	Mouse	Chicken	-	0.6 mg/ml	1:1000	Invitrogen	18-0092
Cathepsin E	IgG, pAb	Goat	Mouse	-	0.1mg/ml	1:500	R&D Systems	AF1130
CFH	IgG, pAb	Goat	Human	-	Undiluted serum	1:1000	Calbiochem	AF1130
RPE-65	IgG, mAb	Mouse	Bovine	-	1 mg/ml	1:2500	Chemicon	MAB5428MI
Mouse IgG, IgA & IgM	IgG, pAb	Goat	Mouse	Horseradish peroxidase	1 mg/ml	1:2000	Dako Cytomation	P0447
Goat Ig, all subclasses	IgG, pAb	Rabbit	Goat	Horseradish peroxidase	0.5 mg /ml	1:2000	Dako Cytomation	P0449

Table 2.1. Primary and secondary antibodies used in western blotting
Ig, immunoglobublin; pAb, polyclonal antibody; mAb, monoclonal antibody

2.3. *In Vivo* techniques

2.3.1. Animals

Cfh$^{-/-}$ mice were a generous gift from Prof. Matthew Pickering (Imperial College). Mice were generated through disruption of *Cfh* exon 3 using a gene targeting vector in embryonic stem cells. *Cfh*$^{-/-}$ mice have a 129/Sv x C57Bl/6 hybrid background (Pickering *et al.,* 2002). Ex-breeding C57Bl/6 control mice of 6-9 months were purchased from Harlan Laboratories. Young C57Bl/6 mice were bred in house. Mice were housed in the Biological Resources Unit at the Institute of Ophthalmology; a UK Home Office approved animal facility. *Cfh*$^{-/-}$ breeding pairs were housed in isolated ventilated cages and all breeding pairs were fed a diet of Teklad global 19% protein extruded rodent diet (Harlan Laboratories, 2019). All other mice were housed on the open shelf and fed a diet of Teklad global 18% protein extruded rodent diet (Harlan Laboratories, 2018). All mice were exposed to 12 h light and 12 h dark cycles.

Mice used for RNA isolation underwent cervical dislocation. Perfused mice were first anaesthetised prior to perfusion with fixative. All other mice were killed with a rising CO_2 concentration with subsequent cervical dislocation. After death, mice were immediately enucleated using curved forceps.

Mice were used at either 7-8 weeks or 1 year ± 11 days for all analyses except for microarray analysis where mice were 7-8 weeks and 1 year 140 days ± 6 days. Mice

were killed at various times throughout the day except for ultrastructural analysis (see Section 2.4).

2.3.2. Electroretinograms and visual evoked potentials

Electroretinogram (ERG) and visual evoked potential (VEP) recordings were performed on 1 year 14 day ± 11 days mice in conjunction with Dr. E. Rebecca Longbottom of the cell biology department at The Institute of Ophthalmology.

2.3.2.1. Animal preparation

Mice were dark-adapted overnight and prepared for recordings under dim red illumination. Mice were anaesthetised by intraperitoneal injection with ketamix, 2 μl/g body weight (37.5% ketamine, 25% Dormitor, Fort Dodge Animal Health Ltd) and 10 μl atropine sulphate (600 μg/ml, Hameln Pharmaceuticals) to aid breathing. The right eye was patched over to exclude light, and to the left eye, 2.5% phenylephrine hydrochloride and 1% tropicamide eye drops (Minims-Bausch & Lomb) were administered for dilation of the pupil and a local anaesthetic, 0.5% proxymetacaine hydrochloride (Minims-Bausch & Lomb) was applied. Each mouse was placed in the recording chamber on an electrically heated pad (CWE Inc., TC-100) to maintain a 37°C body temperature and secured to a bite bar before placing platinum electrodes. All needle electrodes were inserted subcutaneously using a 21 gauge (G) needle moistened with Kreb's solution (NaCl 124 mM, KCL 2 mM, KH_2PO_4 1.25 mM, $MgSO_4$ 1 mM, $CaCl_2$ 2 mM, $NaHCO_3$ 26 mM, glucose 10 mM). The VEP recording needle electrode was positioned at the skull in the region of the contralateral visual cortex and the VEP reference needle electrode was positioned at the nose. The ERG reference needle electrode was placed at the temple near the left eye and the ERG recording loop electrode was placed on the left cornea. The earth needle electrode was placed at the back near the tail of the mouse. The light-emitting diode stimulator was positioned over the left eye and the recording chamber sealed.

2.3.2.2. Scotopic and photopic recordings

Stimuli for the scotopic recordings were brief full field flashes of white light from darkness at varying intensity (-5.5 to 1 log cd/s/m^2) by altering both the duration (3 μs-

1 ms) and attenuation (1000-1) of the stimulus. The frequency of the flashes was 0.67 Hz at lower intensities, which was decreased to 0.33 and 0.17 Hz at the intermediate and higher intensities.

For photopic recordings, mice were light adapted in the recording chamber for 20 min with a rod adapting background light (20 cd). Background light was maintained throughout photopic recordings where brief full field flashes of white light were applied at varying intensity (-1.4 to 1 log cd/s/m^2) by altering both the duration (1-3 ms) and attenuation (1000-1) of the stimulus. The frequency of flashes was 0.5 Hz.

2.3.2.3. Data collection and analysis

Electrode recordings from ERG and VEP electrodes were collected at the same time and were sent to an analogue to digital interface. Digital data were sent to the computer and interpreted by Observer software (Breakpoint Pty Ltd). After recordings, mice were sacrificed by cervical dislocation.

ERG and VEP recordings were analysed using Reviewer software (Breakpoint Pty Ltd). For ERG data, amplitude and time to peak of the a-wave were measured from the baseline to the trough. The amplitude of the b-wave was measured from the trough of the a-wave to the peak of the b-wave. Time to peak of the b-wave was measured from baseline to the peak of the b-wave. VEP amplitude were measured from the peak of the positive wave to the trough of the negative wave, and time to peak was measured from baseline to the trough of the negative peak.

2.4. Electron Microscopy

2.4.1. Fixation

For ultrastructural analysis all samples were prepared in the afternoon. For analysis of the RPE, enucleated eyes were immersed in Karnovsky's fixative (3% glutaraldehyde (EM grade-TAAB, G002), 1% paraformaldehyde in 0.07 M sodium cacodylate (Agar Scientific, R1104), pH 7.4) for 2 h at RT. For analysis of retinal vessels, mice were perfused with Karnovsky's fixative. For this, mice were first anaesthetised with a 100 µl intraperitoneal injection of Euthatal (contains 20% w/v sodium pentabarbitone BP,

Merial Animal Health Ltd) and the chest cavity opened. The descending aorta was clamped, an incision was made in the right ventricle and a shunt inserted. Karnovsky's fixative was pumped through the shunt, and into the head of the mouse via the right ventricle. The right aorta was cut open, and approximately 20 ml of fixative was pumped into the right ventricle until the fluid from the right aorta ran clear. Perfused eyes were enucleated and immersed in Karnovsky's fixative for a further 2 h at RT. Eyes were washed with 0.1 M cacodylate and the lens was removed by cutting a small hole into the cornea.

2.4.2. Embedding

Eyes were osmicated in 1% osmium tetroxide (Agar Scientific, R1015) - 0.1 M cacodylate in the dark for 2 h on ice then washed twice with 0.1 M cacodylate. Eyes were dehydrated in successive washes of 70%, 90% and 100% ethanol for 15 min in each wash with two 100% washes followed by two 100% propylene oxide (Agar Scientific, R1080) washes. Eyes were immersed in a 1:1 mixture of propylene oxide and araldite resin (50% dodecenyl succinic anhydride (Agar Scientific, R1051) 40% Araldite CY212 (Agar Scientific, R1040) 1.6% DMP30 (TAAB, D032)) overnight at RT. The following day, eyes were placed in fresh 100% araldite resin in open tubes and the resin replaced after 3-4 h for a further 3-4 h. Eyes were transferred to fresh 100% araldite resin and polymerised by baking overnight at 60°C.

2.4.3. Semithin sections and imaging

Eyes were sectioned and stained by Robin Howes of the electron microscopy department at The Institute of Ophthalmology, UCL. Semithin resin sections of 2 μm were cut on a Leica ultracut S microtome with a diamond knife through the optic nerve. Semithin sections were stained with 1% toluidine blue in 1% borax, 50% ethanol for 30 s, washed in 50% ethanol then dried at 60°C for 10 min. Sections were dried and mounted in DPX resin (Agar Scientific, R1340). Phase contrast images of semithin resin sections were obtained using a 20X objective on an inverted Leica DMIL microscope. Digital images were captured with a Leica DC200 digital camera. Density of nuclei in the ONL was quantified by manual counting.

2.4.4. Ultrathin sections and imaging

Eyes were sectioned and stained by Robin Howes of the electron microscopy department at The Institute of Ophthalmology, UCL. Ultrathin resin sections of 70-80 nm were cut on a Leica ultracut S microtome with a diamond knife through the optic nerve. Sections were stained for 10 min with lead citrate (1.33 g lead nitrate (EM grade, TAAB, L019), 1.76 g trisodium citrate in 8 ml 1 M sodium hydroxide and 42 ml deionised water). Sections were imaged on a Joel 1010 transmission electron microscope at 1500X magnification and digital images were taken using a Gatan Orius SC1000B CCD camera.

2.4.5. Organelle distribution analysis

Organelle distribution was analysed in transmission electron micrographs without a nucleus. Mitochondria were identified by their characteristic internal membraneous stacks, and melanosomes by their uniform electron dense appearance. The distance from the RPE basal lamina to the centre of each organelle was measured using Image J software (Rasband, 2011). Over 200 mitochondria and 300 melanosomes were quantified from two mice in each group.

2.5. Protein analysis

2.5.1. Immunohistochemistry

Sections and flatmounts were imaged using a confocal laser scanning microscope, LSM 710 and ZEN software (Carl Zeiss Inc.).

2.5.1.1. Tissue sections

Upon recovery, eyes were immediately immersed in 4% paraformaldehyde (PFA)-PBS for 10 min at RT. A small hole was made into the cornea to enable removal of the lens and vitreous humour. Eyes were further fixed in 4% PFA-PBS for 2 h at RT or overnight at 4°C. Eyes underwent sucrose infiltration (30% sucrose-PBS) overnight at 4°C. Eyes were embedded in OCT embedding matrix (Raymond A Lamb, LAMB-OCT) and frozen on dry ice then initially stored at -20°C and subsequently at -80°C. 12 μm sections were cut on a cryostat (CM 1850, Leica Microsystems) at -20°C and adhered to superfrost adhesion slides (VWR International, 631-0446). Sections were stored in a sealed box at

-80°C. Prior to staining, slides were thawed to RT in the sealed box, removed and dried for a minimum of 2 h under a fan at RT.

Prior to staining, sections were surrounded with wax (Pap-pen, VWR, 720-0169) to prevent dehydration of sections during long incubation times. Sections were blocked in 500 µl blocking/permeabilising solution (PBS - 5% normal donkey serum, 1% bovine serum albumin (BSA), 0.5% Triton, 0.12% NaN_3) for a minimum of 1 h at RT. Primary antibodies were diluted according to Table 2.2 in blocking/permeabilising solution, 200 µl added per slide and incubated overnight at 4°C. As a primary antibody control, non-specific IgG antibodies which matched the species of the primary antibody were applied to sections in the same fashion as the primary antibody. As a secondary antibody control, sections were also incubated with blocking/permeabilising solution containing no antibody. The following day, slides were washed 3 x 5 min in washing buffer (PBS-0.1% Tween). Fluorophore-conjugated secondary antibodies were diluted according to Table 2.2 in blocking/permeabilising solution, 200 µl added per slide and incubated for 1 h at RT in the dark. As a control, secondary antibodies were applied to sections which had not been stained with primary or non-specific antibody. Slides were washed 3 x 5 min in washing buffer and incubated with 4',6-diamidino-2-phenylindole (DAPI, 1 µg/ml) for 2 min at RT. Slides were washed 2 x 5 min in PBS and mounted with VECTASHIELD® mounting medium (Vector Labs, H-1000) and cover slips.

2.5.1.2. Flatmounts

Eyes were fixed briefly for 5 min in 2% PFA-1.5X PBS before dissection in 2X PBS. External muscle and the optic nerve were trimmed to aid flattening and the eye was cut in half with the incision following posterior to the ora-serrata. The anterior eyecup, lens and vitreous humour were discarded. The neuroretina was carefully peeled away from the RPE using forceps and detached at the optic nerve head. 4-6 incisions 2/3 in towards the centre were made in order to enable flattening. After PBS aspiration, flattened neuroretinas were re-fixed and stored in ice cold methanol at -20°C.

Antibody target	Antibody Clone/Type	Antibody Species	Immunogen Species	Conjugated	Antibody Concentration	Dilution	Source	Catalogue Number
Bassoon	SAP7F407, IgG_{2a}, mAb	Mouse	Rat	-	1 mg/ml	1:500	Stressgen Bioreagents	VAM-PS003
Short Wave Cone Opsin	N-20, IgG, pAb	Goat	Human	-	200 mg/ml	1:500	Santa Cruz Biotechnology	sc14363
C3	IgG, pAb	Goat	Mouse	FITC	4 mg/ml	1:100	MP Biomedicals	55500
C3b/iC3b/C3c	2/11, IgG1, mAb	Rat	Mouse	-	100 mg/ml	1:50	Hycult biotech	HM1065
C5	IgG, pAb	Rabbit	Mouse	-	100 mg/ml	1:10	abcam	ab11898
Collagen IV	IgG, pAb	Rabbit	Mouse	-	-	1:500	AbD seroTec	2150-1470
Crry	5D5, IgG_1, mAb	Rat	Mouse	-	5 mg/ml	1:100	Paul Morgan*	-
DAF	MD1, IgG_1, mAb	Rat	Mouse	-	1.4 mg/ml	1:50	Paul Morgan*	-
GFAP	G-A-5, IgG_1, mAb	Mouse	Pig	Cy3	-	1:500	Sigma Aldrich	C9205
MAC	IgG, pAb	Rabbit	Human	-	5 mg/ml	1:50	Abcam	ab55811
CD59a	7A6, IgG_1, mAb	Mouse	Mouse	-	1mg/ml	1:50	Paul Morgan*	-
CD59a	MEL4, IgG_1, mAb	Rat	Mouse	-	-	1:50	Paul Morgan*	-
Goat IgG	IgG, pAb	Donkey	Goat	AlexaFluor 488	2 mg/ml	1:200	Invitrogen	A-11055
Mouse IgG	IgG, pAb	Donkey	Mouse	AlexaFluor 488	2 mg/ml	1:200	Invitrogen	A-21202
Rat IgG	IgG, pAb	Donkey	Rat	AlexaFluor 488	2 mg/ml	1:200	Invitrogen	A-21208
Rabbit IgG	IgG, pAb	Donkey	Rabbit	AlexaFluor 555	2 mg/ml	1:200	Invitrogen	A-31572
Rat IgG	IgG, pAb	Donkey	Rat	AlexaFluor 555	2 mg/ml	1:200	Invitrogen	A-21434
Mouse IgG	IgG, pAb	Donkey	Mouse	AlexaFluor 647	2 mg/ml	1:200	Invitrogen	A-31571
Rabbit IgG	IgG, pAb	Donkey	Rabbit	AlexaFluor 647	2 mg/ml	1:200	Invitrogen	A-31573

Table 2.2. Primary and secondary antibodies used for immunohistochemistry
Ig, immuoglublin; pAb, polyclonal antibody; mAb, monoclonal antibody; FITC, fluoroscein-5-isothiocyanate; Cy3, cyanine 3. * Kind gifts from Prof. B. Paul Morgan, University of Cardiff.

All incubation steps were carried out on an orbital shaker. Prior to staining, neuroretinas were re-fixed in 4% PFA-PBS for 2 min at RT, washed in 2X PBS and blocked for 1 h at RT (blocking/permeabilising solution: 2X PBS, 3% Triton, 1% BSA-fraction V, 0.5% Tween, 0.1% NaN_3). Primary antibodies were made up in blocking/permeabilising solution according to Table 2.2 100 µl of primary antibody was applied to each neuroretina in a 96 well plate (Nunc) overnight at RT. The following day, neuroretinas were washed 3 x 10 min in blocking/permeabilising solution. Fluorophore-conjugated secondary antibodies were made up in blocking/ permeabilising solution according to Table 2.2 and 100 µl applied for 2 h at RT. Neuroretinas were washed 2 x 10 min in blocking/permeabilising solution and for 10 min in 2X PBS. Neuroretinas were re-fixed in 4% PFA-PBS for 10 min at RT and washed 2 x 5 min in 2X PBS. Neuroretinas were mounted on slides in MOWIAL® mounting medium (see following Section).

2.5.1.2.1. Mowial mounting medium

2.6 g MOWIAL® (Calbiochem, 475904) was added to 6 g glycerol and mixed for 1 h at RT on a roller. To this, 6 ml of deionised water was added and mixing continued overnight at RT. The following day, 12 ml 0.25 M Tris-HCl (pH 8.5) was added and the mixture heated to 50°C, for 5 h shaking every 30 min. Mountant was stored in aliquots at -20°C.

2.5.2. Protein isolation

Unfixed eyes were immediately dissected as in Section 2.5.1.2 The neuroretina and remaining eyecup were separately immersed in 200 µl 2X SDS-PAGE sample buffer (described in Section 2.1.3) and rotated overnight to disrupt the tissue. The following day, the neuroretina lysate was passed through a 21G needle and the eyecup removed leaving the pigmented lysate of the RPE/choroid remaining. Samples were heated to 95°C for 5 min and stored at -20°C.

2.6. Gene expression analysis

2.6.1. RNA isolation

Isolation of RNA for microarray analysis and subsequent analysis of data was performed in collaboration with Dr. Carsten Faber (University of Copenhagen).

All surfaces and dissection equipment were thoroughly cleaned with RNase*Zap*® (Ambion Inc, AM9780) and rinsed with 0.1% diethylpyrocarbonate treated water. Dissection of each eye was within 5 min of enucleation. Eyes were dissected as detailed in Section 2.5.1.2.

For microarray analysis, neuroretinas were removed and placed in RNA*later*®, stored at 4°C overnight and on the following day RNA*later*® was removed and the tissue frozen at -80°C. Thawed neuroretinas were treated with TRIzol® reagent (Invitrogen, 15596-026) for RNA isolation and passed through a QIAshredder (QIAGEN, 79654).

RNA isolation from RPE was tested by applying TRIzol® reagent to the remaining eyecup in either an Eppendorf tube which was rotated for 10 min or on a petri dish

where the pigmented cells were scraped off using a 21 G needle. For microarray samples, RPE/choroid RNA was isolated using the scraping method. RNA and protein isolation from TRIzol® reagent for both RPE/choroid and neuroretina samples was performed according to the manufacturer's protocol.

Isolated RNA underwent a clean-up procedure using the RNeasy kit (QIAGEN, 74104). RNA was eluted in 30 µl RNase free water. DNA was degraded by treating each 30 µl sample with 1 µl of amplification grade DNase I (Invitrogen, 18068-015) and 3.44 µl of the accompanying buffer (200 mM Tris-HCl (pH 8.4), 20 mM $MgCl_2$, 500 mM KCl) and incubating for 15 min at RT. The reaction was stopped by addition of 1 µl of 25 mM EDTA (pH 8.0) and incubating for 15 min at 60°C. RNA was stored at -80°C.

For real-time quantitative polymerase chain reactions (RT qPCR), RNA was isolated using the RNEasy kit. After dissection, the neuroretina was placed in 350 µl of buffer RLT. To the remaining eyecup, 350 µl buffer RLT was applied and the RPE/choroid scraped off using a 21 G needle. RNA was isolated following the manufacturer's protocol.

2.6.2. Reverse transcription of RNA

RNA concentration was quantified using a NanoDrop spectrophotometer (Thermo Scientific). 350 ng of RPE/choroid or 600 ng of neuroretina RNA was used for reverse transcription into complementary DNA (cDNA) using the QuantiTect Reverse Transcription kit (QIAGEN, 205311) following the manufacturer's protocol. Briefly, genomic DNA was eliminated in a 5 min reaction followed by reverse transcription using an reverse transcription primer mix (containing an optimised blend of oligo-dT and random primers) for 15 min at 42°C followed by a 3 min inactivation step at 95°C.

2.6.3. Real-time quantitative polymerase chain reactions

RT qPCR reactions were set up on ice, in triplicate, using Power SYBR® green mastermix (Applied Biosystems, 4309155). Each 25 µl reaction contained 12.5 µl mastermix (SYBR® green 1 dye, AmpliTaq Gold® DNA polymerase, dNTPs, dUTPs,

passive reference and optimised buffers), 1.5 μl forward primer (5 μM), 1.5 μl reverse primer (5 μM) (Table 2.3), 1 μl cDNA template and 8.5 μl RNase free water.

Primer Target	Species	Orientation	Sequence (5' → 3')
Actin	Mouse	Forward	TCCAAGTATCCATGAAATAAGTGG
Actin	Mouse	Reverse	GCAGTACATAATTTACACAGAAGC
Pecam1	Mouse	Forward	GCCAGTCACTTGAAGACAGACC
Pecam1	Mouse	Reverse	TGGAACGGAAAGGAAGATCAAGG
Rbp7	Mouse	Forward	CTCCACCTGGAAATGTTCTG
Rbp7	Mouse	Reverse	ACGAGATAACTTGGCATTGAG

Table 2.3. Primer sequences used in real-time quantitative PCR
Pecam1, platelet endothelial cell adhesion molecule 1; *Rbp7*, retinol binding protein 7.

Samples were run on 7900HT Fast Real-Time PCR System (Applied Biosystems) using the following programme:

1. Denaturation at 95°C for 10 min
2. 40 cycles of denaturation at 95°C for 15 s > amplification at 60°C for 1 min
3. 1 cycle of denaturation 95°C for 15 s > amplification 60°C for 15 s
4. Denaturation at 95°C for 15 s

Dissociation curves were checked after each run to ensure only one peak was present. Raw fluorescence data and cycle information were imported into Data analysis for real-time PCR (DART-PCR) version 1.0 (Peirson *et al.,* 2003) in an excel workbook. This programme converts raw data into relative expression values (R_0) after the following steps:

1. Groups and triplicates are assigned
2. Samples which are outliers for amplification efficiency are removed
3. Amplification efficiency and threshold set

Relative expression of the gene of interest was normalised to β-actin as an internal control.

2.6.4. Microarray analysis

Quality control and processing of RNA, and statistical analysis, was performed by the UCL Genomics Facility. RNA was isolated from *Cfh*$^{-/-}$ and C57Bl/6 mice of 7-8 weeks and 1 year 140 days ± 6 days (according to Section 2.6.1).

2.6.4.1. Quantitative and qualitative analysis of RNA

RNA quality and quantity were assessed using Agilent RNA 6000 pico and nano kits (Agilent, 5067-1511/3) which use a fluorescent dye that intercalates with nucleic acids that are subsequently separated by electrophoresis in an Agilent Bioanalyzer 2100. RPE/choroid RNA was loaded onto pico microfluidic chips (detection of RNA > 50 pg/μl) and neuroretina RNA onto nano microfluidic chips (detection of RNA > 25-500 ng/μl) and the manufacturer's protocol followed.

2.6.4.2. Linear amplification of RNA

RPE/choroid RNA quantity was below the minimum requirement for microarray analysis (1 μg) therefore it was linearly amplified using an Ovation WGA amplification kit according to the manufacturer's protocol (NuGEN Technologies, 6100-012). This kit averages a 15,000 x linear amplification of all mRNA. Amplification is initiated both at the 3' end and randomly throughout the whole mRNA transcript to enable amplification of non-poly (A) transcripts and compromised RNA samples.

2.6.4.3. Amplification, fragmentation and terminal labelling

RNA underwent sense target labelling assay prior to hybridisation to Affymetrix Mouse Gene 1.0 ST Array GeneChips® (Affymetrix, 9011680). Each GeneChip® comprised of more than 750,000 unique 25-mer oligonucleotides representing more than 28,853 gene-level probe sets. Each probe set contains ≈ 27 probes spread across the full length of the gene.

2.6.4.4. Statistical analyses of microarray data

After general array quality control and data export, the data were normalised using robust multiarray average (RMA) and imported into Partek software. Array data were then checked for any outliers and overall grouping/separation using principal

component analysis (PCA), and signal histograms. ANOVA analysis of data generated a standard p-value. The p-values were adjusted using the Benjamini & Hochberg method to reduce false positives due to multiple testing. Comparison of the data was carried out using a false discovery rate of ≤ 0.05 to create gene lists which showed significant differentially expressed genes and exons between the different groups.

2.6.4.5. Pathway analysis

Ingenuity Pathway Analysis® (IPA) software was used to analyse the lists of genes which were identified as being significantly differentially expressed between groups. This identified whether there were any direct or indirect links between genes in each list to a single pathway. It also identified which canonical and cellular functions were most affected in each gene list. Some genes in each list were classified as 'unmapped' and were therefore excluded from the analysis. This work was carried out using a free trial licence registered to Jennifer Williams.

2.7. Statistical tests

Standard deviations (S.D.) and unpaired, two-tailed, Student t-tests were calculated using Microsoft® Excel. One-way Analysis of Variance (ANOVA) tests were calculated in GraphPad Prism® software. Spearman's Rank correlation coefficient was calculated using the following formula: $1 – (6\Sigma d^2/n^2-1)$, where Σd = sum of the differences and n = number of data points. Differences are calculated by ranking each data set separately in numerical order, data points are given a value dependent on their rank (e.g. 1-8 if n = 8). The difference in values assigned to each comparable data point in each data set is the difference.

Chapter 3: Results

A Study of the Secretion of Complement Factor H from Retinal Pigment Epithelial Cells

Since the discovery of complement proteins in drusen (Mullins *et al.,* 2000), it has been speculated that complement plays a pathogenic role in AMD, though whether it had a direct or indirect role was undecided. In 2005 however, four separate studies identified the same SNP in CFH that confers increased risk for AMD (Edwards *et al.,* 2005; Hageman *et al.,* 2005; Haines *et al.,* 2005; Klein *et al.,* 2005) (see Section 1.4.3.2). Together these studies suggested that up to 50% of all AMD cases could be linked to this SNP in the CFH gene. Previous to this, most research into CFH focused on its role in kidney diseases where its dysfunction or absence had been shown to be one of the causes of DDD and aHUS (Zipfel *et al.,* 2006).

The largest pool of CFH is in the blood where in humans the concentration ranges from 120-790 μg/ml (see Section 1.2.3). Most serum CFH is made by the liver and, via the blood, it helps to protect against inappropriate complement attack for all organs and tissues it has access to. In addition to the CFH provided from the blood, most organs produce their own CFH; this is thought to increase local concentrations to offer additional protection against uncontrolled complement activation.

The eye is capable of producing its own CFH and in contrast to other organs it may depend on this resource more heavily than the supply from the blood because of the blood-retinal barrier which restricts the movement of proteins from the blood into the retina. In human eyes CFH protein expression has been reported in several tissues including the optic nerve, lens, RPE, ciliary body, sclera and retina (Mandal and Ayyagari, 2006). RPE cells are thought to be the main producers of CFH in the eye, as mRNA expression is higher than in any other ocular cell type (Hageman *et al.,* 2005).

The RPE is considered central to the pathogenesis of AMD since it is believed to be partly responsible for the development of drusen, and several of its key functions in maintaining homeostasis in the retina become dysregulated in AMD. Since both CFH and the RPE are central to the pathogenesis of AMD and the RPE is thought to be the

major local producer of CFH in the eye, the first aim of this study was to investigate the secretion of CFH from the RPE. Since 2005 only a handful of publications have explored the secretion of CFH from RPE cells (An *et al*., 2006; Chen *et al.,* 2007; Yu *et al.,* 2007; Kim *et al.,* 2009; Juel *et al.,* 2011; Lau *et al.,* 2011). This chapter describes studies of CFH secretion from RPE cells in culture.

3.1. Optimisation of ARPE19 secretion assay for the quantification of CFH

In order to quantify CFH secretion from RPE cells in culture the RPE cell line ARPE19 was chosen as a model cell line for optimising the secretion assay. The quantification of CFH from ARPE19 culture supernatants was complicated by the presence of CFH in FCS used to supplement DMEM for culturing ARPE19 cells. ARPE19 cells were therefore grown to confluency in the presence of serum, but after thorough washing with PBS, secretion assays were performed in serum-free DMEM. Culture supernatants were collected from ARPE19 cells maintained for 72 h in serum-free DMEM and the proteins were resolved by SDS-PAGE and western blotted for CFH. CFH was not identified in the culture supernatant (data not shown), most likely because it was below the threshold for detection. Therefore, in order to maximise the protein loading from each culture supernatant sample, proteins were first concentrated by precipitation. Two protein precipitating agents, acetone and TCA were tested. A culture supernatant sample collected from ARPE19 cells maintained in serum-free DMEM for 24 h was divided equally and precipitated with either acetone or TCA. Subsequent SDS-PAGE and western blotting for CFH revealed that TCA was more efficient at precipitating CFH than acetone (Figure 3.1). TCA was therefore chosen as the precipitating agent for concentrating proteins to enable CFH quantification from the dilute culture supernatants. This result also confirmed that ARPE19 cells secrete CFH, consistent with Juel *et al.* (2011), who were the first to report this.

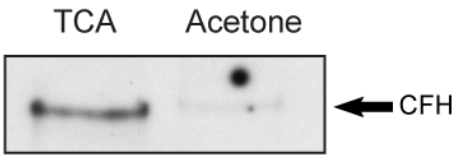

Figure 3.1. Precipitation of secreted CFH from ARPE19 culture supernatant
ARPE19 cells, cultured in a 6-well plate, were serum starved in DMEM for 24 h. One culture supernatant sample was collected and divided, half was precipitated with 60% acetone and the other half was precipitated with 25% TCA. All precipitated proteins were resolved by SDS-PAGE and western blotted for CFH. CFH was visualised as an approximately 155 kDa polypeptide band using enhanced chemiluminescence.

3.2. Serum starvation causes a similar pattern of CFH secretion in both ARPE19 and primary porcine RPE cells

It was important to examine the consequences of serum starvation on CFH secretion in order to interpret the effects of any agonist treatment applied to the cells in future experiments. Two RPE cell types were used, the RPE cell line ARPE19 and primary RPE cells isolated from porcine eyes. RPE cells were cultured in DMEM containing serum, until they reached confluency. Confluent cells were used to limit the complication of cell growth over the time of the assay, to improve the ability of the cells to withstand serum withdrawal and to represent the *in vivo* situation where the RPE exists as a confluent monolayer. RPE cells were washed twice in PBS in order to remove any traces of CFH in the media. In a 6-well plate, 4 wells were treated with serum-free DMEM in an 'accumulative' fashion whereby medium was removed after 2, 4, 6 and 8 h. In order to analyse CFH secretion in between each time point, one well was treated 'serially', whereby fresh serum-free DMEM was added and removed every 2 h up until 8 h. There were no visible signs of cell stress or change in cell density after 8 h of serum starvation (Figure 3.2A).

Western blot analysis of ARPE19 culture supernatants showed that CFH accumulated in the media over the 8 h period (Figure 3.2B). Serial ARPE19 samples revealed that CFH was secreted in increasing amounts with each change of media; this peaked at 6 h and subsequently decreased. Similarly, CFH secreted by primary porcine RPE accumulated in the media over 8 h and had a comparable secretory pattern to ARPE19 cells when the media were changed serially.

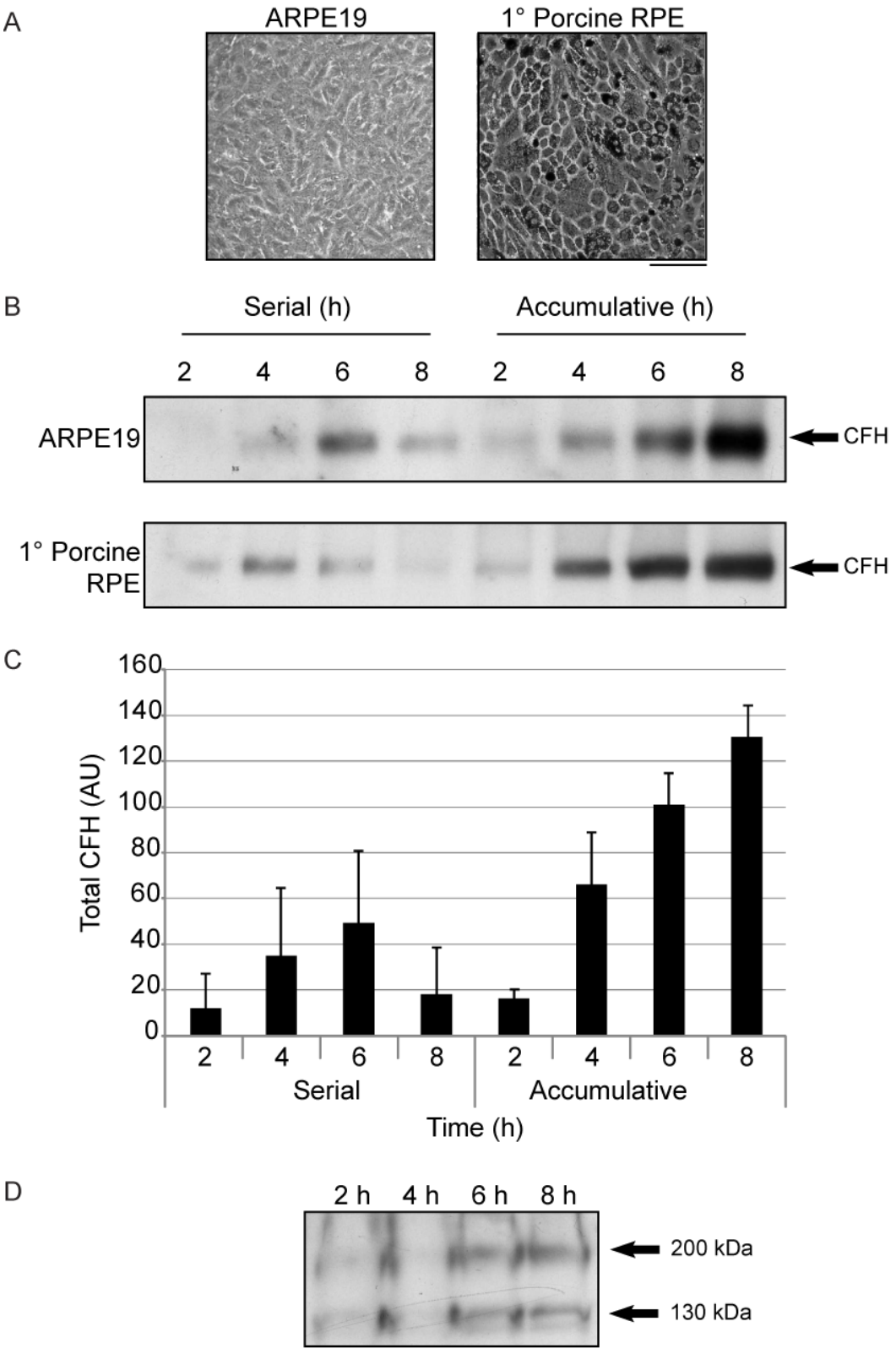

Figure 3.2. ARPE19 cells secrete CFH in a similar fashion to primary porcine RPE in culture
Confluent ARPE19 or primary porcine RPE cells were serum starved in DMEM for up to 8 h. (A) Phase contrast images of the cells following serum starvation. Scale bar represents 100 μm. (B) During serum starvation, culture supernatants were collected serially (from same well) or accumulatively (from different wells) and precipitated with 25% TCA. Proteins were resolved by SDS-PAGE and western blotted for CFH as described in the legend to Figure 3.1. (C) CFH bands shown in (B) were quantified by densitometric analysis. (D) At the end of the secretion assay, ARPE19 cells treated in an accumulative fashion were lysed in SDS-PAGE sample buffer. Proteins were resolved by SDS-PAGE and western blotted for CFH as above. Data are means ± S.D.

By densitometric analysis of each band, CFH was quantified and an average of the mean pixel intensity (MPI) of ARPE19 and primary porcine RPE bands were plotted against time (Figure 3.2C). The graph shows that the relationship between the accumulation of CFH and time was largely linear between 4-8 h. The increase in CFH secretion from 2-4 h does not fit this linear relationship, between these two time points the gradient increased, indicating an increased rate of CFH secretion between these time points. The relationship between time and CFH secretion from the serial samples was linear up until 6 h but after this CFH secretion decreased. This decline in the capacity to secrete CFH after 6 h was likely caused by the sequential serum-free media changes applied to the serial samples since this decrease was not observed in RPE cells treated in an accumulative fashion.

At the end of the secretion assay, the ARPE19 cells which had been treated with DMEM in an accumulative fashion were lysed in SDS-PAGE sample buffer. Cellular proteins were resolved by SDS-PAGE and western blotted for CFH. Protein bands were visible at approximately 130 kDa and 200 kDa but no bands of 155 kDa were identified (Figure 3.2D). This suggests that CFH secreted into the media did not adhere to the cells, as this would have been expected to yield a similar sized band to the CFH present in the culture supernatant. The intensity of the 130 kDa and 200 kDa bands did not change at the different time points of the accumulative samples. Other reports where CFH was quantified from cell lysates used a different antibody to the one used in these experiments and this may account for the difference in band sizes observed.

In summary, these results show that serum starvation causes similar patterns of CFH secretion from both ARPE19 and primary porcine RPE cells. A Spearman's rank statistical test for non-parametric statistical dependence between two variables showed a positive correlation of 0.7. Since ARPE19 cells behaved similarly to primary porcine RPE, we were confident in using ARPE19 cells as a model for RPE secretion of CFH in further experiments.

3.3. Alternative methods of concentrating CFH are not as efficient as TCA precipitation for CFH quantification

The rise and fall of CFH secretion by RPE cells in Figure 3.2 could have several explanations. The removal of serum may stimulate a burst of secretion as a stress-response which peaks at 4-6 h. To circumvent the possibility of a stress-response induced by serum withdrawal, we tested the secretion of CFH in a serum-free supplemented medium, X-VIVO™ 15, which does not contain CFH, and is specifically designed to support cells in a serum-free environment (Juel *et al.,* 2011). However, X-VIVO™ 15 contains added proteins which when precipitated with TCA formed an insoluble protein pellet. In order to use X-VIVO™ 15 medium in secretion assays, CFH would therefore have to be isolated from the culture supernatants using a method that avoided generating an unworkable protein pellet. In principle this could be achieved by performing an ammonium sulphate cut, where proteins of different solubility are precipitated at different salt concentrations.

To test whether this technique would be suitable for the isolation of CFH, an ammonium sulphate cut was performed on culture supernatants from ARPE19 cells cultured in serum-free DMEM for 72 h. Ammonium sulphate was added in increasing concentrations of 29%, 55%, 62%, 67% and 71% to the same sample in a stepwise fashion and the precipitates removed at each step. The largest yield of CFH came from the 29% ammonium sulphate cut (Figure 3.3A), which was similar to the amount recovered in a comparable sample precipitated with TCA. However, repeating the experiment with a lower starting concentration of ammonium sulphate and increasing in smaller steps (5%, 14%, 25%, 32%, 41% and 50%), appeared to reduce the efficiency of CFH precipitation (Figure 3.3B). In practise, we concluded that this was not an accurate method of obtaining CFH protein for absolute quantification.

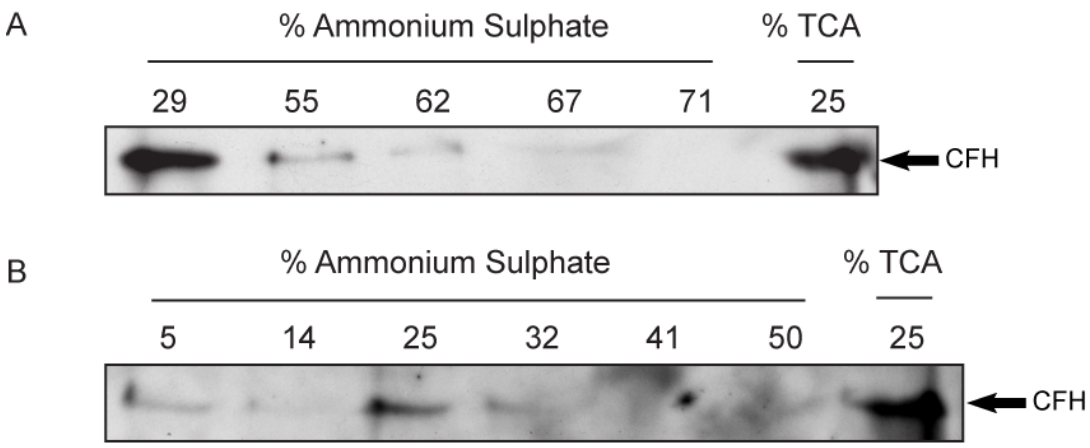

Figure 3.3. Ammonium sulphate precipitation of secreted CFH from ARPE19 culture supernatant
ARPE19 cells, cultured in a 6-well plate, were serum starved in DMEM for 72 h. Ammonium sulphate precipitation was carried out by increasing the concentration of ammonium sulphate in a stepwise fashion in the culture supernatant from one well whereby precipitate was recovered at each step. (A) Culture supernatants were collected from two separate wells, one was precipitated with 29-71% ammonium sulphate and compared to the other precipitated with 25% TCA. (B) As in (A) except a lower range of 5-50% ammonium sulphate was used. Precipitated proteins were resolved by SDS-PAGE and western blotted for CFH as described in the legend to Figure 3.1.

As an alternative to protein precipitation, we next attempted to exploit the binding properties of CFH in order to isolate the protein from X-VIVO™ 15. CFH is known to bind glycosaminoglycans such as heparin (Blackmore *et al.,* 1996), suggesting that heparin-agarose beads could therefore be used for this purpose. Supernatants from ARPE19 cells cultured in either serum-free DMEM or X-VIVO™ 15 for 48 h were mixed with heparin-agarose beads in order to isolate CFH. After 3.5 h of incubation, the beads were removed from the culture supernatants by centrifugation and the isolated proteins were recovered from the beads by boiling in SDS-PAGE sample buffer. Western blot analysis of the isolated proteins showed that CFH recovery from ARPE19 culture supernatants was successful (Figure 3.4A). A similar level of CFH secretion was seen using ARPE19 cells whether cultured in either serum-free DMEM or X-VIVO™ 15. CFH was not present in DMEM or X-VIVO™15 media itself which had not been in contact with ARPE19 cells (Figure 3.4A).

In order to determine whether heparin-agarose was efficient at isolating all the CFH present in the samples, the culture supernatants, post heparin-agarose bead incubation, were precipitated with TCA. TCA precipitated proteins were western blotted for CFH (Figure 3.4B). The DMEM sample showed a significant CFH band

indicating that heparin-agarose did not isolate all the CFH from the sample. The X-VIVO™ 15 sample only had a faint CFH band which would suggest that the vast majority of CFH was recovered. However, when the X-VIVO™ 15 sample was treated with TCA an insoluble pellet formed, making subsequent analysis by SDS-PAGE and western blotting impossible. These results indicate that under these conditions, efficient CFH isolation by heparin-agarose for quantification was not possible. Nevertheless, it could be that by increasing the amount of heparin-agarose beads or incubation time, or altering other parameters, this method could be optimised to increase the efficiency of CFH isolation. But taking into consideration the large volume of heparin-agarose beads that would be required, long incubation times and inefficient CFH isolation, this method was not considered suitable to enable robust quantification of secreted CFH. It was therefore decided to perform RPE secretion assays in serum-free DMEM rather than X-VIVO™ 15.

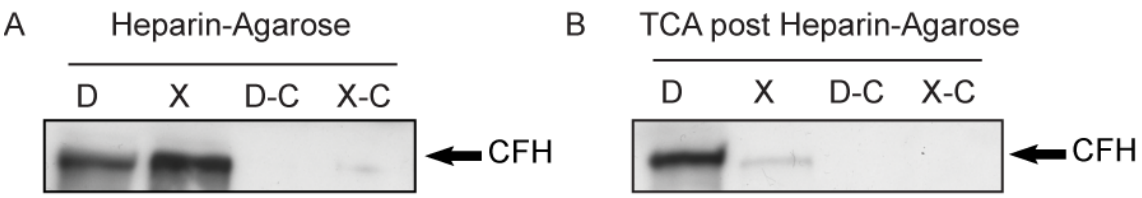

Figure 3.4. Heparin-agarose pulldown of secreted CFH from ARPE19 culture supernatant
ARPE19 cells, cultured in a 6-well plate, were serum starved in DMEM (D) or X-VIVO™ 15 (X) for 48 h. CFH recovery from culture supernatants by heparin-agarose pulldown was compared to protein precipitation with 25% TCA. (A) Heparin-agarose pulldown was performed by incubating culture supernatant from one well with heparin-agarose beads for 3.5 h. Beads were recovered through centrifugation and supernatants were kept on ice. The beads were washed and incubated with hot SDS-PAGE sample buffer to recover pulled-down proteins. Beads were removed from the sample buffer by centrifugation. As controls both DMEM (D-C) and X-VIVO™ 15 (X-C) media which had not been in contact with cells went through the same heparin-agarose pulldown procedure. (B) After removal of beads, the culture supernantants kept on ice from (A) were subsequently precipitated with 25% TCA. Proteins were resolved by SDS-PAGE and western blotted for CFH as described in the legend to Figure 3.1.

3.4. Secretion of CFH from ARPE19 cells is similar whether cultured in 10% or 1% FCS

Results from our Institute have suggested that ARPE19 cells become more quiescent and 'RPE-like' when the serum concentration is reduced to 1% compared to 10% (personal communication, Ahmado A.). On account of these observations we speculated that the culture conditions pre serum starvation could affect CFH secretion. We therefore performed an 8 h secretion assay, as described in Section 3.2, on ARPE19 cells that had been grown for a minimum of two weeks in either 10% or 1% FCS. No differences were observed in cell density or morphology when the cells were visualised using phase contrast microscopy (data not shown). In order to control for precipitation efficiency, goat IgG was added to the collected culture supernatants prior to precipitation with TCA. CFH bands were quantified by calculating the MPI, and normalised to the MPI of their respective goat IgG bands. Even though the same amount of goat IgG was added to each sample it was clear from the densities of the IgG bands on the western blot that protein recovery was variable (Figure 3.5A). This may have been the result of protein lost during washing, or different precipitation or transfer efficiencies, and it showed the importance of normalising CFH secretion data to IgG bands.

Quantification and normalisation of the CFH bands from three experiments showed that the pattern of CFH secretion was similar between ARPE19 cells cultured in 10% and 1% FCS (Figure 3.5B). CFH secretion from the serial well showed that with successive media changes less CFH was secreted at later time points, similar to previous results which showed a peak of secretion from the serial well at 4-6 h. The results from the accumulative samples were consistent with previous results (Figure 3.2) in which CFH accumulated rapidly from 2-6 h, and more slowly thereafter.

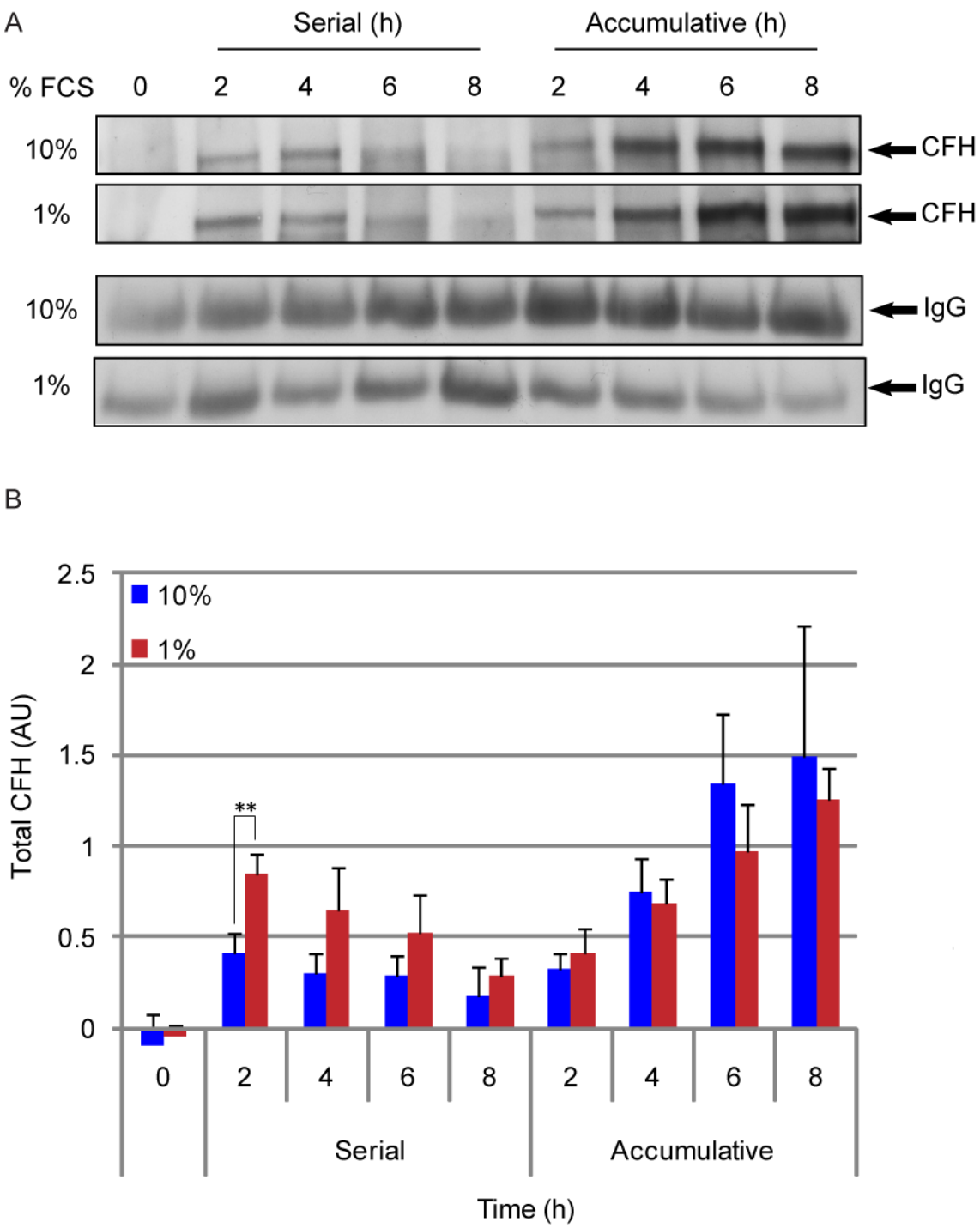

Figure 3.5. Secretion of CFH from ARPE19 cells is similar whether cultured in 10% or 1% FCS
ARPE19 cells, allowed to grow to confluency in DMEM containing either 10% (blue bars) or 1% (red bars) FCS were serum starved in DMEM for up to 8 h. (A) During serum starvation, culture supernatants were collected serially (from same well) or accumulatively (from different wells). Prior to precipitation with 25% TCA, 1 μg of goat IgG was added to each collected sample to control for precipitation efficiency. Proteins were resolved by SDS-PAGE and western blotted for CFH and goat IgG. CFH was visualised as an approximately 155 kDa polypeptide band and goat IgG heavy chains as an approximately 55 kDa polypeptide band using enhanced chemiluminescence. (B) CFH and goat IgG bands were quantified by densitometric analysis. MPI of each CFH band was normalised to the MPI of its respective IgG band. Data are means ± S.D, n = 3. Unpaired Student t-tests were applied to data, ** p = < 0.01.

CFH secretion was on average higher from ARPE19 cells cultured in 1% FCS than in 10% FCS in serial samples. However, unpaired Student t-tests for each time point revealed a significant difference in CFH secretion at the serial 2 h time point only ($p = < 0.01$). This difference may reflect CFH secretion prior to serum starvation which could have been higher due to the lower concentration of CFH in 1% FCS supplemented DMEM. However, CFH secretion from accumulative samples showed higher CFH secretion from cells cultured in 10% FCS.

3.5. CFH secretion pattern from ARPE19 cells over an extended time course

In order to address whether the drop in CFH secretion after 4-6 h was a consequence of stress caused by serum withdrawal, we extended the time course of the secretion assay up to 72 h with time points at 0, 8, 24, 48 and 72 h. The assay was carried out in the same manner as the 8 h assay with culture supernatants removed in both an accumulative and serial fashion.

No differences were observed in cell density or morphology when ARPE19 cells were visualised using phase contrast microscopy after 72 h in serum-free media (data not shown). Results from four experiments showed that the ARPE19 cells continued to secrete CFH after more than 8 h in serum-free conditions (Figure 3.6A). The normalised accumulative data show that CFH accumulated in the culture supernatant over time in an approximately linear manner (Figure 3.6B). Analyses of the serial samples revealed that CFH secretion was maximal in the second 24 h period (48 h time point). However, note that the serial 24 h time point should be regarded as 16 h of actual secretion time. When this is added to the 8 h serial time point the total value is similar to the full 24 h value observed in the accumulative well. These results suggest that ARPE19 cells secrete CFH in serum-free conditions for at least three days and perhaps longer.

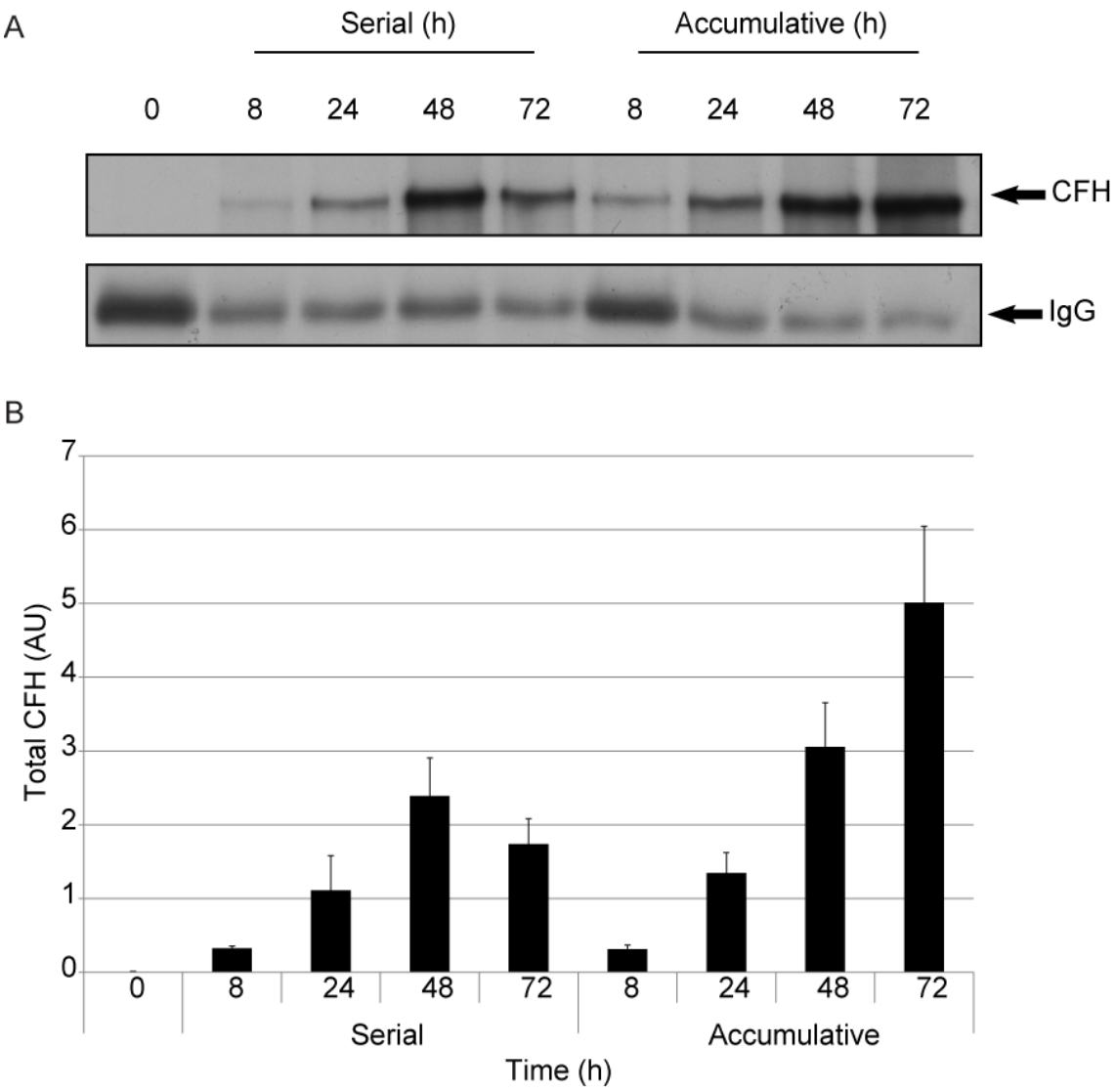

Figure 3.6. Secretion of CFH from ARPE19 cells over an extended time course
Confluent ARPE19 cells were serum starved for up to 72 h in DMEM. (A) During serum starvation, culture supernatants were collected serially (from same well) or accumulatively (from different wells). Prior to precipitation with 25% TCA, 1 μg of goat IgG was added to each sample to control for precipitation efficiency. Proteins were resolved by SDS-PAGE and western blotted for CFH and goat IgG as described in the legend to Figure 3.5. (B) CFH and goat IgG bands were quantified by densitometric analysis. MPI of each CFH band was normalised to the MPI of its respective IgG band. Data are means ± S.D., n = 4.

3.6. The effect of inflammatory cytokines on CFH secretion

Consistent with the involvement of complement in inflammatory reactions the expression of complement proteins is influenced by the cytokine environment. The CFH gene promoter region contains an IFNγ responsive site and acute phase response elements which indicate that pro-inflammatory cytokines can regulate gene expression (Section 1.2.3). Indeed, IFNγ has been shown to stimulate CFH expression in several cell types (Lappin *et al.,* 1992) and this has been shown to be mediated by the activation of the transcription factor, signal transducer and activator of transcription 1 (STAT1) in RPE cells (Wu *et al.,* 2007). Other pro-inflammatory cytokines such as IL-1β (Halme *et al.,* 2009) and TNFα (Katz and Strunk, 1989; Thomas *et al.,* 2000) have also been shown to stimulate CFH expression although reports are not consistent between groups and different cell types (Schlaf *et al.,* 2002; Timar *et al.,* 2006). RPE cells express soluble and cell surface cytokine receptors and it is well documented that cytokines influence the expression of many proteins expressed by RPE cells (Holtkamp *et al.,* 2001; An *et al.,* 2008; Shi *et al.,* 2008). However, only a handful of papers have addressed the influence of pro-inflammatory cytokines on CFH secretion by RPE cells, and the results of these studies are not all in agreement with one another (Chen *et al.,* 2007; Wu *et al.,* 2007; Kim *et al.,* 2009; Juel *et al.,* 2011; Luo *et al.,* 2011; Lau *et al.,* 2011). Given the likely importance of CFH secretion by RPE in AMD, and the conflicts in the literature, we therefore tested the effects of three pro-inflammatory cytokines, IFNγ, TNFα and IL-1β, on CFH secretion.

Confluent ARPE19 cells were treated with serum-free DMEM containing 0-200 ng/ml of IFNγ, TNFα or IL-1β and incubated for 8 h. The culture supernatants were precipitated with TCA, resolved by SDS-PAGE and western blotted for CFH. TNFα did not have a detectable effect on CFH secretion, however both IL-1β and IFNγ stimulated an increase in CFH secretion (Figure 3.7A). Quantification of the protein bands indicated that CFH secretion was enhanced with increasing concentrations of IFNγ and IL-1β (Figure 3.7B).

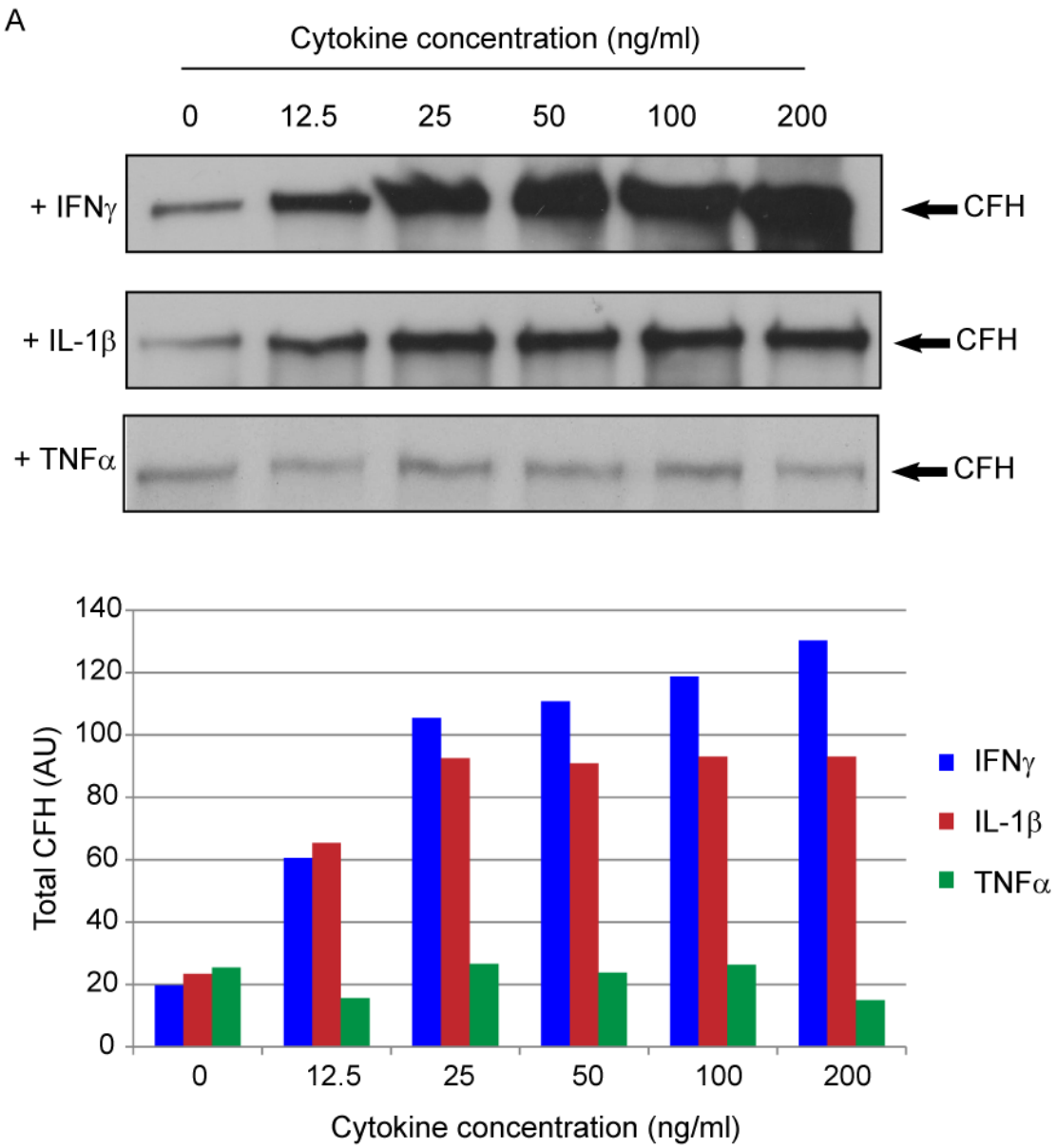

Figure 3.7. IFNγ and IL-1β enhance CFH secretion from ARPE19 cells
Confluent ARPE19 cells were serum starved for 8 h in DMEM or DMEM containing 12.5-200 ng/ml IFNγ, IL-1β or TNFα. (A) Culture supernatants were collected after 8 h of cytokine exposure and precipitated with 25% TCA. Proteins were resolved by SDS-PAGE and western blotted for CFH as described in the legend to Figure 3.1. (B) CFH bands shown in (A) were quantified by densitometric analysis.

To address the speed at which ARPE19 cells are able to respond to cytokine stimulation, IFNγ mediated CFH secretion was tested over an 8 h time course. Confluent ARPE19 cells were treated with serum-free DMEM containing either 0 or 100 ng/ml of IFNγ. Accumulative samples were taken after 0, 2, 4, 6 or 8 h. The culture supernatants were precipitated with TCA, resolved by SDS-PAGE and western blotted for CFH (Figure 3.8A). Quantification of the CFH bands showed that ARPE19 cells

respond to IFNγ within 2 h, and that this response was enhanced at each subsequent time point (Figure 3.8B). This indicated that the effect of IFNγ was sustained over 8 h suggesting that under inflammatory situations where IFNγ is present, RPE cells may chronically increase the amount of CFH they secrete. *In vivo* this response would likely contribute to protecting the neighbouring photoreceptors and the RPE cells themselves from potential damage caused by complement activation during an inflammatory event.

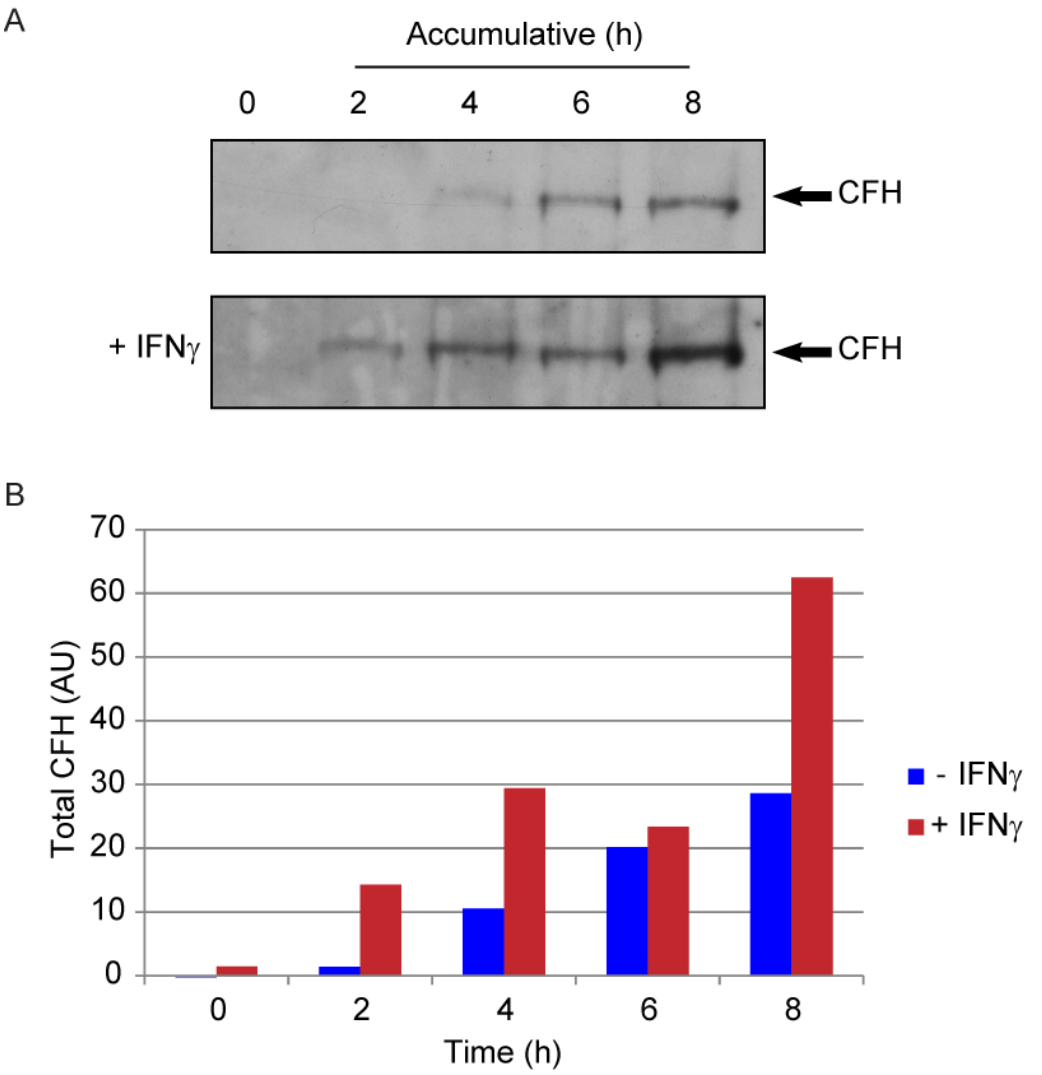

Figure 3.8. IFNγ sustainably enhances CFH secretion from ARPE19 over an 8 h time course
Confluent ARPE19 cells were serum starved for up to 8 h in DMEM or DMEM containing 100 ng/ml IFNγ. (A) During serum starvation, culture supernatants were collected accumulatively (from different wells) and precipitated with 25% TCA. Proteins were resolved by SDS-PAGE and western blotted for CFH as described in the legend to Figure 3.1. (B) CFH bands shown in (A) were quantified by densitometric analysis.

3.7. ARPE19 cells synthesise CFH *de novo* under serum-free conditions

To determine whether the CFH secreted from ARPE19 cells was derived from intracellular stores or was synthesised *de novo*, cycloheximide was added to secretion assays. Cycloheximide inhibits the translation of mRNA but does not affect the secretion of stored proteins. Confluent ARPE19 cells were serum-starved in DMEM either in the presence of 10 µM cycloheximide or the equivalent dilution of DMSO (vehicle). Serial and accumulative samples were taken at 0, 2, 4, 6, and 8 h.

Results showed that after 2 h, CFH secretion was markedly inhibited by the presence of cycloheximide in the accumulative samples (Figure 3.9A). A Student t-test for each time point revealed a significant difference between cycloheximide and vehicle treated samples when collected accumulatively. The CFH which was secreted during the first 2 h may represent release of a small intracellular store, or protein that had been translated and was en route to the secretory pathway before incubation with cycloheximide. Quantification and normalisation of the CFH bands revealed a small increase in CFH in the accumulative samples over time in the presence of cycloheximide (Figure 3.9B). This suggests either that ARPE19 cells indeed have a small store of CFH which is slowly released over 8 h, or that cycloheximide does not completely block mRNA translation. The serial and accumulative results from the DMSO controls were largely consistent with previous results. The experiment reveals a significant block in CFH secretion in the presence of cycloheximide in comparison to control, suggesting that the majority of CFH secretion from ARPE19 cells following serum withdrawal is the result of *de novo* protein synthesis.

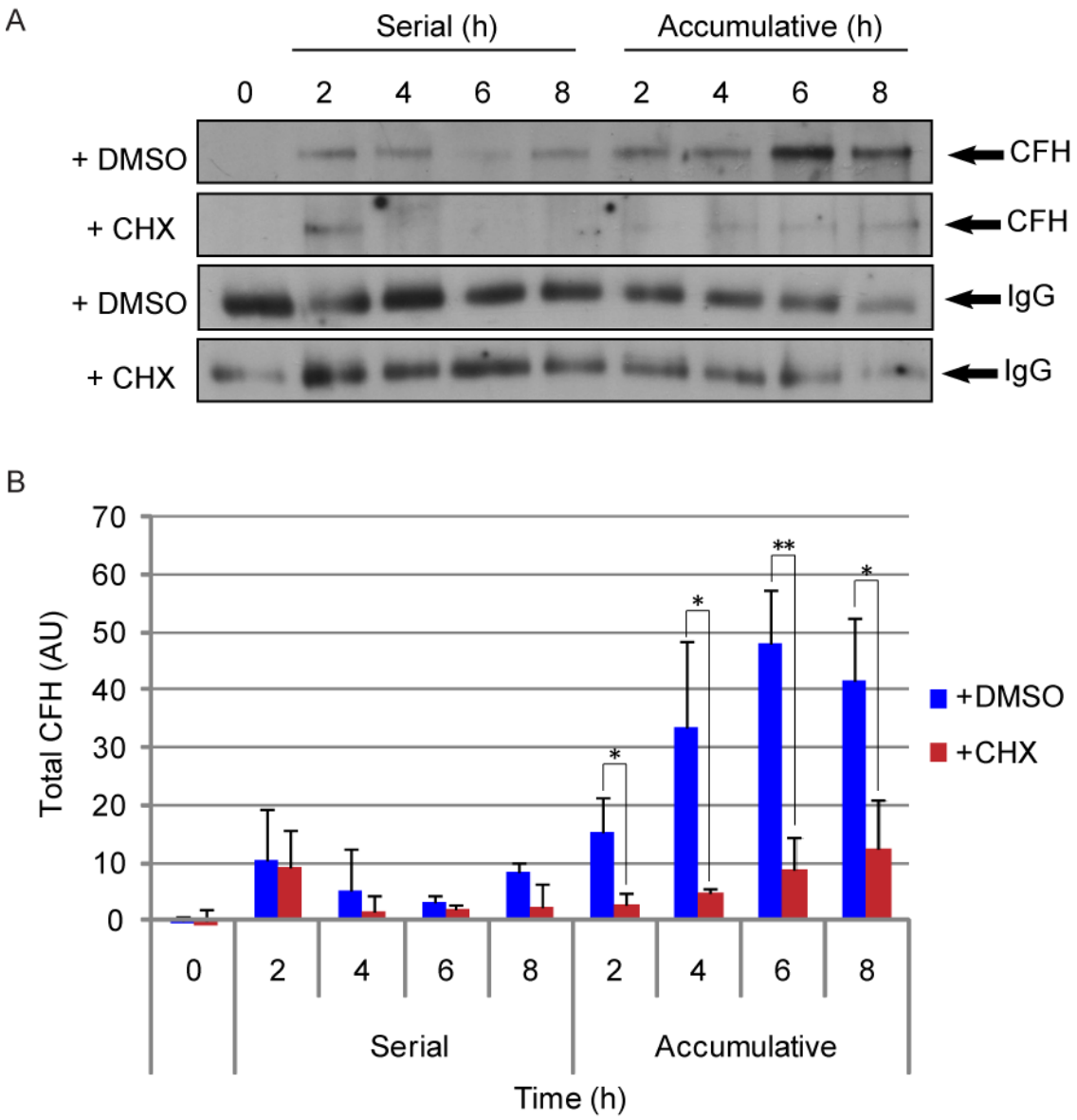

Figure 3.9. Serum starvation stimulates *de novo* CFH synthesis by ARPE19 cells
Confluent ARPE19 cells were serum starved for up to 8 h in DMEM containing either 10 μM cycloheximide (CHX) or DMSO. (A) During serum starvation, culture supernatants were collected serially (from same well) or accumulatively (from different wells). Prior to precipitation with 25% TCA, 1 μg of goat IgG was added to each collected sample to control for precipitation efficiency. Proteins were resolved by SDS-PAGE and western blotted for CFH and goat IgG as described in the legend to Figure 3.5. (B) CFH and goat IgG bands were quantified by densitometric analysis. MPI of each CFH band was normalised to the MPI of its respective IgG band. Data are means ± S.D., n = 3. Unpaired Student t-tests were applied to data, * p = < 0.05, ** p = < 0.01.

3.8. Discussion

The presence of CFH in drusen, the early hallmark of AMD, and the Y402H SNP in CFH that is linked to AMD susceptibility together present a strong case for the involvement of this protein in the pathogenesis of AMD. The source of CFH in drusen is believed to be the RPE because of its close proximity. Both primary isolated mouse and human RPE express CFH mRNA (Mandal and Ayyagari, 2006) and it has been suggested that CFH transcript levels in RPE are as high as those in the liver (Hageman *et al.,* 2005). Although CFH is expressed in a variety of cell types, regulation of CFH expression is believed to cell-type specific (Friese *et al.,* 1999). Several factors including cytokines, phagocytosis, oxidative stress and co-culture with activated T-cells have been shown to alter the expression of CFH by RPE cells (Chen *et al.,* 2007; Wu *et al.,* 2007; Kim *et al.,* 2009; Juel *et al.,* 2011; Luo *et al.,* 2011; Lau *et al.,* 2011). However, changes in CFH mRNA do not always correspond to a change in protein expression as demonstrated by Chen *et al.,* (2007) who reported a decrease in *Cfh* mRNA after IL-6 exposure with no subsequent change in CFH protein expression. Taking these points into consideration, together with the fact that CFH must be secreted in order for it to carry out its function as a regulator of the alternative pathway, we decided to investigate the secretion and expression of CFH in RPE cells.

To date there are only six published reports of CFH secretion by RPE cells (An *et al.,* 2006; Chen *et al.,* 2007; Yu *et al.,* 2007; Kim *et al.,* 2009; Juel *et al.,* 2011; Lau *et al.,* 2011), of which three have shown that this can be manipulated by exposure to IFNγ or co-culture with activated T-cells (Kim *et al.,* 2009; Juel *et al.,* 2011; Lau *et al.,* 2011). The paucity of literature on this topic, given that it is six years since CFH was linked to AMD, may be due to the difficult nature of studying secretion of a protein which is itself present in the serum used to culture the cells. An *et al.,* (2006) were the first to show that RPE cells are capable of secreting CFH, in experiments in which they used stable isotope labelling of amino acids in cell culture. With the limited literature on CFH secretion from RPE cells we attempted to develop an *in vitro* assay in which to study CFH secretion.

Due to the limited availability of primary human RPE cells, we chose to use the cell line ARPE19, which spontaneously arose from RPE cultured from a male donor in the University of California (Dunn *et al.,* 1996). Unlike transformed RPE cell lines, ARPE19 cells retain their normal RPE karyology as well as structural and functional characteristics of RPE cells *in vivo*. However, a study comparing the gene expression of ARPE19 cells to primary human RPE, showed that ARPE19 cells exclusively express 9 genes which are not expressed by primary human RPE, and conversely do not express 35 genes which primary human RPE cells do express (Cai and Del Priore, 2006). These genes represent less than 1% of all the genes expressed by either cell type, and of these none were complement genes. However, this study also showed that almost 2% of the genes expressed were either up or down-regulated >3 fold in ARPE19 cells compared to primary human RPE, and that these could be sorted into two distinct hierarchical clusters. Although our results show that in serum-free conditions ARPE19 cells secrete CFH in a similar manner to primary porcine RPE, the limitations of using a cell line must be considered when extrapolating these results to an *in vivo* scenario.

Developing this assay presented several challenges. Firstly CFH is present in FCS which is routinely used to culture RPE cells *in vitro*. Our CFH antibody recognised bovine CFH, the presence of which in the media of secretion assays masked any endogenous CFH secreted by the cells even when FCS was lowered to 1% of the total volume. A second challenge was accurately measuring the low levels of CFH secreted into the media. We dealt with this problem by precipitating spent media. Other techniques such as enzyme-linked immunosorbent assay may have also been applied, however this would have required species-specific CFH antibodies, which we were unable to identify from commercial sources.

Another consideration was the choice of culture conditions for the ARPE19 cells. Tian *et al.,* (2005) showed that serum added to the culture media for ARPE19 cells caused more changes in gene expression than when the cells were in serum-free conditions as compared to gene expression by primary RPE. Here we observed that culturing ARPE19 cells in low or high serum did not significantly affect the overall secretion pattern of CFH in response to serum starvation.

Upon initial removal of serum from cultured RPE cells, we observed secretion of CFH within 2 h. In serially collected samples, where precipitation efficacy was controlled for by spiking the samples with IgG, CFH secretion diminished with each serial change of media. However, the accumulative data showed that CFH secretion continued after 2 h since CFH levels accumulated in a largely linear fashion over an 8 h period. Therefore the drop in CFH secretion in serial samples after 2 h is most likely due to serial media changes causing stress to the cells. The extended time course revealed similar results where CFH accumulated over a 72 h period in accumulative samples but serial samples showed a failure to secrete CFH after the third replenishment of media. The accumulative data suggest that CFH is constitutively secreted since CFH levels did not plateau by 72 h. If CFH secretion is not constitutive it would be interesting to test whether serum depleted of CFH initiates the same secretory pattern as complete serum removal. As CFH depleted serum is commercially unavailable, we attempted to deplete FCS of CFH by separation through a heparin column, however complete removal was unachievable due to the high concentration of CFH in serum.

The peak in CFH secretion seen after serum removal is largely the result of *de novo* synthesis since it was largely abrogated in the presence of cycloheximide. The CFH secretion measured after 2 h in cycloheximide could represent release of a small store of CFH within the RPE, or may be protein that had already been translated and was being processed in the secretory pathway, before the cycloheximide took effect.

Chen *et al.,* (2007) were the first to investigate the effect of pro-inflammatory cytokines on CFH expression by RPE cells. They showed that TNFα significantly decreased the expression of CFH expression whereas IL-1, IL-4, IL-6 and IFNγ had no effect. Four further studies generated opposing data, that IFNγ stimulates both expression and secretion of CFH by RPE cells (Wu *et al.,* 2007; Kim *et al.,* 2009; Luo *et al.,* 2011; Lau *et al.,* 2011). Our results also disagree with those of Mei *et al.,* (2007) in that we observed that TNFα had no effect on CFH secretion and that IFNγ and IL-1β were capable of stimulating CFH secretion. A significant difference in experimental strategies is that Mei *et al.,* (2007) conducted their studies on a mouse RPE line. Thus, it is also possible that in addition to being cell type specific, the regulation of CFH by

pro-inflammatory cytokines is species specific too. Our results should be repeated in primary cells to show that this is not a cell-line specific effect due to differences in transcription such as those shown by Cai *et al.* (2009). One of the 90 genes they showed to be differentially expressed was the transcription factor, STAT1, whose expression was 3.2 fold increased in native human RPE cells compared to ARPE19 cells. STAT1 has been shown to mediate IFNγ enhanced CFH secretion by RPE (Wu *et al.,* 2007) and therefore ARPE19 cells may be less responsive to IFNγ compared to primary cells.

In conclusion, we have shown that ARPE19 cells secrete *de novo* synthesised CFH for at least 72 h in serum-free conditions. The secretory pattern suggests that RPE cells secrete CFH constitutively but that this secretion may be enhanced in inflammatory conditions perhaps to strengthen their own protection and that of their surroundings from complement bystander damage.

Chapter 4: Results

Characterisation of the Retina in 7-8 week and 1 year old *Cfh*$^{-/-}$ Mice

Previous work from our group has shown that CFH is required for normal visual function in 2 year old mice (Coffey *et al.,* 2007). In the absence of CFH, mice have reduced visual acuity and a diminished rod photoreceptor response. Subretinal C3 and autofluorescent deposits were shown to accumulate but electron-dense material decreased. Bruch's membrane became thinner and there was disorganisation of RPE organelles and rod photoreceptors. However, it is unknown when these functional and anatomical abnormalities begin in *Cfh*$^{-/-}$ mice. This chapter characterises the retina of *Cfh*$^{-/-}$ mice at 7-8 weeks and 1 year and investigates whether any of the abnormalities reported at 2 years are evident at 1 year or earlier.

4.1. Loss of CFH leads to a reduction in photoreceptor density at 1 year

First we assessed whether the loss of CFH caused any morphological disorganisation in the retinas of young or 1 year *Cfh*$^{-/-}$ mice. We compared *Cfh*$^{-/-}$ mice at 7-8 weeks (young) and 1 year (aged), and used wild-type age-matched controls to monitor changes associated with normal ageing. Semithin resin sections were cut from fixed eyes in all four groups and stained with toluidine blue (Figure 4.1A-D). We observed a greater tendency for photoreceptor detachment in the 1 year *Cfh*$^{-/-}$ samples than in aged-matched wild-type samples (data not shown) and that photoreceptor density appeared reduced in comparison to all other groups. Quantification of the nuclei in the ONL revealed that there was a significant reduction in their number with age in both wild-type and *Cfh*$^{-/-}$ mice (Figure 4.1E). Nuclei density in the ONL was not significantly different between young wild-type and *Cfh*$^{-/-}$ mice however it was significantly reduced in the 1 year samples. In addition to the ONL, the OPL and INL of the 1 year *Cfh*$^{-/-}$ samples appeared less dense than those of age-matched wild-type controls.

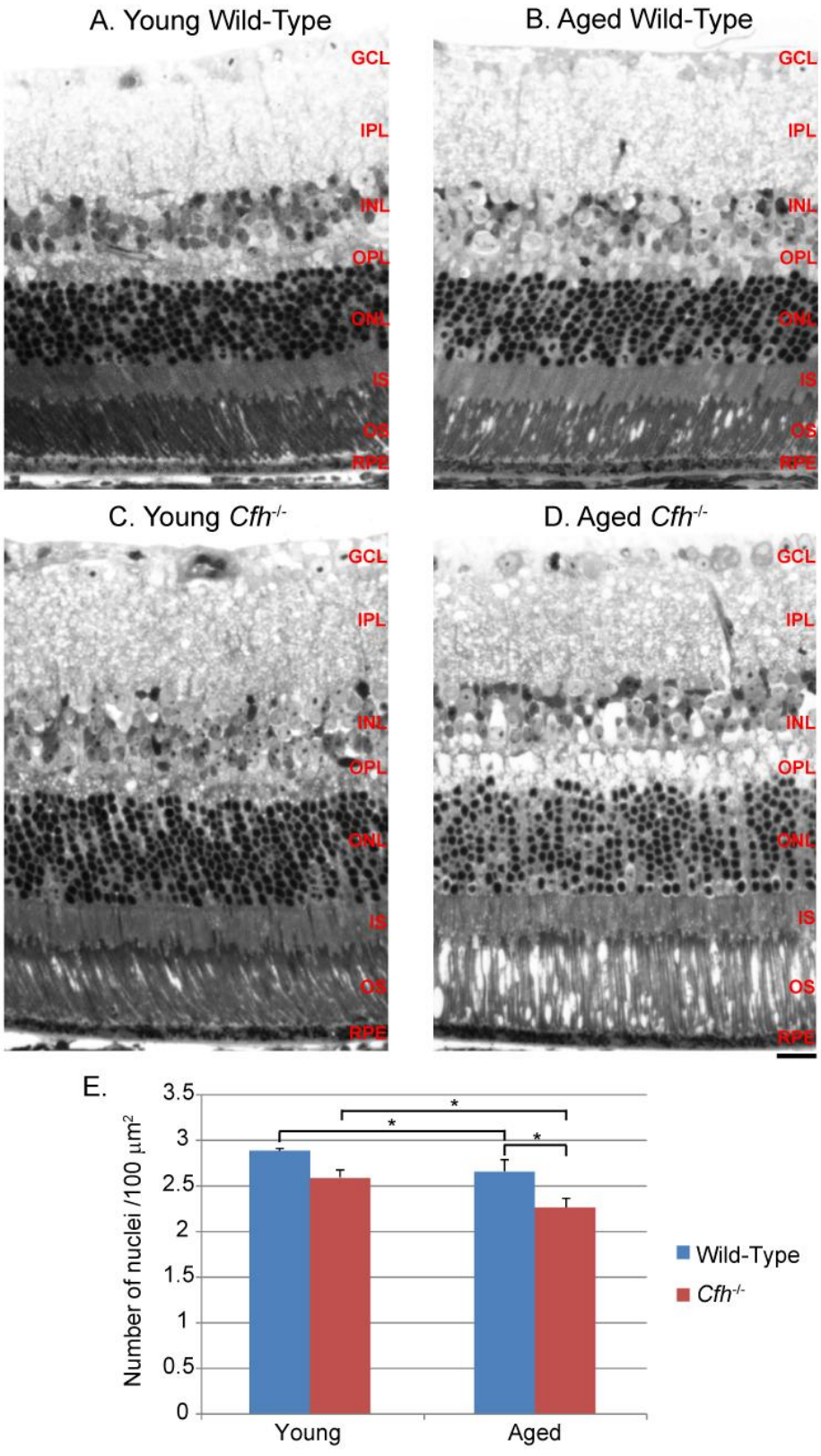

Figure 4.1. Morphological organisation of the retina in young and aged *Cfh*-/- and wild-type mice (A&B) Wild-type and (C&D) *Cfh*$^{-/-}$ mouse eyes were fixed in Karnovsky's fixative and embedded in resin. 2 µm semithin sections were cut and stained with toluidine blue by Robin Howes. Images were obtained using a 20X objective. (A&C) Young mice were 7-8 weeks old and (B&D) aged mice were 1 year old. GCL, ganglion cell layer; IPL, inner plexiform layer; INL, inner nuclear layer; OPL, outer plexiform layer; ONL, outer nuclear layer; IS, inner segments; OS, outer segments; RPE, retinal pigment epithelium. Scale bar represents 20 µm. (E) Average nuclei number in 100 µm^2 area of the ONL. Data are means ± S.D., n=3. Student t-tests were applied to data, * p = < 0.05.

4.2. Ultrastructural analysis reveals both ageing and *Cfh* deletion affect the positioning of mitochondria and melanosomes in RPE

A healthy functioning RPE is key in maintaining homeostasis across the retina, and age-related changes are well documented in the RPE (see Sections 1.4.4.1-5). *Cfh* gene knock-out reversed some of these age-related ultrastructural changes and advanced others, when examined in 2 year old mice (Coffey *et al.,* 2007). In order to allow detailed ultrastructural examination of the RPE, transmission electron micrographs were prepared from 7-8 week (Figure 4.2) and 1 year (Figure 4.3) $Cfh^{-/-}$ and wild-type mice. It was reported that in 2 year wild-type mice, electron-dense material accumulates in the basal region within the RPE and that this is decreased in $Cfh^{-/-}$ retinas (Coffey *et al.,* 2007). In both young and 1 year old samples, electron micrographs showed clear basal infoldings with no sign of any accumulation of electron-dense material towards the basal surface. In both $Cfh^{-/-}$ and wild-type samples there was an expected increase in lipofuscin with age which is consistent with previous studies (Wing *et al.,* 1978), although levels of lipofuscin did not appear significantly different between genotypes. Ageing was associated with a large proportion of photoreceptors dissociating from the apical processes of the RPE in both $Cfh^{-/-}$ and wild-type mice. However, we did not observe photoreceptors lying horizontally across the RPE as was observed in the 2 year $Cfh^{-/-}$ retinas (Coffey *et al.,* 2007).

A. Young Wild-Type

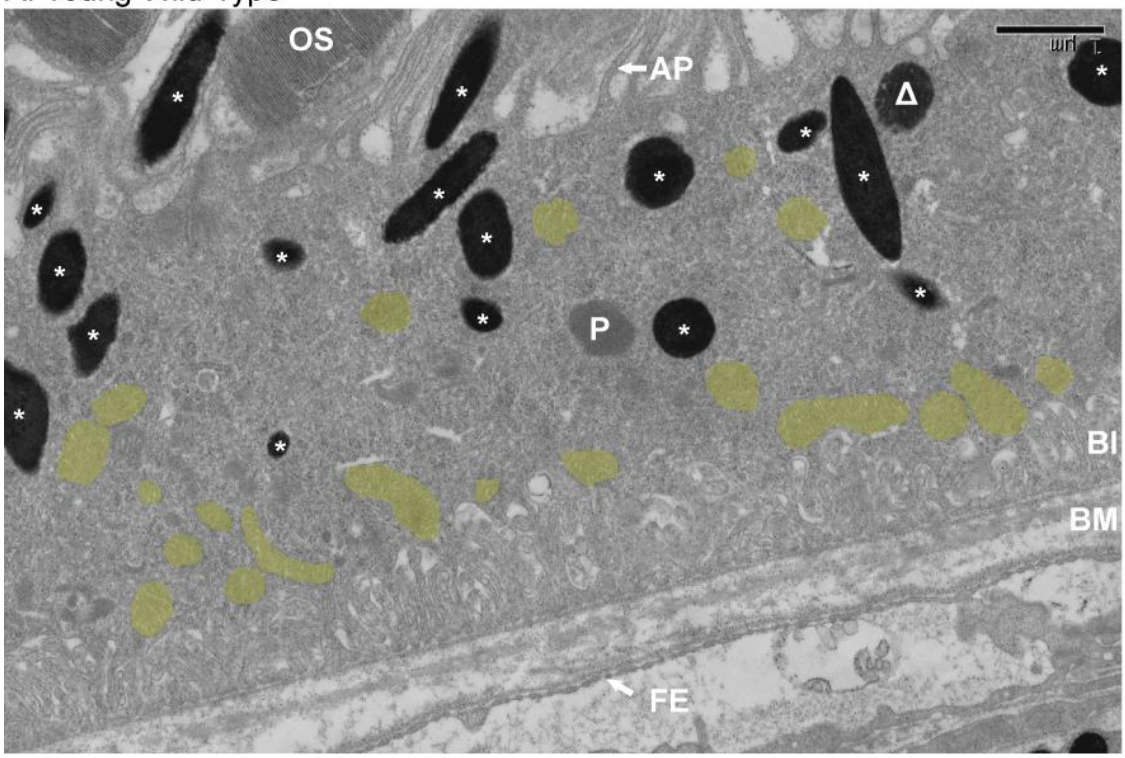

B. Young *Cfh*$^{-/-}$

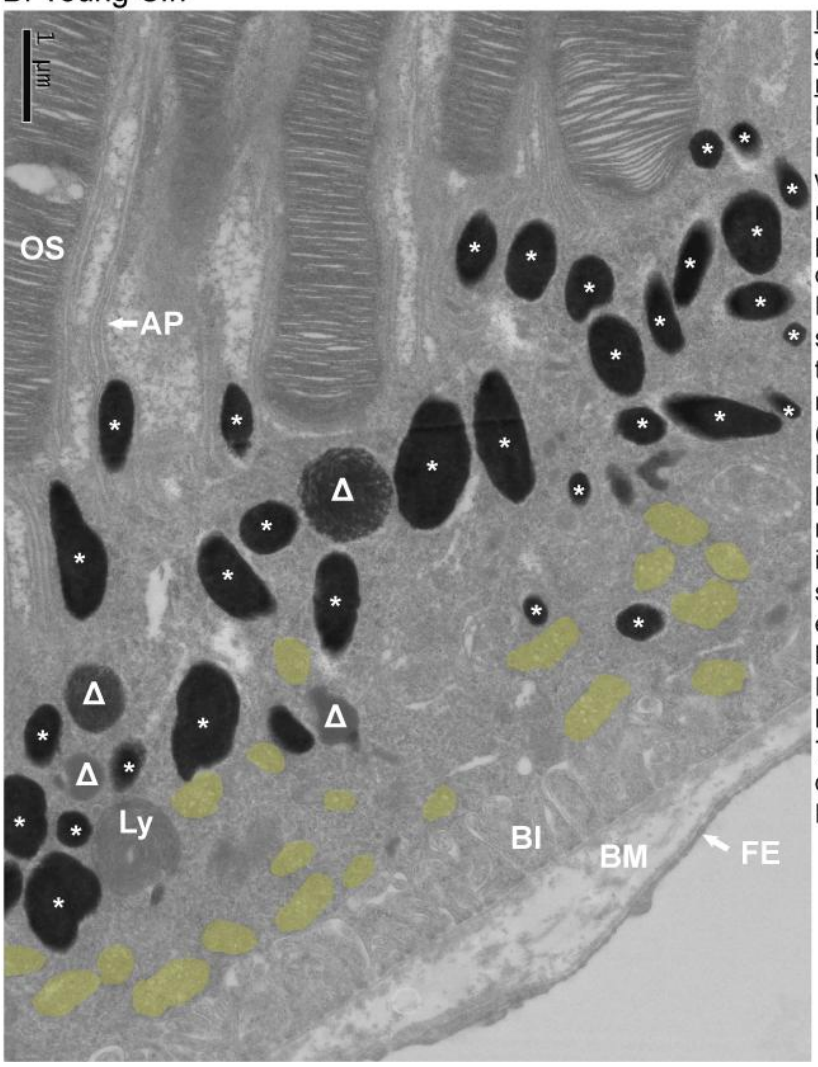

Figure 4.2. Transmission electron micrographs of mouse RPE

Representative images of RPE from 7-8 week old (A) wild-type and (B) *Cfh*$^{-/-}$ mice. Images show the polarised distribution of organelles in RPE. Electron-dense melanosomes (marked with *) tend to be apical with respect to mitochondria (yellow) which are basal. P, phagosome; Ly, lysosome; Δ; maturing melanosome (not counted in analysis); OS, outer segments; AP, apical processes; BM, Bruch's membrane; BI, basal infoldings; FE, fenestrated endothelium of the choriocapillaris. 70-80 nm sections were cut and stained by Robin Howes.

A. Aged Wild-Type

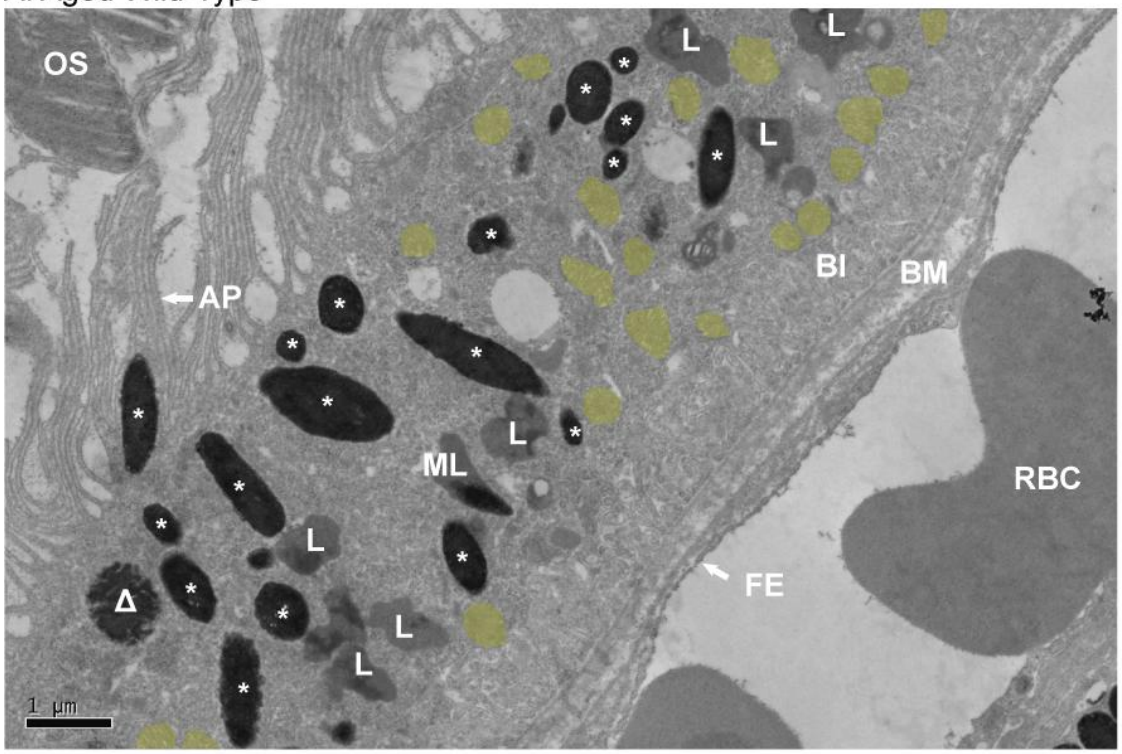

B. Aged *Cfh*$^{-/-}$

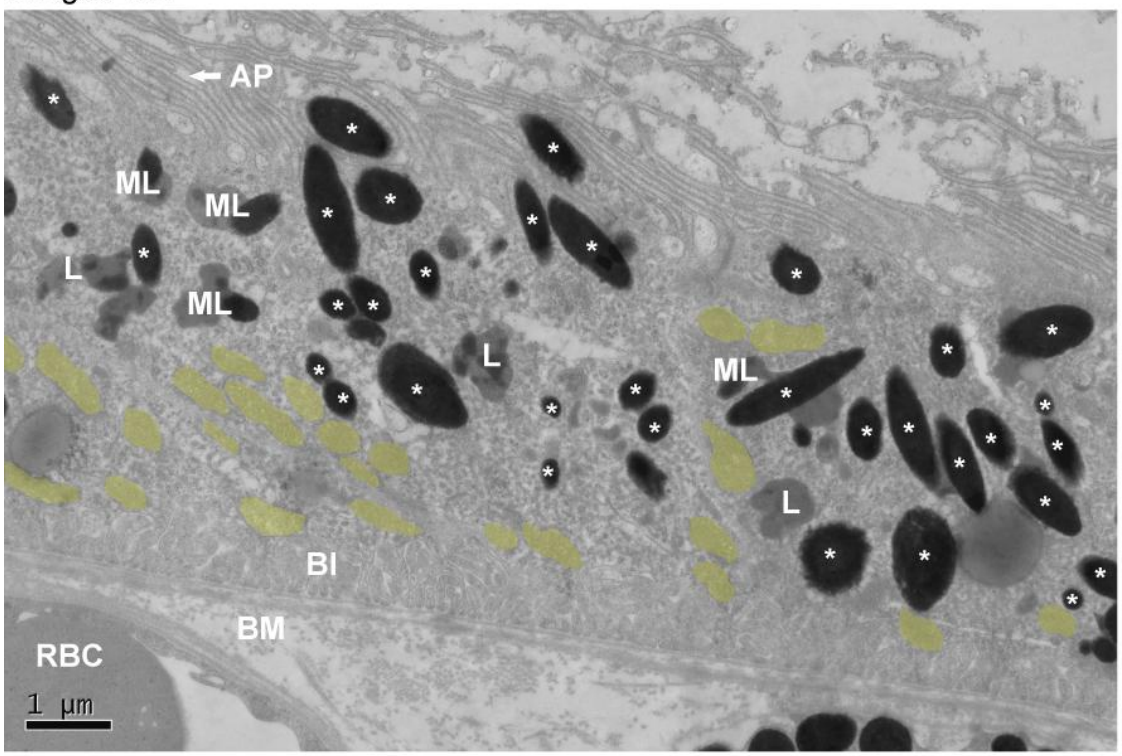

Figure 4.3. Transmission electron micrographs of aged mouse RPE

Representative images of RPE from 1 year old (A) wild-type and (B) *Cfh*$^{-/-}$ mice. Images show the polarised distribution of organelles in RPE. Electron-dense melanosomes (marked with *) tend to be apical with respect to mitochondria (yellow) which are basal. OS, outer segments; AP, apical processes; L, lipofuscin; ML, melano-lipofuscin; BM, Bruch's membrane; BI, basal infoldings; FE, fenestrated endothelium of the choriocapillaris. 70-80 nm sections were cut and stained by Robin Howes.

In the 2 year *Cfh*$^{-/-}$ animals it was reported that melanin and lipofuscin-containing organelles were more evenly distributed throughout the cell compared to age-matched wild-type controls where they were predominantly apical. The previous study did not address the localisation of mitochondria. In light of this, we analysed the distribution of both mitochondria and melanosomes in the RPE of both young (7-8 weeks) and aged (1 year) *Cfh*$^{-/-}$ and age-matched wild-type mice (Figure 4.4). The cross-sectional depth of the RPE cells, measured from the basal lamina to the base of the apical processes, was not significantly different across the four groups with an average height of 5 μm. Mitochondria are normally localised towards the basal side of RPE where there is a large energy demand (Gouras *et al.,* 2010). The distribution of mitochondria was unaffected by the loss of CFH at 7-8 weeks (Figure 4.4A). However, ageing caused mitochondria in wild-type RPE to become less polarised and were on average further from the basal lamina which is consistent with published data (Mishima and Kondo, 1981). In 1 year *Cfh*$^{-/-}$ samples we observed the opposite whereby mitochondria were found closer to the basal lamina.

Melanosomes are typically polarised towards the apical surface of RPE. Their position is suited to the absorption of scattered light, and thus protection of free radical generation in the basally arranged mitochondria. In wild-type retinas, melanosomes were on average 2 μm further from the basal lamina than mitochondria and their position were not altered with ageing (Figure 4.4B) However, in the RPE of young *Cfh*$^{-/-}$ mice, melanosomes were slightly more apical than in wild-type mice. In contrast, in 1 year *Cfh*$^{-/-}$ retinas, the opposite effect was observed, in that melanosomes were less polarised and on average 1 μm from mitochondria. These analyses show that in 1 year *Cfh*$^{-/-}$ samples the basal polarity of mitochondria was accentuated, whereas there was a loss of apical polarity of melanosomes.

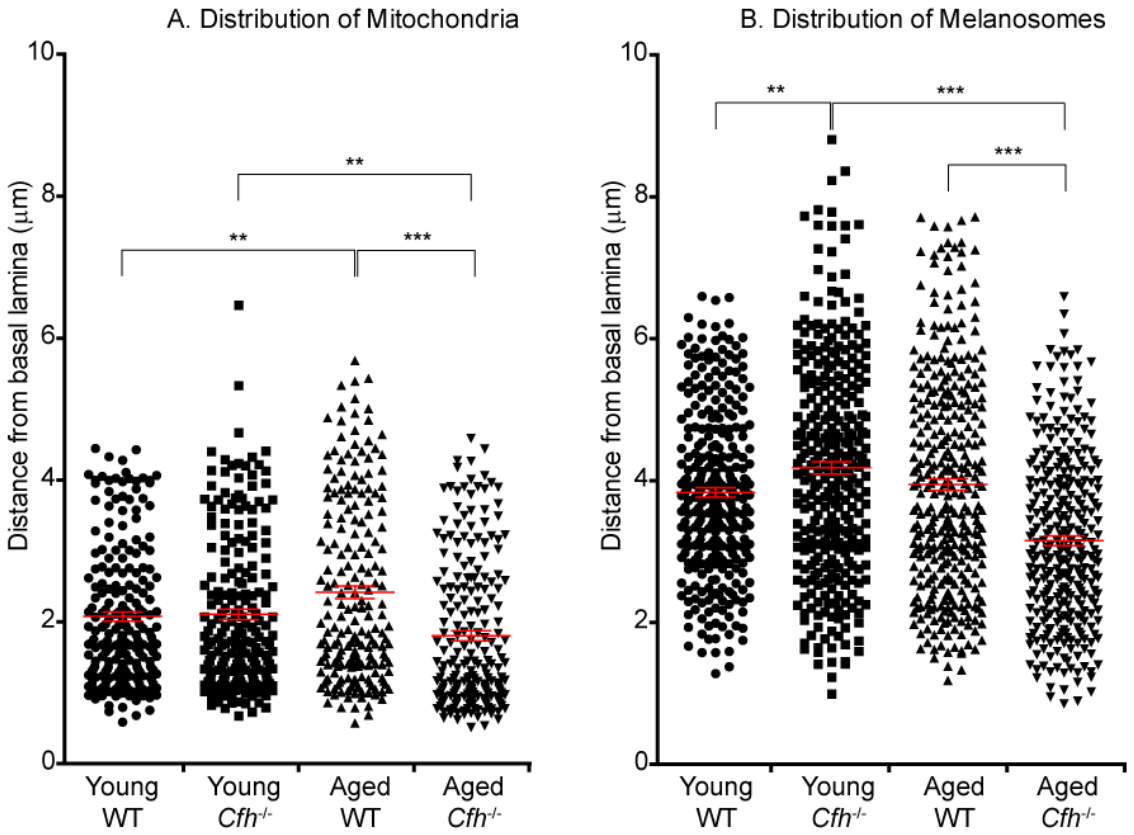

Figure 4.4. Analysis of the effect of ageing and *Cfh* gene deletion on the distribution of organelles in mouse RPE

The distance of (A) mitochondria or (B) melanosomes from the basal lamina was measured from electron micrographs of the RPE. The scatter plots show quantification of >200 mitochondria and >300 melanosomes per group where each dot represents one organelle. n=2 for each group. Unpaired Student t-tests were applied to data, **, p = < 0.01, ***, p = < 0.001.

4.3. Retinal function is impaired in 1 year *Cfh*$^{-/-}$ mice

In order to assess whether the morphological changes described here had any functional significance we performed ERGs. ERGs measure the electrical response of the retina to flashes of light stimuli by placing a small electrode on the surface of the cornea. A normal ERG trace is composed of a negative a-wave followed by a positive b-wave. The a-wave records largely the activity of the photoreceptors whereas the b-wave is mainly due to depolarisation of intermediate neurons in response to photoreceptor stimulation. Dark-adapted 1 year *Cfh*$^{-/-}$ and age-matched wild-type mice were exposed to flashes of light of increasing intensity. Overlaid scotopic ERG traces from both *Cfh*$^{-/-}$ and wild-type mice showed clear a- and b- waves (Figure 4.5A-B). Retinal function was assessed between groups by comparing the amplitude and time to peak for each wave. The amplitudes of both the a- and b-waves were not significantly different in 1 year *Cfh*$^{-/-}$ mice compared to wild-type controls (Figure 4.5C-

D), and were similar to values reported in other 1 year pigmented mice (Chang *et al.,* 2008). However, the time to reach the peak of the a- and b-wave was modestly increased in the 1 year *Cfh*$^{-/-}$ mice compared to wild-type (Figure 4.5E-F). An ANOVA showed that this increase was significant for the a-wave ($p = 0.004$) but not for the b-wave. An unpaired Student t-test for each light intensity revealed that half of the a-wave measurements were significantly increased in *Cfh*$^{-/-}$ mice. The slower response of the b-wave was not statistically significant. Given that the a-wave was significantly slower, the fact that the time to reach the peak of the b-wave (which is measured from t0) was not significantly different, suggests that neuronal activity after the photoreceptor response was not affected by the loss of CFH.

After recording scotopic ERGs, mice were light-adapted for photopic ERGs in order to assess their cone-mediated responses. In rodents, photopic ERG recordings are smaller than scotopic measurements because cones account for only 3% of photoreceptors (Carter-Dawson and LaVail, 1979). Overlaid photopic ERG traces from both *Cfh*$^{-/-}$ and wild-type mice showed small a-wave responses at higher light intensities but clear b-wave responses at lower light intensities (Figure 4.6A-B). Measurements of the a- and b-wave amplitudes showed no significant difference between 1 year *Cfh*$^{-/-}$ and age-matched wild-type controls (Figure 4.6C-D). There were also no significant differences in the time to peak for both the a- and b-wave responses (Figure 4.6E-F). These results suggest that cone-mediated vision is unaffected by the loss of CFH in mice at 1 year of age.

VEPs were recorded simultaneously to confirm that neuronal stimulation in the eye elicited subsequent neuronal activity in the visual cortex. VEP recordings from both *Cfh*$^{-/-}$ and wild-mice showed a negative wave that followed the b-wave of the ERG, indicating normal neural transmission (data not shown). Comparing the amplitude and time to peak for the negative wave of *Cfh*$^{-/-}$ to wild-type mice did not show any significant differences.

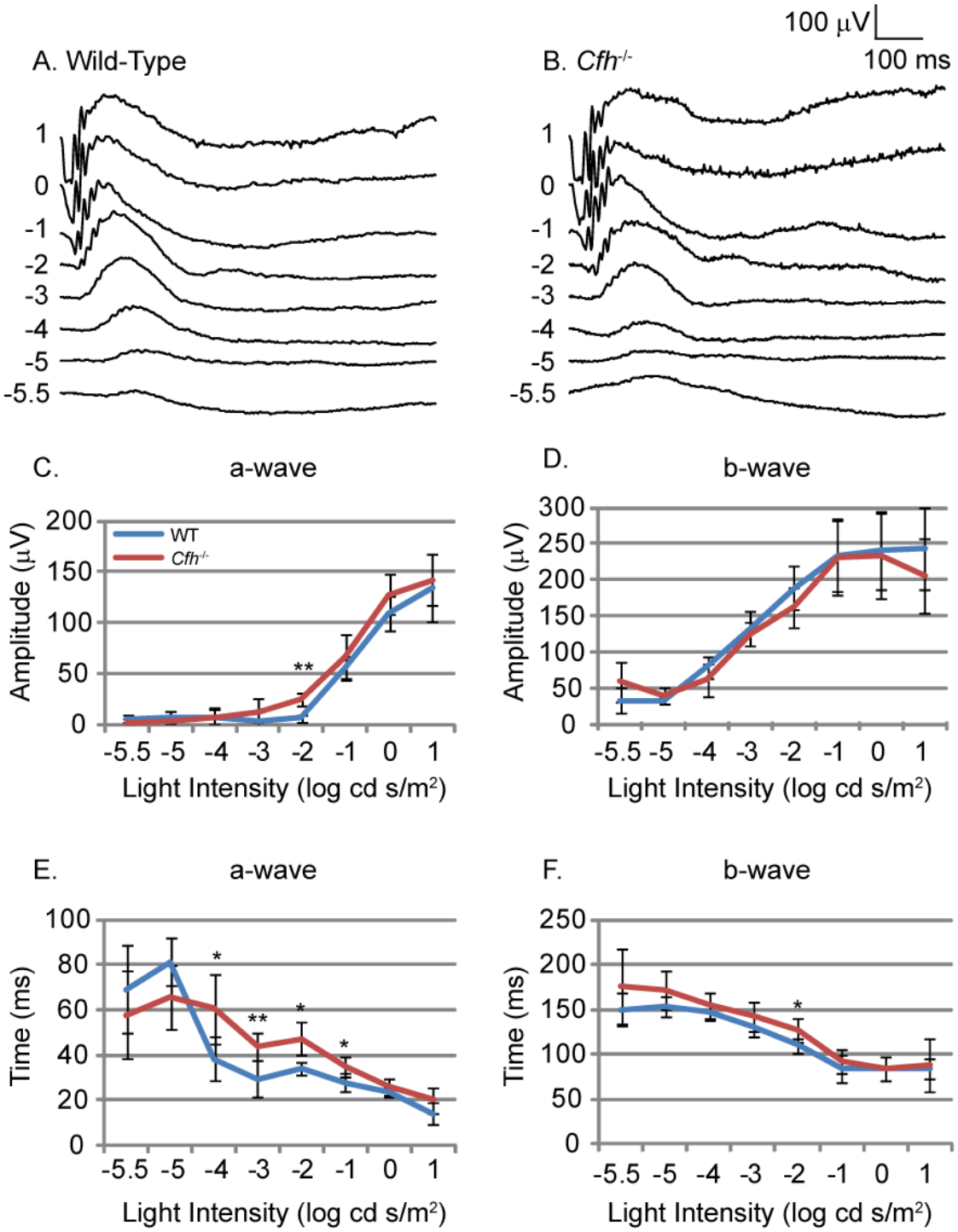

Figure 4.5. Electroretinogram response to light under scotopic condtions in *Cfh-/-* and wild-type age-matched mice

Electrophysical assessment of retinal function by ERG was performed on 1 year old *Cfh*$^{-/-}$ and wild-type (WT) mice. Dark adapted mice were used to assess scotopic neural retinal responses. (A and B) Representative ERG traces in response to flash stimuli of increasing log intensity. Mean amplitude of the (C) a-wave and (D) b-wave measured from wild-type (blue line) and *Cfh*$^{-/-}$ (red line) mice. Time to peak of the (E) a-wave and (F) b-wave measured from wild-type and *Cfh*$^{-/-}$ mice. WT n = 6, KO n = 5. Unpaired Student t-tests were applied to data,* p = < 0.05, ** p = < 0.01. ANOVA showed a significant increase in time to peak of a-wave (p = < 0.01). ERG recordings were performed in conjunction with Dr. E. Rebecca Longbottom.

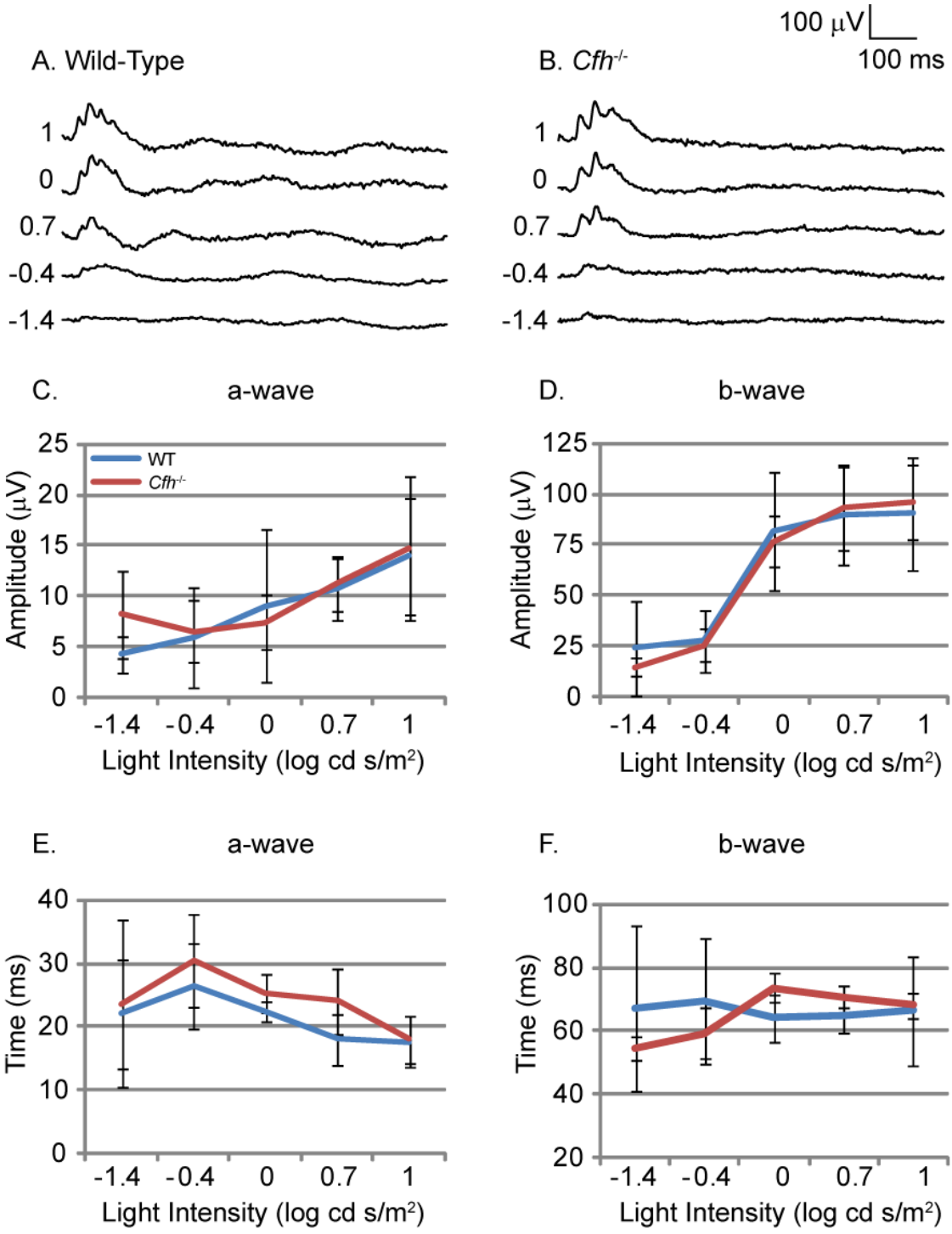

Figure 4.6. Electroretinogram response to light under photopic condtions in *Cfh*-/- and wild-type age-matched mice

Electrophysical assessment of retinal function by ERG was performed on 1 year old *Cfh*$^{-/-}$ and wild-type mice. Light adapted mice were used to assess photopic neural retinal responses. (A and B) Representative ERG traces in response to flash stimuli of increasing log intensity. Mean amplitude of the (C) a-wave and (D) b-wave measured from wild-type (blue line) and *Cfh*$^{-/-}$ (red line) mice. Time to peak of the (E) a-wave and (F) b-wave measured from wild-type and *Cfh*$^{-/-}$ mice. WT n = 6, KO n = 5. ERG recordings were performed in conjunction with Dr. E. Rebecca Longbottom.

4.4. Stress related responses in the retina of 1 year *Cfh*$^{-/-}$ mice

In view of the previous results suggesting features of accelerated ageing in the absence of CFH, we examined whether there were other signs of retinal stress in 1 year *Cfh*$^{-/-}$ mice. In the 2 year *Cfh*$^{-/-}$ animals it was reported that in some photoreceptors, short-wavelength cone opsin was redistributed into the apical compartment of the cell (Coffey *et al.,* 2007). Mislocalisation of opsins can indicate RPE dysfunction and may precede photoreceptor degeneration (Zhang *et al.,* 2011). However, immunohistochemical staining of *Cfh*$^{-/-}$ and wild-type retinas for short-wavelength cone opsin showed normal distribution localised to the outer segments in both young (7-8 weeks) and aged (1 year) mice (Figure 4.7).

Another indicator of retinal stress is up-regulation of expression of glial fibrillary acidic protein (GFAP). GFAP, an intermediate filament protein, is expressed by astrocytes and the endfeet of Müller cells in the GCL. In retinas stressed by injury or disease pathologies, GFAP expression is up-regulated in what is termed reactive gliosis (Bringmann *et al.,* 2006). GFAP expression in the wild-type and young *Cfh*$^{-/-}$ retinas was restricted to astroglia in the GCL (Figure 4.8A-C). However, in 1 year *Cfh*$^{-/-}$ mice the GFAP positive cell processes were more disorganised than the structures seen in the control retinas. Additionally these processes were seen extending towards the IPL (Figure 4.8D), indicating that astroglial activation is evident in 1 year *Cfh*$^{-/-}$ retinas.

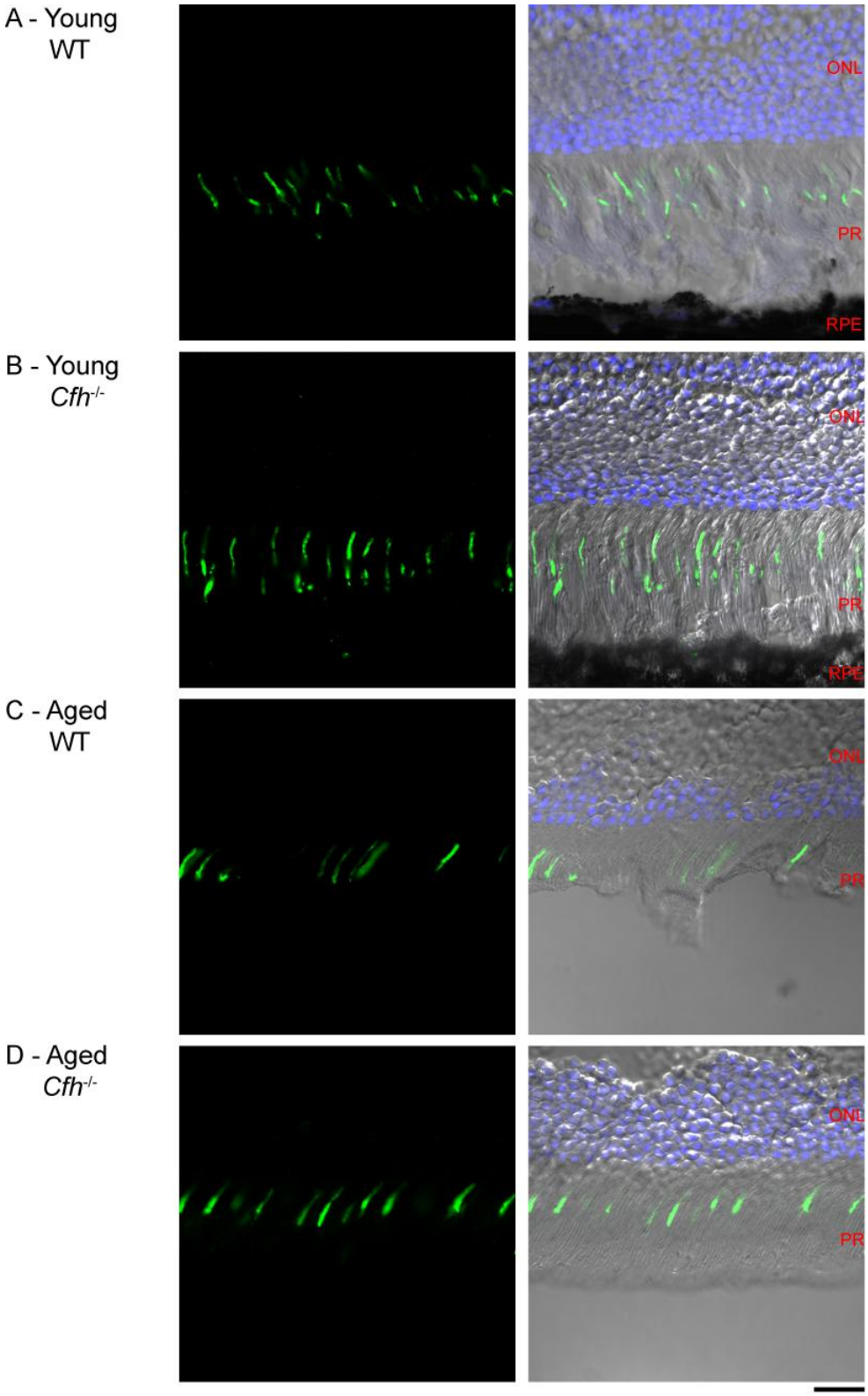

Figure 4.7. Distribution of short-wavelength cone opsin in *Cfh-/-* and wild-type mice
12 μm sections from (A&B) young (7-8 weeks) or (C&D) aged (1 year) (A&C) wild-type or (B&D) *Cfh*$^{-/-}$ fixed mouse eyes were stained for short-wave cone opsin (green) and nuclei (blue). Sections were imaged using confocal and differential inteference contrast microscopy. Dissociation of the photoreceptors from RPE in aged samples was a common occurence. ONL, outer nuclear layer; PR, photoreceptors; RPE, retinal pigment epithelium. Images represent three independent experiments. Scale bar represents 20 μm.

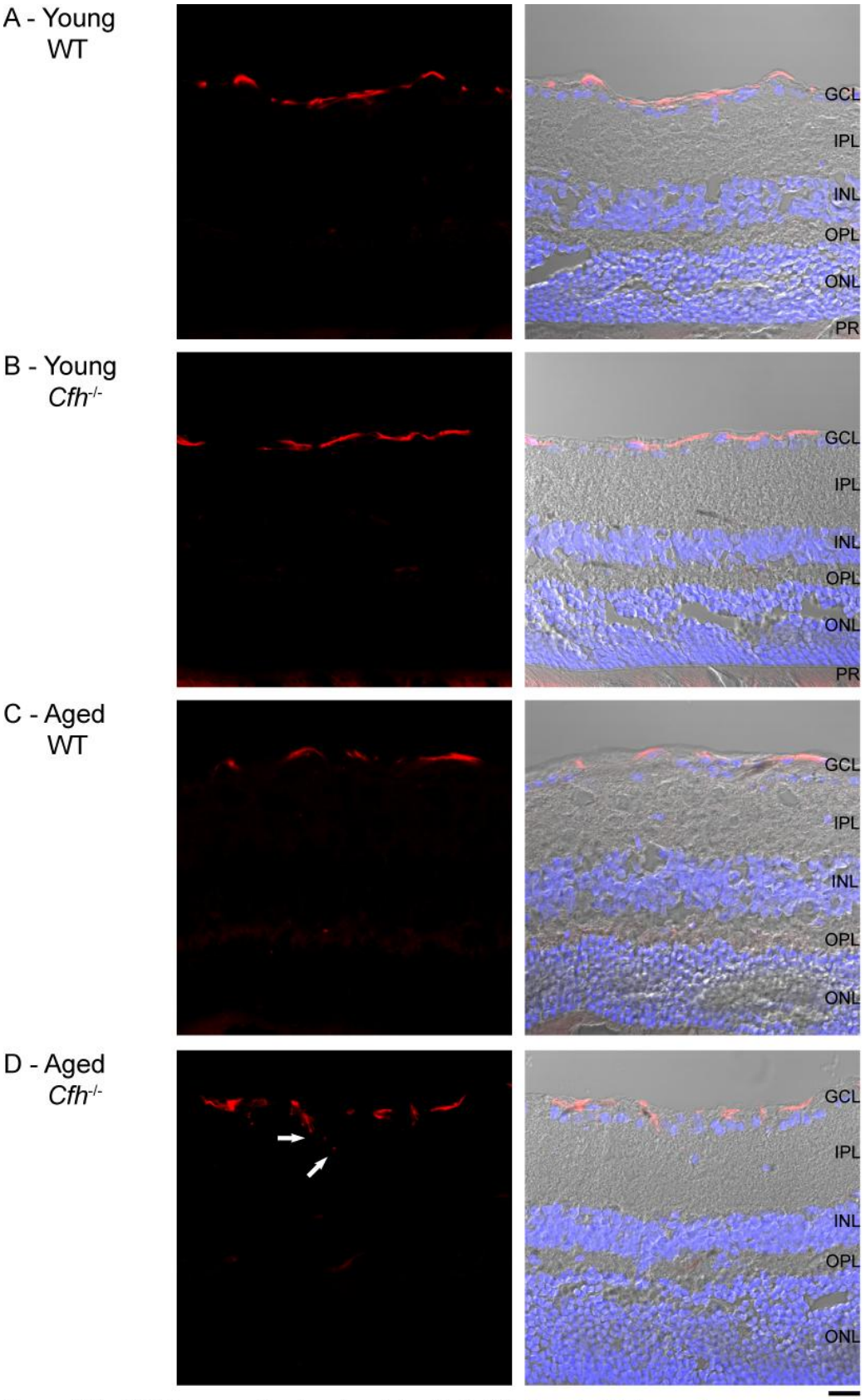

Figure 4.8. GFAP expression in astroglial cells in *Cfh-/-* and wild-type mice

12 μm sections from (A&B) young (7-8 weeks) or (C&D) aged (1 year) (A&C) wild-type or (B&D) *Cfh*$^{-/-}$ fixed mouse eyes were stained for GFAP (red) and nuclei (blue). Sections were imaged using confocal and differential inteference contrast microscopy. Arrows indicate astrocytic processes extending into IPL. GCL, ganglion cell layer; IPL, inner plexiform layer; INL, inner nuclear layer; OPL, outer plexiform layer, ONL, outer nuclear layer; PR, photoreceptors. Images represent three independent experiments. Scale bar represents 20 μm.

4.5. Organisation of the retinal vasculature is unaffected by the loss of CFH

Previous reports on 1 and 2 year *Cfh*$^{-/-}$ mice generated conflicting data on whether the retinal vasculature is affected by the loss of CFH. The retinal vasculature is organised into three plexuses, the inner, intermediate and deep (see Section 1.3.4). Previous research has suggested that the deep plexus of 1 year *Cfh*$^{-/-}$ mice is significantly withered and has a reduced density when imaged by fluorescein angiography (Lundh von *et al.,* 2009). We examined the retinal vasculature by flatmounting whole retinas to allow analysis of each plexus by confocal microscopy. Flatmounts of young (7-8 weeks) and 1 year *Cfh*$^{-/-}$ and age-matched wild-type retinas were stained for collagen IV in the basement membrane, C3 and mouse IgG within vessels. In all retinas examined, the three plexuses could clearly be identified by collagen IV and IgG staining (Figures 4.9-10, data for intermediate and deep plexuses not shown) and no differences were observed between wild-type and *Cfh*$^{-/-}$ retinas. As expected, C3 was present in the blood vessels of all three plexuses in wild-type mice. However C3 staining was weak in the deep and intermediate plexuses of the *Cfh*$^{-/-}$ retinas but was stronger in larger vessels in the inner plexus though still below the level seen in wild-type retinas. This is consistent with previous reports showing that plasma in *Cfh*$^{-/-}$ mice is deficient for C3 because its breakdown is able to continue unhindered (Pickering *et al.,* 2002). Electron micrographs did not reveal any major structural defects in the retinal vessels of *Cfh*$^{-/-}$ mice (data not shown).

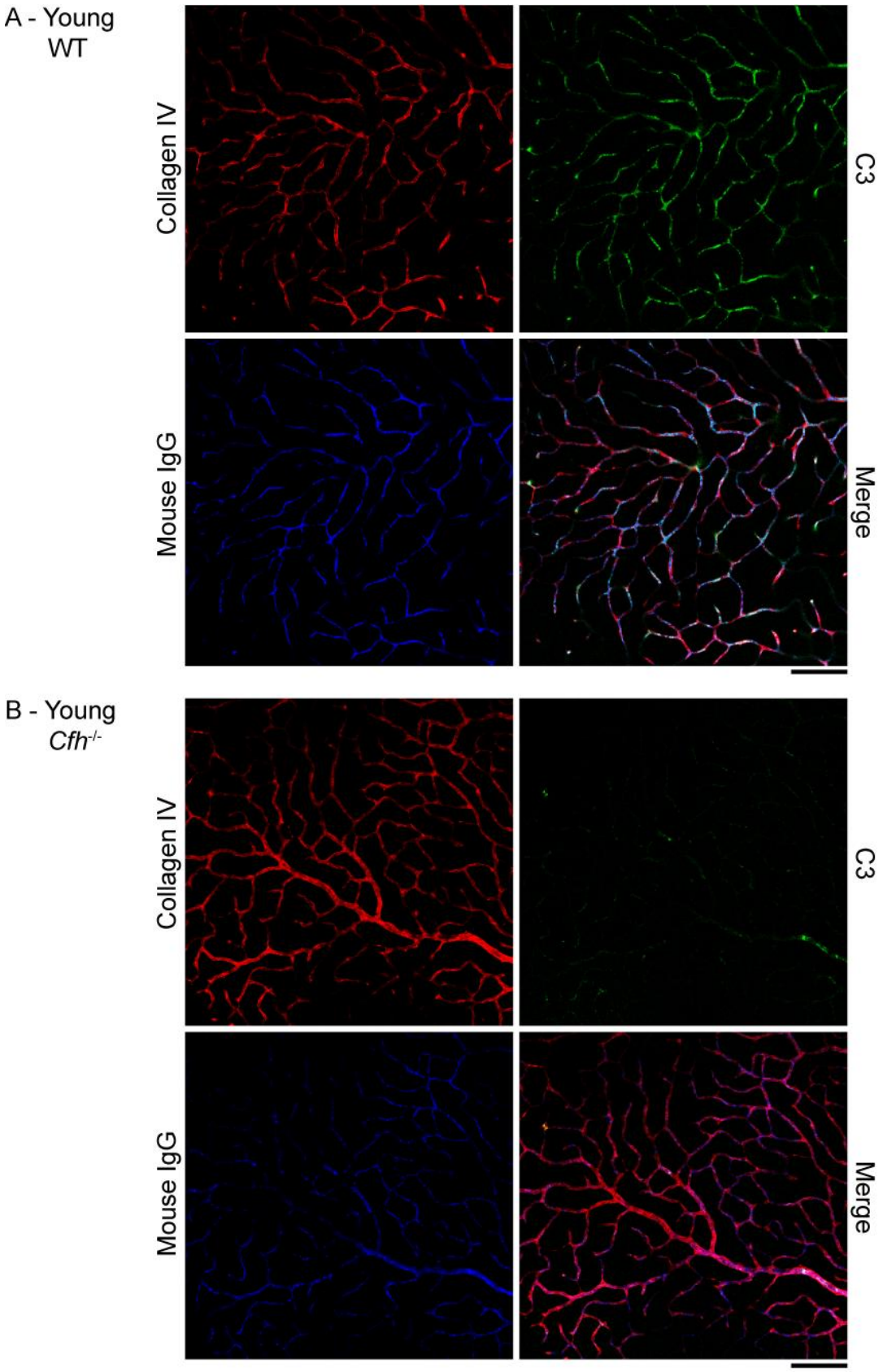

Figure 4.9. The organisation of the deep plexus of the retinal vasculature is unaffected by the loss of CFH in young mice

Neuroretinas from young (7-8 weeks) (A) wild-type and (B) *Cfh*$^{-/-}$ mice were flatmounted and fixed in ice cold methanol. Vessels were stained for collagen IV (red), C3 (green) and mouse IgG (blue) and imaged using confocal microscopy. *Cfh*$^{-/-}$ mice show reduced levels of circulating C3. Images represent three independent experiments. Scale bars represent 100 μm.

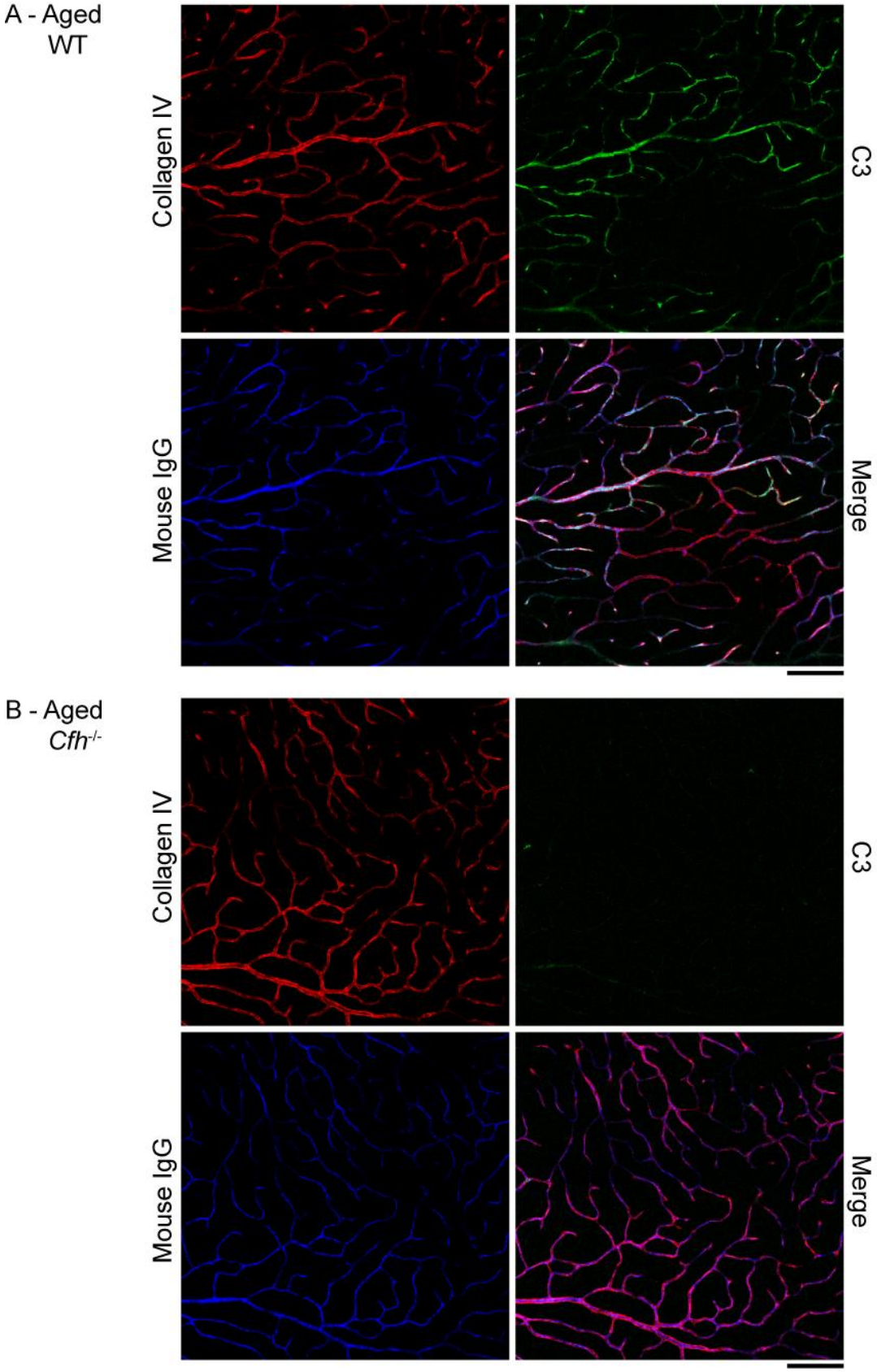

Figure 4.10. The organisation of the deep plexus of the retinal vasculature is unaffected by the loss of CFH in aged mice

Neuroretinas from aged (1 year) (A) wild-type and (B) *Cfh*$^{-/-}$ mice were flatmounted and fixed in ice cold methanol. Vessels were stained for collagen IV (red), C3 (green) and mouse IgG (blue) and imaged using confocal microscopy. *Cfh*$^{-/-}$ mice show reduced levels of circulating C3. Images represent three independent experiments. Scale bars represent 100 μm.

4.6. Activated C3 breakdown products are increased in the retinal vasculature of 1 year *Cfh*$^{-/-}$ mice

Since there is a continual breakdown of C3 in the plasma of *Cfh*$^{-/-}$ mice, we investigated whether by-products of C3 breakdown were present in the retinas of young and 1 year *Cfh*$^{-/-}$ mice and compared this to age-matched wild-type controls. Lundh von *et al.,* (2009) reported C3b deposition along endothelial surfaces of inner and deep retinal vessels of 1 year *Cfh*$^{-/-}$ mice which correlated with vascular constrictions. Flatmounted retinas were stained for C3b, iC3b and C3c. Breakdown products were faintly observed at a similar intensity in the vessels of the deep and intermediate plexuses for both *Cfh*$^{-/-}$ and wild-type retinas in young and 1 year mice (data not shown). Brighter staining was detected in vessels of the inner plexus (Figure 4.11-12), with the most intense staining clearly associated with red blood cells in the larger vessels. C3b and iC3b-coated red blood cells appeared brighter in *Cfh*$^{-/-}$ mice compared to wild-type mice demonstrating the increase in C3 breakdown in *Cfh*$^{-/-}$ mice. Red blood cells express CR1, a receptor for C3b and iC3b, and this allows the clearance of complement-coated immune complexes to the liver for degradation (Fearon, 1980). Staining of breakdown products in the smaller vessels of the inner plexus did not have the definitive shape of red blood cells nor did staining localise to the walls of the vessels but rather looked to be diffuse within vessels. 1 year *Cfh*$^{-/-}$ mice had an increase in C3 breakdown products which appeared diffuse within the smaller vessels of the inner plexus in comparison to 1 year wild-type controls. No accumulation of C3 breakdown products was observed in the RPE or Bruch's membrane region (data not shown).

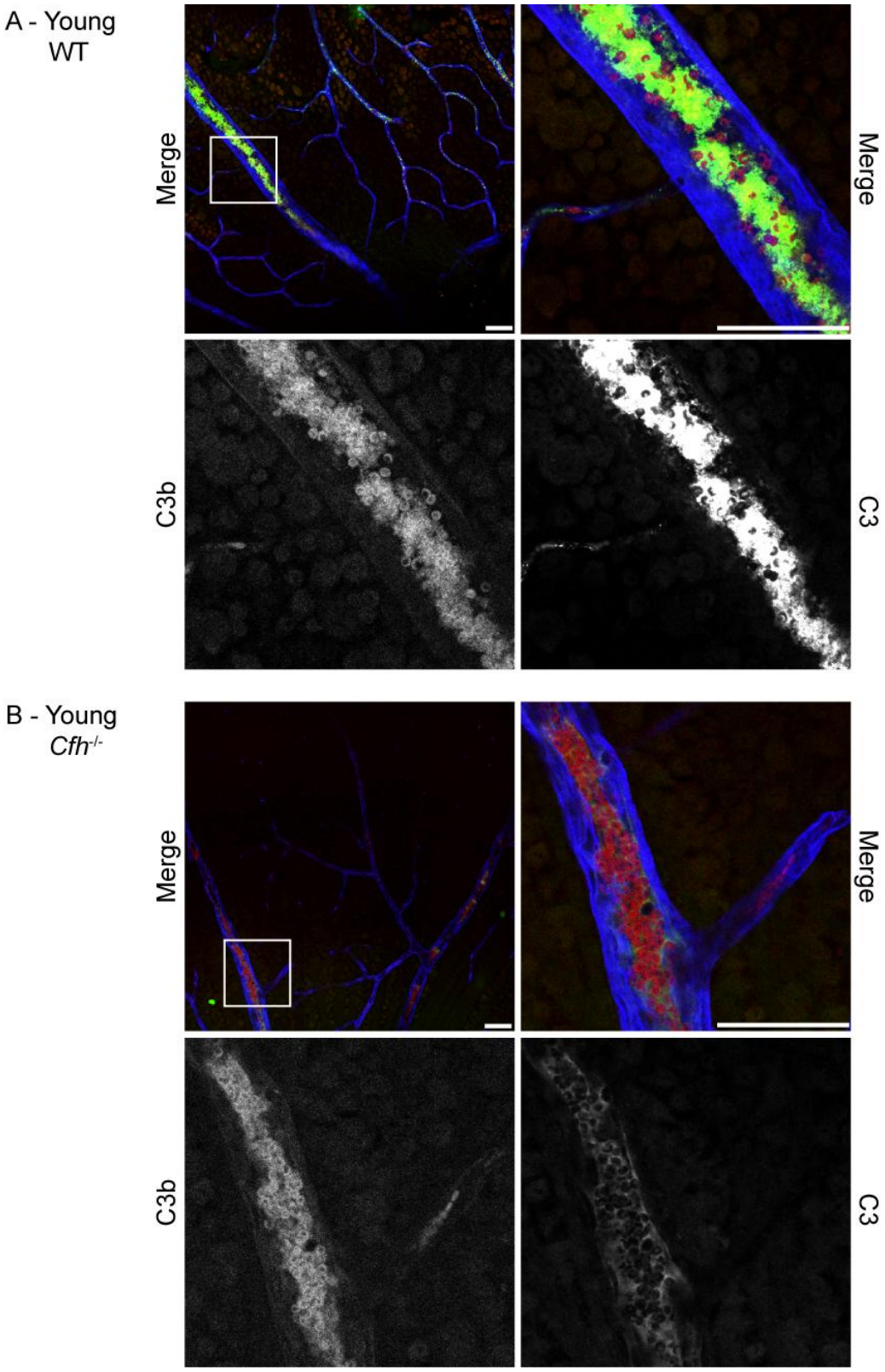

Figure 4.11. C3 and C3 activation fragments in the inner retinal vasculature of young wild-type and *Cfh*-/- mice

Neuroretinas from 7-8 week old (A) wild-type and (B) *Cfh*$^{-/-}$ mice were flatmounted and fixed in ice cold methanol. Vessels were stained for C3 (green), activated C3b/iC3b/C3c (red) and collagen IV (blue) and imaged using confocal microscopy. *Cfh*$^{-/-}$ mice show reduced levels of circulating C3 and enhanced levels of activation fragments on red blood cells. Scale bars represent 50 μm.

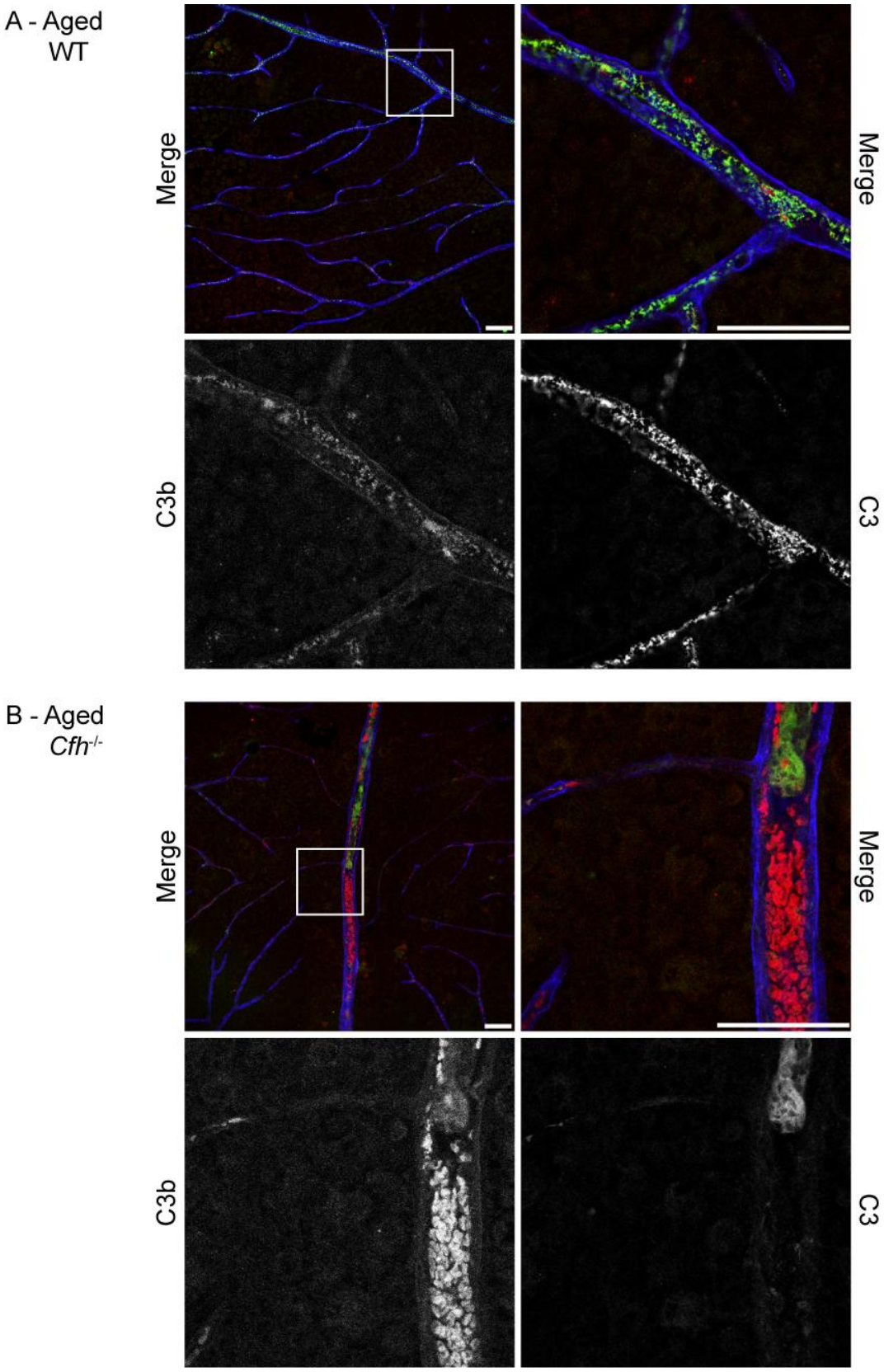

Figure 4.12. C3 and C3 activation fragments in the inner retinal vasculature of aged wild-type and *Cfh*-/- mice

Neuroretinas from 1 year old (A) wild-type and (B) *Cfh*$^{-/-}$ mice were flatmounted and fixed in ice cold methanol. Vessels were stained for C3 (green), activated C3b/iC3b/C3c (red) and collagen IV (blue) and imaged using confocal microscopy. *Cfh*$^{-/-}$ mice show reduced levels of circulating C3 and an increased level of activation fragments on red blood vessels and diffuse within smaller vessels. Scale bars represent 50 μm.

4.7. Expression of regulatory complement components in the retina

In view of the uncontrolled C3 breakdown in *Cfh*$^{-/-}$ mice, we explored whether there was activation of the complement pathway downstream of C3 in the retina. Neither C5 nor MAC staining were identified above that of the non-specific antibody control in either *Cfh*$^{-/-}$ or wild-type retinas (data not shown).

We speculated that the lack of downstream complement activation, when there is unregulated C3 breakdown, could be due to up-regulation of complement regulators that compensate for the loss of CFH. CRRY is a rodent-specific complement regulator which serves both the co-factor and decay-accelerating roles of CFH. Immunohistochemical staining of 1 year *Cfh*$^{-/-}$ and age-matched wild-type retinas showed increased expression of CRRY on the inner side of the OPL. In some retinas, the staining pattern appeared clustered around densely packed areas of ribbon synapses marked by bassoon (Figure 4.13).

DAF, like CFH can accelerate the decay of C3 convertases. Staining of DAF in retinal sections revealed positive staining in the GCL in wild-type mice which was unaffected by age (Figure 4.14A-B). This expression pattern was unchanged in young *Cfh*$^{-/-}$ mice (Figure 4.14C). In 1 year *Cfh*$^{-/-}$ retina, DAF antibody stained projections extending from the GCL into the IPL (Figure 4.14D). Positive staining was also present amongst the nuclei of the INL and in the OPL but did not extend into the ONL. Due to their different shape, it is unlikely that the DAF positive processes are the same as those positive for GFAP. We also attempted to examine the expression pattern of MIRL, a complement regulator which inhibits the formation of MAC. Testing two antibodies we were unable to identify specific staining that was different from that of the non-specific antibody control (data not shown).

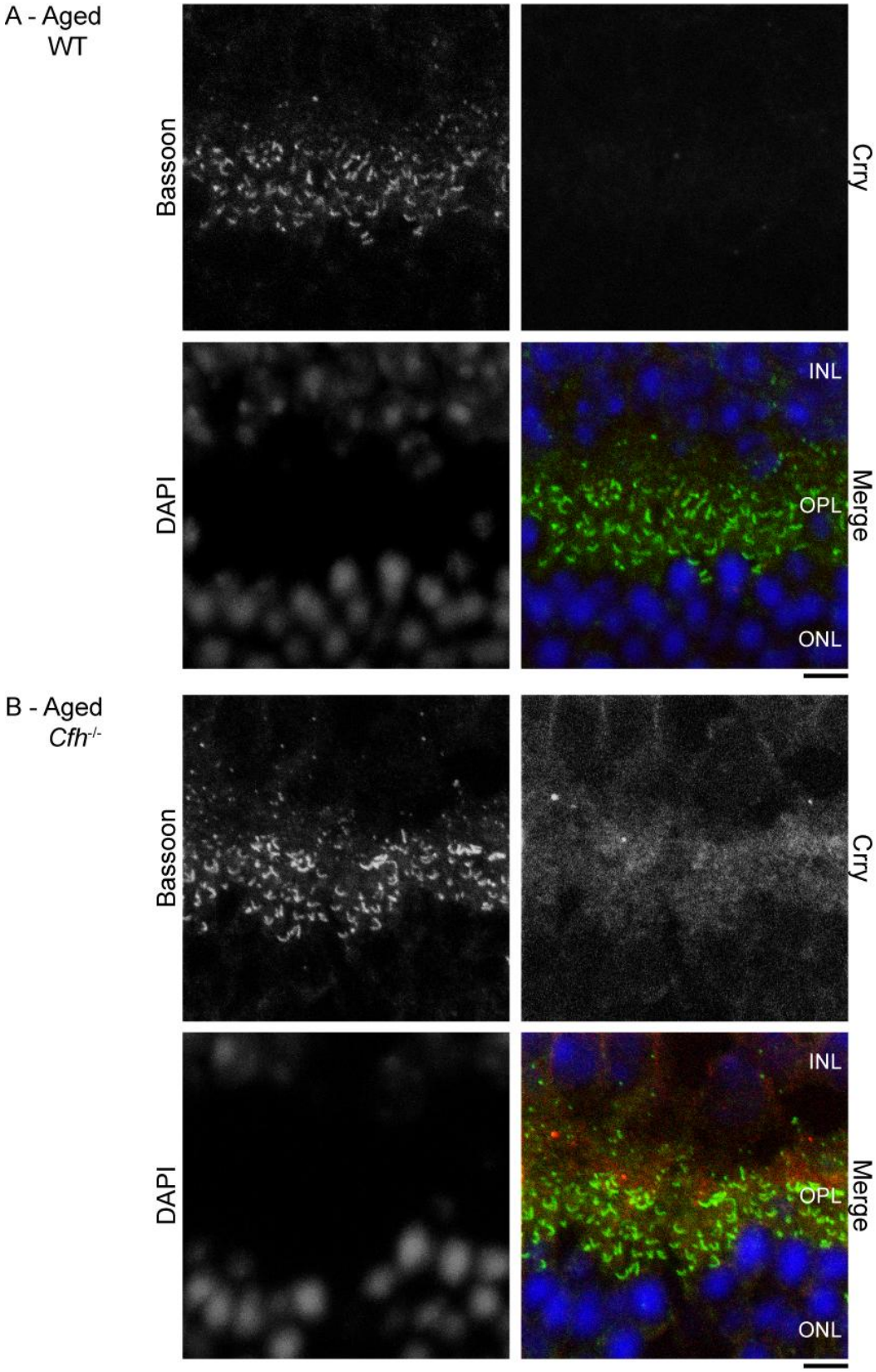

Figure 4.13. CRRY expression is enhanced in the outer plexiform layer of aged *Cfh-/-* mice
12 μm PFA fixed sections from 1 year (A) wild-type (WT) or (B) *Cfh*$^{-/-}$ mouse eyes were stained for bassoon (green), CRRY (red) and nuclei (blue). Z-stacks were imaged using confocal microscopy and projections of 2.7 μm are represented. INL, inner nuclear layer; OPL, outer plexiform layer; ONL, outer nuclear layer. Scale bars represent 5 μm.

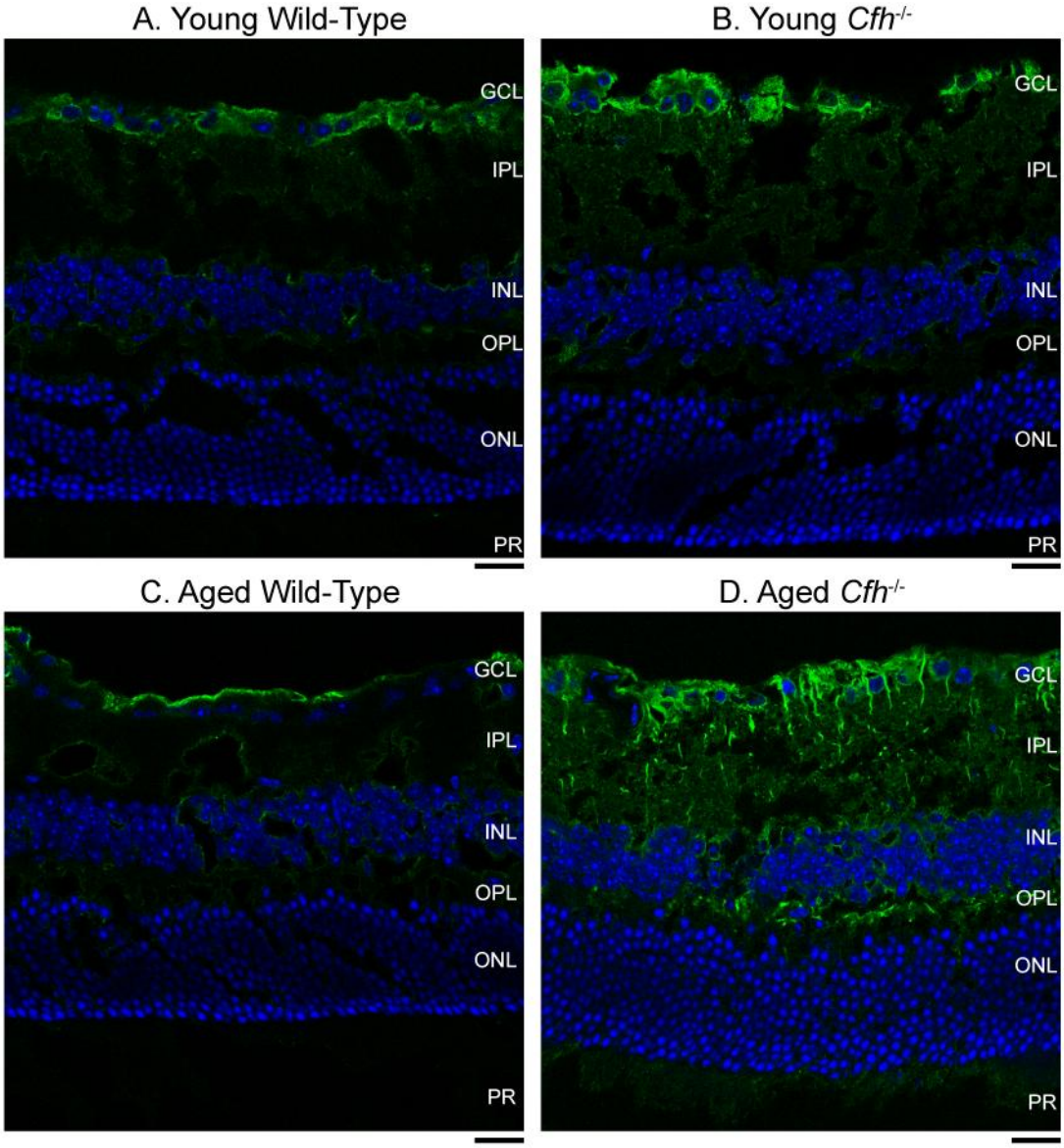

Figure 4.14. Decay-accelerating factor expression is enhanced in aged *Cfh*-/- mice
12 μm PFA fixed sections from (A & B) young (7-8 weeks) or (C & D) aged (1 year) (A & C) wild-type or (B & D) *Cfh*$^{-/-}$ mouse retina were stained for DAF (green) and nuclei (blue). Sections were imaged using confocal microscopy. GCL, ganglion cell layer; IPL, inner plexiform layer; INL, inner nuclear layer; OPL, outer plexiform layer; ONL, outer nuclear layer; PR, photoreceptors. Scale bars represent 20 μm.

4.8. Discussion

Ageing of the retina is a well characterised process in both the human and mouse. Ageing leads to structural and functional changes in all compartments of the retina including the neuroretina, RPE, Bruch's membrane and ocular perfusion. In wild-type mice this study showed several features which were consistent with normal ageing such as accumulation of lipofuscin in the RPE, a decrease in photoreceptor density, a higher propensity for the photoreceptors to detach and loss of polarisation of the mitochondria. The majority of these features which occurred in the ageing of wild-type mice also occurred in *Cfh*$^{-/-}$ mice except the loss of polarisation of mitochondria. Here we showed that mitochondria became more polarised with ageing in *Cfh*$^{-/-}$ mice. We speculate that this may reflect a higher energy requirement of the RPE in aged *Cfh*$^{-/-}$ RPE compared to age-matched wild-type mice.

Several features of ageing were not identified in this study, such as an accumulation of debris in the basal infoldings of the RPE or Bruch's membrane. Since we studied ageing from 7-8 weeks to 1 year we would not expect all features of ageing to be present.

Although analysing the effect of CFH deficiency at a young age was not the major focus of this study we revealed only two features of all those analysed which were different between young wild-type and *Cfh*$^{-/-}$ retinas. Firstly we showed that loss of CFH caused C3 depletion in the plasma of the retinal vessels. This is consistent with Pickering *et al.,* (2002) who show that C3 is markedly reduced in serum of *Cfh*$^{-/-}$ mice. Secondly we showed that melanosomes were more polarised towards the apical membrane in young *Cfh*$^{-/-}$ mice compared to young wild-type mice. We speculate that this may be an early defensive mechanism utilised by the RPE in response to enhanced C3b breakdown products. Peculiarly this feature was reversed when we compared 1 year wild-type mice to 1 year *Cfh*$^{-/-}$ mice. Here we found that melanosomes were less polarised in 1 year *Cfh*$^{-/-}$ RPE which suggests mild RPE dysfunction. However, in order to draw any firm conclusions, these analyses should be repeated in several more mice.

One of the aims of this study was to analyse whether any of the structural or functional defects found in 2 year *Cfh*$^{-/-}$ mice (Coffey *et al.,* 2007) were present in

younger *Cfh*$^{-/-}$ mice. We have observed that as in 2 year *Cfh*$^{-/-}$ mice, photoreceptors in 1 year *Cfh*$^{-/-}$ mice showed a greater tendency to detach from the apical processes of the RPE than age-matched wild-type controls. We took this analysis further by measuring the density of nuclei in the ONL, and showed that thinning of the photoreceptors was enhanced in 1 year *Cfh*$^{-/-}$ mice compared to age-matched wild-type controls. This may be due to a combination of neuroretinal stress and RPE dysfunction. Unlike in the 2 year *Cfh*$^{-/-}$ mice, ERG results showed that in the in 1 year *Cfh*$^{-/-}$ mice there was not a significant difference in the amplitude of either the a- or b-wave under scotopic conditions from age-matched wild-type controls. However we did see an increased time to peak of the scotopic a-wave in 1 year *Cfh*$^{-/-}$ mice compared to age-matched wild-type controls. This is perhaps an early indicator of the loss of visual function seen in older animals. Immunohistochemical analysis did not reveal any stress-related redistribution of opsins in the photoreceptors. However, we did find early signs of retinal stress in astroglia of 1 year *Cfh*$^{-/-}$ mice, characterised by GFAP staining. The shape and length of the GFAP positive cell processes suggested these cells were astrocytes rather than Müller cells. In order to confirm this, sections could be co-stained with a marker for astrocytes but not Müller cells and co-localisation quantified. In conclusion, we have shown early features of most of the structural and functional differences reported between 2 year *Cfh*$^{-/-}$ mice and age-matched wild-type controls.

One study on 1 year *Cfh*$^{-/-}$ mice proposed a role for CFH in ocular perfusion (Lundh von *et al.,* 2009). These investigators reported that the deep plexus of the retinal vessels is withered due to deposition of C3b along endothelial surfaces. However, in this study we observed that the retinal vasculature appeared normal in young and 1 year *Cfh*$^{-/-}$ mice and that there was no sign of C3b deposition on endothelial surfaces. The discrepancy between these reports may be due to fixation methods since unlike Lundh von *et al.,*(2009), we did not perfuse fix the retinas.

The presence of both structural and functional changes, although mild in the 1 year *Cfh*$^{-/-}$ mice, indicated that the retina was responsive to the deficiency of CFH by the age of 1 year. This led us to investigate whether the retina was able to compensate for the

deficiency in CFH by up-regulating other complement regulators. Here we have shown that there was indeed a redistribution of complement regulators in the retinas of 1 year *Cfh*$^{-/-}$ mice. The enhancement of complement regulation in the neuroretina suggests that this area is particularly vulnerable to complement activation, in light of which, it would be interesting to analyse the expression of CRRY and DAF in 2 year *Cfh*$^{-/-}$ mice.

Age-related ocular pathologies are often due to an added stress such as a genetic or environmental factor which makes the retina unable to cope with the normal ageing process. Here we show that many of the more severe structural and functional changes identified in 2 year *Cfh*$^{-/-}$ mice are not present in 1 year *Cfh*$^{-/-}$ mice. This highlights the importance of ageing in the pathology of 2 year *Cfh*$^{-/-}$ mice.

Chapter 5: Results

Microarray Analysis of RPE/Choroid and Neuroretina of *Cfh*$^{-/-}$ Mice

It is evident that ageing is a key contributor to the retinal phenotype in the 2 year old *Cfh*$^{-/-}$ mice since not all the functional and morphological changes were present in 1 year old *Cfh*$^{-/-}$ mice. With the aim of understanding the mechanisms involved in this process we used a genome-wide microarray in order to analyse the gene expression profile of both the RPE and neuroretina of *Cfh*$^{-/-}$ mice at 7-8 weeks and 16 months of age. This allowed us to analyse the effect of both *Cfh* genotype and ageing on the retinal gene expression. This analysis required processing two tissues (RPE/choroid and neuroretina) from six mice in each of the four groups (Figure 5.1). This work was carried out in collaboration with Dr. Carsten Faber (University of Copenhagen).

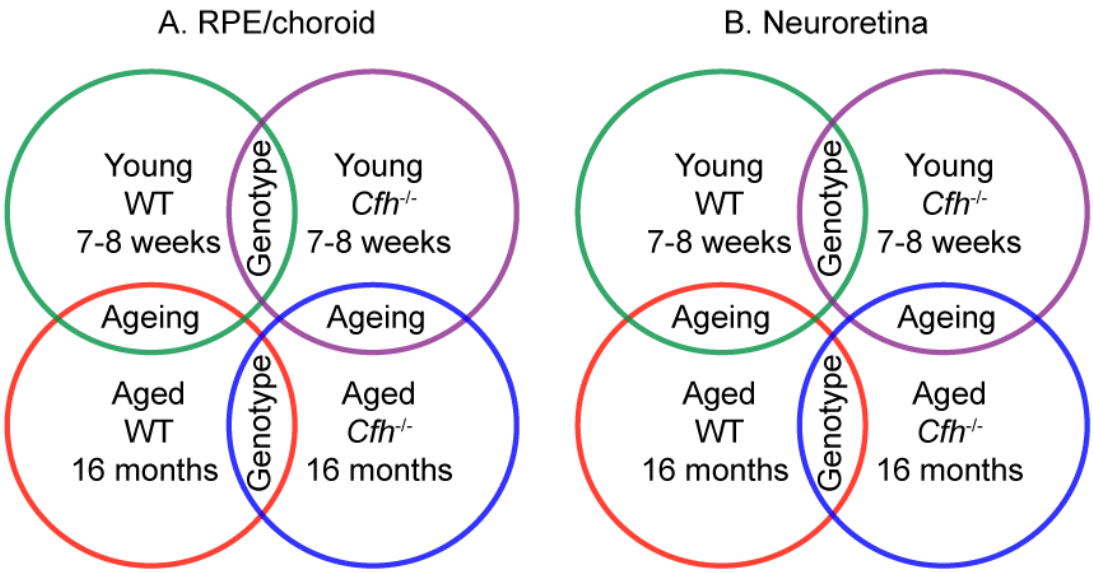

Figure 5.1. Groups of mice used for microarray analysis
RNA was isolated from two tissues (A) RPE/choroid and (B) neuroretina. Four groups of mice were used; young (7-8 weeks) and aged (16 months) *Cfh*$^{-/-}$ mice and age-matched wild-type (WT) controls. RNA was isolated from 6 mice per group, where both the RPE and neuroretina were isolated from each mouse. Four comparisons were made per tissue; the effect of *Cfh* genotype at a young and older age and the effect of ageing on wild-type and *Cfh*$^{-/-}$ mice. RNA isolation was carried out with equal contribution from Dr. Carsten Faber.

5.1. Isolation of RNA from RPE and neuroretina

Isolation of neuroretina was achieved by dissecting the posterior eyecup and peeling out the neuroretina. Isolation of RNA from the neuroretina gave a good yield of RNA, ranging from 3.8-6.4 μg RNA per pair of eyes. Since the RPE is a monolayer, isolation of sufficient RNA for microarray analysis required initial optimisation. First, separation of

the RPE from the choroid was attempted by incubation of posterior eyecups in trypsin or dispase. The yield of RNA using this method was low and to be suitable in this study would have required pooling multiple eyes from several mice. Moreover, RT qPCR analysis of the RNA isolated revealed endothelial-specific *Pecam1* gene expression, showing that there was vessel contamination from the choroid (data not shown). Nevertheless, isolation of both the RPE and choroid allowed recovery of a larger proportion of the total RPE cells, so isolation of RPE/choroid by incubation with TRIzol® or manual scraping of the pigmented cells was compared. After isolation of RNA, proteins were extracted from the same preparation and resolved by SDS-PAGE. Western blotting for RPE65 showed that manual scraping of the pigmented cells from the posterior eyecup achieved a higher proportion of the RPE-specific protein compared to incubation of the posterior eyecup in TRIzol® (Figure 5.2). Manual scraping produced yields of 0.5-1.2 μg RNA per pair of eyes.

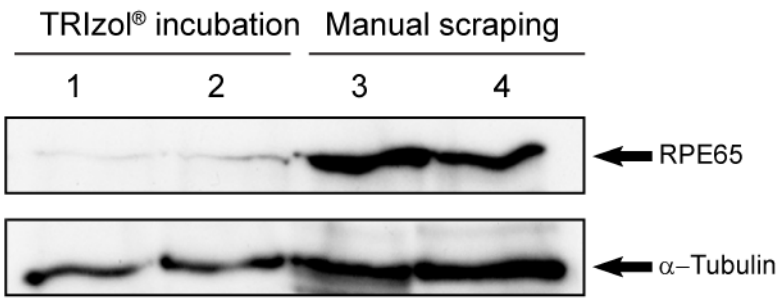

Figure 5.2. Manual scraping led to a better yield of RPE than TRIzol incubation
Posterior eyecups were dissected from 4 pairs of eyes isolated from C57BL/6 mice (1-4). RPE cells were dissociated using two methods. Pairs 1 & 2 were rotated in TRIzol for 10 min at RT. RPE cells from pairs 3 & 4 were carefully scraped off using a 28 G needle. RNA and DNA were extracted from TRIzol® solution before proteins were precipitated with isopropanol. Precipitated proteins were resolved by SDS-PAGE and western blotted for RPE65 and α-tubulin. RPE65 and α-tubulin were visualised, using enhanced chemiluminescence, as approximately 65 kDa and 55 kDa polypeptide bands respectively.

5.2. RNA quality assessment prior to microarray analysis

Microarray analysis requires RNA of a high integrity. Here, RNA quality was assessed using a bioanalyzer where a fluorescent dye intercalates with nucleic acids which are subsequently separated by electrophoresis (Figure 5.3A). Analysis of the 18S and 28S ribosomal RNA (rRNA) peaks on the electrophoresis traces gives an indication of any RNA degradation (Figure 5.3B). The traces also indicate the presence of any DNA or phenol contamination. The bioanalyzer software generates a RNA integrity number

(RIN) by applying an algorithm to the entire electrophoresis trace. This number ranges from 1-10, with 10 representing the maximum integrity value. Using the highest RIN scores, four of the six RNA samples collected were chosen for microarray analysis. The average RIN score for RPE/choroid RNA was less than that of neuroretina RNA which is likely due to low yield of RPE/choroid RNA compared to the neuroretina (Figure 5.3C).

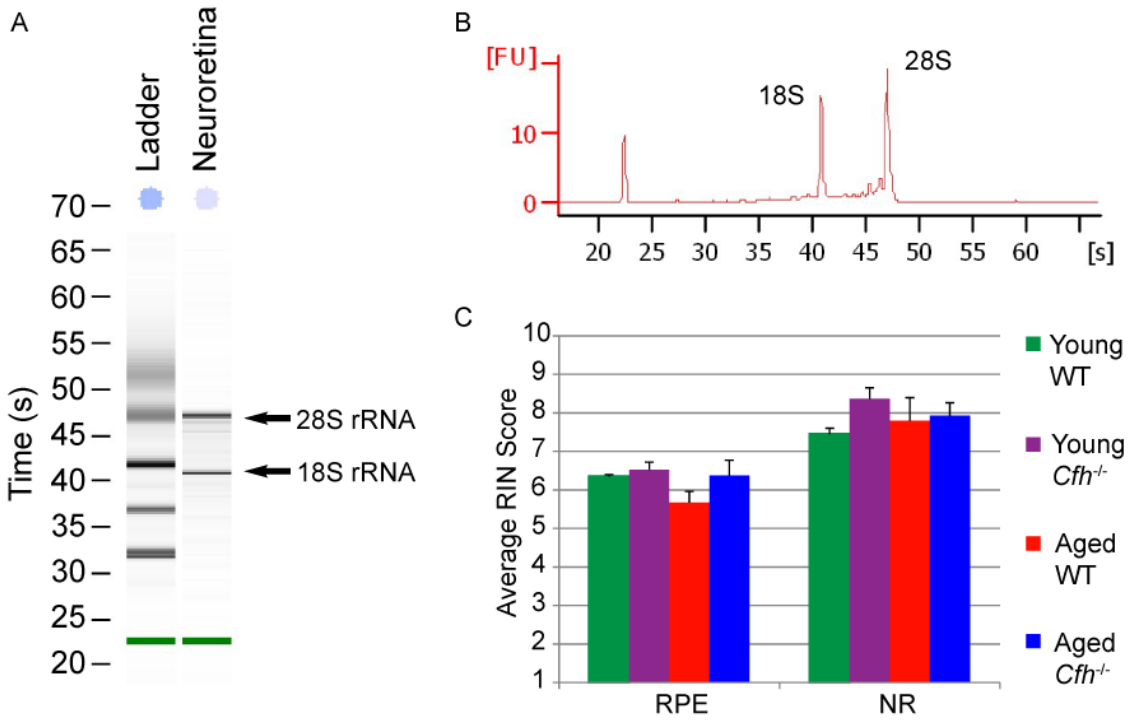

Figure 5.3. RNA quality assessment
RNA quality was assessed using Agilent Pico Chips and a Bioanalyzer. (A) Representative electropherogram showing ribosomal RNA bands, 28S and 18S. (B) Gel-like image plotting fluorescence units (FU) against time (s). (C) Average RNA Integrity number (RIN) for each group was calculated from the traces in (B). Data are means ± S.D., n = 4. Samples were ran on the Bioanalyzer by UCL Genomics Facility.

5.3. Microarray analysis

RNA was processed at the UCL genomics facility and underwent a sense target labelling assay to generate amplified biotinylated sense-strand DNA. Due to the low concentration of RPE/choroid RNA, the RNA was linearly amplified prior to the labelling assay. Each sample was hybridised to an Affymetrix Mouse Gene 1.0 ST Array GeneChip® then stained and scanned. Each chip contained approximately 27 probes for every known gene and Ensembl predicted EnsGene, equating to 28,853 genes across the mouse genome.

UCL Genomics carried out statistical analysis of the microarray raw data using Partek® software. Using this software, data underwent background adjustment and normalisation to account for variance in labelling and hybridisation between chips. Differential expression between groups was analysed by ANOVA whilst controlling for false discovery rate.

PCA was applied to all genes to assess variance within and between groups. PCA of the RPE/choroid samples showed that samples within the young wild-type group had the most variance whereas the four samples in the other three groups largely clustered together (Figure 5.4A). PCA analysis of the neuroretina samples showed that the young groups had less variance between samples than the aged groups (Figure 5.4B). Overall, the neuroretina groups were more variable than the RPE/choroid groups, which may be due to the multicellular nature of the neuroretina in comparison to the RPE/choroid. One outlier in the young *Cfh*$^{-/-}$ neuroretina group was removed from analyses because it was vastly different to the other three samples of its group. Overall variance between samples of each group was expected since RNA was not pooled from multiple mice but each sample represented RNA from one mouse. Additionally, comparisons between varied groups should give more confidence in the genes which are shown to be significantly different between them.

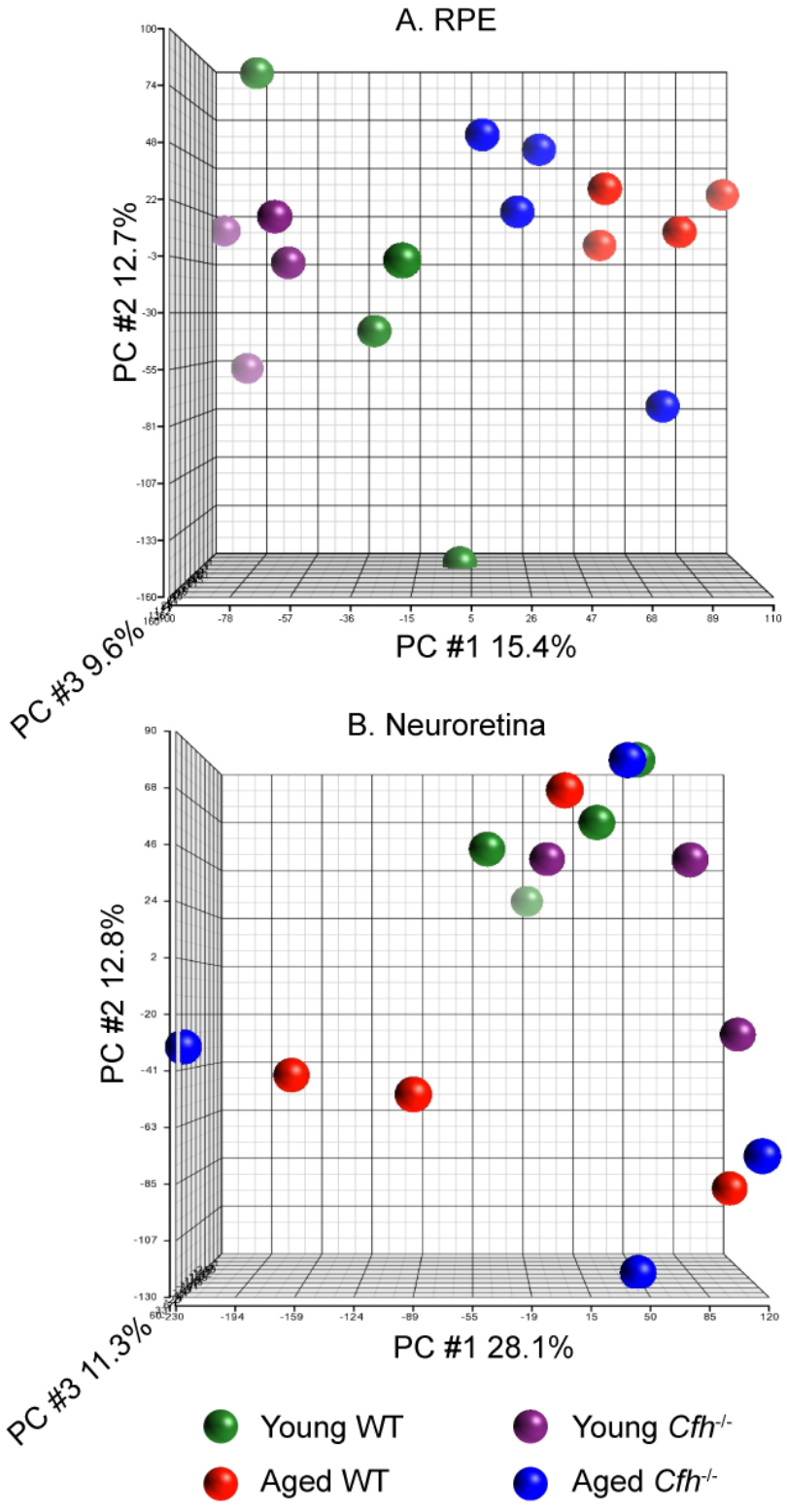

Figure 5.4. Principal components analysis of variance between samples
Principal components analysis (PCA) reduces the variability of all genes between samples to three uncorrelated prinicipal components (PC #1-3). Variability within (B) neuroretina groups is larger than that within (A) RPE/choroid groups. Each sphere represents one mouse. PCA plots were generated by UCL Genomics Facility.

Statistical analysis of the microarray data was performed to compare the effect of either *Cfh* genotype or age between groups. These comparisons identified which genes were significantly changed in either the RPE/choroid or the neuroretina as a result of the loss of CFH or ageing. Analysis of the RPE/choroid showed that in both wild-type and *Cfh*$^{-/-}$ mice, approximately 450-550 genes exhibited changes in expression as a function of ageing that met the criteria for significance (Figure 5.5A). In contrast, age-related gene expression was more stable in the neuroretina, though as with RPE/choroid, somewhat fewer changes in gene expression were observed in the *Cfh*$^{-/-}$ mice (Figure 5.5B). Interestingly, despite the large number of age-related changes in gene expression in the RPE/choroid, only a few differences were noted between wild-type and *Cfh*$^{-/-}$ mice, namely 5 in the young and 21 in the aged animals. However, in the neuroretina there were 12 significant differences between the young wild-type and *Cfh*$^{-/-}$ animals and >100 between the aged counterparts. Thus, deletion of *Cfh* appears to have a greater impact on the transcriptomics of ageing in the neuroretina than the RPE/choroid. This may appear counter-intuitive in light of the fact that CFH expression in the retina is predominantly in the RPE but is consistent with the observed changes in visual function in the aged *Cfh*$^{-/-}$ mice (Coffey *et al.,* 2007).

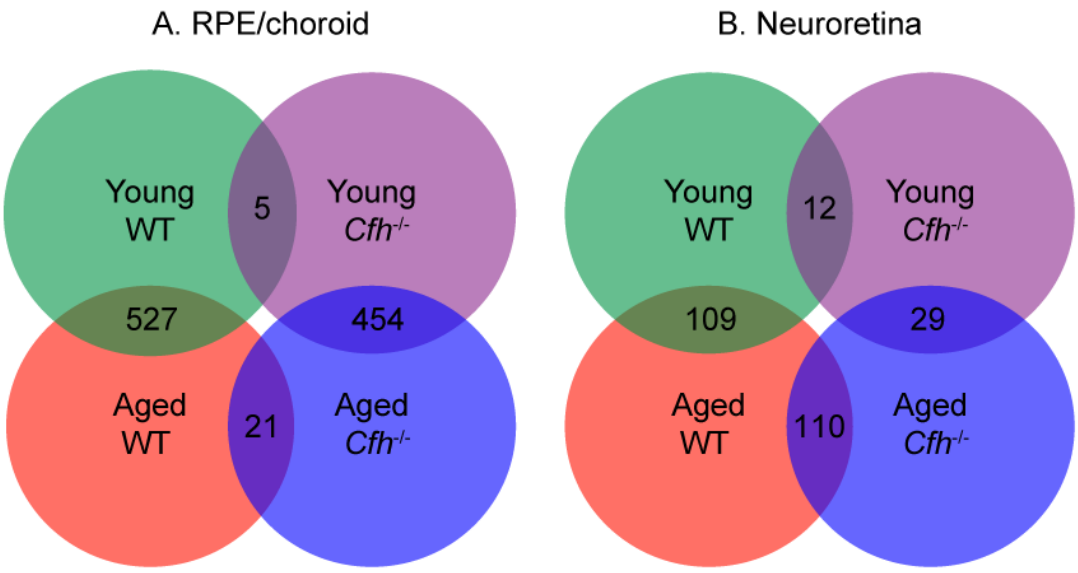

Figure 5.5. The number of genes identified from microarray analysis whose expression were significanlty different between groups

Microarray analysis was performed on RNA isolated from (A) RPE/choroid and (B) neuroretina of young (7-8 weeks) and aged (16 months) *Cfh*$^{-/-}$ mice and age-matched wild-type (WT) controls. Numbers indicate how many genes were significantly different between groups, adjusted p value < 0.05, n = 4 for all except young *Cfh*$^{-/-}$ where n = 3. Statistical analysis was performed by UCL Genomics Facility.

5.4. The effect of *Cfh* genotype on gene expression in the RPE/choroid

In young animals, as expected, *Cfh* was the most down-regulated gene in *Cfh*$^{-/-}$ mice. In addition to *Cfh*, only four other genes were significantly altered compared to age-matched wild-type controls (Table 5.1). These four genes were all down-regulated in *Cfh*$^{-/-}$ mice but their functions could not be linked to a single pathway. Of the four genes, both diazepam binding inhibitor (*Dbi*) and minichromosome maintenance deficient 6 (*Mcm6*) remained significantly altered when comparing aged *Cfh*$^{-/-}$ RPE/choroid to age-matched wild-type controls.

Gene Symbol	Key	Gene Name	FC	p-value
Mapk14		mitogen-activated protein kinase 14	-1.47	4.7E-06
1700029I15Rik		RIKEN cDNA 1700029I15 gene	-1.47	1.2E-06
Dbi	1 ♣ Ψ	diazepam binding inhibitor	-1.52	1.0E-06
Mcm6	1 ♣ Ψ	minichromosome maintenance deficient 6	-3.05	1.4E-06
Cfh	1 ♣ Ψ	complement component factor h	-7.08	3.4E-09

Table 5.1. Genes differentially expressed in RPE/choroid of young *Cfh*-/- mice
Microarray analysis revealed which genes were significantly differentially expressed in the RPE/choroid of young (7-8 weeks) *Cfh*$^{-/-}$ mice compared to age-matched wild-type controls. Genes listed in fold change (FC) order; light blue signifies genes with a down-regulation < -2 and dark blue ≥ -2. Key: 1, gene located on mouse chromosome 1; ♣, gene remains differentially expressed in aged (16 months) *Cfh*$^{-/-}$ RPE/choroid in comparison to age-matched wild-type controls; Ψ, gene also differentially expressed in neuroretina of *Cfh*$^{-/-}$ mice when compared to age-matched wild-type controls.

The loss of CFH had a greater impact on the RPE/choroidal gene expression of aged mice than that of younger mice (Table 5.2). In addition to *Cfh*, 20 genes were differentially expressed between aged *Cfh*$^{-/-}$ mice and age-matched wild-type controls. Ingenuity Pathway Analysis® did not reveal a direct or known functional link between any of these 20 genes.

Pituitary tumour-transforming gene 1 (*Pttg1*) was the most up-regulated gene in the RPE/choroid of aged *Cfh*$^{-/-}$ mice compared to age-matched wild-type controls with over a six fold change. However *Pttg1* expression was also down-regulated with age in wild-type mice therefore the apparent up-regulation in aged *Cfh*$^{-/-}$ mice may actually be the consequence of the gene not being down-regulated with ageing in these mice. *Pttg1* is a proto-oncogene involved in sister chromatid segregation important for mitotic checkpoints and cell proliferation (Pei and Melmed, 1997). *Pttg1* has also been shown to be involved in regulation of transcription, apoptosis and endothelial cell survival

(Bernal *et al.,* 2002), and dysregulation of this gene has been identified in mouse models of photoreceptor degeneration and retinal dystrophy (van de Pavert *et al.,* 2007; Fernandez-Medarde *et al.,* 2009; Yetemian *et al*., 2010). However characterisation of the *Pttg1*$^{-/-}$ mouse reported no morphological or functional changes in the retina, suggesting that *Pttg1* dysregulation is a secondary event to perhaps cell stress or neovascularisation (Yetemian and Craft, 2011). The significance of *Pttg1* expression in relation to *Cfh* gene knock-out is not clear.

Gene Symbol	Key	Gene Name	FC	p-value
Pttg1	Ψ	pituitary tumor-transforming gene 1	6.47	2.8E-08
Ctse	1	cathepsin E	3.41	2.6E-06
5830417I10Rik	Ψ	RIKEN cDNA 5830417I10 gene	3.39	3.0E-07
Cd5l		CD5 antigen-like	2.37	1.4E-05
4933409K07Rik	Ψ*	RIKEN cDNA 4933409K07 gene	2.11	1.2E-05
Cck		cholecystokinin	2.01	2.3E-06
Fstl4		follistatin-like 4	1.84	1.0E-05
Cd99l2		CD99 antigen-like 2	1.46	2.3E-05
Klhl9		kelch-like 9 (Drosophila)	1.40	4.2E-05
Dct		dopachrome tautomerase	1.39	1.0E-05
1700029I15Rik		RIKEN cDNA 1700029I15 gene	1.32	3.4E-05
Ubxn4	1	UBX domain protein 4	-1.19	3.0E-05
Dbi	1 ♣ Ψ	diazepam binding inhibitor	-1.67	1.1E-07
Dynlt1	Ψ *	dynein light chain Tctex-type 1	-1.74	3.6E-05
Igl-V1		immunoglobulin lambda chain, variable 1	-2.11	3.3E-06
H60b		histocompatibility 60b	-2.30	4.9E-05
Mcm6	1 ♣ Ψ	minichromosome maintenance deficient 6 (MIS5 homolog, S. pombe) (S. cerevisiae)	-2.46	1.2E-05
H2-M2		histocompatibility 2, M region locus 2	-3.05	1.1E-07
Rbp7		retinol binding protein 7, cellular	-4.24	7.6E-07
Cfh	1 ♣ Ψ	complement component factor h	-5.08	2.8E-08
Snca	Ψ	synuclein, alpha	-7.00	4.6E-10

Table 5.2. Genes differentially expressed in RPE/choroid of aged *Cfh*-/- mice
Microarray analysis revealed which genes were significantly differentially expressed in the RPE/choroid of aged (16 months) *Cfh*$^{-/-}$ mice compared to age-matched wild-type controls. Genes listed in fold change (FC) order; red signifies genes with an up-regulation ≥ 2, pink an up-regulation < 2, light blue a down-regulation < -2 and dark blue a down-regulation ≥ -2. Key: 1, gene located on mouse chromosome 1; ♣, gene also differentially expressed in young (7-8 weeks) *Cfh*$^{-/-}$ RPE/choroid in comparison to age-matched wild-type controls; Ψ, gene also differentially expressed in neuroretina of *Cfh*$^{-/-}$ mice when compared to age matched wild-type controls; *, large gene with more than one probe set that showed significant differential expression.

Cathepsin E (*Ctse*) gene expression was over three fold higher in RPE/choroid in aged *Cfh*$^{-/-}$ samples compared to age-matched wild-type controls, but its expression did not significantly change with ageing in either *Cfh*$^{-/-}$ or wild-type mice. However cathepsins B, H, K and S were all up-regulated with age in both *Cfh*$^{-/-}$ and wild-type mice. CTSE is an intracellular non-lysosomal aspartic proteinase, and has been reported to

accumulate in neural tissue with ageing and neurodegeneration, and co-localises with lipofuscin. One retinal study reported CTSE expression in the neurons of the inner, OPL and GCL (Bernstein *et al.,* 1998). However, attempts to validate this up-regulation by western blot analysis of RPE/choroid lysates from aged *Cfh*$^{-/-}$ mice were thwarted because protein expression was below the detectable limit of the assay (data not shown).

At 16 months, synuclein alpha (*Snca*) gene expression was even more down-regulated than that of *Cfh*. This gene was up-regulated with age in wild-type mice, therefore the down-regulation in aged *Cfh*$^{-/-}$ mice can also be interpreted as a failure to up-regulate the gene with ageing in the *Cf*h$^{-/-}$ mice. SNCA is primarily expressed by neurons; in the eye it is expressed by RPE, photoreceptors, amacrine and bipolar cells (Martinez-Navarrete *et al.,* 2007). The protein is thought to be involved in neuronal transmission and maintenance of the outer segment of the photoreceptors but its function in RPE is unknown.

Retinol binding protein 7 (*Rbp7*) was the most down-regulated gene after *Scna* and *Cfh*. However like *Scna*, *Rbp7* expression was also found to be up-regulated with age in wild-type mice. RBP7 is the most recently identified cellular retinol binding protein and is therefore not yet well characterised (Vogel *et al.,* 2001). RT qPCR analysis of cDNA reverse transcribed from the RNA used for microarray analysis confirmed a down-regulation of *Rbp7* transcript levels in aged *Cfh*$^{-/-}$ RPE/choroid (Figure 5.6).

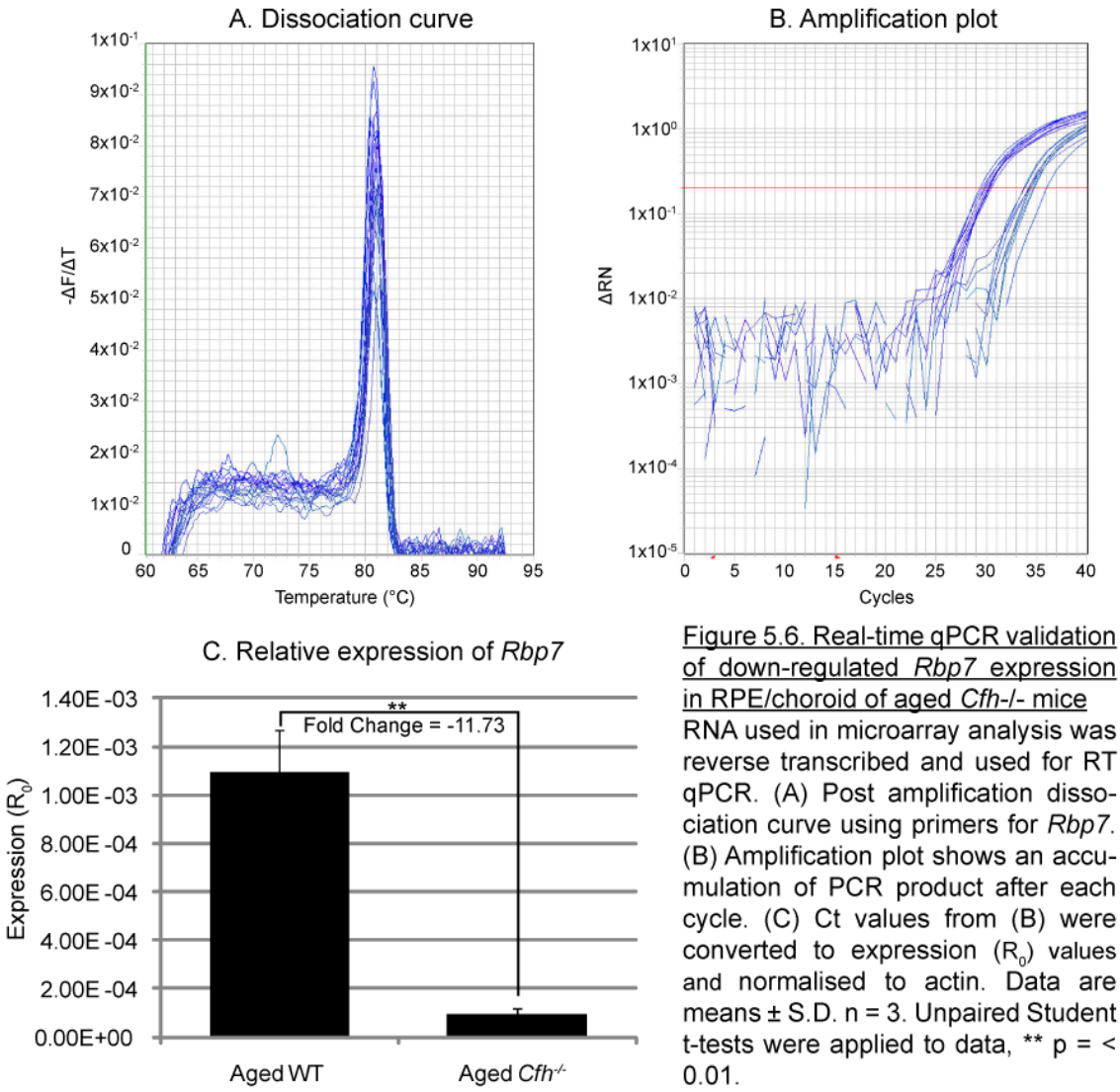

Figure 5.6. Real-time qPCR validation of down-regulated *Rbp7* expression in RPE/choroid of aged *Cfh-/-* mice
RNA used in microarray analysis was reverse transcribed and used for RT qPCR. (A) Post amplification dissociation curve using primers for *Rbp7*. (B) Amplification plot shows an accumulation of PCR product after each cycle. (C) Ct values from (B) were converted to expression (R_0) values and normalised to actin. Data are means ± S.D. n = 3. Unpaired Student t-tests were applied to data, ** p = < 0.01.

5.5. The effect of *Cfh* genotype on gene expression in the neuroretina

The loss of CFH significantly altered the expression of 11 genes in the neuroretina of young mice (Table 5.3). None of the genes that were significantly altered at a young age in RPE/choroid were also altered in the neuroretina which indicated that there was no significant contamination of the neuroretina tissue in the RPE/choroid isolation and vice versa. Of the 11 genes, 10 were down-regulated in aged *Cfh*$^{-/-}$ compared to wild-type age-matched controls. All of these 10 genes, like *Cfh*, are located on mouse chromosome 1, which suggests that targeting of the *Cfh* gene may affect expression of neighbouring genes.

Zinc finger RAN binding domain containing 3 (*Zranb3*) was up-regulated 10.9 fold in young *Cfh*$^{-/-}$ neuroretina. Zranb3 is a member of the SNF2/RAD54 helicase family, its

biological function is not defined but it has been suggested to be involved in G-protein function (Chen *et al.,* 2011).

Gene Symbol	Key	Gene Name	FC	p-value
Zranb3		zinc finger, RAN-binding domain containing 3	10.90	4.3E-07
Shisa4	1 ♣	shisa homolog 4 (Xenopus laevis)	-2.93	8.2E-07
Timm17a	1 ♣	translocase of inner mitochondrial membrane 17a	-3.04	7.3E-07
Tsn	1 ♣	translin	-3.29	1.1E-06
Ppp1r12b	1 ♣	protein phosphatase 1, regulatory (inhibitor) subunit 12B	-3.76	3.2E-06
Cdh7	1 ♣	cadherin 7, type 2	-4.25	1.6E-07
BC026782	1 ♣	cDNA sequence BC026782	-5.28	3.7E-06
Zc3h11a	1 ♣	zinc finger CCCH type containing 11A	-5.91	8.5E-08
Kdm5b	1 ♣	lysine (K)-specific demethylase 5B	-7.21	3.1E-08
Dars	1 ♣ *	aspartyl-tRNA synthetase	-8.65	1.3E-06
Cfh	1 ♣ Ψ *	complement component factor h	-17.74	7.9E-07
EG214403	1 ♣ *	predicted gene, EG214403	-28.32	2.2E-08

Table 5.3. Genes differentially expressed in the neuroretina of young *Cfh*-/- mice
Microarray analysis revealed which genes were significantly differentially expressed in the neuroretina of young (7-8 weeks) *Cfh*$^{-/-}$ mice compared to age-matched wild-type controls. Genes listed in fold change (FC) order; red signifies genes with an up-regulation ≥ 2, and blue a down-regulation ≥ -2. Key: 1, gene located on mouse chromosome 1; ♣, gene remains differentially expressed in aged (16 months) *Cfh*$^{-/-}$ neuroretina in comparison to age-matched wild-type controls; Ψ, gene also differentially expressed in RPE/choroid of *Cfh*$^{-/-}$ mice when compared to age matched wild-type controls; *, large gene with more than one probe set that showed significant differential expression.

In contrast to previous comparisons, the aged neuroretina was markedly affected by the loss of *Cfh*, with 110 genes being significantly different between aged *Cfh*$^{-/-}$ and age-matched wild-type controls (Table 5.4). Of these, 24 were located on mouse chromosome 1, of which 19 were down-regulated in *Cfh*$^{-/-}$ neuroretina.

SLU7 splicing factor homolog (*Slu7*) involved in pre-mRNA splicing exhibited the highest fold change, with 36.57 fold up-regulation in *Cfh*$^{-/-}$ neuroretina. Human *Slu7* is highly expressed in the GCL and INL (Alberstein *et al.,* 2007).

Table 5.4. Genes differentially expressed in neuroretina of aged *Cfh*-/- mice
Microarray analysis revealed which genes were significantly differentially expressed in the neuroretina of aged (16 months) *Cfh*$^{-/-}$ mice compared to age-matched wild-type controls. Genes listed in fold change (FC) order; red signifies genes with an up-regulation ≥ 2, pink an up-regulation < 2, light blue a down-regulation < -2 and dark blue a down-regulation ≥ -2. Key: 1, gene located on mouse chromosome 1; ♣, gene also differentially expressed in young (7-8 weeks) *Cfh*$^{-/-}$ neuroretina in comparison to age-matched wild-type controls; Ψ, gene also differentially expressed in RPE/choroid of *Cfh*$^{-/-}$ mice when compared to age matched wild-type controls; *, large gene with more than one probe set that showed significant differential expression.

Gene Symbol	Key	Gene Name	FC	p-value
Slu7		SLU7 splicing factor homolog (S. cerevisiae)	36.57	7.0E-12
Pttg1	Ψ *	pituitary tumor-transforming gene 1	22.58	5.5E-07
5830417I10Rik	Ψ *	RIKEN cDNA 5830417I10 gene	16.62	6.4E-09
Ublcp1		ubiquitin-like domain containing CTD phosphatase 1	16.12	1.2E-10
Itgav	*	integrin alpha V	13.55	4.6E-06
Gm16432	1 *	predicted gene 16432	9.04	2.1E-06
Pde4b		phosphodiesterase 4B, cAMP specific	8.88	6.1E-08
Glra1		glycine receptor, alpha 1 subunit	8.30	7.7E-07
Grm6		glutamate receptor, metabotropic 6	8.23	4.1E-05
Ush2a	1	Usher syndrome 2A (autosomal recessive, mild) homolog (human)	8.05	9.8E-08
Afg3l2		AFG3(ATPase family gene 3)-like 2 (yeast)	7.72	1.1E-08
Anxa6		annexin A6	7.27	6.2E-08
Atox1		ATX1 (antioxidant protein 1) homolog 1 (yeast)	7.01	1.1E-08
Cgn		cingulin-like 1	6.81	2.3E-05
Wdr78		WD repeat domain 78	5.81	6.6E-06
Pgm2		phosphoglucomutase 2	5.80	1.0E-06
Frzb		frizzled-related protein	5.74	2.8E-09
Ssfa2		sperm specific antigen 2	5.25	2.2E-05
Olfr550		olfactory receptor 550	5.03	1.7E-05
Lrba		LPS-responsive beige-like anchor	4.69	2.8E-10
Cdc16		CDC16 cell division cycle 16 homolog (S. cerevisiae)	4.42	3.5E-06
Slc36a1		solute carrier family 36 (proton/amino acid symporter), member 1	4.10	1.1E-05
Ptprj		protein tyrosine phosphatase, receptor type, J	3.98	1.3E-06
Aldh1a2		aldehyde dehydrogenase family 1, subfamily A2	3.91	3.8E-05
Cdh2		cadherin-2	3.79	4.6E-05
Nfia		nuclear factor I/A	3.51	3.5E-06
Fstl5		follistatin-like 5	3.46	9.6E-07
Ash1l		ash1 (absent, small, or homeotic)-like (Drosophila)	3.31	5.3E-07
Ccl21a	*	chemokine (C-C motif) ligand 21A	3.29	4.9E-06
G3bp1		Ras-GTPase-activating protein SH3-domain binding protein 1	3.27	8.6E-06
Fbxw7		F-box and WD-40 domain protein 7	3.23	1.3E-07
Spire1	*	spire homolog 1 (Drosophila)	3.17	7.6E-07
4933409K07Rik	Ψ *	RIKEN cDNA 4933409K07 gene	3.12	4.4E-06
Arhgef2		rho/rac guanine nucleotide exchange factor (GEF) 2	3.08	9.1E-06
Vdac1		voltage-dependent anion channel 1	3.07	4.1E-08
Trak1		trafficking protein, kinesin binding 1	3.07	9.8E-06
Nav1	1	neuron navigator 1	3.03	4.2E-05
Hnrpdl		heterogeneous nuclear ribonucleoprotein D-like	2.99	4.4E-09
Stard6		StAR-related lipid transfer (START) domain containing 6	2.79	3.6E-05
Pet112l		PET112-like (yeast)	2.65	1.7E-06
Pogz		pogo transposable element with ZNF domain	2.59	2.0E-06
Rapgef2		Rap guanine nucleotide exchange factor (GEF) 2	2.59	1.1E-06
Hnrnph1		heterogeneous nuclear ribonucleoprotein H1	2.45	6.7E-08
Casz1		castor homolog 1, zinc finger (Drosophila)	2.45	9.2E-06
Alg6		asparagine-linked glycosylation 6 homolog (yeast, alpha-1,3,-glucosyltransferase)	2.40	1.2E-05
Cd164		CD164 antigen	2.39	4.3E-07
Lgr5		leucine rich repeat containing G protein coupled receptor 5	2.32	4.4E-05
D030074E01Rik		RIKEN cDNA D030074E01 gene	2.17	3.2E-05
Gabrg2		gamma-aminobutyric acid (GABA) A receptor, subunit gamma 2	2.06	3.7E-06
Tbc1d15		TBC1 domain family, member 15	1.87	1.4E-05
Rps6		ribosomal protein S6 kinase polypeptide 3	1.80	1.3E-09
Pde8b		phosphodiesterase 8B	1.78	3.4E-06
Poli		poliovirus receptor-related 1	1.71	1.7E-05
Zc3h15		zinc finger CCCH-type containing 15	1.60	6.2E-09
Zfp2		zinc finger protein 26	1.54	1.8E-05

Mta2		metastasis-associated gene family, member 2	1.50	9.6E-06
Ctnna1		catenin (cadherin associated protein), alpha 1	1.44	3.6E-05
Asns		asparagine synthetase domain containing 1	1.41	1.3E-06
Clasp1	1	CLIP associating protein 1	1.34	3.1E-05
Creb1	1	cAMP responsive element binding protein 1	1.31	1.5E-06
Cp		ceruloplasmin	1.17	2.9E-06
Tmeff1		transmembrane protein with EGF-like and two follistatin-like domains 1	-1.23	2.5E-05
Guf1		GUF1 GTPase homolog (S. cerevisiae)	-1.30	2.5E-05
C030002C11Rik		hypothetical LOC320400	-1.33	3.9E-05
1700047I17Rik1	*	RIKEN cDNA 1700047I17 gene 1	-1.35	4.4E-05
Rabif	1	RAB interacting factor	-1.35	2.3E-05
Xpa		xeroderma pigmentosum, complementation group A	-1.36	7.4E-06
Snx24		sorting nexing 24	-1.41	2.8E-05
Zdhhc3		zinc finger, DHHC domain containing 3	-1.41	1.7E-05
Dnajc10		DnaJ (Hsp40) homolog, subfamily C, member 10	-1.42	3.3E-07
Cnot10		CCR4-NOT transcription complex, subunit 10	-1.48	1.7E-05
Pin4		protein (peptidyl-prolyl cis/trans isomerase) NIMA-interacting, 4 (parvulin)	-1.48	2.1E-05
Mest	*	mesoderm specific transcript	-1.48	2.2E-05
Cd59a		CD59a antigen	-1.49	9.7E-06
D14Ertd449e	*	DNA segment, Chr 14, ERATO Doi 449, expressed	-1.62	2.4E-06
Slc26a7		solute carrier family 26, member 7	-1.75	7.3E-07
Rbm45		RNA binding motif protein 45	-1.78	4.1E-05
BC016201		cDNA sequence BC016201	-1.82	1.6E-06
Anks1b		ankyrin repeat and sterile alpha motif domain containing 1B	-2.07	5.1E-06
Higd1a		HIG1 domain family, member 1A	-2.30	1.6E-12
Dynlt1	Ψ *	dynein light chain Tctex-type 1	-2.32	1.4E-05
Cerkl	*	ceramide kinase-like	-2.39	5.5E-06
Smc2		structural maintenance of chromosomes 2	-2.41	9.7E-06
Cfhr3	1	complement factor H-related 3	-2.43	2.5E-05
Itga4	*	integrin alpha 4	-2.45	3.0E-06
Ucma		upper zone of growth plate and cartilage matrix associated	-2.49	9.0E-06
Arpc5	1	actin related protein 2/3 complex, subunit 5-like	-2.59	1.1E-05
Shisa4	1 ♣	shisa homolog 4 (Xenopus laevis)	-2.64	1.1E-06
Rgl1	1	ral guanine nucleotide dissociation stimulator,-like 1	-2.64	2.0E-05
Tsn	1 ♣	translin	-2.68	3.2E-06
Gatm		glycine amidinotransferase (L-arginine:glycine amidinotransferase)	-2.75	3.6E-05
Tmem144		transmembrane protein 144	-3.12	1.6E-05
Dpp10	1	dipeptidylpeptidase 10	-3.20	3.9E-05
Nmnat1	*	nicotinamide nucleotide adenylyltransferase 1	-3.40	1.9E-05
Timm17a	1 ♣	translocase of inner mitochondrial membrane 17a	-3.49	1.0E-07
Ppp1r12b	1♣	protein phosphatase 1, regulatory (inhibitor) subunit 12B	-3.54	2.4E-06
Cdh7	1 ♣	cadherin 7, type 2	-4.19	7.9E-08
Lyrm7	*	LYR motif containing 7	-4.66	2.0E-06
Dars	1 ♣ *	aspartyl-tRNA synthetase	-4.75	9.6E-06
Mcm6	1 Ψ *	minichromosome maintenance deficient 6 (MIS5 homolog, S. pombe) (S. cerevisiae)	-5.05	7.5E-06
Ube2t	1 *	ubiquitin-conjugating enzyme E2T (putative)	-5.33	2.9E-05
Dbi	1 Ψ	diazepam binding inhibitor	-6.81	2.6E-06
Kdm5b	1 ♣	lysine (K)-specific demethylase 5B	-6.90	1.7E-08
Zc3h11a	1 ♣	zinc finger CCCH type containing 11A	-7.39	1.1E-08
Cfhr2	1 ♣ *	complement factor H-related 2	-10.14	2.5E-06
Cacna1s	1	calcium channel, voltage-dependent, L type, alpha 1S subunit	-11.39	1.4E-05
Btnl9		butyrophilin-like 9	-14.55	4.4E-08
Snca	Ψ *	synuclein, alpha	-19.11	3.8E-07
Cfh	1 ♣ Ψ *	complement component factor h	-22.76	1.0E-06
EG214403	1 ♣ *	predicted gene, EG214403	-28.09	1.0E-08

Three complement genes were down-regulated in the neuroretina of aged *Cfh*$^{-/-}$ mice compared to age-matched wild-type controls. Two of these, *Cfhr2* and *Cfhr3* are both located close to the *Cfh* locus on mouse chromosome 1 (Figure 5.12). With the large number of differentially expressed genes on chromosome 1 it is difficult to judge whether the down-regulation of *Cfhr2* and *Cfhr3* is an off-target consequence of *Cfh* gene disruption, or a functional response to the loss of CFH protein. The third gene, *Cd59a*, exhibited a small down-regulation of 1.5 fold. CD59a is a regulator of MAC formation also known as MIRL. As with *Rbp7*, *Cd59a* expression was up-regulated 1.6 fold in the wild-type neuroretina by ageing, so again, the down-regulation in aged *Cfh*$^{-/-}$ mice could also be interpreted as a lack of up-regulation with ageing of *Cfh*$^{-/-}$ mice.

Four of the genes not on chromosome one, *Pttg1*, dynein light chain Tctex-type 1 (*Dynlt1*) and two RIKEN cDNA sequences were up-regulated in the *Cfh*$^{-/-}$ mice in both aged RPE/choroid as well as the neuroretina. The two Riken cDNAs have yet to be characterised. *Pttg1* was up-regulated 22.6 fold in comparison to age-matched wild-type controls. As in the RPE/choroid, *Pttg1* was also down-regulated with age in the neuroretina of wild-type with a fold change of -46. Therefore, like in the RPE/choroid, the 22.6 up-regulation measured in aged neuroretina of *Cfh*$^{-/-}$ mice could be interpreted as the absence of down-regulation with age. DYNLT1 forms part of the dynein 1 complex which acts a motor for organelle and vesicle transport along microtubules (King *et al.,* 1996; Nagano *et al.,* 1998). Dynein is involved in the transport of rhodopsin vesicles along microtubules and it is DYNLT1 which binds the dynein complex to rhodopsin in photoreceptors (Tai *et al.,* 1999). Mutations associated with retinitis pigmentosa have been shown to affect the binding of DYNLT1 to rhodopsin.

Ingenuity Pathway Analysis® of the 110 genes revealed the top ten canonical pathways and cellular functions affected in the aged neuroretina of *Cfh*$^{-/-}$ mice (Figure 5.7). The majority of the canonical pathways affected are involved in the metabolism of amino acids or cell signalling. This analysis also showed that cell-to-cell signalling is affected which is relevant to a healthy functioning retina. From this

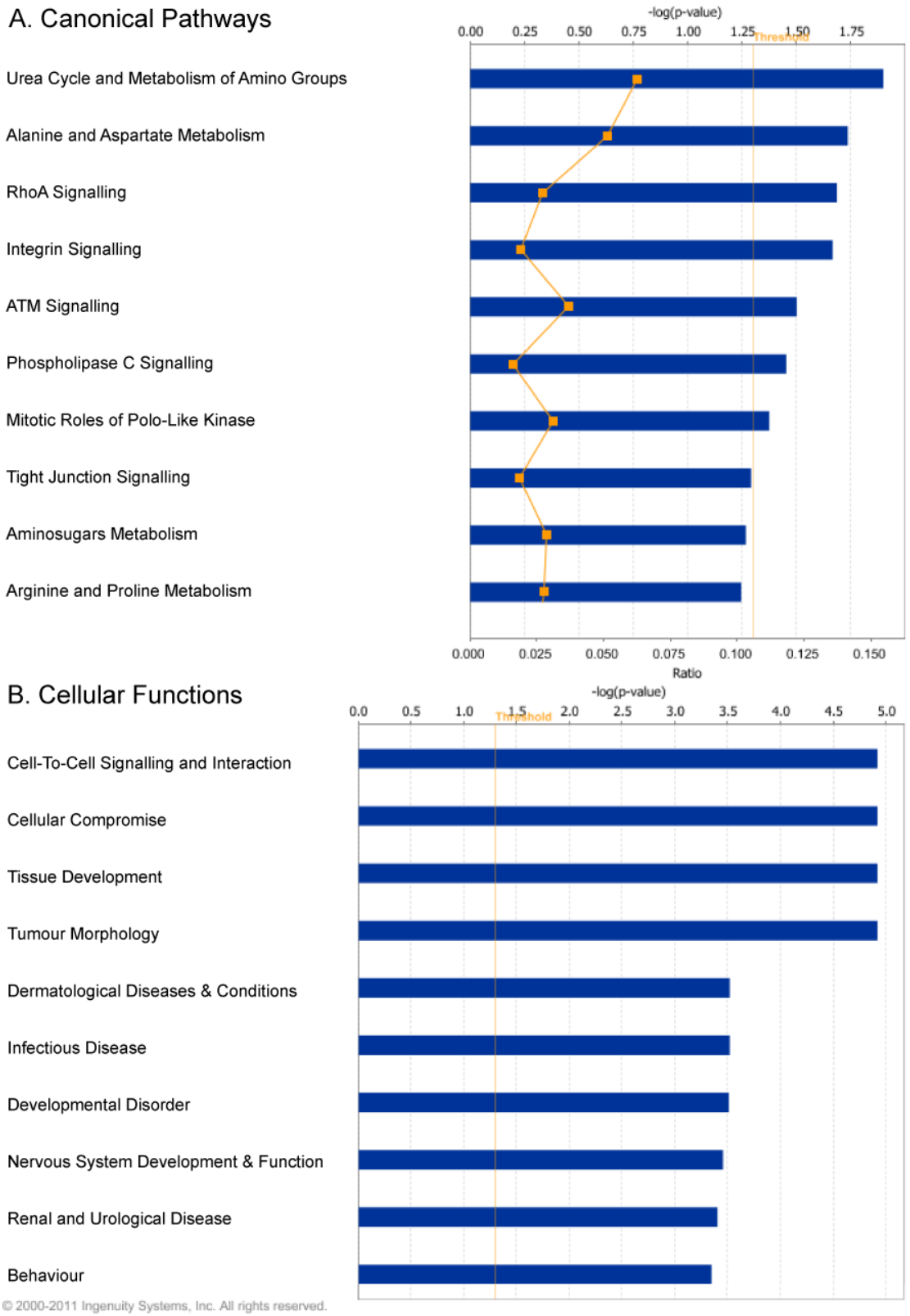

Figure 5.7. Top ten canonical pathways and cellular functions affected in the neuroretina of aged *Cfh-/-* mice

110 genes were differentially expressed in the neuroretina of aged (16 months) *Cfh*$^{-/-}$ mice compared to age-matched wild-type controls. Ingenutiy Pathway Analysis© (IPA) of these 110 genes revealed whch were the top ten (A) canonical pathways and (B) cellular functions involved in this list. Pathways and functions are listed in order of significance. IPA© used Fisher's exact test to calculate p-value. A ratio value for each canonical pathway (yellow squares) compares the number of genes differentially expressed in that pathway to the total number of genes involved for that pathway.

pathway, 4 genes from the list of 110 are represented including AFG3 (ATPase family gene 3)-like 2 (*Afg3l2*), calcium channel, voltage-dependent, L type, alpha 1S subunit (*Cacna1s*), cadherin 2 (*Cdh2*) and integrin alpha V (*Itgav*).

5.6. The effect of ageing on the RPE/choroid

Although ageing affected the expression of a similar number of genes in the RPE/choroid of wild-type (527) and *Cfh*$^{-/-}$ (454) mice, only 192 of these genes were the same genes. This suggests that the ageing process of the RPE/choroid in *Cfh*$^{-/-}$ mice is different to that of wild-type mice. Interestingly, Ingenuity pathway analysis® revealed that the majority of the canonical pathways (Figure 5.8) and cellular functions (Figure 5.9) which were affected, principally involved the immune system in both wild-type and *Cfh*$^{-/-}$ mice. This is consistent with previous literature reporting that RPE/choroid of wild-type mice becomes immunologically active with age (Chen *et al.,* 2008).

5.7. The effect of ageing on the neuroretina

There were fewer gene expression changes associated with ageing of the neuroretina than in the RPE/choroid, suggesting that this tissue is less susceptible to the effects of ageing. But in contrast to the RPE/choroid, there was a large difference in the number of genes which were found to be significantly different in the ageing neuroretinas of wild-type compared to *Cfh*$^{-/-}$ mice. 109 genes were differentially expressed during ageing of the wild-type neuroretina, compared to only 29 in the ageing *Cfh*$^{-/-}$ neuroretina. Of these, 14 genes were found in both groups. Ingenuity pathway analysis® revealed which were the top ten canonical pathways (Figure 5.10) and cellular functions (Figure 5.11) affected. None of the top ten canonical pathways affected by ageing were common to both wild-type and *Cfh*$^{-/-}$ mice, consistent with the notion that gene expression in the ageing of the neuroretina is modified in *Cfh*$^{-/-}$ mice.

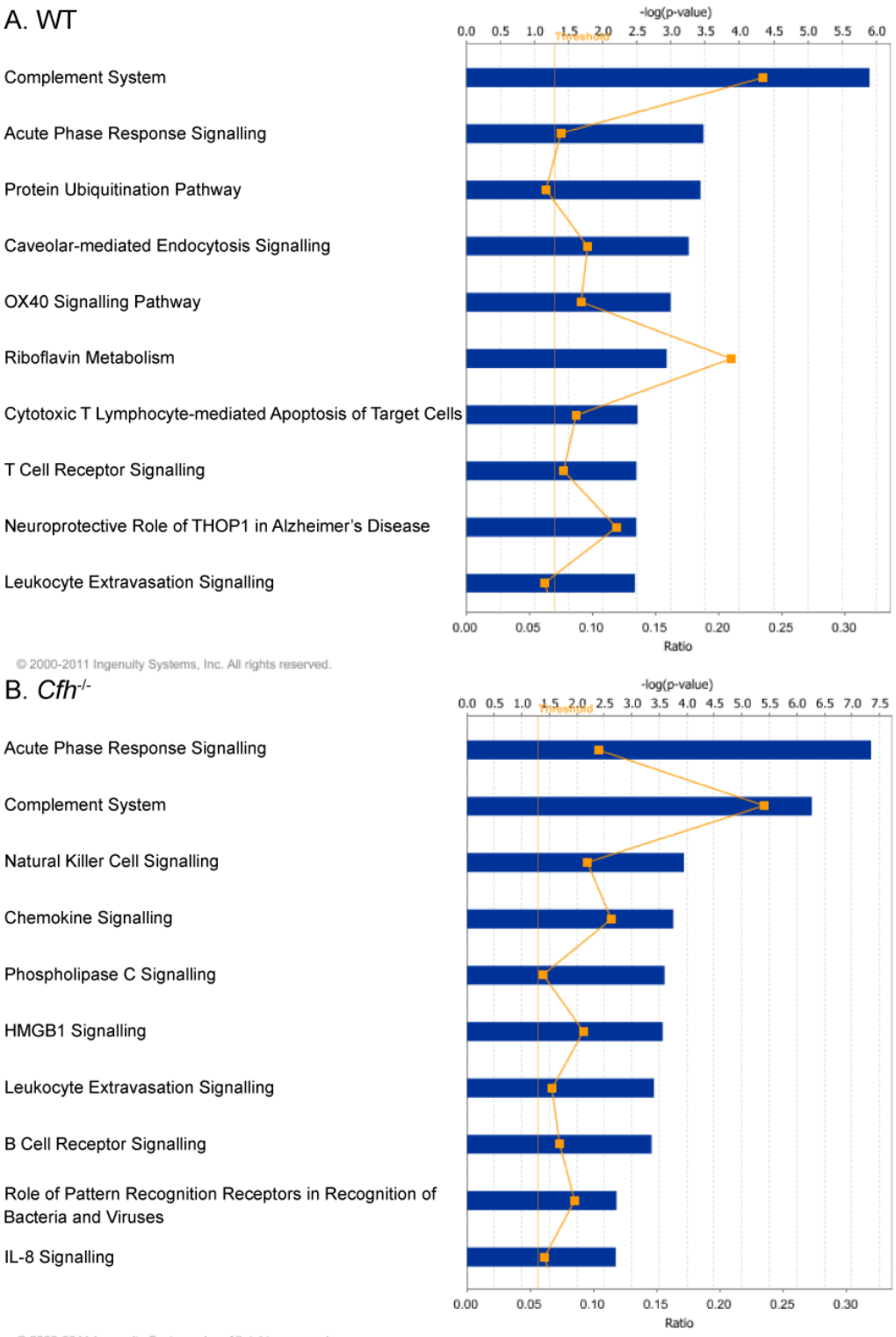

Figure 5.8. Top ten canonical pathways affected by ageing of the RPE/choroid in *Cfh*-/- and wild-type mice

The ageing process from 7-8 weeks to 16 months in the RPE/choroid of wild-type and *Cfh*$^{-/-}$ mice-caused 527 and 454 genes to be differentially expressed respectively. Ingenuity Pathway Analysis© (IPA) identified which canonical pathways were significanlty affected by ageing of the RPE/choroid in (A) wild-type and (B) *Cfh*$^{-/-}$ mice. Pathways are listed in order of significance. IPA© used Fisher's exact test to calculate p-value. A ratio value for each canonical pathway (yellow squares) compares the number of genes differentially expressed in that pathway to the total number of genes involved in that pathway.

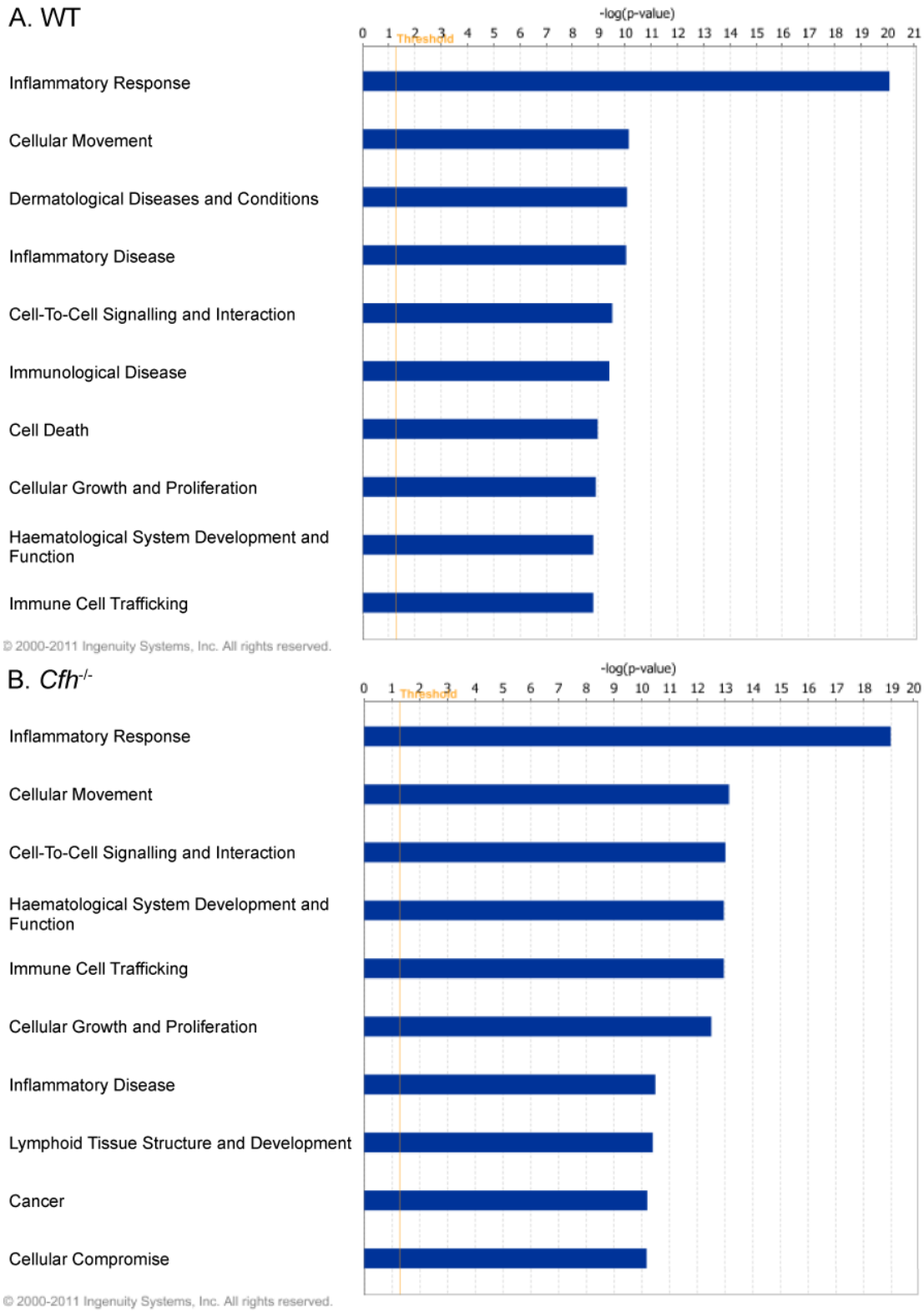

Figure 5.9. Top ten cellular functions affected by ageing of the RPE/choroid in *Cfh-/-* and wild-type mice

The ageing process from 7-8 weeks to 16 months in the RPE/choroid of wild-type and *Cfh*$^{-/-}$ mice-caused 527 and 454 genes to be differentially expressed respectively. Ingenuity Pathway Analysis© (IPA) identified which cellular functions were significanlty affected by ageing of the RPE/choroid in (A) wild-type and (B) *Cfh*$^{-/-}$ mice. Functions are listed in order of significance. IPA© used Fisher's exact test to calculate p-value.

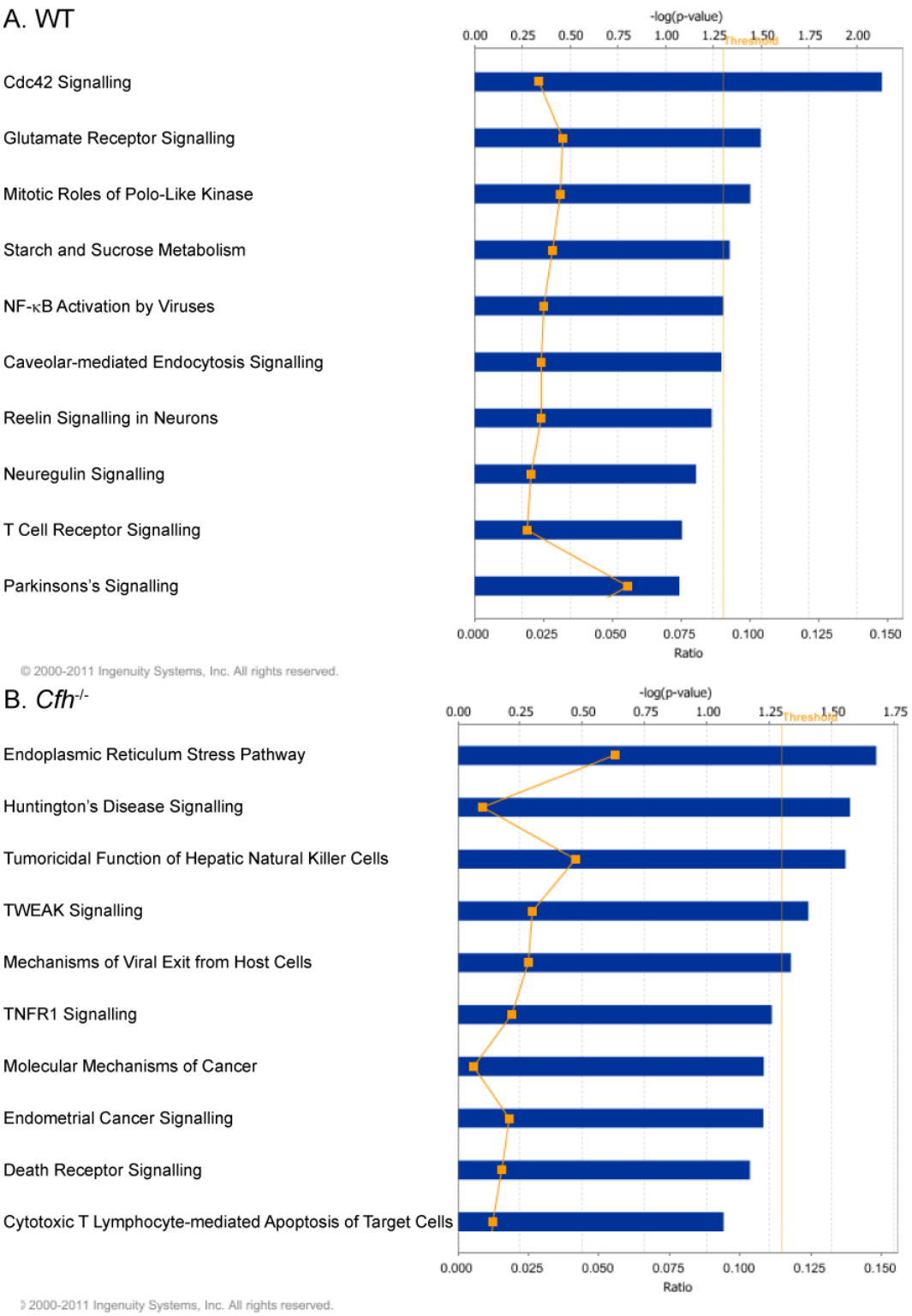

Figure 5.10. Top ten canonical pathways affected by ageing of the neuroretina in *Cfh-/-* and wild-type mice

The ageing process from 7-8 weeks to 16 months in the neuroretina of wild-type and *Cfh*$^{-/-}$ mice-caused 109 and 29 genes to be differentially expressed respectively. Ingenuity Pathway Analysis© (IPA) identified which canonical pathways were significanlty affected by ageing of the neuroretina in (A) wild-type and (B) *Cfh*$^{-/-}$ mice. Pathways are listed in order of significance. IPA© used Fisher's exact test to calculate p-value. A ratio value for each canonical pathway (yellow squares) compares the number of genes differentially expressed in that pathway to the total number of genes involved in that pathway.

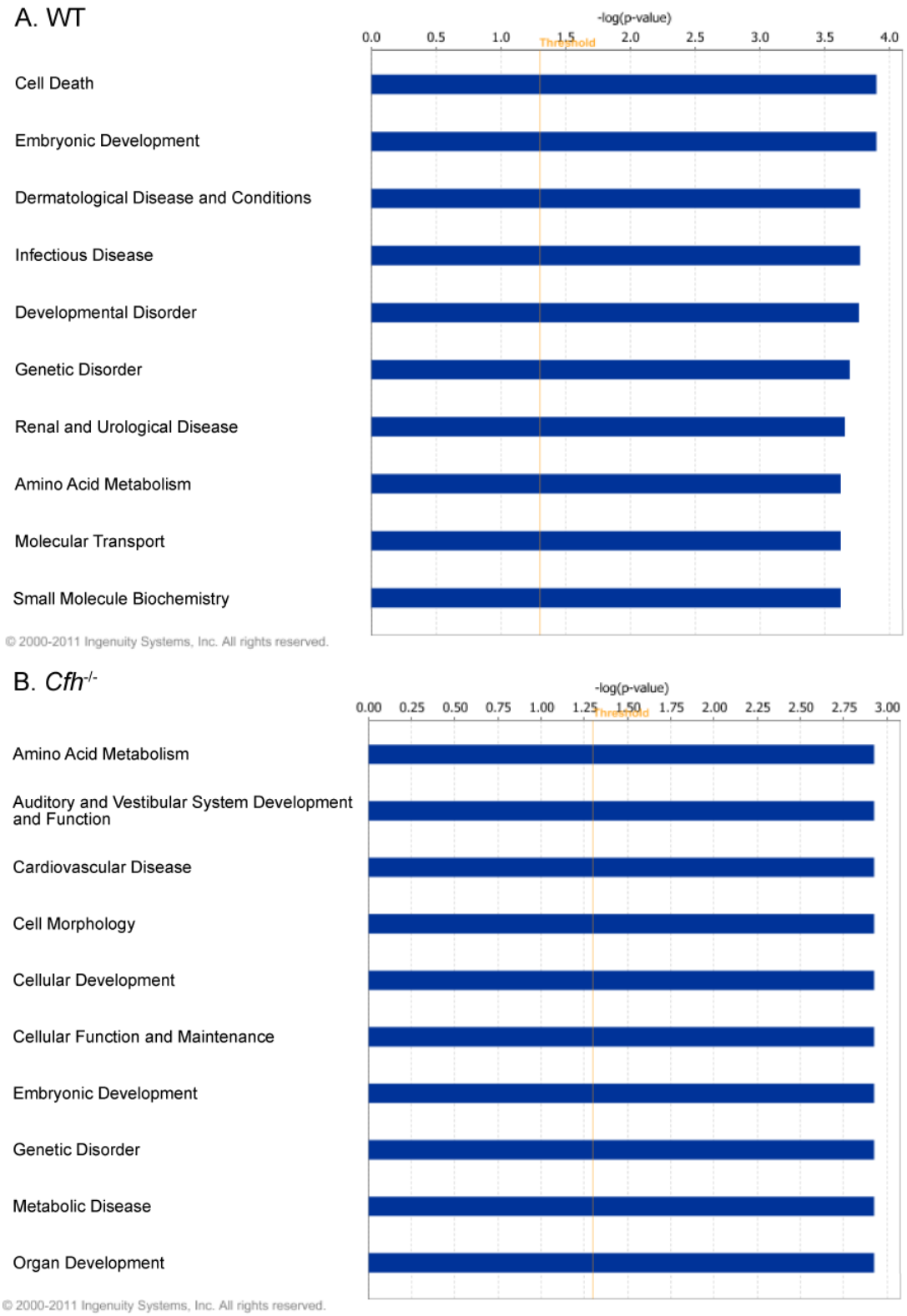

Figure 5.11. Top ten cellular functions affected by ageing of the neuroretina in *Cfh*-/- and wild-type mice

The ageing process from 7-8 weeks to 16 months in the neuroretina of wild-type and *Cfh*$^{-/-}$ mice-caused 109 and 29 genes to be differentially expressed respectively. Ingenuity Pathway Analysis© (IPA) identified which cellular functions were significanlty affected by ageing of the neuroretina in (A) wild-type and (B) *Cfh*$^{-/-}$ mice. Functions are listed in order of significance. IPA© used Fisher's exact test to calculate p-value.

5.8. The effect of ageing on the complement system

Surprisingly no genes directly involved in the complement system were affected by the loss of CFH in RPE/choroid and very few in the neuroretina. However the complement system was the main canonical pathway affected by ageing in the RPE/choroid of both wild-type and *Cfh*$^{-/-}$ mice (Figure 5.8). The majority of these age-related changes were similar in both wild-type and *Cfh*$^{-/-}$ mice (Table 5.5). Complement expression in the neuroretina was largely unaffected by age (Table 5.6).

Cfh expression was not significantly affected by age in either the RPE/choroid or the neuroretina of wild-type mice, consistent with a previous report in humans where *CFH* mRNA was shown not to change with age (Hageman *et al.,* 2005).

Gene Symbol	Gene Name	Young WT RMA	Aged WT RMA	Fold Change	Young *Cfh*$^{-/-}$ RMA	Aged *Cfh*$^{-/-}$ RMA	Fold Change
Complement Activators							
C1qa	C component 1, q subcomponent, alpha polypeptide	162	255	1.58	151	258	1.71
C1qb	C component 1, q subcomponent, beta polypeptide	236	465	1.97	245	408	1.67
C1qc	C component 1, q subcomponent, C chain	357	994	2.78	356	786	2.21
C1ra	C component 1, r subcomponent A	86	105	1.22	73	112	1.53
C1rb	C component 1, r subcomponent B	93	151	1.62	97	140	1.45
C1s	C component 1, s subcomponent	246	466	1.90	214	567	2.65
C2	C component 2 (within H-2S)	205	236	1.15	169	300	1.78
C3	C component 3	257	723	2.81	226	658	2.91
C4a	C component 4A (Rodgers blood group)	86	83	-1.04	74	81	1.10
C4b	C component 4B (Childo blood group)	202	312	1.54	245	354	1.45
C6	C component 6	30	30	1.00	33	30	-1.11
C7	C component 7	23	23	-1.01	23	23	1.01
C8a	C component 8, alpha polypeptide	38	38	1.00	37	39	1.04
C8b	C component 8, beta polypeptide	56	50	-1.11	50	55	1.11
C8g	C component 8, gamma polypeptide	84	84	-1.00	79	81	1.02
C9	C component 9	20	19	-1.04	19	19	1.03
Cfb	C factor B	223	346	1.55	174	422	2.43
Cfd	C factor D (adipsin)	223	155	-1.44	237	157	-1.51
Cfp	C factor properdin	152	142	-1.08	138	162	1.18
Fcna	ficolin A	61	74	1.20	60	66	1.10
Fcnb	ficolin B	73	63	-1.15	67	66	-1.00
Hc (C5)	hemolytic C	29	31	1.08	32	32	1.01
Masp1	mannan-binding lectin serine peptidase 1	59	74	1.27	65	69	1.06
Masp2	mannan-binding lectin serine peptidase 2	51	46	-1.11	46	46	1.01
Mbl1	mannose-binding lectin (protein A) 1	47	46	-1.03	47	47	-1.00
Mbl2	mannose-binding lectin (protein C) 2	77	82	1.06	84	76	-1.10
Complement Regulators							
C1qbp	C component 1, q subcomponent binding protein	753	731	-1.03	715	688	-1.04
C4bp	C component 4 binding protein	30	32	1.08	29	32	1.10
Cd46	CD46 antigen, C regulatory protein	44	53	1.20	41	50	1.22
Cd55	CD55 antigen	114	123	1.07	125	134	1.07
Cd59a	CD59a antigen	251	291	1.16	176	184	1.04
Cd59b	CD59b antigen	86	102	1.19	92	107	1.16
Cfh	C component factor h	2494	2710	1.09	350	539	1.54
Cfhr1	C factor H-related 1	19	17	-1.07	16	16	1.00
Cfhr2	C factor H-related 2	19	22	1.14	15	14	-1.04
Cfhr3	C factor H-related 3	16	16	1.01	12	12	1.00
Cfi	C component factor i	42	45	1.06	36	37	1.03
Clu	clusterin	4802	5283	1.10	5712	5254	-1.09
Cr1l (crry	C component (3b/4b) receptor 1-like	356	370	1.04	367	365	-1.01
Serping1	serine (or cysteine) peptidase inhibitor, clade G, member 1	1187	1850	1.56	1141	2037	1.78
Vtn	vitronectin	818	519	-1.58	627	515	-1.22
Complement Receptors							
C3ar1	C component 3a receptor 1	672	1557	2.32	670	1592	2.38
C5ar1	C component 5a receptor 1	139	126	-1.11	180	125	-1.43
Cr2	C receptor 2	33	34	1.03	31	34	1.10

Table 5.5. The effect of ageing on complement genes in RPE/choroid of WT and *Cfh*-/- mice
Robust multiarray averages (RMA) indicate relative expression for each complement gene in RPE/choroid. RMA values were exported from Affymetrix Expression Console by Dr. Carsten Faber. Orange highlight indicates which genes were significantly up or down-regulated upon comparison. $p = < 0.05$.

Gene Symbol	Gene Name	Young WT RMA	Aged WT RMA	Fold Change	Young *Cfh*$^{-/-}$ RMA	Aged *Cfh*$^{-/-}$ RMA	Fold Change
Complement Activators							
C1qa	C component 1, q subcomponent, alpha polypeptide	83	83	1.00	76	85	1.12
C1qb	C component 1, q subcomponent, beta polypeptide	76	90	1.19	89	85	-1.04
C1qc	C component 1, q subcomponent, C chain	111	136	1.22	116	134	1.16
C1ra	C component 1, r subcomponent A	48	41	-1.16	42	45	1.07
C1rb	C component 1, r subcomponent B	21	20	-1.02	21	22	1.05
C1s	C component 1, s subcomponent	27	19	-1.41	23	21	-1.08
C2	C component 2 (within H-2S)	55	58	1.06	55	53	-1.04
C3	C component 3	99	101	1.03	97	109	1.13
C4a	C component 4A (Rodgers blood group)	57	57	1.00	49	62	1.27
C4b	C component 4B (Childo blood group)	57	63	1.10	60	70	1.17
C6	C component 6	22	22	1.00	22	21	-1.05
C7	C component 7	30	29	-1.06	28	31	1.13
C8a	C component 8, alpha polypeptide	38	39	1.03	37	37	1.00
C8b	C component 8, beta polypeptide	48	59	1.23	52	53	1.02
C8g	C component 8, gamma polypeptide	76	75	-1.01	73	77	1.06
C9	C component 9	37	35	-1.06	32	34	1.04
Cfb	C factor B	144	149	1.04	145	151	1.04
Cfd	C factor D (adipsin)	105	100	-1.05	103	111	1.07
Cfp	C factor properdin	157	144	-1.09	159	150	-1.06
Fcna	ficolin A	61	62	1.01	56	60	1.06
Fcnb	ficolin B	84	73	-1.14	70	74	1.05
Hc (C5)	hemolytic C	31	29	-1.06	29	29	1.01
Masp1	mannan-binding lectin serine peptidase 1	59	53	-1.12	50	57	1.15
Masp2	mannan-binding lectin serine peptidase 2	82	86	1.06	81	77	-1.05
Mbl1	mannose-binding lectin (protein A) 1	33	33	-0.97	33	33	1.02
Mbl2	mannose-binding lectin (protein C) 2	78	80	1.03	77	78	1.01
Complement Regulators							
C1qbp	C component 1, q subcomponent binding protein	1016	1067	1.05	1044	947	-1.10
C4bp	C component 4 binding protein	31	35	1.12	33	34	1.03
Cd46	CD46 antigen, C regulatory protein	57	56	-1.02	55	50	-1.10
Cd55	CD55 antigen	22	22	-1.01	22	20	-1.14
Cd59a	CD59a antigen	1220	1998	1.64	1284	1376	1.07
Cd59b	CD59b antigen	56	74	1.32	58	60	1.03
Cfh	C component factor h	429	642	1.49	43	40	-1.09
Cfhr1	C factor H-related 1	22	19	-1.14	19	19	1.00
Cfhr2	C factor H-related 2	12.09	12.626	1.04	9	10	1.08
Cfhr3	C factor H-related 3	16	16	1.00	11	12	1.10
Cfi	C component factor i	76	84	1.10	66	89	1.33
Clu	clusterin	2121	2092	-1.01	2221	2126	-1.04
Cr1l (crry	C component (3b/4b) receptor 1-like	257	245	-1.04	236	204	-1.15
Serping1	serine (or cysteine) peptidase inhibitor, clade G, member 1	156	244	1.56	175	229	1.31
Vtn	vitronectin	4522	3817	-1.18	4713	4039	-1.17
Complement Receptors							
C3ar1	C component 3a receptor 1	67	86	1.28	66	72	1.09
C5ar1	C component 5a receptor 1	31	28	-1.09	27	29	1.06
Cr2	C receptor 2	27	26	-1.04	25	26	1.04

Table 5.6. The effect of ageing on complement genes in neuroretina of WT and *Cfh*-/- mice
Robust multiarray averages (RMA) indicate relative expression for each complement gene in neuroretina. RMA values were exported from Affymetrix Expression Console by Dr. Carsten Faber. Orange highlight indicates which genes were significantly up or down-regulated upon comparison. p = < 0.05.

5.9. Discussion

This study highlights how ageing has a dramatic effect on the gene expression profile of both the RPE/choroid and the neuroretina. Ageing was associated with more genes being differentially expressed in wild-type retina compared to *Cfh*$^{-/-}$ mice. Nevertheless, ageing has a significant impact on gene expression in the *Cfh*$^{-/-}$ mice, since there were very few differences in gene expression in either the RPE/choroid or neuroretina of young *Cfh*$^{-/-}$ mice when compared with controls. Indeed, all bar three of the genes that were differentially expressed in young *Cfh*$^{-/-}$ mice in both RPE/choroid and the neuroretina were located near the *Cfh* locus on chromosome 1. The number of genes on mouse chromosome 1 which were differentially expressed in *Cfh*$^{-/-}$ mice increased with age. The positions of most of these genes were centromeric to the *Cfh* locus, and those with the highest fold changes were located closest to the *Cfh* locus (Figure 5.12). The majority of these genes were down-regulated in the *Cfh*$^{-/-}$ mice. It is possible from these results that the neomycin selectable cassette inserted into the *Cfh* gene exerts non-specific positional effects on the expression of neighbouring genes. Although the mechanism is not known for how this may occur, several studies have shown effects of selectable marker cassettes on neighbouring genes (Rijli *et al.,* 1994; Meier *et al.,* 2010). Nevertheless, it is possible that some of the genes which were differentially expressed on chromosome 1 are a genuine downstream effect from the loss of CFH.

The functions of the genes differentially regulated on chromosome 1 are diverse including, neural transmission, DNA replication, transcription, cytoskeleton, vesicular transport, cellular junctions, cell signalling and the immune response. This discovery must be considered when interpreting changes in gene expression from genes on other chromosomes and the overall effects on phenotype.

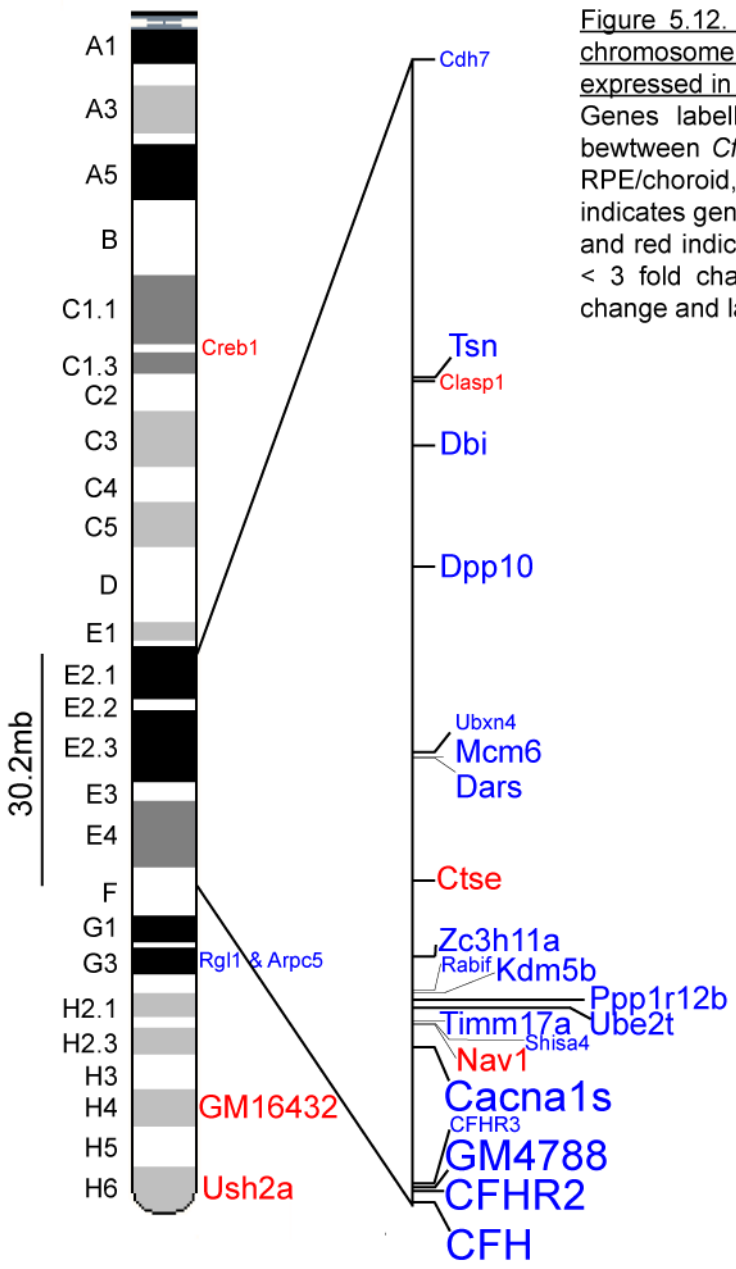

Figure 5.12. Location of genes on mouse chromosome 1 which were differentially expressed in *Cfh*-/- mice

Genes labelled were significantly different bewtween *Cfh*$^{-/-}$ and wild-type mice in either RPE/choroid, neuroretina or both. Blue type indicates genes down-regulated in *Cfh*$^{-/-}$ mice and red indicates up-regulation. Small font = < 3 fold change, medium font = 3-10 fold change and large font = > 10 fold change.

It was surprising to see that *Snca* was down-regulated more than *Cfh*, the original gene disrupted. Since this gene is not located on chromosome 1 it is unlikely that the down-regulation was due to the neo cassette insertion. The role of synuclein alpha outside of neurons is not known. One possible cause of the large down-regulation is that the original mouse strain used to make the knock-out had a disruption in this gene. The mouse strain used had a 129/Sv x C57Bl/6 hybrid genetic background. It is known that C57Bl/6J mice from Harlan contain a chromosomal deletion at the *Scna* locus (Specht and Schoepfer, 2001). In order to clarify if the down-regulation measured in the microarray was genuine, *Cfh*$^{-/-}$ mice would need to be genotyped in the region of the reported deletion (Specht and Schoepfer, 2004).

Chapter 6: Discussion

The complement system is currently emerging as a key feature of several eye diseases. CFH was the first member of the complement system identified as playing a role in the pathogenesis of AMD after the landmark discovery of a SNP present in over 50% of patients (Edwards *et al.,* 2005; Hageman *et al.,* 2005; Haines *et al.,* 2005; Klein *et al.,* 2005). Prior to 2005, little was known about the role of CFH in the healthy retina. This study reports an investigation into the role of CFH in the retina in order to clarify its significance in AMD pathogenesis.

This work was carried out using two experimental systems; *in vitro* through the use of RPE cells in culture and *in vivo* with the use of a knock-out mouse. *In vitro* experiments were informative for understanding the secretory pattern of CFH from RPE cells. Using the RPE cell line, ARPE19, we show that, as in primary porcine RPE, CFH is secreted upon serum removal via *de novo* synthesis. The secretory pattern suggests that CFH is secreted constitutively but only at a low level. However, CFH secretion could be enhanced by the presence of pro-inflammatory cytokines IFNγ or IL-1β. In contrast our *in vivo* model allowed us to investigate the retina as a tissue and using this approach we analysed how the loss of CFH affected the health of the retina when mice were young and at 1 year. Loss of CFH had little effect on the health of the retina at 7-8 weeks with only a mild redistribution of melanosomes in the RPE. Indeed, an analysis of gene expression, revealed only 5 and 12 genes were significantly affected by the loss of CFH in the RPE and neuroretina respectively. At 1 year of age however, the loss of CFH had a greater impact where we were able to identify structural and functional changes and an increased number of genes had altered expression with 21 and 110 genes identified as significantly altered in the RPE and neuroretina respectively. Loss of CFH led to changes observed in the RPE, where organisation of mitochondria and melanosomes were disrupted and in the neuroretina where there was thinning of photoreceptors, re-distribution of complement regulators and early signs of reactive gliosis. Functional tests revealed that the loss of CFH did not impact upon the amplitude of the neural responses but did delay the response of the rod photoreceptors indicating a significant role for CFH in aged mice.

An increased role for CFH with age in the eye fits with the notion that dysfunction of this protein manifests in the age-related eye disease, AMD. In order to understand how regulation of the alternative complement pathway is important to retinal structure and function we chose to use *Cfh*$^{-/-}$ mice to characterise the role of this protein in the retina at a young and intermediate age. For AMD research the use of mouse models seems counter-intuitive since mice do not have a macula, and therefore generation of a mouse which recapitulates all the features of AMD would be challenging. Instead, mouse models are suitable for investigating components of this multifactorial disease.

Immunohistochemical analysis of retinas revealed that due to the loss of CFH several changes were present in the inner retina where we observed altered expression of both GFAP and DAF in 1 year mice. GFAP positive processes extended from the GCL into the IPL in 1 year *Cfh*$^{-/-}$ mice, which we believe to be astrocytic processes indicative of reactive gliosis. Reactive gliosis is one of the first signs that occur when the retina is undergoing stress brought about by injury or disease. In AMD, up-regulation of GFAP in the inner retina is associated with the presence of drusen whereas up-regulation in the outer retina is associated with BRB disruption (Vogt *et al.,* 2006). Within the inner retina lie the three plexuses of the retinal vasculature. Our results indicate that C3b is present in large quantities in these vessels as compared to wild-type mice. We were not able to identify any build up of C3b or C3 on vessel walls as observed by Lundh von *et al.,* (2009) however this may be due to different fixation methods used. One could hypothesise that constant exposure to the enhanced C3b in the retinal vasculature may bring about subtle changes to those vessels or to the perivascular cells, which astroglial cells are capable of detecting. Indeed, Lundh von *et al.,* (2009) reported that in 1 year *Cfh*$^{-/-}$ mice the enhanced deposition of C3 and C3b in the inner vasculature of the retina was associated with withering and reduced perfusion. A reduced rate of perfusion could be one of the causes of retinal stress of the astroglial cells in the inner retina of 1 year *Cfh*$^{-/-}$ mice since GFAP is known to be upregulated in other traditional models of ischaemia such as oxygen-induced retinopathy (DeNiro *et al.,* 2011).

Within the same region of the retina as GFAP, we also observed up-regulation of the complement regulator DAF however their staining patterns were different suggesting that DAF was up-regulated in a different cell type in the inner retina. The DAF positive processes stretching from the GCL to the OPL are characteristic of the shape of Müller cells however this should be confirmed by co-staining for a Müller cell specific marker. This up-regulation shows the ability of the retina to compensate for the loss of CFH by up-regulating a protein which serves several of the same functions of CFH. In human retina, DAF is localised to the ganglion cell layer (Fett *et al.,* 2012) and has recently been shown to be up-regulated in the region of the OLM in patients with AMD (Vogt *et al.,* 2006). Our results suggest that the up-regulation of DAF observed in patients with AMD is directly due to the loss in expression or function of CFH.

Another complement regulator, CD59a, was identified by microarray analysis as being down-regulated (see Chapter 5) in the neuroretina of 1 year *Cfh*$^{-/-}$ mice. In humans, CD59, like DAF, is expressed in the GCL (Sohn *et al.,* 2000) but unlike CRRY and DAF, CD59a inhibits the assembly and function of MAC in the terminal complement pathway. We were unable to verify the presence of MAC formation in the neuroretina of wild-type or *Cfh*$^{-/-}$ mice by immunohistochemistry with the use of several antibodies. MAC has been shown to be constantly active at a low level in the iris, ciliary body, corneal epithelium, sclera and choroid of adult rats (Sohn *et al.,* 2000), however the presence of MAC in the normal mouse retina has not been described in the literature. In AMD, MAC is detected on the RPE, choroidal blood vessels and drusen (Bora *et al.,* 2006). MAC generation is believed to be an important mediator of CNV in laser-induced mouse models since blocking MAC generation using *C5*$^{-/-}$ mice or by up-regulating CD59a significantly reduced development of CNV lesions (Bora *et al.,* 2006; Bora *et al.,* 2007). The generation of MAC via activation of the alternative pathway is important for CNV development since CNV is inhibited in *Cfb*$^{-/-}$ but not *C4*$^{-/-}$ mice (Brooimans *et al.,* 1989). Given this, one would expect CNV lesions to be exacerbated in *Cfh*$^{-/-}$ mice due to a less controlled regulation of the alternative pathway. However Lundh von *et al.,* (2009) report that laser-induced CNV is less severe in *Cfh*$^{-/-}$ mice compared to wild-type mice which they believe is due to lower perfusion rates in the choriocapillaris. Although we were unable to verify whether there was low level MAC

generation present in 1 year wild-type, it may be that up-regulation of DAF and CRRY protein expression in 1 year *Cfh*$^{-/-}$ mice enabled better control of terminal pathway activation and redundancy of CD59a function leading to its down-regulation in *Cfh*$^{-/-}$ mice. Better control of the terminal pathway in 1 year *Cfh*$^{-/-}$ mice may be a reason for the reduced lesion size observed by Lundh von *et al.,* in their laser induced CNV experiments. Alternatively, the down-regulation of CD59a seen in 1 year *Cfh*$^{-/-}$ mice may lead to deposition of MAC but at levels below the limit of detection by immunohistochemistry. Uncontrolled MAC generation can cause harmful bystander damage to healthy tissue and may have contributed to the mild degeneration seen at 1 year in *Cfh*$^{-/-}$ mice where there was thinning in the photoreceptors, ONL and INL. MAC can also have sub-lytic effects where in RPE it has been shown to stimulate the secretion of IL-6, IL-8, MCP-1 and VEGF (Lueck *et al.,* 2011). Gene expression analysis did not reveal a significant increase in the expression of these molecules suggesting that either MAC formation did not occur in *Cfh*$^{-/-}$ mice or that it was formed elsewhere in the retina. In future experiments it will be important to validate CD59a protein expression by immunohistochemistry or immunoblot and to analyse MAC expression by immunoblot in the retina of *Cfh*$^{-/-}$ mice.

In contrast to the inner retina where we observed differences in GFAP and DAF expression but the overall morphology was normal, in the outer neuroretina we observed altered morphology with thinning of the photoreceptors and reduced nuclei density in the ONL in 1 year *Cfh*$^{-/-}$ mice. Close to this region we also observed up-regulation of the complement regulator CRRY clustered around the ribbon synapses of the OPL, demonstrating that this area is responsive to changes in the complement system. We are uncertain as to the direct cause of the cell death observed in the photoreceptors of 1 year *Cfh*$^{-/-}$ mice however some clues can be taken from gene expression analysis of the neuroretina. There were 109 genes which were significantly differentially expressed in 1 year *Cfh*$^{-/-}$ mice as compared to age-matched wild-type controls. Of these 109 genes, *Pttg1* is of particular interest since it is dysregulated in other models of photoreceptor degeneration (van de Pavert *et al.,* 2007; Fernandez-Medarde *et al.,* 2009; Yetemian *et al.,* 2010). Pathway analysis identified amino acid metabolism and signalling between cells to be the main pathways affected by the loss

of CFH in the neuroretina at 1 year. These two functions are integral to the normal functioning of the neuroretina. We speculate that photoreceptor cell death may be the result of reduced interaction of the photoreceptors with neighbouring cells such as the RPE. Indeed we observed a greater tendency for the photoreceptors to detach from the RPE in 1 year *Cfh*$^{-/-}$ mice when preparing fixed sections for electron microscopy and immunohistochemistry. The death of photoreceptors in 1 year *Cfh*$^{-/-}$ mice had an impact on visual function since we recorded a decreased time to peak of the a-wave when stimulating the rod photoreceptors under scotopic conditions.

The phenotype characterised in these mice at 1 year is mild, with subtle differences revealed by ERG in the scotopic a-wave, RPE organelle distribution, ONL density and GFAP expression. The ability of the retina to cope with the loss of CFH may be due to the up-regulation we observed of membrane-bound complement regulators, CRRY in the OPL, and DAF in the GCL, IPL, INL and OPL. Our results highlight the ability of the neuroretina to adapt its expression of complement regulators in response to loss of CFH. Surprisingly this up-regulation, observed by immunohistochemistry, was not observed upon gene expression analysis of the neuroretina of 1 year *Cfh*$^{-/-}$ mice. This suggests that the up-regulation of these proteins was due to an effect occurring post-translation, emphasising the importance of not assuming that mRNA expression is equivalent to protein expression. Alternatively it could suggest that up-regulation of DAF or CRRY was in a small subset of cells which did not reach statistical significance over the background of the other cells present in the neuroretina. However, we should also consider, that these two analyses were carried out using mice of slightly different ages (1 year and 1 year 4 months), therefore it is possible (albeit unlikely), that protein expression although enhanced at 1 year in *Cfh*$^{-/-}$ mice, returned to that of age-matched wild-type controls by 1 year 4 months, or that age-matched wild-type controls also up-regulated these genes within the 4 months these analyses were carried out.

Gene expression analysis did reveal that in 1 year *Cfh*$^{-/-}$ mice, more genes in the neuroretina were differentially regulated as compared to the RPE/choroid. This suggests that the absence of CFH has a larger impact on the neuroretina than the RPE/choroid. Similarly, the majority of the differences between 1 year *Cfh*$^{-/-}$ and age-

matched wild-type controls identified in Chapter 4 were in the neuroretina. These results draw attention away from the RPE, dysfunction of which is central to AMD, to focus instead on the neuroretina. Conversely an analysis of ageing of both the wild-type and *Cfh*$^{-/-}$ mice revealed significantly more genes were differentially regulated in the RPE/choroid as compared to the neuroretina. We speculate that the ability of the RPE/choroid to adapt gene expression to a larger extent with age may render these tissues more protection against the damaging effects of ageing. Interestingly the main cellular and canonical pathways affected by ageing in the RPE/choroid of both genotypes were the complement system, acute phase response signalling and inflammatory responses highlighting how the innate immune system is the most significantly affected pathway by ageing in this tissue.

Although the use of *Cfh*$^{-/-}$ mice was informative in understanding the role of CFH in the retina we also wanted to investigate the expression pattern of CFH by RPE which is believed to be the main source of CFH in the eye. Our results corroborate this belief since gene expression analysis of wild-type mice showed that *Cfh* gene expression was higher in RPE/choroid as compared to the neuroretina. To investigate CFH secretion we used an *in vitro* approach and developed a secretory assay using ARPE19 cells, where spent media was precipitated with TCA and proteins were subsequently resolved by SDS PAGE and western blotted for CFH. This approach allowed us to test whether external stimuli could modulate CFH secretion. For quantitative analysis, samples were spiked with goat IgG to act as a loading control. In hindsight, the development of an enzyme-linked immunosorbent assay would have had several advantages including more sensitive detection of CFH, increased accuracy and being a faster technique.

Since different tissues express different members of the complement system at various levels, some of which are constitutively expressed and some factors that are only expressed in response to inflammation, we used our *in vitro* assay to determine secretion patterns from RPE. We have confirmed that RPE cells in culture secrete CFH *de novo* consistent with human umbilical vein endothelial cells (Penfold *et al.,* 2001), and provide evidence that this secretion is constitutive. Constitutive expression of CFH

by ARPE19 cells has previously been disputed by Wu *et al.,* (2007) who reported that IFNγ stimulation is required for CFH expression from ARPE19 cells. This discrepancy in results is most likely because we were able to detect a lower level of expression by concentrating spent media with TCA. Our results are in agreement with data from primary human RPE where CFH is shown to be secreted in a constitutive manner (Kim *et al.,* 2009). Constitutive secretion of CFH from RPE suggests that there is a constant requirement for complement regulation in the retina which is not met by a systemic contribution. However because the concentration of secreted CFH was not high enough to be detected by western blotting without prior concentration this suggests that constitutive secretion, at least by ARPE19 cells in culture, is only at a low level. It is possible therefore that complement regulation in the retina is supplemented by systemic CFH from the choroid. This would imply that gene or stem cell therapy to correct a SNP in CFH in RPE may not be a successful approach for treating AMD.

Several pathological mechanisms involved in AMD can influence the behaviour of RPE cells including oxidative stress, lipid metabolism and inflammation. We chose to investigate the effect of inflammation on CFH secretion in our secretion assay since complement expression is known to be modified by this process in several cell types. As in other cell types, we showed that RPE cells in culture enhance secretion of CFH in response to IFNγ. Kim *et al.,* (2009) have previously shown this using cultured human foetal RPE however this is the first report showing that CFH secretion from ARPE19 cells is similar to primary human RPE cells. Additionally, we showed for the first time in this cell type that another pro-inflammatory cytokine, IL-1β, also enhanced CFH secretion from RPE cells in culture. In AMD, the RPE is exposed to cytokines from several sources, including activated microglial cells which migrate towards the sub-RPE space with age (Tsutsumi *et al.,* 2003), macrophage infiltration during CNV (Yu *et al.,* 2007) and from the RPE cells themselves in an autocrine or paracrine manner. Our experiments however, reflect the response of healthy RPE cells to pro-inflammatory cytokines. In AMD, where RPE cells are exposed to several stresses such as oxidative stress (see Section 1.4.4.1) and altered lipid metabolism (see Section 1.4.4.2) the RPE may have an altered response to pro-inflammatory cytokines where perhaps an enhanced CFH secretion is not able to be maintained allowing complement activation

to ensue. Evidence for this comes from the data collected from our serial samples where the RPE cells were exposed to the stress of the media being changed every two hours. In this case we observed a drop in CFH secretion over time, suggesting that cell stress may diminish CFH secretion.

At present it is not known whether CFH secreted by RPE cells is functionally active. In order to test this, CFH collected from RPE cells in culture could be used in a haemolytic assay where sheep red blood cells are incubated with CFH free serum with or without adding back the collected CFH and percentage lysis is assessed. In future work it will be important to demonstrate that CFH secreted by RPE cells is active and that its concentration in the retina is functionally significant.

ARPE19 cells are heterozygous for the C/T AMD-risk SNP (unpublished data from our group) and are therefore ideal to study how the Y/H protein variants may differ in their function or secretion. It is not known whether the Y/H CFH variants are secreted at a similar level. Over-expression of these variants in human embryonic kidney 293 cells (Yu *et al.,* 2007) suggests that this is not the case, however An *et al.,* (2006) report enhanced CFH secretion from human RPE genotyped as homozygous for the AMD-associated H-variant. It would be interesting to study whether one of the variants in ARPE19 cells is preferentially secreted at the apical or basal membrane. In order to carry out these experiments, Y/H specific CFH antibodies and polarised ARPE19 monolayers would be required.

Use of an *in vitro* assay does not allow an investigation into how CFH secretion changes with ageing. Gene expression analysis of wild-type mice showed that there was no change in *Cfh* RNA expression from 7-8 weeks to 1 year 4 months suggesting that tight regulation of *Cfh* RNA expression is likely to be important to the health of the retina over time. This result is in agreement with similar reports where in mice, Mandal and Ayyagari (2006) show no particular transcription pattern in the posterior segment from P30-600 and in humans, Hageman *et al.,* (2005) report no change to CFH transcription with age. Para-inflammation associated with the ageing of the retina has previously been associated with up-regulation of TNFα (Xu *et al.,* 2009), and our data showing

that TNFα has no impact on CFH secretion by RPE cells would support the notion that there is no change in the regulation of *CFH* transcription with age and para-inflammation.

This study overall has attempted to answer some of the questions relating to the expression of CFH from the RPE and its function in the retina as a whole. We show that RPE cells constitutively secrete CFH *de novo* at a low level but that this can be enhanced by pro-inflammatory cytokines IFNγ and IL-1β. We show that the retina is reactive to changes in complement regulation and plays on the redundancy between complement regulators by compensating for loss of CFH with the up-regulation of DAF and CRRY. However, CFH must play a role beyond that which other complement regulators can compensate since early signs of photoreceptor degeneration are evident in 1 year *Cfh*$^{-/-}$ retinas. Overall the phenotype of the 1 year *Cfh*$^{-/-}$ mice was subtle and this may reflect the additional deficiency in these mice which are also low in circulating C3. Since patients with AMD have normal circulating levels of C3, it would be of interest to generate a RPE-specific *Cfh*$^{-/-}$ mouse where mice would have normal levels of circulating CFH and C3. The presence of normal levels of circulating C3 may attenuate or generate a more severe phenotype in the retina as compared to global *Cfh*$^{-/-}$ mice. Using the *Cfh*$^{-/-}$ mouse we were unable to distinguish whether the phenotype which developed was due to loss of ocular or systemic CFH, or both. Using RPE-specific *Cfh* gene deletion would allow us to separate the contribution of local as compared to systemic CFH to the health of the retina. This transgenic mouse we are currently creating using cre-loxP technology, where a transgenic mouse expressing inducible Cre recombinase under the control of the RPE specific monocarboxylate transporter 3 gene promoter (Longbottom *et al.,* 2009) is crossed with a transgenic mouse expressing floxed *Cfh* alleles.

Reference List

(2001). A randomized, placebo-controlled, clinical trial of high-dose supplementation with vitamins C and E, beta carotene, and zinc for age-related macular degeneration and vision loss: AREDS report no. 8. *Arch. Ophthalmol.* **119,** 1417-1436.

Adinolfi,M., Dobson,N.C., and Bradwell,A.R. (1981). Synthesis of two components of human complement, beta 1H and C3bINA, during fetal life. *Acta Paediatr. Scand.* **70,** 705-710.

Alberstein,M., Amit,M., Vaknin,K., O'Donnell,A., Farhy,C., Lerenthal,Y., Shomron,N., Shaham,O., Sharrocks,A.D., shery-Padan,R. et al. (2007). Regulation of transcription of the RNA splicing factor hSlu7 by Elk-1 and Sp1 affects alternative splicing. *RNA.* **13,** 1988-1999.

Allikmets,R. (2000). Further evidence for an association of ABCR alleles with age-related macular degeneration. The International ABCR Screening Consortium. *Am. J. Hum. Genet.* **67,** 487-491.

Ambati,J., Anand,A., Fernandez,S., Sakurai,E., Lynn,B.C., Kuziel,W.A., Rollins,B.J., and Ambati,B.K. (2003). An animal model of age-related macular degeneration in senescent Ccl-2- or Ccr-2-deficient mice. *Nat. Med.* **9,** 1390-1397.

An,E., Gordish-Dressman,H., and Hathout,Y. (2008). Effect of TNF-alpha on human ARPE-19-secreted proteins. *Mol. Vis.* **14,** 2292-2303.

An,E., Lu,X., Flippin,J., Devaney,J.M., Halligan,B., Hoffman,E.P., Strunnikova,N., Csaky,K., and Hathout,Y. (2006). Secreted proteome profiling in human RPE cell cultures derived from donors with age related macular degeneration and age matched healthy donors. *J. Proteome. Res.* **5,** 2599-2610.

An,E., Sen,S., Park,S.K., Gordish-Dressman,H., and Hathout,Y. (2010). Identification of novel substrates for the serine protease HTRA1 in the human RPE secretome. *Invest Ophthalmol. Vis. Sci.* **51,** 3379-3386.

An,F., Li,Q., Tu,Z., Bu,H., Chan,C.C., Caspi,R.R., and Lin,F. (2009). Role of DAF in protecting against T-cell autoreactivity that leads to experimental autoimmune uveitis. *Invest Ophthalmol. Vis. Sci.* **50,** 3778-3782.

Anderson,D.H., Ozaki,S., Nealon,M., Neitz,J., Mullins,R.F., Hageman,G.S., and Johnson,L.V. (2001). Local cellular sources of apolipoprotein E in the human retina and retinal pigmented epithelium: implications for the process of drusen formation. *Am. J. Ophthalmol.* **131,** 767-781.

Aslam,M. and Perkins,S.J. (2001). Folded-back solution structure of monomeric factor H of human complement by synchrotron X-ray and neutron scattering, analytical ultracentrifugation and constrained molecular modelling. *J. Mol. Biol.* **309,** 1117-1138.

Austin,B.A., Liu,B., Li,Z., and Nussenblatt,R.B. (2009). Biologically active fibronectin fragments stimulate release of MCP-1 and catabolic cytokines from murine retinal pigment epithelium. *Invest Ophthalmol. Vis. Sci.* **50,** 2896-2902.

Baalasubramanian,S., Harris,C.L., Donev,R.M., Mizuno,M., Omidvar,N., Song,W.C., and Morgan,B.P. (2004). CD59a is the primary regulator of membrane attack complex assembly in the mouse. *J. Immunol.* **173,** 3684-3692.

Baynes,J.W. (2001). The role of AGEs in aging: causation or correlation. *Exp. Gerontol.* **36,** 1527-1537.

Beatty,S., Koh,H., Phil,M., Henson,D., and Boulton,M. (2000). The role of oxidative stress in the pathogenesis of age-related macular degeneration. *Surv. Ophthalmol.* **45,** 115-134.

Becerra,S.P., Fariss,R.N., Wu,Y.Q., Montuenga,L.M., Wong,P., and Pfeffer,B.A. (2004). Pigment epithelium-derived factor in the monkey retinal pigment epithelium and interphotoreceptor matrix: apical secretion and distribution. *Exp. Eye Res.* **78,** 223-234.

Bernal,J.A., Luna,R., Espina,A., Lazaro,I., Ramos-Morales,F., Romero,F., Arias,C., Silva,A., Tortolero,M., and Pintor-Toro,J.A. (2002). Human securin interacts with p53 and modulates p53-mediated transcriptional activity and apoptosis. *Nat. Genet.* **32,** 306-311.

Bernstein,H.G., Reichenbach,A., and Wiederanders,B. (1998). Cathepsin E immunoreactivity in human ocular tissues: influence of aging and pathological states. *Neurosci. Lett.* **240,** 135-138.

Bettman,J.W., Fellows,V., and Chao,P. (1958). The effect of cigarette smoking on the intraocular circulation. *AMA. Arch. Ophthalmol.* **59,** 481-488.

Bexborn,F., Andersson,P.O., Chen,H., Nilsson,B., and Ekdahl,K.N. (2008). The tick-over theory revisited: formation and regulation of the soluble alternative complement C3 convertase (C3(H2O)Bb). *Mol. Immunol.* **45,** 2370-2379.

Blackmore,T.K., Fischetti,V.A., Sadlon,T.A., Ward,H.M., and Gordon,D.L. (1998a). M protein of the group A Streptococcus binds to the seventh short consensus repeat of human complement factor H. *Infect. Immun.* **66,** 1427-1431.

Blackmore,T.K., Hellwage,J., Sadlon,T.A., Higgs,N., Zipfel,P.F., Ward,H.M., and Gordon,D.L. (1998b). Identification of the second heparin-binding domain in human complement factor H. *J. Immunol.* **160,** 3342-3348.

Blackmore,T.K., Sadlon,T.A., Ward,H.M., Lublin,D.M., and Gordon,D.L. (1996). Identification of a heparin binding domain in the seventh short consensus repeat of complement factor H. *J. Immunol.* **157,** 5422-5427.

Bokisch,V.A., Dierich,M.P., and Muller-Eberhard,H.J. (1975). Third component of complement (C3): structural properties in relation to functions. *Proc. Natl. Acad. Sci. U. S. A* **72,** 1989-1993.

Bokisch,V.A. and Muller-Eberhard,H.J. (1970). Anaphylatoxin inactivator of human plasma: its isolation and characterization as a carboxypeptidase. *J. Clin. Invest* **49,** 2427-2436.

Bone,R.A., Landrum,J.T., and Tarsis,S.L. (1985). Preliminary identification of the human macular pigment. *Vision Res.* **25,** 1531-1535.

Bonilha,V.L. (2008). Age and disease-related structural changes in the retinal pigment epithelium. *Clin. Ophthalmol.* **2,** 413-424.

Booij,J.C., Baas,D.C., Beisekeeva,J., Gorgels,T.G., and Bergen,A.A. (2010). The dynamic nature of Bruch's membrane. *Prog. Retin. Eye Res.* **29,** 1-18.

Bora,N.S., Jha,P., Lyzogubov,V.V., Kaliappan,S., Liu,J., Tytarenko,R.G., Fraser,D.A., Morgan,B.P., and Bora,P.S. (2010). Recombinant membrane-targeted form of CD59 inhibits the growth of choroidal neovascular complex in mice. *J. Biol. Chem.* **285,** 33826-33833.

Bora,N.S., Kaliappan,S., Jha,P., Xu,Q., Sivasankar,B., Harris,C.L., Morgan,B.P., and Bora,P.S. (2007). CD59, a complement regulatory protein, controls choroidal

neovascularization in a mouse model of wet-type age-related macular degeneration. *J. Immunol.* **178,** 1783-1790.

Bora,N.S., Kaliappan,S., Jha,P., Xu,Q., Sohn,J.H., Dhaulakhandi,D.B., Kaplan,H.J., and Bora,P.S. (2006). Complement activation via alternative pathway is critical in the development of laser-induced choroidal neovascularization: role of factor B and factor H. *J. Immunol.* **177,** 1872-1878.

Bora,P.S., Sohn,J.H., Cruz,J.M., Jha,P., Nishihori,H., Wang,Y., Kaliappan,S., Kaplan,H.J., and Bora,N.S. (2005). Role of complement and complement membrane attack complex in laser-induced choroidal neovascularization. *J. Immunol.* **174,** 491-497.

Braley,A.E. (1966). Dystrophy of the macula. *Am. J. Ophthalmol.* **61,** 1-24.

Bringmann,A., Pannicke,T., Grosche,J., Francke,M., Wiedemann,P., Skatchkov,S.N., Osborne,N.N., and Reichenbach,A. (2006). Muller cells in the healthy and diseased retina. *Prog. Retin. Eye Res.* **25,** 397-424.

Brooimans,R.A., Hiemstra,P.S., van der Ark,A.A., Sim,R.B., van Es,L.A., and Daha,M.R. (1989). Biosynthesis of complement factor H by human umbilical vein endothelial cells. Regulation by T cell growth factor and IFN-gamma. *J. Immunol.* **142,** 2024-2030.

Cai,H. and Del Priore,L.V. (2006). Gene expression profile of cultured adult compared to immortalized human RPE. *Mol. Vis.* **12,** 1-14.

Cai,J., Nelson,K.C., Wu,M., Sternberg,P., Jr., and Jones,D.P. (2000). Oxidative damage and protection of the RPE. *Prog. Retin. Eye Res.* **19,** 205-221.

Carroll,M.V. and Sim,R.B. (2011). Complement in health and disease. *Adv. Drug Deliv. Rev.* **63,** 965-975.

Carter-Dawson,L.D. and LaVail,M.M. (1979). Rods and cones in the mouse retina. I. Structural analysis using light and electron microscopy. *J. Comp Neurol.* **188,** 245-262.

Chang,B., Mandal,M.N., Chavali,V.R., Hawes,N.L., Khan,N.W., Hurd,R.E., Smith,R.S., Davisson,M.L., Kopplin,L., Klein,B.E. et al. (2008). Age-related retinal degeneration (arrd2) in a novel mouse model due to a nonsense mutation in the Mdm1 gene. *Hum. Mol. Genet.* **17,** 3929-3941.

Charlesworth,J.A., Scott,D.M., Pussell,B.A., and Peters,D.K. (1979). Metabolism of human beta 1H: studies in man and experimental animals. *Clin. Exp. Immunol.* **38,** 397-404.

Chen,H., Liu,B., Lukas,T.J., and Neufeld,A.H. (2008). The aged retinal pigment epithelium/choroid: a potential substratum for the pathogenesis of age-related macular degeneration. *PLoS. One.* **3,** e2339.

Chen,M., Forrester,J.V., and Xu,H. (2007). Synthesis of complement factor H by retinal pigment epithelial cells is down-regulated by oxidized photoreceptor outer segments. *Exp. Eye Res.* **84,** 635-645.

Chen,M., Muckersie,E., Forrester,J.V., and Xu,H. (2010). Immune activation in retinal aging: a gene expression study. *Invest Ophthalmol. Vis. Sci.* **51,** 5888-5896.

Chen,P.C., Chen,Y.C., Lai,L.C., Tsai,M.H., Chen,S.K., Yang,P.W., Lee,Y.C., Hsiao,C.K., Lee,J.M., and Chuang,E.Y. (2011). Use of Germline Polymorphisms in Predicting Concurrent Chemoradiotherapy Response in Esophageal Cancer. *Int. J. Radiat. Oncol. Biol. Phys.*

Chong,E.W., Kreis,A.J., Wong,T.Y., Simpson,J.A., and Guymer,R.H. (2008). Alcohol consumption and the risk of age-related macular degeneration: a systematic review and meta-analysis. *Am. J. Ophthalmol.* **145,** 707-715.

Chong,N.H., Keonin,J., Luthert,P.J., Frennesson,C.I., Weingeist,D.M., Wolf,R.L., Mullins,R.F., and Hageman,G.S. (2005). Decreased thickness and integrity of the macular elastic layer of Bruch's membrane correspond to the distribution of lesions associated with age-related macular degeneration. *Am. J. Pathol.* **166,** 241-251.

Cicardi,M., Zingale,L., Zanichelli,A., Pappalardo,E., and Cicardi,B. (2005). C1 inhibitor: molecular and clinical aspects. *Springer Semin. Immunopathol.* **27,** 286-298.

Ciulla,T.A. and Rosenfeld,P.J. (2009). Antivascular endothelial growth factor therapy for neovascular age-related macular degeneration. *Curr. Opin. Ophthalmol.* **20,** 158-165.

Clark,S.J., Higman,V.A., Mulloy,B., Perkins,S.J., Lea,S.M., Sim,R.B., and Day,A.J. (2006). His-384 allotypic variant of factor H associated with age-related macular degeneration has different heparin binding properties from the non-disease-associated form. *J. Biol. Chem.* **281,** 24713-24720.

Clark,S.J., Perveen,R., Hakobyan,S., Morgan,B.P., Sim,R.B., Bishop,P.N., and Day,A.J. (2010). Impaired binding of the age-related macular degeneration-associated complement factor H 402H allotype to Bruch's membrane in human retina. *J. Biol. Chem.* **285,** 30192-30202.

Cleveland,R.P., Hazlett,L.D., Leon,M.A., and Berk,R.S. (1983). Role of complement in murine corneal infection caused by Pseudomonas aeruginosa. *Invest Ophthalmol. Vis. Sci.* **24,** 237-242.

Coffey,P.J., Gias,C., McDermott,C.J., Lundh,P., Pickering,M.C., Sethi,C., Bird,A., Fitzke,F.W., Maass,A., Chen,L.L. et al. (2007). Complement factor H deficiency in aged mice causes retinal abnormalities and visual dysfunction. *Proc. Natl. Acad. Sci. U. S. A* **104,** 16651-16656.

Cousins,S.W., Espinosa-Heidmann,D.G., and Csaky,K.G. (2004). Monocyte activation in patients with age-related macular degeneration: a biomarker of risk for choroidal neovascularization? *Arch. Ophthalmol.* **122,** 1013-1018.

Crabb,J.W., Miyagi,M., Gu,X., Shadrach,K., West,K.A., Sakaguchi,H., Kamei,M., Hasan,A., Yan,L., Rayborn,M.E. et al. (2002). Drusen proteome analysis: an approach to the etiology of age-related macular degeneration. *Proc. Natl. Acad. Sci. U. S. A* **99,** 14682-14687.

Curcio,C.A. and Millican,C.L. (1999). Basal linear deposit and large drusen are specific for early age-related maculopathy. *Arch. Ophthalmol.* **117,** 329-339.

D'souza,Y.B., Jones,C.J., Short,C.D., Roberts,I.S., and Bonshek,R.E. (2009). Oligosaccharide composition is similar in drusen and dense deposits in membranoproliferative glomerulonephritis type II. *Kidney Int.* **75,** 824-827.

Deangelis,M.M., Silveira,A.C., Carr,E.A., and Kim,I.K. (2011). Genetics of age-related macular degeneration: current concepts, future directions. *Semin. Ophthalmol.* **26,** 77-93.

Degn,S.E., Jensen,L., Gal,P., Dobo,J., Holmvad,S.H., Jensenius,J.C., and Thiel,S. (2010). Biological variations of MASP-3 and MAp44, two splice products of the MASP1 gene involved in regulation of the complement system. *J. Immunol. Methods* **361,** 37-50.

Degn,S.E., Jensenius,J.C., and Thiel,S. (2011). Disease-causing mutations in genes of the complement system. *Am. J. Hum. Genet.* **88,** 689-705.

Dempsey,P.W., Allison,M.E., Akkaraju,S., Goodnow,C.C., and Fearon,D.T. (1996). C3d of complement as a molecular adjuvant: bridging innate and acquired immunity. *Science* **271,** 348-350.

DeNiro,M., Al-Mohanna,F.H., and Al-Mohanna,F.A. (2011). Inhibition of reactive gliosis prevents neovascular growth in the mouse model of oxygen-induced retinopathy. *PLoS. One.* **6,** e22244.

Detrick,B. and Hooks,J.J. (2010). Immune regulation in the retina. *Immunol. Res.* **47,** 153-161.

Du,H., Lim,S.L., Grob,S., and Zhang,K. (2011). Induced pluripotent stem cell therapies for geographic atrophy of age-related macular degeneration. *Semin. Ophthalmol.* **26,** 216-224.

Dunn,K.C., Aotaki-Keen,A.E., Putkey,F.R., and Hjelmeland,L.M. (1996). ARPE-19, a human retinal pigment epithelial cell line with differentiated properties. *Exp. Eye Res.* **62,** 155-169.

Ebrahem,Q., Renganathan,K., Sears,J., Vasanji,A., Gu,X., Lu,L., Salomon,R.G., Crabb,J.W., and nand-Apte,B. (2006). Carboxyethylpyrrole oxidative protein modifications stimulate neovascularization: Implications for age-related macular degeneration. *Proc. Natl. Acad. Sci. U. S. A* **103,** 13480-13484.

Edwards,A.O., Ritter,R., III, Abel,K.J., Manning,A., Panhuysen,C., and Farrer,L.A. (2005). Complement factor H polymorphism and age-related macular degeneration. *Science* **308,** 421-424.

Esparza-Gordillo,J., Soria,J.M., Buil,A., Almasy,L., Blangero,J., Fontcuberta,J., and Rodriguez de,C.S. (2004). Genetic and environmental factors influencing the human factor H plasma levels. *Immunogenetics* **56,** 77-82.

Estaller,C., Schwaeble,W., Dierich,M., and Weiss,E.H. (1991). Human complement factor H: two factor H proteins are derived from alternatively spliced transcripts. *Eur. J. Immunol.* **21,** 799-802.

Fearon,D.T. (1980). Identification of the membrane glycoprotein that is the C3b receptor of the human erythrocyte, polymorphonuclear leukocyte, B lymphocyte, and monocyte. *J. Exp. Med.* **152,** 20-30.

Fearon,D.T. and Austen,K.F. (1975). Properdin: binding to C3b and stabilization of the C3b-dependent C3 convertase. *J. Exp. Med.* **142,** 856-863.

Fernandez-Medarde,A., Barhoum,R., Riquelme,R., Porteros,A., Nunez,A., de,L.A., de Las,R.J., de,l., V, Varela-Nieto,I., and Santos,E. (2009). RasGRF1 disruption causes retinal photoreception defects and associated transcriptomic alterations. *J. Neurochem.* **110,** 641-652.

Fernando,A.N., Furtado,P.B., Clark,S.J., Gilbert,H.E., Day,A.J., Sim,R.B., and Perkins,S.J. (2007). Associative and structural properties of the region of complement factor H encompassing the Tyr402His disease-related polymorphism and its interactions with heparin. *J. Mol. Biol.* **368,** 564-581.

Ferris,F.L., III, Fine,S.L., and Hyman,L. (1984). Age-related macular degeneration and blindness due to neovascular maculopathy. *Arch. Ophthalmol.* **102,** 1640-1642.

Fett,A.L., Hermann,M.M., Muether,P.S., Kirchhof,B., and Fauser,S. (2012). Immunohistochemical localization of complement regulatory proteins in the human retina. *Histol. Histopathol.* **27,** 357-364.

Finnemann,S.C., Bonilha,V.L., Marmorstein,A.D., and Rodriguez-Boulan,E. (1997). Phagocytosis of rod outer segments by retinal pigment epithelial cells requires alpha(v)beta5 integrin for binding but not for internalization. *Proc. Natl. Acad. Sci. U. S. A* **94,** 12932-12937.

Fremeaux-Bacchi,V., Miller,E.C., Liszewski,M.K., Strain,L., Blouin,J., Brown,A.L., Moghal,N., Kaplan,B.S., Weiss,R.A., Lhotta,K. et al. (2008). Mutations in complement C3 predispose to development of atypical hemolytic uremic syndrome. *Blood* **112,** 4948-4952.

Friedman,D.S., O'Colmain,B.J., Munoz,B., Tomany,S.C., McCarty,C., de Jong,P.T., Nemesure,B., Mitchell,P., and Kempen,J. (2004). Prevalence of age-related macular degeneration in the United States. *Arch. Ophthalmol.* **122,** 564-572.

Friese,M.A., Hellwage,J., Jokiranta,T.S., Meri,S., Peter,H.H., Eibel,H., and Zipfel,P.F. (1999). FHL-1/reconectin and factor H: two human complement regulators which are encoded by the same gene are differently expressed and regulated. *Mol. Immunol.* **36,** 809-818.

Fukuoka,Y., Strainic,M., and Medof,M.E. (2003). Differential cytokine expression of human retinal pigment epithelial cells in response to stimulation by C5a. *Clin. Exp. Immunol.* **131,** 248-253.

Futter,C.E., Ramalho,J.S., Jaissle,G.B., Seeliger,M.W., and Seabra,M.C. (2004). The role of Rab27a in the regulation of melanosome distribution within retinal pigment epithelial cells. *Mol. Biol. Cell* **15,** 2264-2275.

Gariano,R.F., Provis,J.M., and Hendrickson,A.E. (2000). Development of the foveal avascular zone. *Ophthalmology* **107,** 1026.

Garlatti,V., Chouquet,A., Lunardi,T., Vives,R., Paidassi,H., Lortat-Jacob,H., Thielens,N.M., Arlaud,G.J., and Gaboriaud,C. (2010). Cutting edge: C1q binds deoxyribose and heparan sulfate through neighboring sites of its recognition domain. *J. Immunol.* **185,** 808-812.

Glenn,J.V., Mahaffy,H., Wu,K., Smith,G., Nagai,R., Simpson,D.A., Boulton,M.E., and Stitt,A.W. (2009). Advanced glycation end product (AGE) accumulation on Bruch's membrane: links to age-related RPE dysfunction. *Invest Ophthalmol. Vis. Sci.* **50,** 441-451.

Gordon,D.L., Kaufman,R.M., Blackmore,T.K., Kwong,J., and Lublin,D.M. (1995). Identification of complement regulatory domains in human factor H. *J. Immunol.* **155,** 348-356.

Gouras,P., Ivert,L., Neuringer,M., and Mattison,J.A. (2010). Topographic and age-related changes of the retinal epithelium and Bruch's membrane of rhesus monkeys. *Graefes Arch. Clin. Exp. Ophthalmol.* **248,** 973-984.

Gu,X., Meer,S.G., Miyagi,M., Rayborn,M.E., Hollyfield,J.G., Crabb,J.W., and Salomon,R.G. (2003). Carboxyethylpyrrole protein adducts and autoantibodies, biomarkers for age-related macular degeneration. *J. Biol. Chem.* **278,** 42027-42035.

Haddad,S., Chen,C.A., Santangelo,S.L., and Seddon,J.M. (2006). The genetics of age-related macular degeneration: a review of progress to date. *Surv. Ophthalmol.* **51,** 316-363.

Hageman,G.S., Anderson,D.H., Johnson,L.V., Hancox,L.S., Taiber,A.J., Hardisty,L.I., Hageman,J.L., Stockman,H.A., Borchardt,J.D., Gehrs,K.M. et al. (2005). A common haplotype in the complement regulatory gene factor H (HF1/CFH) predisposes individuals to age-related macular degeneration. *Proc. Natl. Acad. Sci. U. S. A* **102,** 7227-7232.

Hageman,G.S., Luthert,P.J., Victor Chong,N.H., Johnson,L.V., Anderson,D.H., and Mullins,R.F. (2001). An integrated hypothesis that considers drusen as biomarkers of immune-

mediated processes at the RPE-Bruch's membrane interface in aging and age-related macular degeneration. *Prog. Retin. Eye Res.* **20,** 705-732.

Haines,J.L., Hauser,M.A., Schmidt,S., Scott,W.K., Olson,L.M., Gallins,P., Spencer,K.L., Kwan,S.Y., Noureddine,M., Gilbert,J.R. et al. (2005). Complement factor H variant increases the risk of age-related macular degeneration. *Science* **308,** 419-421.

Hakobyan,S., Harris,C.L., van den Berg,C.W., Fernandez-Alonso,M.C., de Jorge,E.G., de,C., Sr., Rivas,G., Mangione,P., Pepys,M.B., and Morgan,B.P. (2008). Complement factor H binds to denatured rather than to native pentameric C-reactive protein. *J. Biol. Chem.* **283,** 30451-30460.

Halme,J., Sachse,M., Vogel,H., Giese,T., Klar,E., and Kirschfink,M. (2009). Primary human hepatocytes are protected against complement by multiple regulators. *Mol. Immunol.* **46,** 2284-2289.

Hamilton,G., Proitsi,P., Williams,J., O'Donovan,M., Owen,M., Powell,J., and Lovestone,S. (2007). Complement factor H Y402H polymorphism is not associated with late-onset Alzheimer's disease. *Neuromolecular. Med.* **9,** 331-334.

Hammond,B.R., Jr., Wooten,B.R., and Snodderly,D.M. (1996). Cigarette smoking and retinal carotenoids: implications for age-related macular degeneration. *Vision Res.* **36,** 3003-3009.

Harris,C.L., Hanna,S.M., Mizuno,M., Holt,D.S., Marchbank,K.J., and Morgan,B.P. (2003). Characterization of the mouse analogues of CD59 using novel monoclonal antibodies: tissue distribution and functional comparison. *Immunology* **109,** 117-126.

Hartmann,K., Corvey,C., Skerka,C., Kirschfink,M., Karas,M., Brade,V., Miller,J.C., Stevenson,B., Wallich,R., Zipfel,P.F. et al. (2006). Functional characterization of BbCRASP-2, a distinct outer membrane protein of Borrelia burgdorferi that binds host complement regulators factor H and FHL-1. *Mol. Microbiol.* **61,** 1220-1236.

Heier,J.S., Boyer,D., Nguyen,Q.D., Marcus,D., Roth,D.B., Yancopoulos,G., Stahl,N., Ingerman,A., Vitti,R., Berliner,A.J. et al. (2011). The 1-year results of CLEAR-IT 2, a phase 2 study of vascular endothelial growth factor trap-eye dosed as-needed after 12-week fixed dosing. *Ophthalmology* **118,** 1098-1106.

Heinen,S., Hartmann,A., Lauer,N., Wiehl,U., Dahse,H.M., Schirmer,S., Gropp,K., Enghardt,T., Wallich,R., Halbich,S. et al. (2009). Factor H-related protein 1 (CFHR-1) inhibits complement C5 convertase activity and terminal complex formation. *Blood* **114,** 2439-2447.

Hellwage,J., Jokiranta,T.S., Koistinen,V., Vaarala,O., Meri,S., and Zipfel,P.F. (1999). Functional properties of complement factor H-related proteins FHR-3 and FHR-4: binding to the C3d region of C3b and differential regulation by heparin. *FEBS Lett.* **462,** 345-352.

Hellwage,J., Meri,T., Heikkila,T., Alitalo,A., Panelius,J., Lahdenne,P., Seppala,I.J., and Meri,S. (2001). The complement regulator factor H binds to the surface protein OspE of Borrelia burgdorferi. *J. Biol. Chem.* **276,** 8427-8435.

Herbert,A.P., Deakin,J.A., Schmidt,C.Q., Blaum,B.S., Egan,C., Ferreira,V.P., Pangburn,M.K., Lyon,M., Uhrin,D., and Barlow,P.N. (2007). Structure shows that a glycosaminoglycan and protein recognition site in factor H is perturbed by age-related macular degeneration-linked single nucleotide polymorphism. *J. Biol. Chem.* **282,** 18960-18968.

Hogg,R.E., Woodside,J.V., Gilchrist,S.E., Graydon,R., Fletcher,A.E., Chan,W., Knox,A., Cartmill,B., and Chakravarthy,U. (2008). Cardiovascular disease and hypertension are strong risk factors for choroidal neovascularization. *Ophthalmology* **115,** 1046-1052.

Holers,V.M. (2008). The spectrum of complement alternative pathway-mediated diseases. *Immunol. Rev.* **223,** 300-316.

Hollyfield,J.G., Bonilha,V.L., Rayborn,M.E., Yang,X., Shadrach,K.G., Lu,L., Ufret,R.L., Salomon,R.G., and Perez,V.L. (2008). Oxidative damage-induced inflammation initiates age-related macular degeneration. *Nat. Med.* **14,** 194-198.

Hollyfield,J.G., Perez,V.L., and Salomon,R.G. (2010). A hapten generated from an oxidation fragment of docosahexaenoic acid is sufficient to initiate age-related macular degeneration. *Mol. Neurobiol.* **41,** 290-298.

Holtkamp,G.M., Kijlstra,A., Peek,R., and de Vos,A.F. (2001). Retinal pigment epithelium-immune system interactions: cytokine production and cytokine-induced changes. *Prog. Retin. Eye Res.* **20,** 29-48.

Holtkamp,G.M., Van,R.M., de Vos,A.F., Willekens,B., Peek,R., and Kijlstra,A. (1998). Polarized secretion of IL-6 and IL-8 by human retinal pigment epithelial cells. *Clin. Exp. Immunol.* **112,** 34-43.

Horster,R., Ristau,T., Sadda,S.R., and Liakopoulos,S. (2011). Individual recurrence intervals after anti-VEGF therapy for age-related macular degeneration. *Graefes Arch. Clin. Exp. Ophthalmol.* **249,** 645-652.

Horstmann,R.D., Sievertsen,H.J., Knobloch,J., and Fischetti,V.A. (1988). Antiphagocytic activity of streptococcal M protein: selective binding of complement control protein factor H. *Proc. Natl. Acad. Sci. U. S. A* **85,** 1657-1661.

Huber-Lang,M., Sarma,J.V., Zetoune,F.S., Rittirsch,D., Neff,T.A., McGuire,S.R., Lambris,J.D., Warner,R.L., Flierl,M.A., Hoesel,L.M. et al. (2006). Generation of C5a in the absence of C3: a new complement activation pathway. *Nat. Med.* **12,** 682-687.

Imamura,Y., Noda,S., Hashizume,K., Shinoda,K., Yamaguchi,M., Uchiyama,S., Shimizu,T., Mizushima,Y., Shirasawa,T., and Tsubota,K. (2006). Drusen, choroidal neovascularization, and retinal pigment epithelium dysfunction in SOD1-deficient mice: a model of age-related macular degeneration. *Proc. Natl. Acad. Sci. U. S. A* **103,** 11282-11287.

Inal,J.M., Hui,K.M., Miot,S., Lange,S., Ramirez,M.I., Schneider,B., Krueger,G., and Schifferli,J.A. (2005). Complement C2 receptor inhibitor trispanning: a novel human complement inhibitory receptor. *J. Immunol.* **174,** 356-366.

Iriyama,A., Inoue,Y., Takahashi,H., Tamaki,Y., Jang,W.D., and Yanagi,Y. (2009). A2E, a component of lipofuscin, is pro-angiogenic in vivo. *J. Cell Physiol* **220,** 469-475.

Jarrett,S.G., Lin,H., Godley,B.F., and Boulton,M.E. (2008). Mitochondrial DNA damage and its potential role in retinal degeneration. *Prog. Retin. Eye Res.* **27,** 596-607.

Jarva,H., Jokiranta,T.S., Hellwage,J., Zipfel,P.F., and Meri,S. (1999). Regulation of complement activation by C-reactive protein: targeting the complement inhibitory activity of factor H by an interaction with short consensus repeat domains 7 and 8-11. *J. Immunol.* **163,** 3957-3962.

Jha,P., Sohn,J.H., Xu,Q., Nishihori,H., Wang,Y., Nishihori,S., Manickam,B., Kaplan,H.J., Bora,P.S., and Bora,N.S. (2006a). The complement system plays a critical role in the

development of experimental autoimmune anterior uveitis. *Invest Ophthalmol. Vis. Sci.* **47,** 1030-1038.

Jha,P., Sohn,J.H., Xu,Q., Wang,Y., Kaplan,H.J., Bora,P.S., and Bora,N.S. (2006b). Suppression of complement regulatory proteins (CRPs) exacerbates experimental autoimmune anterior uveitis (EAAU). *J. Immunol.* **176,** 7221-7231.

Johnson,L.V., Leitner,W.P., Staples,M.K., and Anderson,D.H. (2001). Complement activation and inflammatory processes in Drusen formation and age related macular degeneration. *Exp. Eye Res.* **73,** 887-896.

Johnson,L.V., Ozaki,S., Staples,M.K., Erickson,P.A., and Anderson,D.H. (2000). A potential role for immune complex pathogenesis in drusen formation. *Exp. Eye Res.* **70,** 441-449.

Johnson,P.T., Betts,K.E., Radeke,M.J., Hageman,G.S., Anderson,D.H., and Johnson,L.V. (2006). Individuals homozygous for the age-related macular degeneration risk-conferring variant of complement factor H have elevated levels of CRP in the choroid. *Proc. Natl. Acad. Sci. U. S. A* **103,** 17456-17461.

Jokiranta,T.S., Hellwage,J., Koistinen,V., Zipfel,P.F., and Meri,S. (2000). Each of the three binding sites on complement factor H interacts with a distinct site on C3b. *J. Biol. Chem.* **275,** 27657-27662.

Juel,H.B., Kaestel,C., Folkersen,L., Faber,C., Heegaard,N.H., Borup,R., and Nissen,M.H. (2011). Retinal pigment epithelial cells upregulate expression of complement factors after co-culture with activated T cells. *Exp. Eye Res.* **92,** 180-188.

Kallitsis,A., Moschos,M.M., and Ladas,I.D. (2007). Photodynamic therapy versus thermal laser photocoagulation for the treatment of recurrent choroidal neovascularization due to AMD. *In Vivo* **21,** 1049-1052.

Kamei,M. and Hollyfield,J.G. (1999). TIMP-3 in Bruch's membrane: changes during aging and in age-related macular degeneration. *Invest Ophthalmol. Vis. Sci.* **40,** 2367-2375.

Kanda,A., Chen,W., Othman,M., Branham,K.E., Brooks,M., Khanna,R., He,S., Lyons,R., Abecasis,G.R., and Swaroop,A. (2007). A variant of mitochondrial protein LOC387715/ARMS2, not HTRA1, is strongly associated with age-related macular degeneration. *Proc. Natl. Acad. Sci. U. S. A* **104,** 16227-16232.

Kardys,I., Klaver,C.C., Despriet,D.D., Bergen,A.A., Uitterlinden,A.G., Hofman,A., Oostra,B.A., Van Duijn,C.M., de Jong,P.T., and Witteman,J.C. (2006). A common polymorphism in the complement factor H gene is associated with increased risk of myocardial infarction: the Rotterdam Study. *J. Am. Coll. Cardiol.* **47,** 1568-1575.

Katta,S., Kaur,I., and Chakrabarti,S. (2009). The molecular genetic basis of age-related macular degeneration: an overview. *J. Genet.* **88,** 425-449.

Katz,Y. and Strunk,R.C. (1989). IL-1 and tumor necrosis factor. Similarities and differences in stimulation of expression of alternative pathway of complement and IFN-beta 2/IL-6 genes in human fibroblasts. *J. Immunol.* **142,** 3862-3867.

Kelly,U., Yu,L., Kumar,P., Ding,J.D., Jiang,H., Hageman,G.S., Arshavsky,V.Y., Frank,M.M., Hauser,M.A., and Rickman,C.B. (2010). Heparan sulfate, including that in Bruch's membrane, inhibits the complement alternative pathway: implications for age-related macular degeneration. *J. Immunol.* **185,** 5486-5494.

Kevany,B.M. and Palczewski,K. (2010). Phagocytosis of retinal rod and cone photoreceptors. *Physiology. (Bethesda.)* **25,** 8-15.

Kim,Y.H., He,S., Kase,S., Kitamura,M., Ryan,S.J., and Hinton,D.R. (2009). Regulated secretion of complement factor H by RPE and its role in RPE migration. *Graefes Arch. Clin. Exp. Ophthalmol.* **247,** 651-659.

King,S.M., Dillman,J.F., III, Benashski,S.E., Lye,R.J., Patel-King,R.S., and Pfister,K.K. (1996). The mouse t-complex-encoded protein Tctex-1 is a light chain of brain cytoplasmic dynein. *J. Biol. Chem.* **271,** 32281-32287.

Klaver,C.C., Wolfs,R.C., Assink,J.J., Van Duijn,C.M., Hofman,A., and de Jong,P.T. (1998). Genetic risk of age-related maculopathy. Population-based familial aggregation study. *Arch. Ophthalmol.* **116,** 1646-1651.

Klein,R., Klein,B.E., and Linton,K.L. (1992). Prevalence of age-related maculopathy. The Beaver Dam Eye Study. *Ophthalmology* **99,** 933-943.

Klein,R., Knudtson,M.D., Cruickshanks,K.J., and Klein,B.E. (2008). Further observations on the association between smoking and the long-term incidence and progression of age-related macular degeneration: the Beaver Dam Eye Study. *Arch. Ophthalmol.* **126,** 115-121.

Klein,R.J., Zeiss,C., Chew,E.Y., Tsai,J.Y., Sackler,R.S., Haynes,C., Henning,A.K., SanGiovanni,J.P., Mane,S.M., Mayne,S.T. et al. (2005). Complement factor H polymorphism in age-related macular degeneration. *Science* **308,** 385-389.

Klos,A., Tenner,A.J., Johswich,K.O., Ager,R.R., Reis,E.S., and Kohl,J. (2009). The role of the anaphylatoxins in health and disease. *Mol. Immunol.* **46,** 2753-2766.

Korb,L.C. and Ahearn,J.M. (1997). C1q binds directly and specifically to surface blebs of apoptotic human keratinocytes: complement deficiency and systemic lupus erythematosus revisited. *J. Immunol.* **158,** 4525-4528.

Kortvely,E., Hauck,S.M., Duetsch,G., Gloeckner,C.J., Kremmer,E., ge-Priglinger,C.S., Deeg,C.A., and Ueffing,M. (2010). ARMS2 is a constituent of the extracellular matrix providing a link between familial and sporadic age-related macular degenerations. *Invest Ophthalmol. Vis. Sci.* **51,** 79-88.

Kotarsky,H., Hellwage,J., Johnsson,E., Skerka,C., Svensson,H.G., Lindahl,G., Sjobring,U., and Zipfel,P.F. (1998). Identification of a domain in human factor H and factor H-like protein-1 required for the interaction with streptococcal M proteins. *J. Immunol.* **160,** 3349-3354.

Kraiczy,P., Hellwage,J., Skerka,C., Becker,H., Kirschfink,M., Simon,M.M., Brade,V., Zipfel,P.F., and Wallich,R. (2004). Complement resistance of Borrelia burgdorferi correlates with the expression of BbCRASP-1, a novel linear plasmid-encoded surface protein that interacts with human factor H and FHL-1 and is unrelated to Erp proteins. *J. Biol. Chem.* **279,** 2421-2429.

Kraiczy,P., Hellwage,J., Skerka,C., Kirschfink,M., Brade,V., Zipfel,P.F., and Wallich,R. (2003). Immune evasion of Borrelia burgdorferi: mapping of a complement-inhibitor factor H-binding site of BbCRASP-3, a novel member of the Erp protein family. *Eur. J. Immunol.* **33,** 697-707.

Kregel,K.C. and Zhang,H.J. (2007). An integrated view of oxidative stress in aging: basic mechanisms, functional effects, and pathological considerations. *Am. J. Physiol Regul. Integr. Comp Physiol* **292,** R18-R36.

Krohne,T.U., Kaemmerer,E., Holz,F.G., and Kopitz,J. (2010). Lipid peroxidation products reduce lysosomal protease activities in human retinal pigment epithelial cells via two different mechanisms of action. *Exp. Eye Res.* **90,** 261-266.

Kunert,A., Losse,J., Gruszin,C., Huhn,M., Kaendler,K., Mikkat,S., Volke,D., Hoffmann,R., Jokiranta,T.S., Seeberger,H. et al. (2007). Immune evasion of the human pathogen Pseudomonas aeruginosa: elongation factor Tuf is a factor H and plasminogen binding protein. *J. Immunol.* **179,** 2979-2988.

Kutty,R.K., Nagineni,C.N., Samuel,W., Vijayasarathy,C., Hooks,J.J., and Redmond,T.M. (2010). Inflammatory cytokines regulate microRNA-155 expression in human retinal pigment epithelial cells by activating JAK/STAT pathway. *Biochem. Biophys. Res. Commun.* **402,** 390-395.

Lachmann,P.J. and Halbwachs,L. (1975). The influence of C3b inactivator (KAF) concentration on the ability of serum to support complement activation. *Clin. Exp. Immunol.* **21,** 109-114.

Laine,M., Jarva,H., Seitsonen,S., Haapasalo,K., Lehtinen,M.J., Lindeman,N., Anderson,D.H., Johnson,P.T., Jarvela,I., Jokiranta,T.S. et al. (2007). Y402H polymorphism of complement factor H affects binding affinity to C-reactive protein. *J. Immunol.* **178,** 3831-3836.

Lappin,D.F., Guc,D., Hill,A., McShane,T., and Whaley,K. (1992). Effect of interferon-gamma on complement gene expression in different cell types. *Biochem. J.* **281 (Pt 2),** 437-442.

Lau,L.I., Chiou,S.H., Liu,C.J., Yen,M.Y., and Wei,Y.H. (2011). The Effect of Photooxidative Stress and Inflammatory Cytokine on Complement Factor H Expression in Retinal Pigment Epithelial Cells. *Invest Ophthalmol. Vis. Sci.*

Law,A.L., Ling,Q., Hajjar,K.A., Futter,C.E., Greenwood,J., Adamson,P., Wavre-Shapton,S.T., Moss,S.E., and Hayes,M.J. (2009). Annexin A2 regulates phagocytosis of photoreceptor outer segments in the mouse retina. *Mol. Biol. Cell* **20,** 3896-3904.

Leffler,J., Herbert,A.P., Norstrom,E., Schmidt,C.Q., Barlow,P.N., Blom,A.M., and Martin,M. (2010). Annexin-II, DNA, and histones serve as factor H ligands on the surface of apoptotic cells. *J. Biol. Chem.* **285,** 3766-3776.

Li,M., tmaca-Sonmez,P., Othman,M., Branham,K.E., Khanna,R., Wade,M.S., Li,Y., Liang,L., Zareparsi,S., Swaroop,A. et al. (2006). CFH haplotypes without the Y402H coding variant show strong association with susceptibility to age-related macular degeneration. *Nat. Genet.* **38,** 1049-1054.

Li,R., Maminishkis,A., Wang,F.E., and Miller,S.S. (2007). PDGF-C and -D induced proliferation/migration of human RPE is abolished by inflammatory cytokines. *Invest Ophthalmol. Vis. Sci.* **48,** 5722-5732.

Licht,C., Heinen,S., Jozsi,M., Loschmann,I., Saunders,R.E., Perkins,S.J., Waldherr,R., Skerka,C., Kirschfink,M., Hoppe,B. et al. (2006). Deletion of Lys224 in regulatory domain 4 of Factor H reveals a novel pathomechanism for dense deposit disease (MPGN II). *Kidney Int.* **70,** 42-50.

Longbottom,R., Fruttiger,M., Douglas,R.H., Martinez-Barbera,J.P., Greenwood,J., and Moss,S.E. (2009). Genetic ablation of retinal pigment epithelial cells reveals the adaptive response of the epithelium and impact on photoreceptors. *Proc. Natl. Acad. Sci. U. S. A* **106,** 18728-18733.

Lotery,A. and Trump,D. (2007). Progress in defining the molecular biology of age related macular degeneration. *Hum. Genet.* **122,** 219-236.

Lueck,K., Wasmuth,S., Williams,J., Hughes,T.R., Morgan,B.P., Lommatzsch,A., Greenwood,J., Moss,S.E., and Pauleikhoff,D. (2011). Sub-lytic C5b-9 induces functional changes in retinal pigment epithelial cells consistent with age-related macular degeneration. *Eye (Lond)* **25,** 1074-1082.

Lundh von,L.P., Kam,J.H., Bainbridge,J., Catchpole,I., Gough,G., Coffey,P., and Jeffery,G. (2009). Complement factor h is critical in the maintenance of retinal perfusion. *Am. J. Pathol.* **175,** 412-421.

Luo,C., Chen,M., and Xu,H. (2011). Complement gene expression and regulation in mouse retina and retinal pigment epithelium/choroid. *Mol. Vis.* **17,** 1588-1597.

Madico,G., Welsch,J.A., Lewis,L.A., McNaughton,A., Perlman,D.H., Costello,C.E., Ngampasutadol,J., Vogel,U., Granoff,D.M., and Ram,S. (2006). The meningococcal vaccine candidate GNA1870 binds the complement regulatory protein factor H and enhances serum resistance. *J. Immunol.* **177,** 501-510.

Malek,G., Li,C.M., Guidry,C., Medeiros,N.E., and Curcio,C.A. (2003). Apolipoprotein B in cholesterol-containing drusen and basal deposits of human eyes with age-related maculopathy. *Am. J. Pathol.* **162,** 413-425.

Maller,J., George,S., Purcell,S., Fagerness,J., Altshuler,D., Daly,M.J., and Seddon,J.M. (2006). Common variation in three genes, including a noncoding variant in CFH, strongly influences risk of age-related macular degeneration. *Nat. Genet.* **38,** 1055-1059.

Mandal,M.N. and Ayyagari,R. (2006). Complement factor H: spatial and temporal expression and localization in the eye. *Invest Ophthalmol. Vis. Sci.* **47,** 4091-4097.

Manickam,B., Jha,P., Hepburn,N.J., Morgan,B.P., Harris,C.L., Bora,P.S., and Bora,N.S. (2010). Suppression of complement activation by recombinant Crry inhibits experimental autoimmune anterior uveitis (EAAU). *Mol. Immunol.* **48,** 231-239.

Manickam,B., Jha,P., Matta,B., Liu,J., Bora,P.S., and Bora,N.S. (2011). Inhibition of complement alternative pathway suppresses experimental autoimmune anterior uveitis by modulating T cell responses. *J. Biol. Chem.* **286,** 8472-8480.

Marmorstein,A.D., Marmorstein,L.Y., Sakaguchi,H., and Hollyfield,J.G. (2002). Spectral profiling of autofluorescence associated with lipofuscin, Bruch's Membrane, and sub-RPE deposits in normal and AMD eyes. *Invest Ophthalmol. Vis. Sci.* **43,** 2435-2441.

Martinez,A., Pio,R., Zipfel,P.F., and Cuttitta,F. (2003). Mapping of the adrenomedullin-binding domains in human complement factor H. *Hypertens. Res.* **26 Suppl,** S55-S59.

Martinez-Navarrete,G.C., Martin-Nieto,J., Esteve-Rudd,J., Angulo,A., and Cuenca,N. (2007). Alpha synuclein gene expression profile in the retina of vertebrates. *Mol. Vis.* **13,** 949-961.

McRae,J.L., Duthy,T.G., Griggs,K.M., Ormsby,R.J., Cowan,P.J., Cromer,B.A., McKinstry,W.J., Parker,M.W., Murphy,B.F., and Gordon,D.L. (2005). Human factor H-related protein 5 has cofactor activity, inhibits C3 convertase activity, binds heparin and C-reactive protein, and associates with lipoprotein. *J. Immunol.* **174,** 6250-6256.

Meier,I.D., Bernreuther,C., Tilling,T., Neidhardt,J., Wong,Y.W., Schulze,C., Streichert,T., and Schachner,M. (2010). Short DNA sequences inserted for gene targeting can accidentally interfere with off-target gene expression. *FASEB J.* **24,** 1714-1724.

Meri,S. and Pangburn,M.K. (1990). Discrimination between activators and nonactivators of the alternative pathway of complement: regulation via a sialic acid/polyanion binding site on factor H. *Proc. Natl. Acad. Sci. U. S. A* **87,** 3982-3986.

Mihlan,M., Blom,A.M., Kupreishvili,K., Lauer,N., Stelzner,K., Bergstrom,F., Niessen,H.W., and Zipfel,P.F. (2011). Monomeric C-reactive protein modulates classic complement activation on necrotic cells. *FASEB J.*

Mihlan,M., Stippa,S., Jozsi,M., and Zipfel,P.F. (2009). Monomeric CRP contributes to complement control in fluid phase and on cellular surfaces and increases phagocytosis by recruiting factor H. *Cell Death. Differ.* **16,** 1630-1640.

Mintz,C.S., Arnold,P.I., Johnson,W., and Schultz,D.R. (1995). Antibody-independent binding of complement component C1q by Legionella pneumophila. *Infect. Immun.* **63,** 4939-4943.

Misasi,R., Huemer,H.P., Schwaeble,W., Solder,E., Larcher,C., and Dierich,M.P. (1989). Human complement factor H: an additional gene product of 43 kDa isolated from human plasma shows cofactor activity for the cleavage of the third component of complement. *Eur. J. Immunol.* **19,** 1765-1768.

Mishima,H. and Kondo,K. (1981). Ultrastructure of age changes in the basal infoldings of aged mouse retinal pigment epithelium. *Exp. Eye Res.* **33,** 75-84.

Mitchell,P., Smith,W., Attebo,K., and Wang,J.J. (1995). Prevalence of age-related maculopathy in Australia. The Blue Mountains Eye Study. *Ophthalmology* **102,** 1450-1460.

Molina,H. (2002). The murine complement regulator Crry: new insights into the immunobiology of complement regulation. *Cell Mol. Life Sci.* **59,** 220-229.

Mondino,B.J., Brown,S.I., Rabin,B.S., and Bruno,J. (1978). Alternate pathway activation of complement in a Proteus mirabilis ulceration of the cornea. *Arch. Ophthalmol.* **96,** 1659-1661.

Mondino,B.J., Chou,H.J., and Sumner,H.L. (1996). Generation of complement membrane attack complex in normal human corneas. *Invest Ophthalmol. Vis. Sci.* **37,** 1576-1581.

Mondino,B.J. and Sumner,H.L. (1990). Generation of complement-derived anaphylatoxins in normal human donor corneas. *Invest Ophthalmol. Vis. Sci.* **31,** 1945-1949.

Morgan,B.P. and Gasque,P. (1997). Extrahepatic complement biosynthesis: where, when and why? *Clin. Exp. Immunol.* **107,** 1-7.

Morgan,H.P., Schmidt,C.Q., Guariento,M., Blaum,B.S., Gillespie,D., Herbert,A.P., Kavanagh,D., Mertens,H.D., Svergun,D.I., Johansson,C.M. et al. (2011). Structural basis for engagement by complement factor H of C3b on a self surface. *Nat. Struct. Mol. Biol.* **18,** 463-470.

Morris,K.M., Aden,D.P., Knowles,B.B., and Colten,H.R. (1982). Complement biosynthesis by the human hepatoma-derived cell line HepG2. *J. Clin. Invest* **70,** 906-913.

Mullins,R.F., Russell,S.R., Anderson,D.H., and Hageman,G.S. (2000). Drusen associated with aging and age-related macular degeneration contain proteins common to extracellular

deposits associated with atherosclerosis, elastosis, amyloidosis, and dense deposit disease. *FASEB J.* **14,** 835-846.

Munoz-Canoves,P., Vik,D.P., and Tack,B.F. (1990). Mapping of a retinoic acid-responsive element in the promoter region of the complement factor H gene. *J. Biol. Chem.* **265,** 20065-20068.

Nagano,F., Orita,S., Sasaki,T., Naito,A., Sakaguchi,G., Maeda,M., Watanabe,T., Kominami,E., Uchiyama,Y., and Takai,Y. (1998). Interaction of Doc2 with tctex-1, a light chain of cytoplasmic dynein. Implication in dynein-dependent vesicle transport. *J. Biol. Chem.* **273,** 30065-30068.

Nagineni,C.N., Cherukuri,K.S., Kutty,V., Detrick,B., and Hooks,J.J. (2007). Interferon-gamma differentially regulates TGF-beta1 and TGF-beta2 expression in human retinal pigment epithelial cells through JAK-STAT pathway. *J. Cell Physiol* **210,** 192-200.

Nagineni,C.N., Kommineni,V.K., William,A., Detrick,B., and Hooks,J.J. (2011). Regulation of VEGF expression in human retinal cells by cytokines: implications for the role of inflammation in age-related macular degeneration. *J. Cell Physiol.*

Nan,R., Gor,J., Lengyel,I., and Perkins,S.J. (2008a). Uncontrolled zinc- and copper-induced oligomerisation of the human complement regulator factor H and its possible implications for function and disease. *J. Mol. Biol.* **384,** 1341-1352.

Nan,R., Gor,J., and Perkins,S.J. (2008b). Implications of the progressive self-association of wild-type human factor H for complement regulation and disease. *J. Mol. Biol.* **375,** 891-900.

Nauta,A.J., Bottazzi,B., Mantovani,A., Salvatori,G., Kishore,U., Schwaeble,W.J., Gingras,A.R., Tzima,S., Vivanco,F., Egido,J. et al. (2003). Biochemical and functional characterization of the interaction between pentraxin 3 and C1q. *Eur. J. Immunol.* **33,** 465-473.

Nelson,R.A., Jr. (1953). The immune-adherence phenomenon; an immunologically specific reaction between microorganisms and erythrocytes leading to enhanced phagocytosis. *Science* **118,** 733-737.

Nilsson,U.R. and Mueller-Eberhard,H.J. (1965). Isolation of beta IF-globulin from human serum and its characterization as the fifth component of complement. *J. Exp. Med.* **122,** 277-298.

Nischler,C., Oberkofler,H., Ortner,C., Paikl,D., Riha,W., Lang,N., Patsch,W., and Egger,S.F. (2011). Complement factor H Y402H gene polymorphism and response to intravitreal bevacizumab in exudative age-related macular degeneration. *Acta Ophthalmol.* **89,** e344-e349.

Okemefuna,A.I., Nan,R., Miller,A., Gor,J., and Perkins,S.J. (2010). Complement factor H binds at two independent sites to C-reactive protein in acute phase concentrations. *J. Biol. Chem.* **285,** 1053-1065.

Okubo,A., Rosa,R.H., Jr., Bunce,C.V., Alexander,R.A., Fan,J.T., Bird,A.C., and Luthert,P.J. (1999). The relationships of age changes in retinal pigment epithelium and Bruch's membrane. *Invest Ophthalmol. Vis. Sci.* **40,** 443-449.

Ollert,M.W., Kadlec,J.V., David,K., Petrella,E.C., Bredehorst,R., and Vogel,C.W. (1994). Antibody-mediated complement activation on nucleated cells. A quantitative analysis of the individual reaction steps. *J. Immunol.* **153,** 2213-2221.

Olson,J.H., Erie,J.C., and Bakri,S.J. (2011). Nutritional supplementation and age-related macular degeneration. *Semin. Ophthalmol.* **26,** 131-136.

Pauleikhoff,D., Barondes,M.J., Minassian,D., Chisholm,I.H., and Bird,A.C. (1990). Drusen as risk factors in age-related macular disease. *Am. J. Ophthalmol.* **109,** 38-43.

Pei,L. and Melmed,S. (1997). Isolation and characterization of a pituitary tumor-transforming gene (PTTG). *Mol. Endocrinol.* **11,** 433-441.

Peirson,S.N., Butler,J.N., and Foster,R.G. (2003). Experimental validation of novel and conventional approaches to quantitative real-time PCR data analysis. *Nucleic Acids Res.* **31,** e73.

Penfold,P.L., Madigan,M.C., Gillies,M.C., and Provis,J.M. (2001). Immunological and aetiological aspects of macular degeneration. *Prog. Retin. Eye Res.* **20,** 385-414.

Perez-Caballero,D., Gonzalez-Rubio,C., Gallardo,M.E., Vera,M., Lopez-Trascasa,M., Rodriguez de,C.S., and Sanchez-Corral,P. (2001). Clustering of missense mutations in the C-terminal region of factor H in atypical hemolytic uremic syndrome. *Am. J. Hum. Genet.* **68,** 478-484.

Perkins,S.J., Nealis,A.S., and Sim,R.B. (1991). Oligomeric domain structure of human complement factor H by X-ray and neutron solution scattering. *Biochemistry* **30,** 2847-2857.

Perkins,S.J., Okemefuna,A.I., and Nan,R. (2010). Unravelling protein-protein interactions between complement factor H and C-reactive protein using a multidisciplinary strategy. *Biochem. Soc. Trans.* **38,** 894-900.

Pickering,M.C., Cook,H.T., Warren,J., Bygrave,A.E., Moss,J., Walport,M.J., and Botto,M. (2002). Uncontrolled C3 activation causes membranoproliferative glomerulonephritis in mice deficient in complement factor H. *Nat. Genet.* **31,** 424-428.

Pickering,M.C., de Jorge,E.G., Martinez-Barricarte,R., Recalde,S., Garcia-Layana,A., Rose,K.L., Moss,J., Walport,M.J., Cook,H.T., de,C., Sr. et al. (2007). Spontaneous hemolytic uremic syndrome triggered by complement factor H lacking surface recognition domains. *J. Exp. Med.* **204,** 1249-1256.

Pio,R., Martinez,A., Unsworth,E.J., Kowalak,J.A., Bengoechea,J.A., Zipfel,P.F., Elsasser,T.H., and Cuttitta,F. (2001). Complement factor H is a serum-binding protein for adrenomedullin, and the resulting complex modulates the bioactivities of both partners. *J. Biol. Chem.* **276,** 12292-12300.

Poltermann,S., Kunert,A., von der,H.M., Eck,R., Hartmann,A., and Zipfel,P.F. (2007). Gpm1p is a factor H-, FHL-1-, and plasminogen-binding surface protein of Candida albicans. *J. Biol. Chem.* **282,** 37537-37544.

Pryor,W.A., Hales,B.J., Premovic,P.I., and Church,D.F. (1983). The radicals in cigarette tar: their nature and suggested physiological implications. *Science* **220,** 425-427.

Rajawat,Y.S., Hilioti,Z., and Bossis,I. (2009). Aging: central role for autophagy and the lysosomal degradative system. *Ageing Res. Rev.* **8,** 199-213.

Rasband,W.S. ImageJ. (2011). National Institutes of Health, Bethesda, Maryland, USA. Ref Type: Computer Program

Rasmussen,H., Chu,K.W., Campochiaro,P., Gehlbach,P.L., Haller,J.A., Handa,J.T., Nguyen,Q.D., and Sung,J.U. (2001). Clinical protocol. An open-label, phase I, single

administration, dose-escalation study of ADGVPEDF.11D (ADPEDF) in neovascular age-related macular degeneration (AMD). *Hum. Gene Ther.* **12,** 2029-2032.

Resnikoff,S., Pascolini,D., Etya'ale,D., Kocur,I., Pararajasegaram,R., Pokharel,G.P., and Mariotti,S.P. (2004). Global data on visual impairment in the year 2002. *Bull. World Health Organ* **82,** 844-851.

Rijli,F.M., Dolle,P., Fraulob,V., LeMeur,M., and Chambon,P. (1994). Insertion of a targeting construct in a Hoxd-10 allele can influence the control of Hoxd-9 expression. *Dev. Dyn.* **201,** 366-377.

Ripoche,J., Day,A.J., Harris,T.J., and Sim,R.B. (1988). The complete amino acid sequence of human complement factor H. *Biochem. J.* **249,** 593-602.

Rivera,A., Fisher,S.A., Fritsche,L.G., Keilhauer,C.N., Lichtner,P., Meitinger,T., and Weber,B.H. (2005). Hypothetical LOC387715 is a second major susceptibility gene for age-related macular degeneration, contributing independently of complement factor H to disease risk. *Hum. Mol. Genet.* **14,** 3227-3236.

Rohrer,B., Long,Q., Coughlin,B., Wilson,R.B., Huang,Y., Qiao,F., Tang,P.H., Kunchithapautham,K., Gilkeson,G.S., and Tomlinson,S. (2009). A targeted inhibitor of the alternative complement pathway reduces angiogenesis in a mouse model of age-related macular degeneration. *Invest Ophthalmol. Vis. Sci.* **50,** 3056-3064.

Romano,A.D., Serviddio,G., de,M.A., Bellanti,F., and Vendemiale,G. (2010). Oxidative stress and aging. *J. Nephrol.* **23 Suppl 15,** S29-S36.

Rosenthal,R. and Strauss,O. (2002). Ca2+-channels in the RPE. *Adv. Exp. Med. Biol.* **514,** 225-235.

Sahu,A., Kozel,T.R., and Pangburn,M.K. (1994). Specificity of the thioester-containing reactive site of human C3 and its significance to complement activation. *Biochem. J.* **302 (Pt 2),** 429-436.

Sarna,T., Burke,J.M., Korytowski,W., Rozanowska,M., Skumatz,C.M., Zareba,A., and Zareba,M. (2003). Loss of melanin from human RPE with aging: possible role of melanin photooxidation. *Exp. Eye Res.* **76,** 89-98.

Schlaf,G., Beisel,N., Pollok-Kopp,B., Schieferdecker,H., Demberg,T., and Gotze,O. (2002). Constitutive expression and regulation of rat complement factor H in primary cultures of hepatocytes, Kupffer cells, and two hepatoma cell lines. *Lab Invest* **82,** 183-192.

Schmidt,C.Q., Herbert,A.P., Kavanagh,D., Gandy,C., Fenton,C.J., Blaum,B.S., Lyon,M., Uhrin,D., and Barlow,P.N. (2008). A new map of glycosaminoglycan and C3b binding sites on factor H. *J. Immunol.* **181,** 2610-2619.

Scholl,H.P., Charbel,I.P., Walier,M., Janzer,S., Pollok-Kopp,B., Borncke,F., Fritsche,L.G., Chong,N.V., Fimmers,R., Wienker,T. et al. (2008). Systemic complement activation in age-related macular degeneration. *PLoS. One.* **3,** e2593.

Schraufstatter,I.U., Trieu,K., Sikora,L., Sriramarao,P., and DiScipio,R. (2002). Complement c3a and c5a induce different signal transduction cascades in endothelial cells. *J. Immunol.* **169,** 2102-2110.

Schutt,F., Davies,S., Kopitz,J., Holz,F.G., and Boulton,M.E. (2000). Photodamage to human RPE cells by A2-E, a retinoid component of lipofuscin. *Invest Ophthalmol. Vis. Sci.* **41,** 2303-2308.

Schwaeble,W., Zwirner,J., Schulz,T.F., Linke,R.P., Dierich,M.P., and Weiss,E.H. (1987). Human complement factor H: expression of an additional truncated gene product of 43 kDa in human liver. *Eur. J. Immunol.* **17,** 1485-1489.

Seddon,J.M., Cote,J., Davis,N., and Rosner,B. (2003). Progression of age-related macular degeneration: association with body mass index, waist circumference, and waist-hip ratio. *Arch. Ophthalmol.* **121,** 785-792.

Seddon,J.M., Cote,J., Page,W.F., Aggen,S.H., and Neale,M.C. (2005a). The US twin study of age-related macular degeneration: relative roles of genetic and environmental influences. *Arch. Ophthalmol.* **123,** 321-327.

Seddon,J.M., Gensler,G., Milton,R.C., Klein,M.L., and Rifai,N. (2004). Association between C-reactive protein and age-related macular degeneration. *JAMA* **291,** 704-710.

Seddon,J.M., George,S., and Rosner,B. (2006). Cigarette smoking, fish consumption, omega-3 fatty acid intake, and associations with age-related macular degeneration: the US Twin Study of Age-Related Macular Degeneration. *Arch. Ophthalmol.* **124,** 995-1001.

Seddon,J.M., George,S., Rosner,B., and Rifai,N. (2005b). Progression of age-related macular degeneration: prospective assessment of C-reactive protein, interleukin 6, and other cardiovascular biomarkers. *Arch. Ophthalmol.* **123,** 774-782.

Sharma,A.K. and Pangburn,M.K. (1996). Identification of three physically and functionally distinct binding sites for C3b in human complement factor H by deletion mutagenesis. *Proc. Natl. Acad. Sci. U. S. A* **93,** 10996-11001.

Shi,G., Maminishkis,A., Banzon,T., Jalickee,S., Li,R., Hammer,J., and Miller,S.S. (2008). Control of chemokine gradients by the retinal pigment epithelium. *Invest Ophthalmol. Vis. Sci.* **49,** 4620-4630.

Sim,R.B. and DiScipio,R.G. (1982). Purification and structural studies on the complement-system control protein beta 1H (Factor H). *Biochem. J.* **205,** 285-293.

Sjoberg,A., Onnerfjord,P., Morgelin,M., Heinegard,D., and Blom,A.M. (2005). The extracellular matrix and inflammation: fibromodulin activates the classical pathway of complement by directly binding C1q. *J. Biol. Chem.* **280,** 32301-32308.

Sjoberg,A.P., Trouw,L.A., Clark,S.J., Sjolander,J., Heinegard,D., Sim,R.B., Day,A.J., and Blom,A.M. (2007). The factor H variant associated with age-related macular degeneration (His-384) and the non-disease-associated form bind differentially to C-reactive protein, fibromodulin, DNA, and necrotic cells. *J. Biol. Chem.* **282,** 10894-10900.

Skerka,C., Lauer,N., Weinberger,A.A., Keilhauer,C.N., Suhnel,J., Smith,R., Schlotzer-Schrehardt,U., Fritsche,L., Heinen,S., Hartmann,A. et al. (2007). Defective complement control of factor H (Y402H) and FHL-1 in age-related macular degeneration. *Mol. Immunol.* **44,** 3398-3406.

Sohn,J.H., Bora,P.S., Suk,H.J., Molina,H., Kaplan,H.J., and Bora,N.S. (2003). Tolerance is dependent on complement C3 fragment iC3b binding to antigen-presenting cells. *Nat. Med.* **9,** 206-212.

Sohn,J.H., Kaplan,H.J., Suk,H.J., Bora,P.S., and Bora,N.S. (2000a). Chronic low level complement activation within the eye is controlled by intraocular complement regulatory proteins. *Invest Ophthalmol. Vis. Sci.* **41,** 3492-3502.

Specht,C.G. and Schoepfer,R. (2001). Deletion of the alpha-synuclein locus in a subpopulation of C57BL/6J inbred mice. *BMC. Neurosci.* **2,** 11.

Specht,C.G. and Schoepfer,R. (2004). Deletion of multimerin-1 in alpha-synuclein-deficient mice. *Genomics* **83,** 1176-1178.

Spitzer,D., Mitchell,L.M., Atkinson,J.P., and Hourcade,D.E. (2007). Properdin can initiate complement activation by binding specific target surfaces and providing a platform for de novo convertase assembly. *J. Immunol.* **179,** 2600-2608.

Stark,K., Neureuther,K., Sedlacek,K., Hengstenberg,W., Fischer,M., Baessler,A., Wiedmann,S., Jeron,A., Holmer,S., Erdmann,J. et al. (2007). The common Y402H variant in complement factor H gene is not associated with susceptibility to myocardial infarction and its related risk factors. *Clin. Sci. (Lond)* **113,** 213-218.

Strauss,O. (2005). The retinal pigment epithelium in visual function. *Physiol Rev.* **85,** 845-881.

Streeten,B.W. (1969). Development of the human retinal pigment epithelium and the posterior segment. *Arch. Ophthalmol.* **81,** 383-394.

Streilein,J.W. (2003). Ocular immune privilege: the eye takes a dim but practical view of immunity and inflammation. *J. Leukoc. Biol.* **74,** 179-185.

Suner,I.J., Espinosa-Heidmann,D.G., Marin-Castano,M.E., Hernandez,E.P., Pereira-Simon,S., and Cousins,S.W. (2004). Nicotine increases size and severity of experimental choroidal neovascularization. *Invest Ophthalmol. Vis. Sci.* **45,** 311-317.

Tai,A.W., Chuang,J.Z., Bode,C., Wolfrum,U., and Sung,C.H. (1999). Rhodopsin's carboxy-terminal cytoplasmic tail acts as a membrane receptor for cytoplasmic dynein by binding to the dynein light chain Tctex-1. *Cell* **97,** 877-887.

Taylor,H.R., Munoz,B., West,S., Bressler,N.M., Bressler,S.B., and Rosenthal,F.S. (1990). Visible light and risk of age-related macular degeneration. *Trans. Am. Ophthalmol. Soc.* **88,** 163-173.

Thomas,A., Gasque,P., Vaudry,D., Gonzalez,B., and Fontaine,M. (2000). Expression of a complete and functional complement system by human neuronal cells in vitro. *Int. Immunol.* **12,** 1015-1023.

Thompson,D.A. and Gal,A. (2003). Vitamin A metabolism in the retinal pigment epithelium: genes, mutations, and diseases. *Prog. Retin. Eye Res.* **22,** 683-703.

Thurman,J.M., Renner,B., Kunchithapautham,K., Ferreira,V.P., Pangburn,M.K., Ablonczy,Z., Tomlinson,S., Holers,V.M., and Rohrer,B. (2009). Oxidative stress renders retinal pigment epithelial cells susceptible to complement-mediated injury. *J. Biol. Chem.* **284,** 16939-16947.

Tian,J., Ishibashi,K., Honda,S., Boylan,S.A., Hjelmeland,L.M., and Handa,J.T. (2005). The expression of native and cultured human retinal pigment epithelial cells grown in different culture conditions. *Br. J. Ophthalmol.* **89,** 1510-1517.

Timar,K.K., Pasch,M.C., van den Bosch,N.H., Jarva,H., Junnikkala,S., Meri,S., Bos,J.D., and Asghar,S.S. (2006). Human keratinocytes produce the complement inhibitor factor H: synthesis is regulated by interferon-gamma. *Mol. Immunol.* **43,** 317-325.

Tsutsumi,C., Sonoda,K.H., Egashira,K., Qiao,H., Hisatomi,T., Nakao,S., Ishibashi,M., Charo,I.F., Sakamoto,T., Murata,T. et al. (2003). The critical role of ocular-infiltrating macrophages in the development of choroidal neovascularization. *J. Leukoc. Biol.* **74,** 25-32.

Udono,T., Takahashi,K., Nakayama,M., Murakami,O., Durlu,Y.K., Tamai,M., and Shibahara,S. (2000). Adrenomedullin in cultured human retinal pigment epithelial cells. *Invest Ophthalmol. Vis. Sci.* **41,** 1962-1970.

Ugarte,M., Hussain,A.A., and Marshall,J. (2006). An experimental study of the elastic properties of the human Bruch's membrane-choroid complex: relevance to ageing. *Br. J. Ophthalmol.* **90,** 621-626.

van de Pavert,S.A., Meuleman,J., Malysheva,A., Aartsen,W.M., Versteeg,I., Tonagel,F., Kamphuis,W., McCabe,C.J., Seeliger,M.W., and Wijnholds,J. (2007). A single amino acid substitution (Cys249Trp) in Crb1 causes retinal degeneration and deregulates expression of pituitary tumor transforming gene Pttg1. *J. Neurosci.* **27,** 564-573.

Van,R.H., Hamilton,M.L., and Richardson,A. (2003). Oxidative damage to DNA and aging. *Exerc. Sport Sci. Rev.* **31,** 149-153.

Verma,A., Hellwage,J., Artiushin,S., Zipfel,P.F., Kraiczy,P., Timoney,J.F., and Stevenson,B. (2006). LfhA, a novel factor H-binding protein of Leptospira interrogans. *Infect. Immun.* **74,** 2659-2666.

Vierkotten,S., Muether,P.S., and Fauser,S. (2011). Overexpression of HTRA1 leads to ultrastructural changes in the elastic layer of Bruch's membrane via cleavage of extracellular matrix components. *PLoS. One.* **6,** e22959.

Vik,D.P. (1996). Regulation of expression of the complement factor H gene in a murine liver cell line by interferon-gamma. *Scand. J. Immunol.* **44,** 215-222.

Vingerling,J.R., Dielemans,I., Hofman,A., Grobbee,D.E., Hijmering,M., Kramer,C.F., and de Jong,P.T. (1995). The prevalence of age-related maculopathy in the Rotterdam Study. *Ophthalmology* **102,** 205-210.

Vives-Bauza,C., Anand,M., Shirazi,A.K., Magrane,J., Gao,J., Vollmer-Snarr,H.R., Manfredi,G., and Finnemann,S.C. (2008). The age lipid A2E and mitochondrial dysfunction synergistically impair phagocytosis by retinal pigment epithelial cells. *J. Biol. Chem.* **283,** 24770-24780.

Vogel,S., Mendelsohn,C.L., Mertz,J.R., Piantedosi,R., Waldburger,C., Gottesman,M.E., and Blaner,W.S. (2001). Characterization of a new member of the fatty acid-binding protein family that binds all-trans-retinol. *J. Biol. Chem.* **276,** 1353-1360.

Vogt,S.D., Barnum,S.R., Curcio,C.A., and Read,R.W. (2006). Distribution of complement anaphylatoxin receptors and membrane-bound regulators in normal human retina. *Exp. Eye Res.* **83,** 834-840.

Volanakis,J.E. (1995). Transcriptional regulation of complement genes. *Annu. Rev. Immunol.* **13,** 277-305.

Wang,A.L., Lukas,T.J., Yuan,M., Du,N., Handa,J.T., and Neufeld,A.H. (2009a). Changes in retinal pigment epithelium related to cigarette smoke: possible relevance to smoking as a risk factor for age-related macular degeneration. *PLoS. One.* **4,** e5304.

Wang,G., Spencer,K.L., Court BL, Olson,L.M., Scott,W.K., Haines,J.L., and Pericak-Vance,M.A. (2009b). Localization of age-related macular degeneration-associated ARMS2 in cytosol, not mitochondria. *Invest Ophthalmol. Vis. Sci.* **50,** 3084-3090.

Wang,Y., Bian,Z.M., Yu,W.Z., Yan,Z., Chen,W.C., and Li,X.X. (2010). Induction of interleukin-8 gene expression and protein secretion by C-reactive protein in ARPE-19 cells. *Exp. Eye Res.* **91,** 135-142.

Wang,Z., Dillon,J., and Gaillard,E.R. (2006). Antioxidant properties of melanin in retinal pigment epithelial cells. *Photochem. Photobiol.* **82,** 474-479.

Ward,H.M., Higgs,N.H., Blackmore,T.K., Sadlon,T.A., and Gordon,D.L. (1997). Cloning and analysis of the human complement factor H gene promoter. *Immunol. Cell Biol.* **75,** 508-510.

Wassell,J., Davies,S., Bardsley,W., and Boulton,M. (1999). The photoreactivity of the retinal age pigment lipofuscin. *J. Biol. Chem.* **274,** 23828-23832.

Weiler,J.M., Daha,M.R., Austen,K.F., and Fearon,D.T. (1976). Control of the amplification convertase of complement by the plasma protein beta1H. *Proc. Natl. Acad. Sci. U. S. A* **73,** 3268-3272.

Wickremasinghe,S.S., Xie,J., Lim,J., Chauhan,D.S., Robman,L., Richardson,A.J., Hageman,G., Baird,P.N., and Guymer,R. (2011). Variants in the APOE gene are associated with improved outcome after anti-VEGF treatment for neovascular AMD. *Invest Ophthalmol. Vis. Sci.* **52,** 4072-4079.

Wiesmann,C., Katschke,K.J., Yin,J., Helmy,K.Y., Steffek,M., Fairbrother,W.J., McCallum,S.A., Embuscado,L., DeForge,L., Hass,P.E. et al. (2006). Structure of C3b in complex with CRIg gives insights into regulation of complement activation. *Nature* **444,** 217-220.

Wimmers,S., Karl,M.O., and Strauss,O. (2007). Ion channels in the RPE. *Prog. Retin. Eye Res.* **26,** 263-301.

Wing,G.L., Blanchard,G.C., and Weiter,J.J. (1978). The topography and age relationship of lipofuscin concentration in the retinal pigment epithelium. *Invest Ophthalmol. Vis. Sci.* **17,** 601-607.

Wright,A.F., Chakarova,C.F., bd El-Aziz,M.M., and Bhattacharya,S.S. (2010). Photoreceptor degeneration: genetic and mechanistic dissection of a complex trait. *Nat. Rev. Genet.* **11,** 273-284.

Wu,J., Wu,Y.Q., Ricklin,D., Janssen,B.J., Lambris,J.D., and Gros,P. (2009). Structure of complement fragment C3b-factor H and implications for host protection by complement regulators. *Nat. Immunol.* **10,** 728-733.

Wu,Z., Lauer,T.W., Sick,A., Hackett,S.F., and Campochiaro,P.A. (2007). Oxidative stress modulates complement factor H expression in retinal pigmented epithelial cells by acetylation of FOXO3. *J. Biol. Chem.* **282,** 22414-22425.

Xu,H., Chen,M., and Forrester,J.V. (2009). Para-inflammation in the aging retina. *Prog. Retin. Eye Res.* **28,** 348-368.

Yasukawa,T., Wiedemann,P., Hoffmann,S., Kacza,J., Eichler,W., Wang,Y.S., Nishiwaki,A., Seeger,J., and Ogura,Y. (2007). Glycoxidized particles mimic lipofuscin

accumulation in aging eyes: a new age-related macular degeneration model in rabbits. *Graefes Arch. Clin. Exp. Ophthalmol.* **245,** 1475-1485.

Yehoshua,Z., Rosenfeld,P.J., and Albini,T.A. (2011). Current Clinical Trials in Dry AMD and the Definition of Appropriate Clinical Outcome Measures. *Semin. Ophthalmol.* **26,** 167-180.

Yetemian,R.M., Brown,B.M., and Craft,C.M. (2010). Neovascularization, enhanced inflammatory response, and age-related cone dystrophy in the Nrl-/-Grk1-/- mouse retina. *Invest Ophthalmol. Vis. Sci.* **51,** 6196-6206.

Yetemian,R.M. and Craft,C.M. (2011). Characterization of the pituitary tumor transforming gene 1 knockout mouse retina. *Neurochem. Res.* **36,** 636-644.

Young,R.W. and Bok,D. (1969). Participation of the retinal pigment epithelium in the rod outer segment renewal process. *J. Cell Biol.* **42,** 392-403.

Yu,J., Wiita,P., Kawaguchi,R., Honda,J., Jorgensen,A., Zhang,K., Fischetti,V.A., and Sun,H. (2007). Biochemical analysis of a common human polymorphism associated with age-related macular degeneration. *Biochemistry* **46,** 8451-8461.

Zamiri,P., Sugita,S., and Streilein,J.W. (2007). Immunosuppressive properties of the pigmented epithelial cells and the subretinal space. *Chem. Immunol. Allergy* **92,** 86-93.

Zetterberg,M., Landgren,S., Andersson,M.E., Palmer,M.S., Gustafson,D.R., Skoog,I., Minthon,L., Thelle,D.S., Wallin,A., Bogdanovic,N. et al. (2008). Association of complement factor H Y402H gene polymorphism with Alzheimer's disease. *Am. J. Med. Genet. B Neuropsychiatr. Genet.* **147B,** 720-726.

Zhang,T., Zhang,N., Baehr,W., and Fu,Y. (2011). Cone opsin determines the time course of cone photoreceptor degeneration in Leber congenital amaurosis. *Proc. Natl. Acad. Sci. U. S. A* **108,** 8879-8884.

Zhu,Y., Thangamani,S., Ho,B., and Ding,J.L. (2005). The ancient origin of the complement system. *EMBO J.* **24,** 382-394.

Zipfel,P.F., Heinen,S., Jozsi,M., and Skerka,C. (2006). Complement and diseases: defective alternative pathway control results in kidney and eye diseases. *Mol. Immunol.* **43,** 97-106.

Zipfel,P.F., Jokiranta,T.S., Hellwage,J., Koistinen,V., and Meri,S. (1999). The factor H protein family. *Immunopharmacology* **42,** 53-60.

Zipfel,P.F. and Skerka,C. (1994). Complement factor H and related proteins: an expanding family of complement-regulatory proteins? *Immunol. Today* **15,** 121-126.